Keeyask Generation Project

Physical Environment Monitoring Plan

Physical Environment Monitoring Report

PEMP-2022-01

KEEYASK

Manitoba Environment, Climate and Parks Client File 5550.00
Manitoba Environment Act Licence No. 3107

2021 - 2022

KEEYASK GENERATION PROJECT

PHYSICAL ENVIRONMENT MONITORING PLAN

REPORT #PEMP-2022-01

2021-2022 PHYSICAL ENVIRONMENT MONITORING REPORT: YEAR 1 OPERATION

Prepared by

Manitoba Hydro

June 2022

This report should be cited as follows:

Manitoba Hydro, 2022. 2021-2022 Physical Environment Monitoring Report: Year 1 Operation. Keeyask Generation Project Physical Environment Monitoring Plan Report #PEMP-2022-01. June 2022.

SUMMARY

Background

The Keeyask Generation Project (the Project) involves the construction and operation of the Keeyask Generating Station (GS) on the Nelson River at the former location of Gull Rapids and managing Gull Lake as a reservoir. To obtain a Manitoba Environment Act licence to construct the GS, and before construction began in July 2014, the Keeyask Hydropower Limited Partnership (KHLP) prepared a plan to monitor the effects of the Project on the physical environment. Monitoring results will help the KHLP, government regulators, members of the partner

First Nations communities, and the general public understand how GS construction and operation affects the physical environment. Monitoring will help determine if the actual effects are consistent with predicted effects reported in the Project's environmental impact statement.

The Keeyask Physical Environment Monitoring Plan (PEMP) discusses planned monitoring during construction and operation of the Project, which includes monitoring of water and ice regimes, shoreline erosion, sedimentation, debris, and emission of greenhouse gases from the future reservoir. This report describes the physical environment monitoring activities and results for the 2021/22 monitoring period.

Water and Ice Regime

The water and ice monitoring parameters include water levels, water depth, water velocity, and ice cover. After receiving approval for the Project in the summer of 2014, six automated, continuous water level gauges were installed on the Nelson River between Clark Lake and Gull Rapids to monitor water levels during the construction of the Project.

Nelson River flow decreased in winter from January through April 2021 and was below average at the end of April. In summer 2021, it was near average from mid-May through June, but decreased to near the 5th percentile low flow or lower by August and remained low the rest of the year, varying between about 1,800-2,200 m^3/s. Flows have gradually increased in 2022, approaching average conditions.

In 2021/22, the 7 turbine units were incrementally brought into service, with a new unit coming on line about every 2 months. As units came into service, more of the river flow could be passed through the powerhouse with a corresponding reduction in flow through the spillway. The amount of flow passed over the spillway gradually decreased between April to September 2021, and from mid-September through April 2022 flow has passed through the spillway only intermittently. Since river flows have been low, the powerhouse has been able to pass all the flow.

The 2021/22 monitoring period is the first reported period in which water levels were within the reservoir's operating range the entire time. The open water operating range for the reservoir on Gull Lake is between 158 and 159 m asl. Through the entire period water levels were held between 158.5 and 159 m on Gull Lake. Upstream levels decreased from winter peak levels in

spring and, due to low flows, water levels were relatively flat between the reservoir and Birthday Rapids most of the summer.

In winter, ice effects increase water levels on Split and Clark lakes by about 0.6 m on average above open water levels (KHLP 2012b). Comparing the water levels on Split Lake to levels at the gauge downstream of Clark Lake (05UF759) there is no indication of Split Lake water levels being influenced by the Keeyask GS effects on the ice regime. The EIS predicted there was a possibility that Split Lake could be affected by the Project under low flow conditions like those during the 2021/22 winter for a scenario assuming no ice on Clark Lake. Clark Lake, however, was mostly frozen over in 2021/22, which likely prevented the conditions necessary for the Project to influence levels on Split Lake. Clark Lake normally does not freeze over, although it has occurred prior to the Project.

January 5, 2022

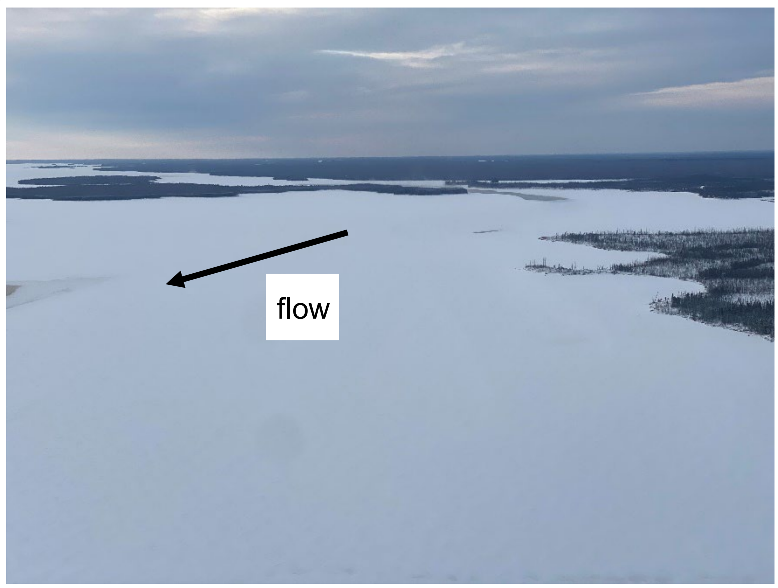

Ice cover on Clark Lake

Ice monitoring is done using satellite imagery and photographs taken along the length of the study area during monthly field trips. Although ice cover development was predicted to occur earlier with the Project than prior to construction and despite low flows, the ice cover in 2021/22 did not develop until the third week of November, about two weeks later than in the previous 5 years. The delay is likely due to somewhat warmer conditions in early winter. The ice cover developed up to about 6.5 km upstream of Birthday Rapids, similar to previous years. The ice cover remained relatively intact until the end of April due to prevailing cold weather, but by the end of May 2022 it was almost entirely gone except for remnants in back bays.

Ice cover thickness was monitored at 5 locations upstream of the Keeyask GS and two downstream to verify the prediction that with the Project a smoother and thinner ice cover would form on the reservoir upstream and at the entrance to Stephens Lake, particularly where rough and thick hanging ice dams previously formed. Monitoring from January to March found ice thicknesses of about 0.7-0.9 m in areas where hanging ice dams several metres thick previously formed at the upstream end of Gull Lake and the entrance to Stephens Lake.

Sedimentation

Sedimentation monitoring includes studying how sediment is carried (sediment transport) in the water and where it is deposited. It involves collecting water samples to measure the amount of sediment suspended in the water (done in a laboratory), using electronic devices that continuously measure turbidity (i.e., the murkiness of the water) over time and by taking readings with a hand-held meter when visiting monitoring sites. Sediment traps are used to collect sediment from the water over time to monitor the potential for sediment to settle out (deposit) near areas of potentially important sturgeon habitat.

Collecting Water Samples for Sedimentation Monitoring

Winter monitoring in 2020/21 included continuous turbidity monitoring at four sites from Clark Lake to just downstream of the Keeyask GS from January to April. Results indicated relatively steady turbidity levels through the reach and, as in previous years, turbidity declined through the winter. Average winter turbidity was similar to winter turbidity observed the previous 6 winter seasons. TSS samples were collected approximately monthly at the continuous turbidity sites and results were comparable with the 5 previous winter seasons, with an overall average TSS that was low at about 3 mg/l. Discrete turbidity was also measured at 12 back bay sites in January and April. Turbidity was generally lower than along the river main stem but showed a similar decline during the winter.

In summer 2021 (Jun–Oct) continuous turbidity was monitored at 5 mainstem sites between Clark Lake and the Kettle GS as well as 6 back bay sites, including one on Stephens Lake. The four sites between Clark Lake to just downstream of Keeyask GS had similar results with little difference between them. The site near Kettle GS generally had lower turbidity, which is consistent with results seen in previous years, Turbidity in Keeyask back bays was variable, but typically lower than along the mainstem, indicating low levels of suspended sediment in these bays. The Stephens Lake back bay had much higher turbidity than the mainstem, which is consistent with what has been seen in the past.

Four times in summer 2021, water samples were collected in bottles at mainstem and back bay sites. Samples were sent to a laboratory to measure total suspended sediment (TSS) in the water. TSS was low overall, both within mainstem areas and back bays. Concentrations were higher in June and July, averaging about 4-8 mg/l across mainstem sites and 2-5 mg/l in back bays. In August and September/October, average concentrations were less than 3 mg/l at the monitoring sites.,. At about 4 mg/l, the summer average TSS concentration across the mainstem sites was significantly lower than the overall average of about 15 mg/l prior to construction and 13 mg/l during construction.

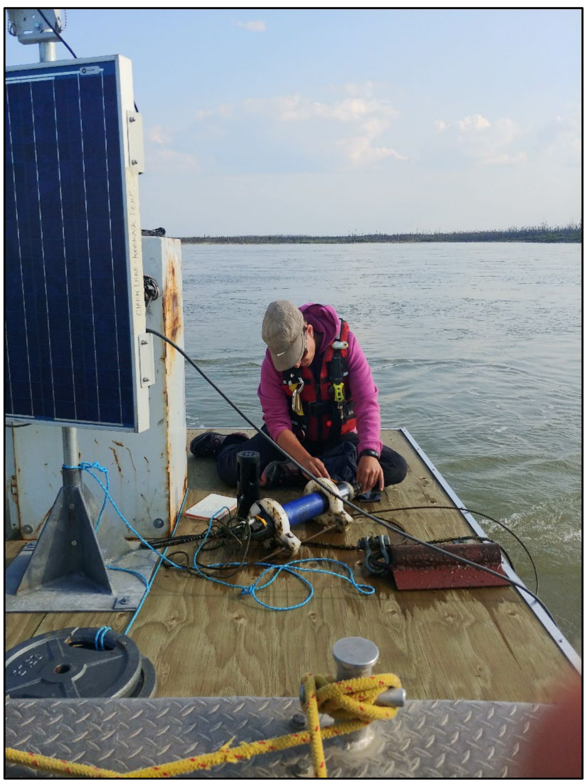

Continuous turbidity monitoring equipment – setting up a turbidity sensor

Dissolved Oxygen (DO)

DO monitoring was performed at 4 mainstem sites and 48 back bay locations in winter 2020/21 (Jan-Apr). Results showed DO to be at or near the saturation concentration (i.e., the maximum DO the water will usually hold depending on water temperature) on the mainstem and was above saturation immediately downstream of the GS because the turbulent flow through the spillway causes extra oxygen to be dissolved in water. About 70% of back bay locations had high DO concentrations, from the top to the bottom of the water. Sites where DO was low were generally shallower and further removed from the mainstem. The results were generally expected.

DO monitoring in the 2021 open water season included continuous monitoring at 5 mainstem sites and in 6 back bays, where two mainstem sites and one back bay site were located on Stephens Lake. The back bay sites used two DO sensors with one near the water surface and one near the bottom of the water to check for differences between the top and bottom. In the back bays, bottom DO was at moderate to low concentrations more often than was predicted. There may be a couple of reasons for this result including less mixing than anticipated due to peat rising to the surface; less mixing of the water by wind: and greater decay of flooded peat and vegetation than anticipated (decay uses oxygen from the water). It was found that there was lower turbidity than expected in the back bays, which means more light was able to get into the water which could result in greater decay and removal of more DO from the water than expected. At all mainstem sites, DO was found to be at or near 100% saturation. The results also showed that increases in the amount of water going through the spillway caused times when DO to increase above the saturation concentration immediately downstream of the GS. DO was not above saturation when all flow was through the powerhouse, which is what would generally be expected.

DO monitoring was also done using a probe to measure DO concentration on site at several depths between the surface and bottom of the water at 11 mainstem sites and 12 back bays sites. Up to 6 separate locations were sampled at each site. The on-site measurements, which were done 4 times in summer 2021, showed high DO concentrations along the mainstem, as observed with the continuous monitoring. Most of the back bay locations, about 83%, had high DO concentrations between the surface and bottom, while 10% and 6% of locations had moderate or low DO respectively. As with winter DO sampling, locations with lower DO tended to be shallower and further removed from the main flow. The discrete results are generally consistent with expectations.

Debris

the boat patrol upstream of Keeyask GS was primarily focused on supporting a 20-person work crew that was tasked with cleaning up woody debris in the vicinity of the Keeyask south dyke. The boat patrol transported the work crew the 60 km distance between the community of Split Lake and the south dyke twice each day. One member of the boat patrol typically remained with the work crew as a supervisor and the patrol boat was used to provide support. While the boat patrol did mark navigation hazards like newly formed reefs created by reservoir impoundment, it did not conduct formal daily patrols of the waterway to find and remove floating debris. The 20-person work crew collected and stockpiled woody debris from about 4 km of shoreline and waterway adjacent to the south dyke. The debris was gathered into several stockpiles that were left over the winter to allow the debris to dry out. In May 2022 the stockpiles were burned to get rid of the debris.

Woody debris adjacent to the south dyke

Reservoir Greenhouse Gas

The purpose of Keeyask reservoir greenhouse gas monitoring program is to enable the comparison of greenhouse gas (GHG) emissions before and after reservoir creation.

Reservoir GHG monitoring was conducted prior to construction of the Project from 2009 to 2013 and during construction in 2014, 2019 and 2020. The 2021 monitoring program monitored GHG conditions using a fixed tower in a flooded back bay and a tower on the south dyke which were the areas that were monitored prior to reservoir impoundment. Two rafts with GHG sensors that were held underwater were also deployed to regularly measure the water at a location in the same back bay as one of the towers as well as a site in the main channel. In addition to the sensors on the towers and rafts, water samples were for laboratory testing were also obtained at a number of sites.

GHG monitoring tower

Monitoring found larger concentrations of the GHGs, carbon dioxide and methane, being released from the shallow, newly flooded areas compared with the deeper existing channel and regions upstream and downstream of the reservoir. The monitoring identified a surge in methane emitted from the reservoir in May 2021 resulting from the release of methane trapped under the ice as the ice cover melted. Generally, the emissions of carbon dioxide and methane from newly flooded areas were larger than observed from the areas prior to impoundment, and flooded areas had higher emissions than areas within the pre-project river channel. Increased GHG emissions following impoundment was predicted in the EIS.

STUDY TEAM

Field Team and Support

Andrew Benger

Darrel Brunet

Keith Dobson

Leslie Flett

Leslie Gbeve

Paiten Harapiak

Leslie Klaassen

Joseph Langan

Jarod Morrison

Greg Petryk

Justin Pollick

Data Analysis, Report Preparation, and Report Review

Wil DeWit

Bob Gill

Martin Hunt

Danielle Kerr

Jennifer Lidgett

Michaelin Lower

Tim Papakyriakou

Russell Schmidt

Ashley Soloway

Marc Totte

TABLE OF CONTENTS

LIST OF TABLES

LIST OF FIGURES

LIST OF MAPS

LIST OF PHOTOS

LIST OF APPENDICES

1.0 INTRODUCTION

Construction of the Keeyask Generation Project (the Project), a 695-megawatt hydroelectric generating station (GS) and associated facilities, began in July 2014. The Project is located at Gull Rapids on the lower Nelson River in northern Manitoba where Gull Lake flows into Stephens Lake, 35 km upstream of the existing Kettle GS.

The *Keeyask Generation Project: Response to EIS Guidelines* (EIS), completed in June 2012, provides a summary of predicted effects and planned mitigation for the Project (KHLP 2012a). Technical supporting information for the physical environment and a summary of proposed monitoring and follow-up programs are provided in the *Keeyask Generation Project Environmental Impact Statement: Physical Environment Supporting Volume* (PESV; KHLP 2012b). As part of the licensing process for the Project, the Keeyask Physical Environment Monitoring Plan (PEMP) was developed detailing the monitoring activities for various components of the physical environment. The PEMP was finalized in 2015 following regulatory review and approval (KHLP 2015a).

This report generally describes the physical environment monitoring performed from April 2021 to March 2022, the first full monitoring season after the reservoir was impounded by raising water levels to the full supply level of 159 m ASL in September 2020. Although construction activities continued in 2021/22 and not all generating units were yet in operation, this period is considered the first year of operation because it is the first season when the reservoir water level was controlled within its licensed operating range of 158-159 m ASL. Note that where information is not yet available or requires further review at the time of the annual report the information will be considered in the following year's report.

The physical environment is defined as the physical and chemical make-up of an ecosystem and describes the area where things live and includes the air, water, and land within the ecosystem. Monitoring and follow-up activities focus on effects to key components of the physical environment to:

- Determine if EIS predictions of Project effects on the physical environment are correct and to identify unanticipated effects.
- Support other monitoring programs (e.g., aquatic and terrestrial) that will monitor Project effects and determine the effectiveness of mitigation and offsetting measures.

The environmental components that are monitored under the PEMP include the following:

- surface water (level/depth) and ice-regimes,
- shoreline erosion and reservoir expansion,
- sedimentation (related to water quality, sediment transport and deposition),
- greenhouse gas,
- woody debris,

- surface water temperature and dissolved oxygen (related to water quality and aquatic habitat), and
- total dissolved gas pressure.

In 2021/22, physical environment monitoring included surface water and ice regime, sedimentation, dissolved oxygen, greenhouse gases, and woody debris monitoring. Monitoring for turbidity, suspended sediment, and water temperature and dissolved oxygen occurred in the 2021/22 winter period and the results will be provided in next years report. Shoreline erosion and reservoir expansion analyses using aerial imagery to map shoreline locations are to be completed based on imagery obtained in 2021. Total dissolved gas pressure monitoring will begin after the powerhouse is fully operating with all 7 turbines in service. The PEMP provides a schedule of the physical environment monitoring activities planned during the construction and operation periods of the Project. The study area generally extends from Clark Lake into Stephens Lake as far as bout 30 km downstream near the Kettle Generating Station as shown on Map 1 (detailed site maps are provided in Appendix 1).

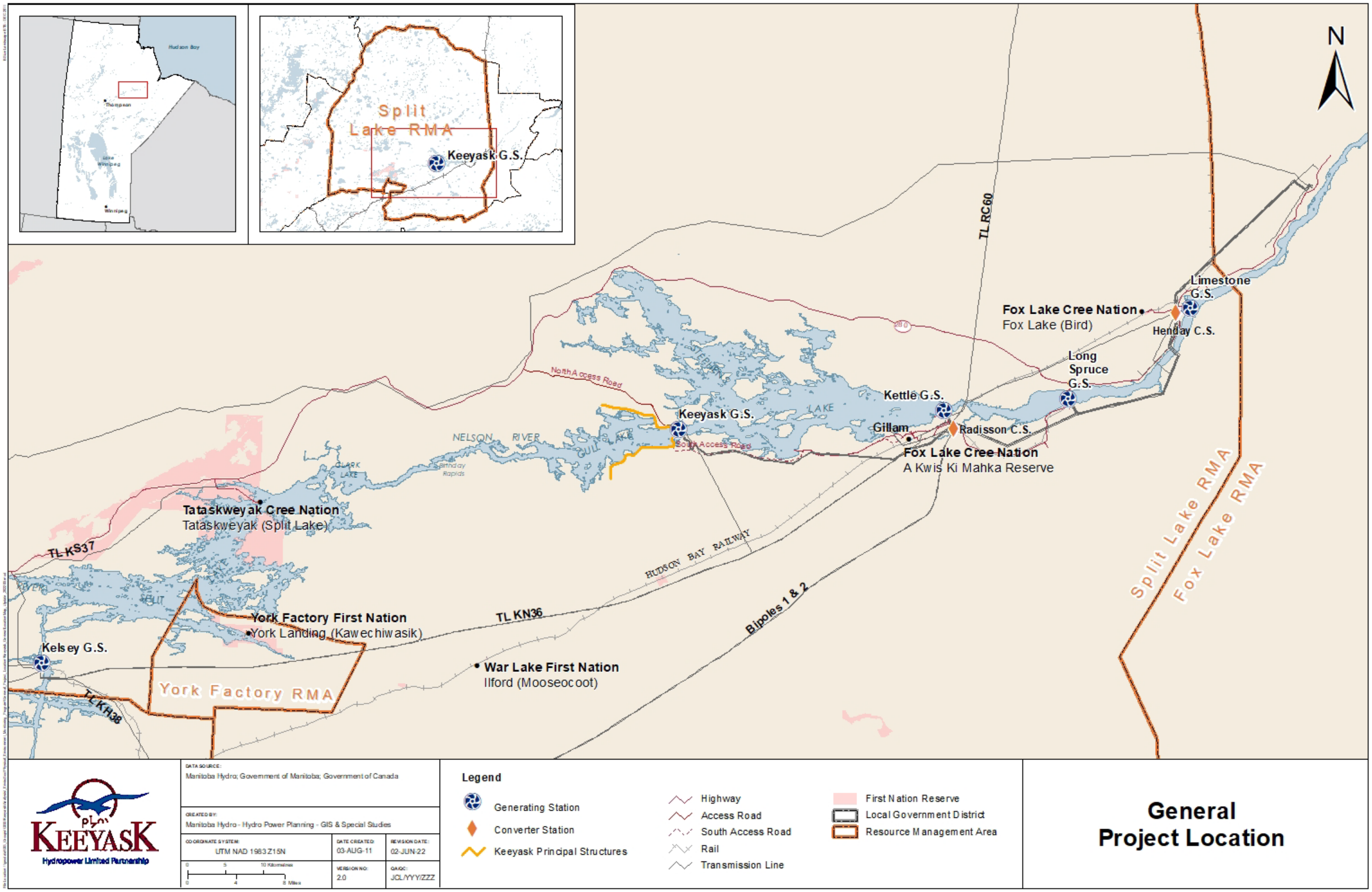

Map 1: General Project location and study area

2.0 SURFACE WATER AND ICE REGIMES

The water regime and ice parameters include water levels, water depth, river and lake-bottom elevation, water velocity, and ice cover. The largest changes to water and ice regimes are expected to occur once the reservoir has been impounded and include increases in water levels, reduction of velocities and development of a smoother ice cover. During the construction period, water levels are expected to increase from the construction of cofferdams used to isolate construction areas and an ice cover is expected to develop earlier from the installation of an ice boom.

The objectives of the water and ice regime monitoring include:

- determining water level regime and verifying expected changes in water levels resulting from the Project;
- confirming that there are no unanticipated Project effects on Split Lake water levels;
- determining water depth/bottom elevation and velocity information to support monitoring being performed under the Aquatic Effects Monitoring Plan (AEMP; KHLP 2015b);
- measuring ice conditions to support understanding of winter water levels, which may be affected by ice processes; and
- confirming that future ice conditions during operation are consistent with predicted effects reported in the EIS.

2.1 NELSON RIVER FLOW CONDITIONS

River discharge (flow) is reported as the outflow from Split Lake which is not affected by the Keeyask Project. Small streams that flow into the monitoring area between Clark Lake and Gull Rapids typically contribute less than 3% of the total flow (KHLP 2012b) and are not included in the total flow. River flows are directly correlated to water levels under open water conditions (i.e. high flow volumes result in high water levels). In winter, the levels are also influenced by ice conditions so the relationship between flow and water level is not consistent between summer and winter months. Split Lake outflows are calculated by Manitoba Hydro based on routing flows from upstream through the lake. The historical daily flow records have been analyzed to characterize flow conditions since September 1, 1977, and represent regulated flow conditions since Lake Winnipeg Regulation and Churchill River Diversion began operating. Average seasonal flows are summarized in Table 1; the summer flows are taken as May through October and winter flows from November through April.

Table 1: Split Lake seasonal discharges since start of Keeyask construction

Year /Season	Minimum Daily (m^3/s)	Mean Daily (m^3/s)	Maximum Daily (m^3/s)
2014 Summer	3438	5245	5907
2014/15 Winter	3340	3865	5057
2015 Summer	3277	3694	4282
2015/16 Winter	3198	3745	4050
2016 Summer	3194	4034	4748
2016/17 Winter	3583	4366	5007
2017 Summer	3082	4838	6594
2017/18 Winter	2880	3396	4093
2018 Summer	2508	3060	3608
2018/19 Winter	2817	3227	3735
2019 Summer	2614	3259	3665
2019/20 Winter	3135	4051	4390
2020 Summer	3350	4913	5944
2020/21 Winter	3008	3516	4111
2021 Summer	1820	2585	3675
2021/22 Winter	1757	2307	2744

The seasonal mean daily discharge (Table 1) during the 2021 Summer and 2021/22 Winter seasons was the lowest recorded since the start of construction, resulting in low water levels and quicker ice development.

River flows (Figure 1) were at or slightly above the median rate until the end of June 2021. In July, flow rates steadily dropped in response to very dry conditions. From August 2021 till February 2022 flow rates were generally at or below the 5th percentile flow. After this, the flow increased slowly and reached the 25th percentile in early April 2022.

Construction of the powerhouse generating units continued in the 2021/22 monitoring season. As work on the seven generating units progressed and additional units came into operation more of the flow passed through the powerhouse and less passed through the spillway (Figure 2). By mid-September all the flow was generally going through the powerhouse as enough units were in operation to handle the river flows that were around 2000 m^3/s. Under normal operating conditions the full capacity of the powerhouse's seven generating units is approximately 4000 m^3/s. In late January and early February, the spillway was utilized for several weeks as not enough units were online to accommodate the river flow.

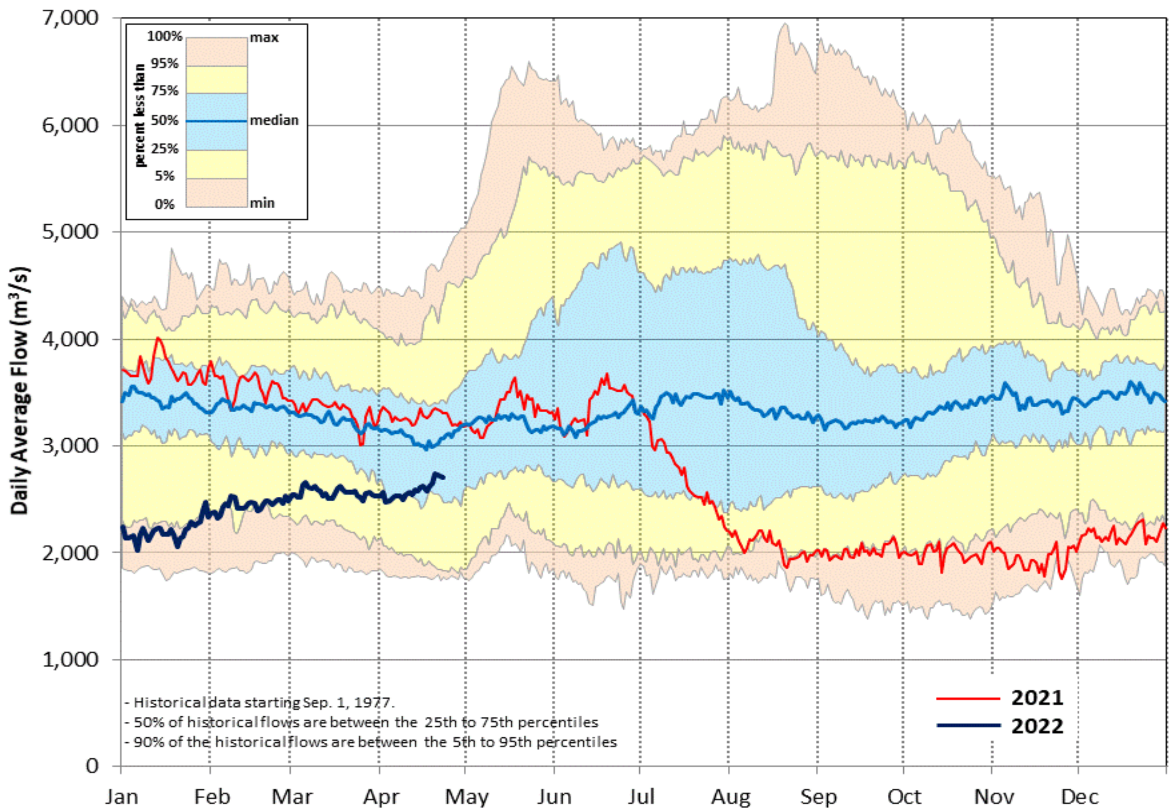

Figure 1: Split Lake 2020/2021 Daily Average Outflow and Historical Statistics

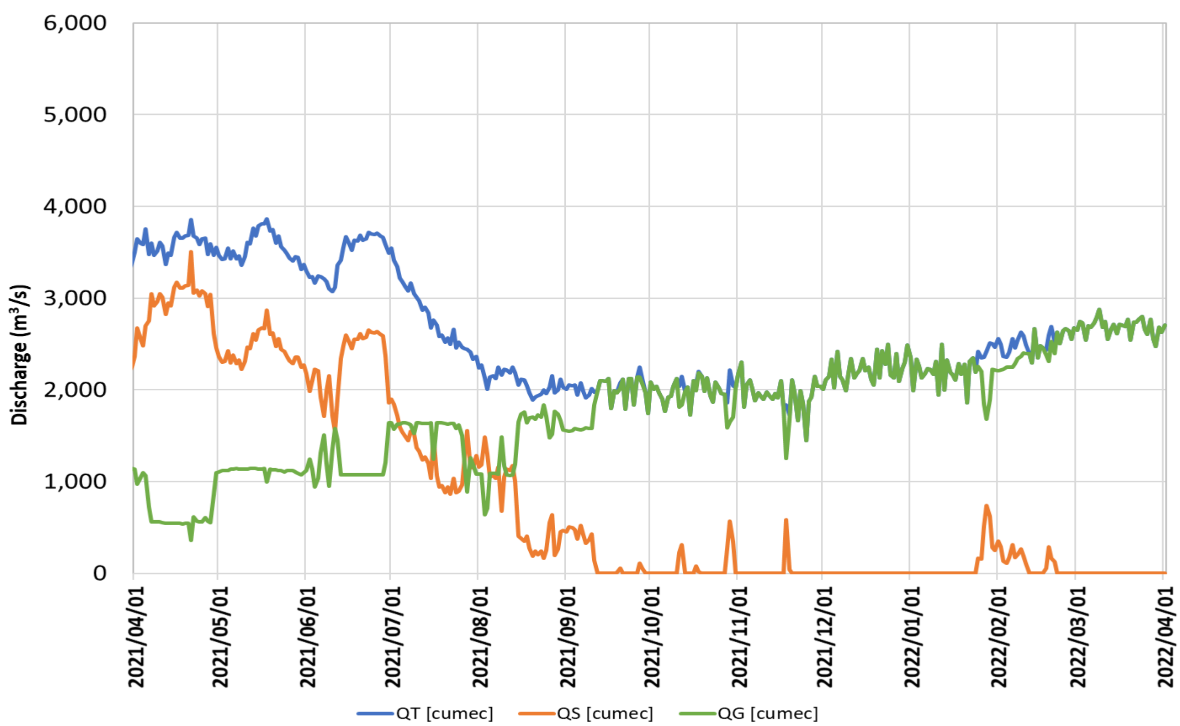

Figure 2: Keeyask Generating Station (GS) and Spillway Discharge

2.2 OBSERVED WATER LEVELS

Water levels are monitored at six sites from Clark Lake to Gull Rapids (Table 2, Map 2). A typical water level gauge is shown in Photo 1. The two Clark Lake sites have been monitored regularly since 2003, while the Gull Lake gauge was installed at the start of construction in mid July 2014. The other three sites were installed after construction started, once the necessary permits and heritage surveys were complete, which were applied for and done after the Environment Act licence was received in early July 2014. The original gauge at the upstream end of Gull Lake (05UF749) was wrecked by ice and was discontinued in May 2016. The gauge was relocated about 3 km upstream to the mouth of Portage Creek and began operation in September 2016 (site 05UF587). In addition to data from the PEMP gauges, data is reported from the existing gauge on Split Lake at the community of Split Lake.

Table 2: List of water level monitoring sites

Site ID	Name	Record	Notes
05UF766	Clark Lake	Oct. 2003 - present	4 km above outlet
05UF759	downstream of Clark Lake	Dec. 2003 - present	1.9 km below outlet
05UF770	upstream of Birthday Rapids	Oct. 2014 - present	1.1 km above rapids
05UF771	downstream of Birthday Rapids	Oct. 2014 - present	2.1 km below rapids
05UF749	upstream of Gull Lake	Oct. 2014 - May 2016	0.26 km above lake
05UF587	upstream of Gull Lake	Sep. 2016 - present	3.0 km above lake
05UF596	Gull Lake	Jul. 2014 - present	7 km above Gull Rapids
05UF701	Split Lake at Split Lake Community	Oct. 1997 - present	existing site

Photo 1: Water level gauging station in winter

The 2021/22 monitoring period is the first reported period in which water levels were within the reservoir's operating range the entire time. The open water operating range for the reservoir on Gull Lake is between 158 and 159 m asl. Through the entire period (Figure 3) water levels were held between 158.5 and 159 m on Gull Lake (station 05UF596).

In the late winter and spring of 2021 water levels were influenced by river ice until mid-May. In mid-May the water level at the gauge upstream of Gull Lake (05UF587) closely matched the Gull Lake gauge indicating that ice was no longer influencing the river levels. As river flows continued to reduce, the water level at the site downstream of Birthday Rapids (05UF771) dropped to be just slightly higher than Gull Lake.

Ice started forming around the third week of November and water levels increased quickly at the two gauges near Birthday Rapids. Both sites experienced a peak level in early December as ice thickness increased before dropping in response to changing ice conditions. With reduced flows, the water levels at the site upstream of Gull Lake experienced only a small increase (<0.3m) compared to the previous winter (<1.3m). All sites experienced lower winter levels in response to both lower flows and reduced ice impacts.

2.3 CLARK LAKE AND SPLIT LAKE WATER LEVELS

The levels on these two lakes show the same pattern of variation, differing by about 0.3-0.5 m with an average difference of approximately 0.4 m. During open water periods, both sites show a clear correlation to variations in flow.

In winter, ice effects typically increase water levels on Split and Clark lakes by about 0.6 m on average above open water levels (KHLP 2012b). Due to the low flows and water levels, the gauge on Clark Lake (05UF766) experienced technical challenges during the 2021/22 winter months. Comparing the water levels on Split Lake to the site downstream of Clark Lake (05UF759) there is no indication of Split Lake water levels being influenced by the downstream site. The EIS predicted there was a possibility that Split Lake would be affected by the Project under low flow conditions similar to what was experienced during the 2021/22 winter. It is likely that with Clark Lake mostly freezing over (see Section 2.4) it reduced the amount of frazil ice formation and limited the downstream ice growth which can increase water levels. Clark Lake has frozen over previously, most recently in the winter of 2011/12 (partial), 2003/04, and 1999/00.

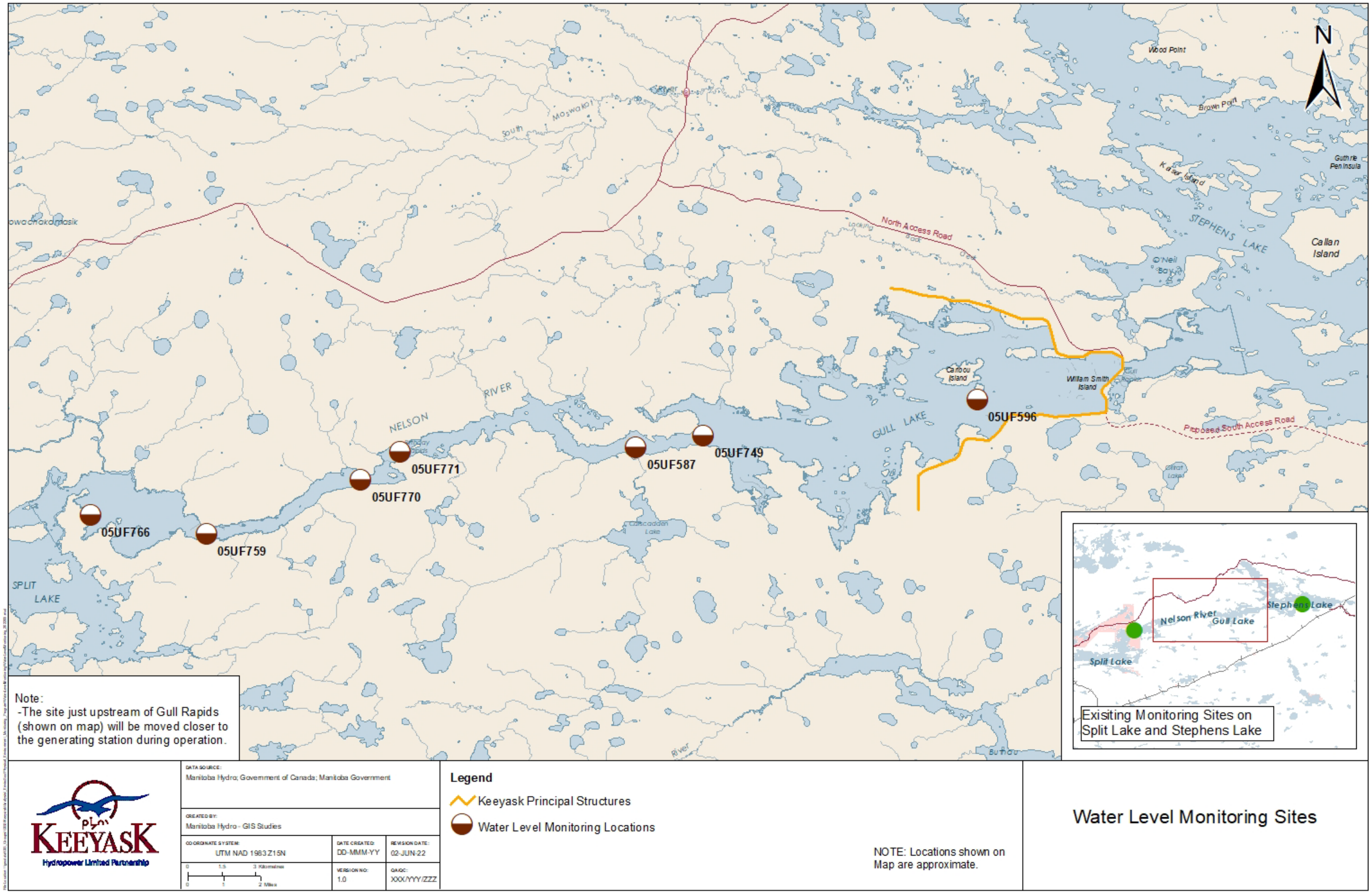

Map 2: **PEMP water level monitoring sites**

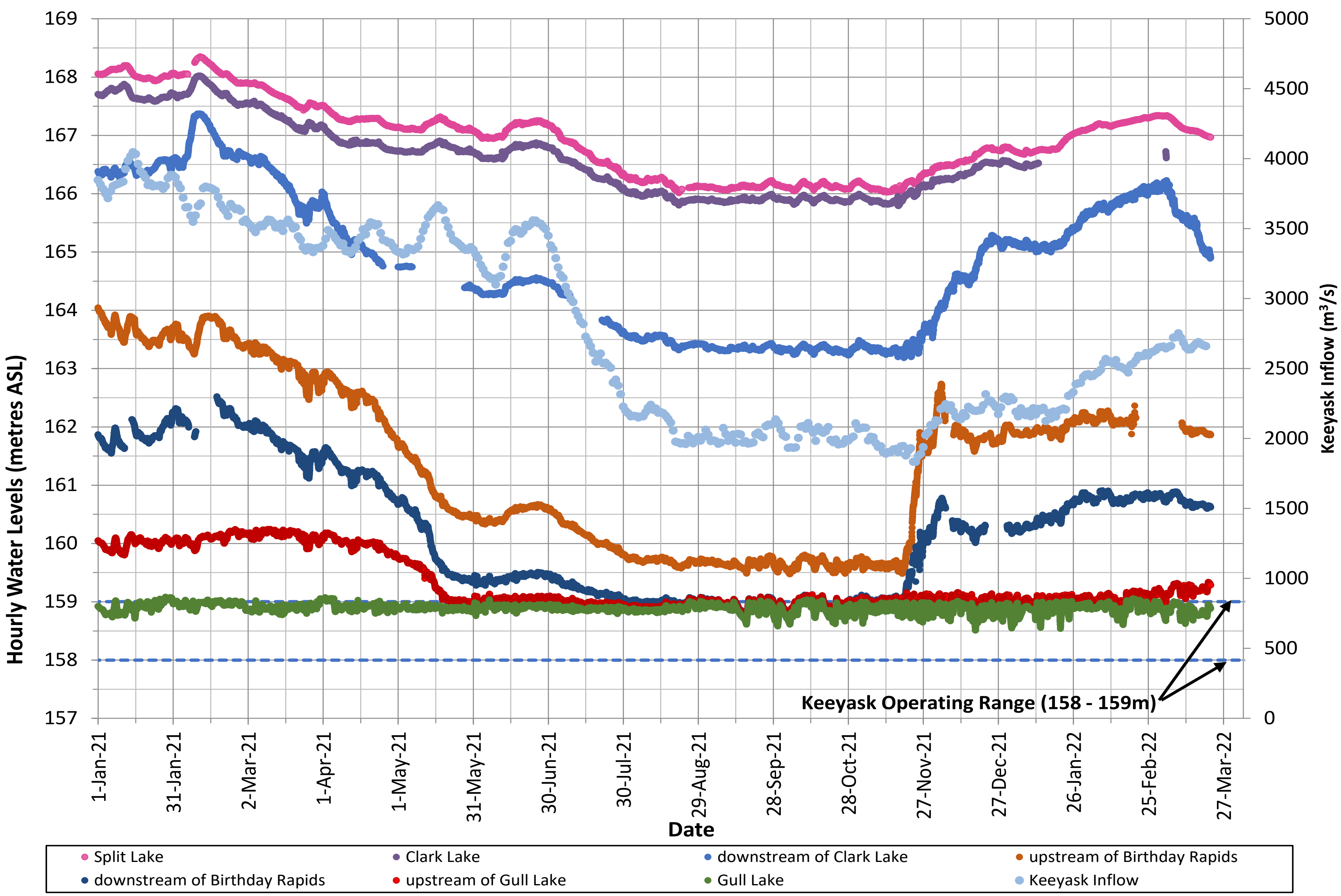

Figure 3: Observed water levels at PEMP monitoring sites in 2021/2022

2.4 ICE REGIME

The PESV (KHLP 2012b, Section 4) discusses ice processes and the pre-Project ice regime in the vicinity of the Project. In the pre-Project environment, a complete ice cover formed most years (approximately 2 out of 3 years) on Gull Lake and the Nelson River up to Birthday Rapids, although the timing and extent varied with flow and climate conditions. A combination of higher flow and/or warmer conditions could prevent an ice bridge from forming in some years so that open water persisted in the central channel from the exit of Split Lake to the entrance of Stephens Lake. In contrast, with early cold temperatures and lower flows the ice front cover could advance upstream of Birthday Rapids. In years when bridging occurred, the date when it formed ranged from as early as November at lower flows to as late as January at higher flows.

The approximate dates for freeze up and breakup on Gull Lake since the start of construction are shown in Table 3. The 2021/22 winter saw the initiation of an ice cover in the third week of November. With the low river flow the ice cover between Birthday Rapids and Gull Lake was smoother than the previous winter (Photo 2). The low flows also provided the necessary conditions for Clark Lake to freeze over (Photo 3) almost entirely. Clark Lake last froze over in 20011/12 (partial) and in 2003/04.

Satellite images show the ice formation (Figure 4, Figure 5, Figure 6) and receding ice conditions (Figure 7, Figure 8, Figure 9) over the course of the winter. With the low river flows, the ice cover progress about 0.5 km further upstream of Birthday Rapids than other years (Table 3).

Table 3: Ice dates and cover advancement / break-up

Year	Initial Freeze-up on Gull Lake	Ice Cover Advancement	Gull Lake Ice Break-up
2014/15	Jan 23, 2015 Nov 9, 2014*	foot of Birthday Rapids	May 13-15, 2015
2015/16	Nov 20, 2015	about 4 km upstream of Birthday Rapids	May 4-9, 2016
2016/17	Nov 19, 2016	about 6 km upstream of Birthday Rapids	May 22-24, 2017
2017/18	Nov 4, 2017	about 6 km upstream of Birthday Rapids	May 19-20, 2018
2018/19	Nov 4-6, 2018	about 6 km upstream of Birthday Rapids	May 13-15 2019
2019/20	Nov 5, 2019	Birthday Rapids	May 21-25, 2020
2020/21	Nov 2-3, 2020	About 6 km upstream of Birthday Rapids	May 22-23, 2021
2021/22	Nov 19-20, 2021	About 6.5 km upstream of Birthday Rapids	May 18-21, 2022

*Ice formation start date before ice boom failed

2021 Photo upstream of Gull Lake

2022 Photo upstream of Gull Lake

Photo 2: Ice formation upstream of Gull Lake

2021 Photo of Clark Lake

2022 Photo of Clark Lake

Photo 3: Ice Cover of Clark Lake

The Keeyask EIS (KHLP, 2012b) predicted that a generally thinner ice cover would develop upstream of the Keeyask GS, particularly at the upstream end of Gull Lake where a thick hanging ice dam would form most years. Similarly, ice within the reach about 4 km downstream of the GS was also predicted to be smoother and thinner because the Project would prevent the formation of a rough and thick hanging ice dam at the entrance to Stephens Lake. The ice cover in the reservoir reach and entrance to Stephens Lake was predicted to develop to a thickness similar to local lake areas (e.g., Split and Stephens lakes), which generally have a maximum ice thickness of about 0.8-1.2 m, depending on specific conditions each winter.

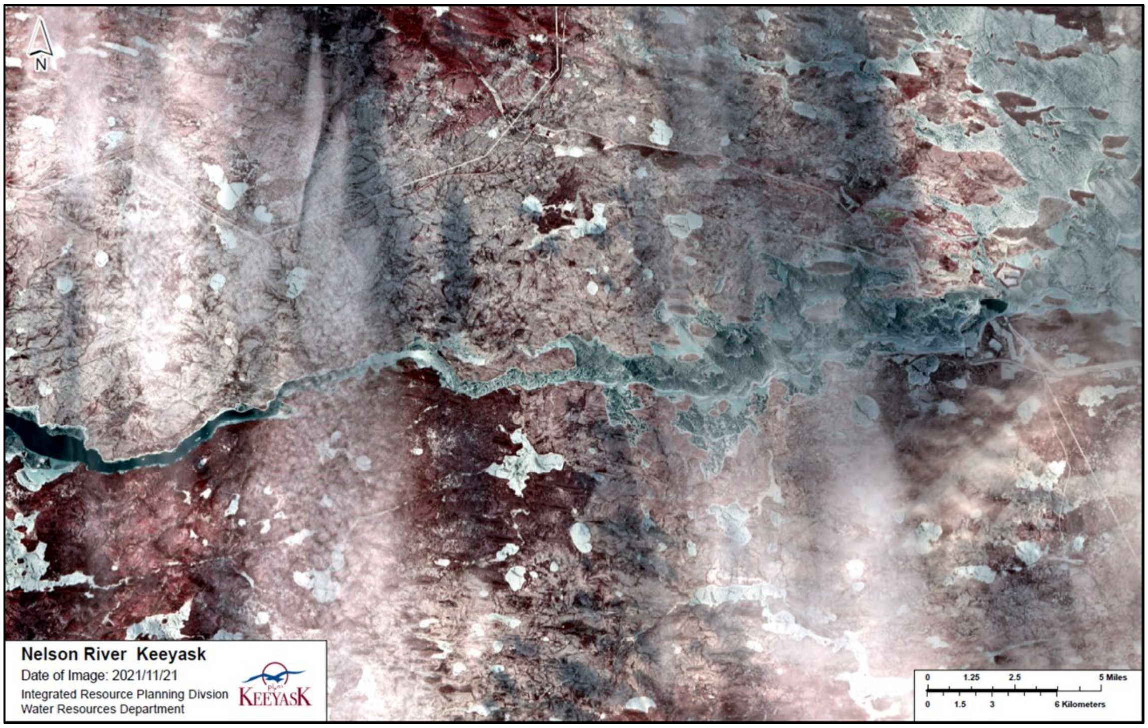

Figure 4: Ice cover development observations from satellite images 2021/11/21

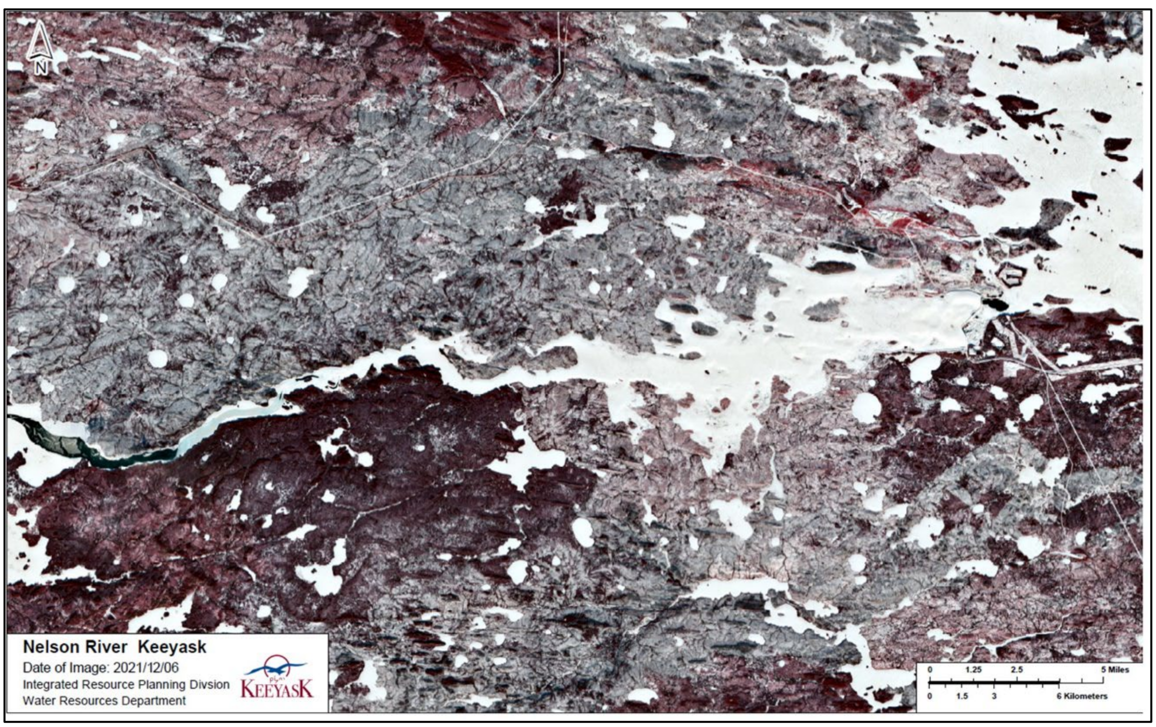

Figure 5: Ice cover development observations from satellite images 2021/12/06

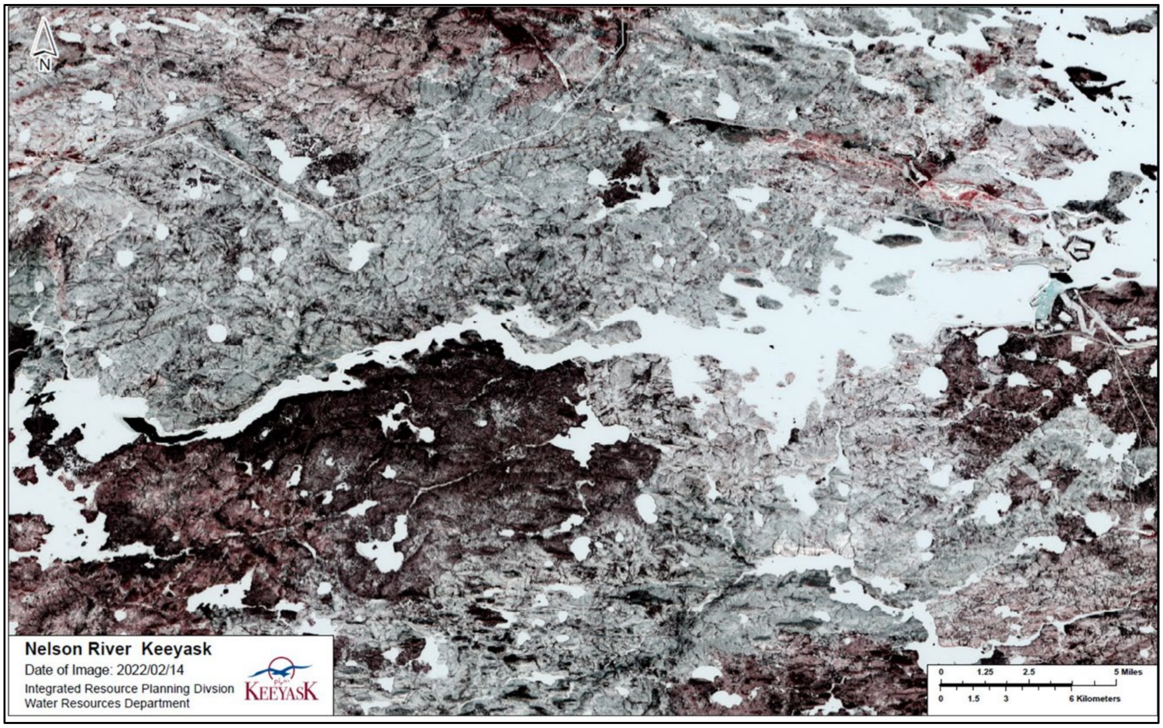

Figure 6: Ice cover development observations from satellite images 2022/02/14

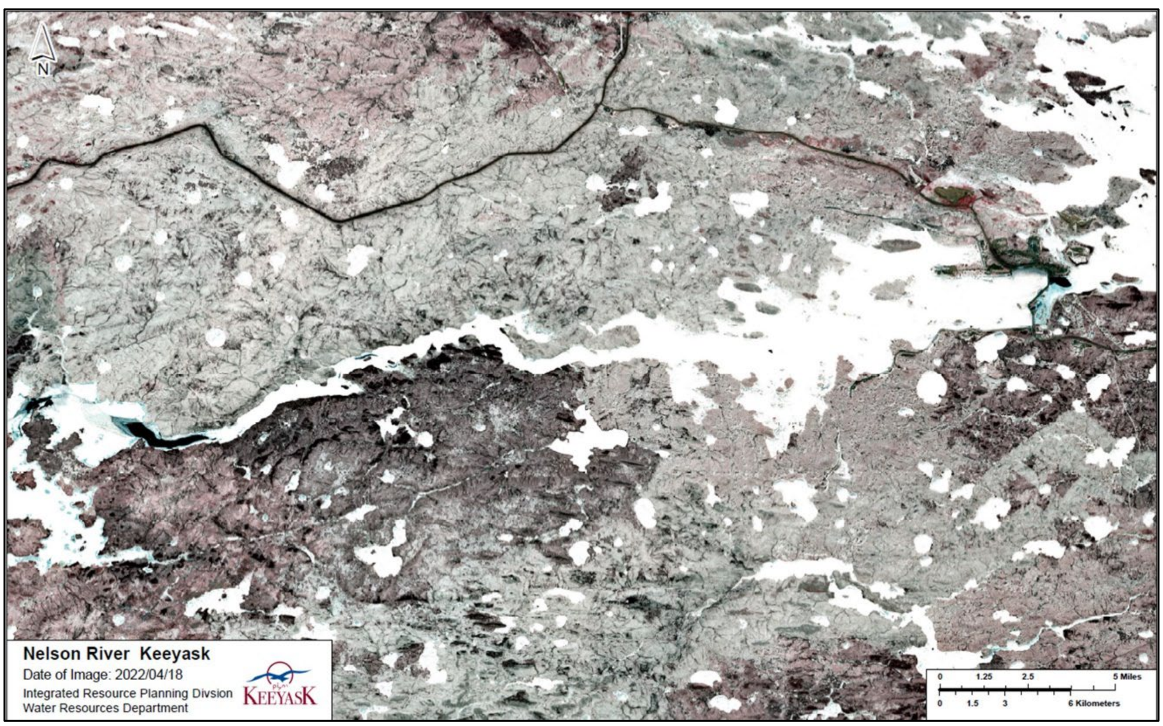

Figure 7: Receding ice cover observations from satellite images 2022/04/18

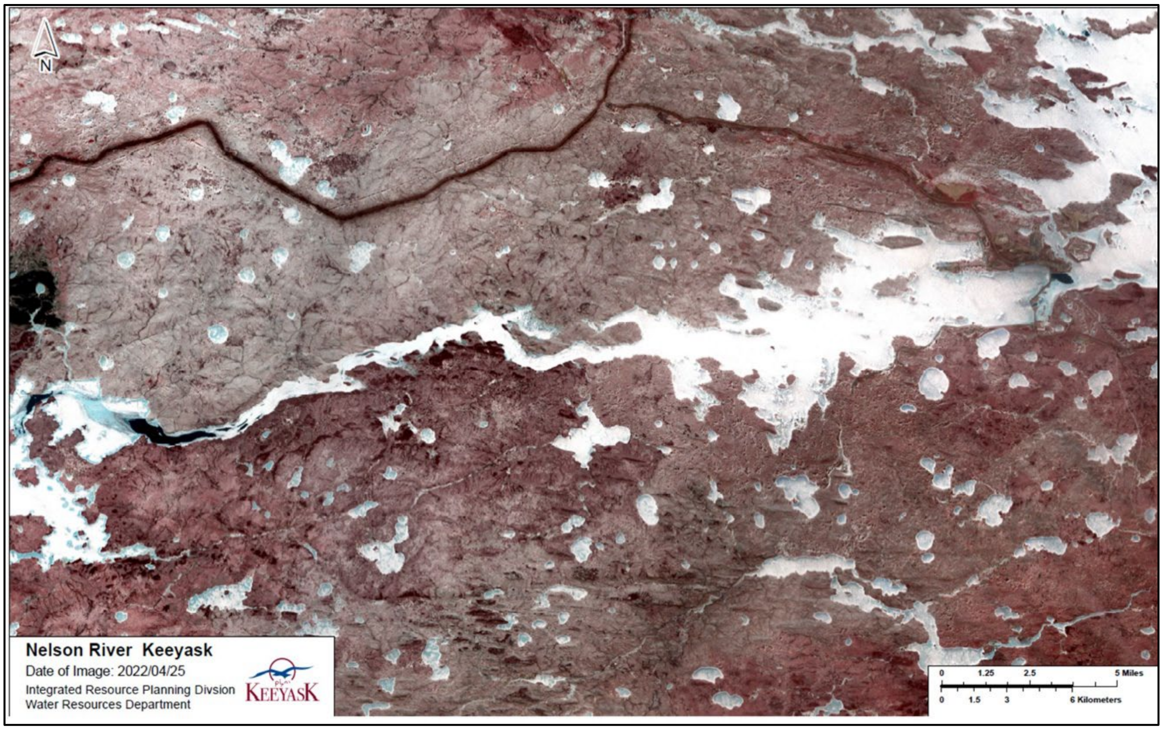

Figure 8: Receding ice cover observations from satellite images 2022/04/25

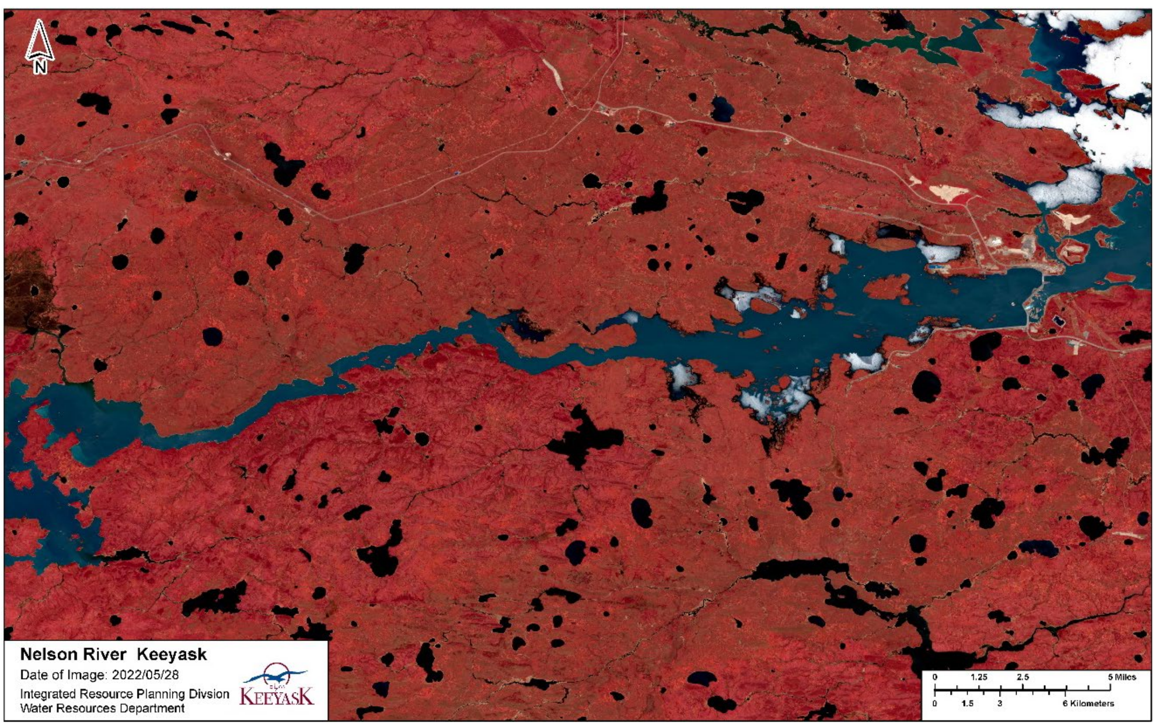

Figure 9: Receding ice cover observations from satellite images 2022/05/28

In accordance with the PEMP, ice thickness was monitored at seven locations in 2021: 5 upstream at about 5 km apart from just upstream of Gull Lake to the GS; and, at two locations approximately two and four kilometres downstream of the GS. Measurements were obtained at these 7 sites on February 5, March 3 and April 23. Upstream of the GS, ice thickness varied from 0.60-0.92 m overall, with maximum thickness ranging from 0.74-0.92 m (Figure 10). Notably, the maximum thickness at the two upstream sites, within the Nelson River channel and the entrance to Gull Lake, was 0.92 m and 0.90 m respectively. This is much less than prior to the Project when the hanging ice dam in this area could grow to 3 m to 5 m thickness or more. Similarly, the maximum ice thickness downstream was 0.7 m and 0.83 m at about 2 km and 4 km downstream respectively, which is significantly less than prior to the Project when the hanging ice dam could attain a thickness of 5-10 m or more (Figure 10). The ice cover was also notably smoother than prior to the Project. Overall, the 2021 monitoring results were consistent with expectations.

2.5 WATER VELOCITY

The Keeyask PEMP committed to measuring water velocities under low, moderate, and high flow conditions (i.e., approximately 5th, 50th, 95th percentile flows) during the operating period to identify the range of velocities occurring in various aquatic habitat areas affected by the project. Because flows in summer 2021 were forecast to be near the post-project 5^{th} percentile low flow of about 2,040 m^3/s (KHLP, 2012b), velocity monitoring was initiated during the open water season. The aquatic monitoring team identified several areas for velocity monitoring from upstream of Birthday Rapids to the entrance of Stephens Lake downstream of the GS. The PEMP monitoring crew measured velocities along more than 80 transects on 11 separate days from July to August (each measurement location included a transect in one direction and a duplicate in the other direction). All required locations upstream of the Keeyask GS were measured. Sites downstream of the GS were not measured because the powerhouse was not operating at capacity so flow conditions were not necessarily representative of operating conditions. Split Lake outflows varied on the days when velocity monitoring was performed:

- July 14 ~2,800 m^3/s (~25^{th} percentile)
- July 19, 20, 21, 22 ~2.500 m^3/s (~15^{th} percentile)
- August 5, 6, 7 ~2,000 m^3/s (~5^{th} percentile)
- August 17, 18, 19 ~2,100 m^3/s (~5^{th} percentile)

The results of from the velocity monitoring were mapped along with the modeled velocities from the Keeyask EIS (KHLP, 2012b) for the 5^{th} percentile flow of 2,040 m^3/s to compare the observed and modeled velocities (Figure 11, Figure 12, Figure 13, Figure 14). In general, the observed velocities were found to be reasonably consistent with the predicted velocities.

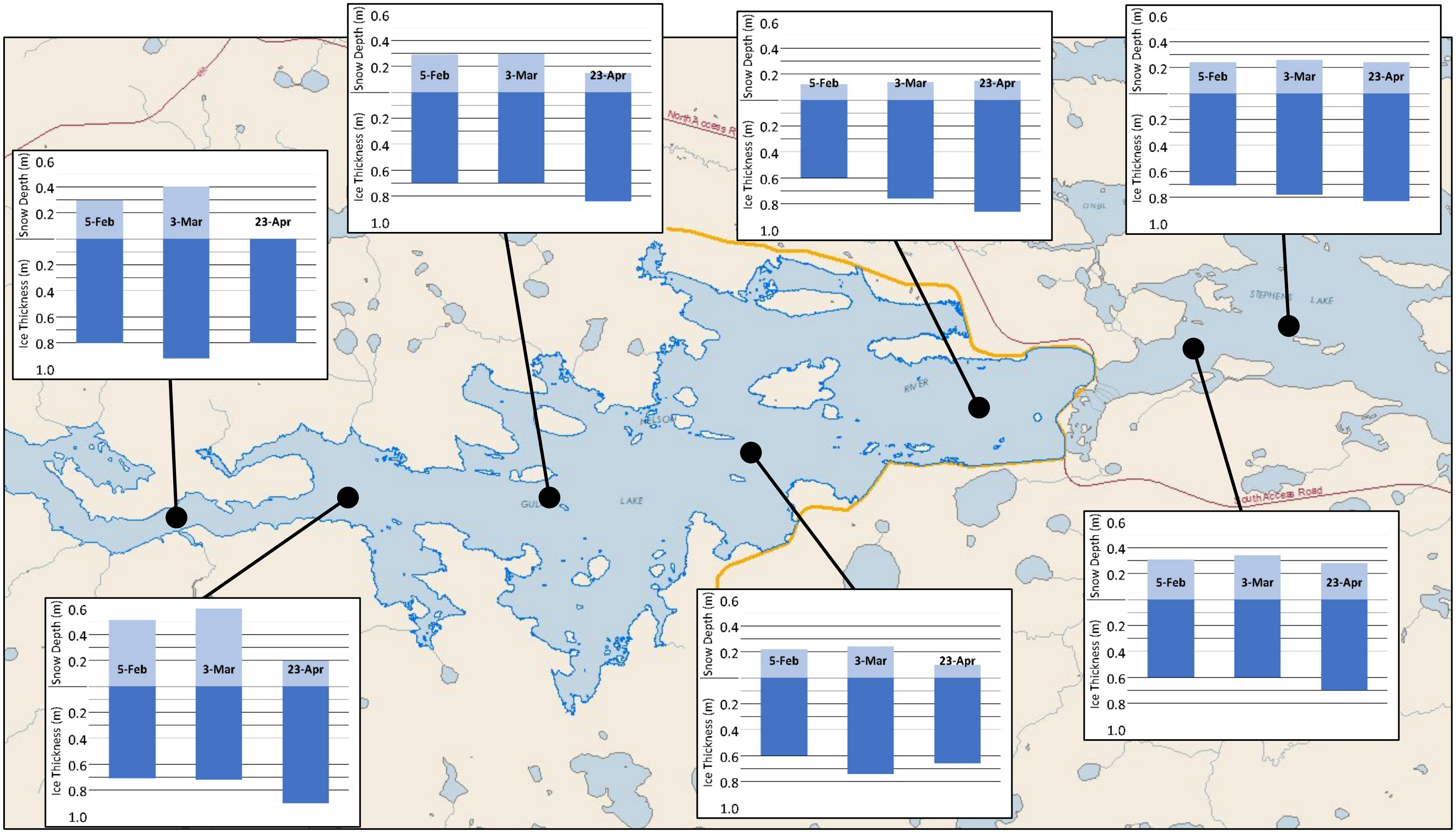

Figure 10: 2021 ice thickness & snow depth measurements

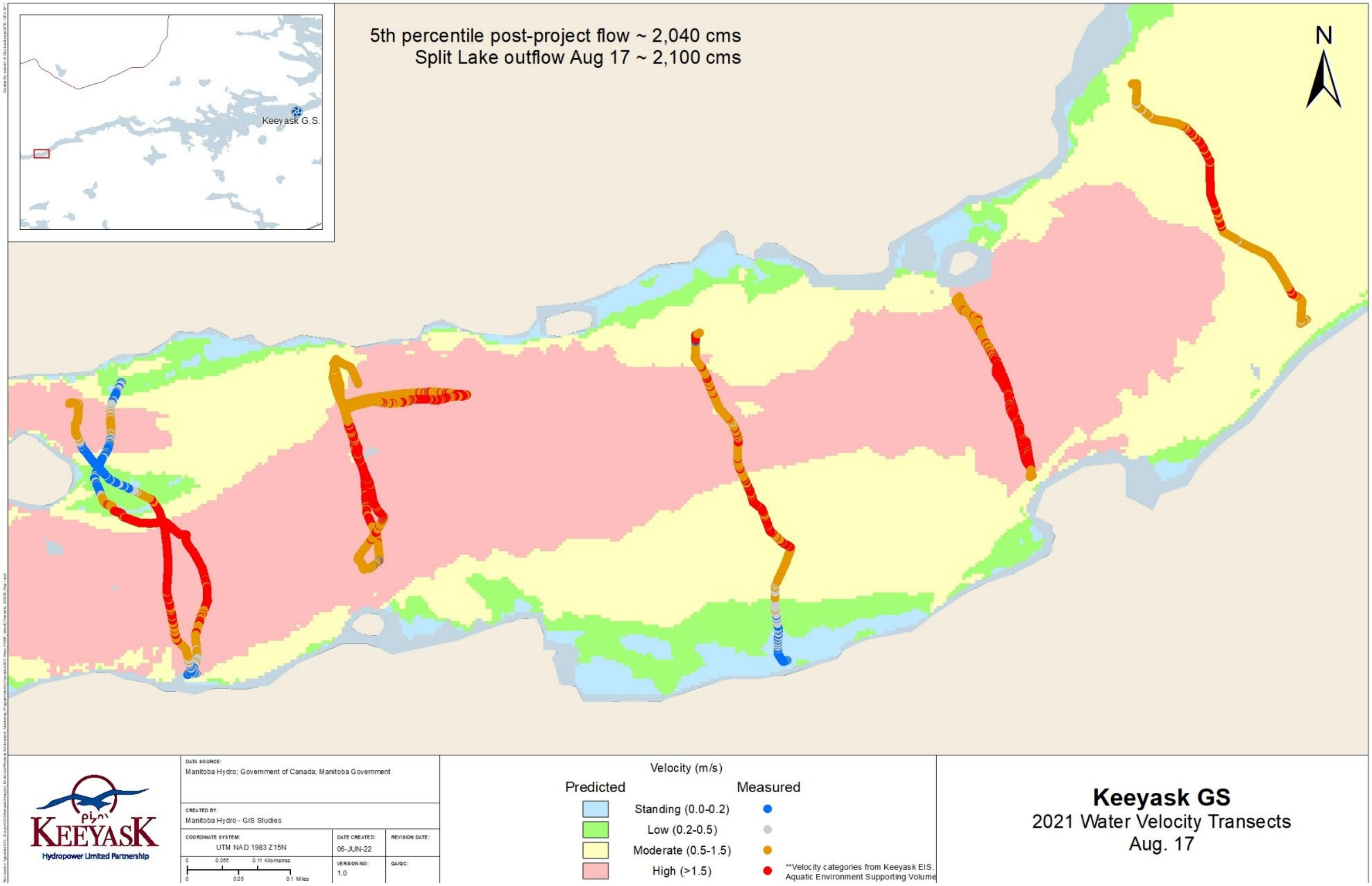

Figure 11: Velocity transects between Clark Lake and Birthday Rapids

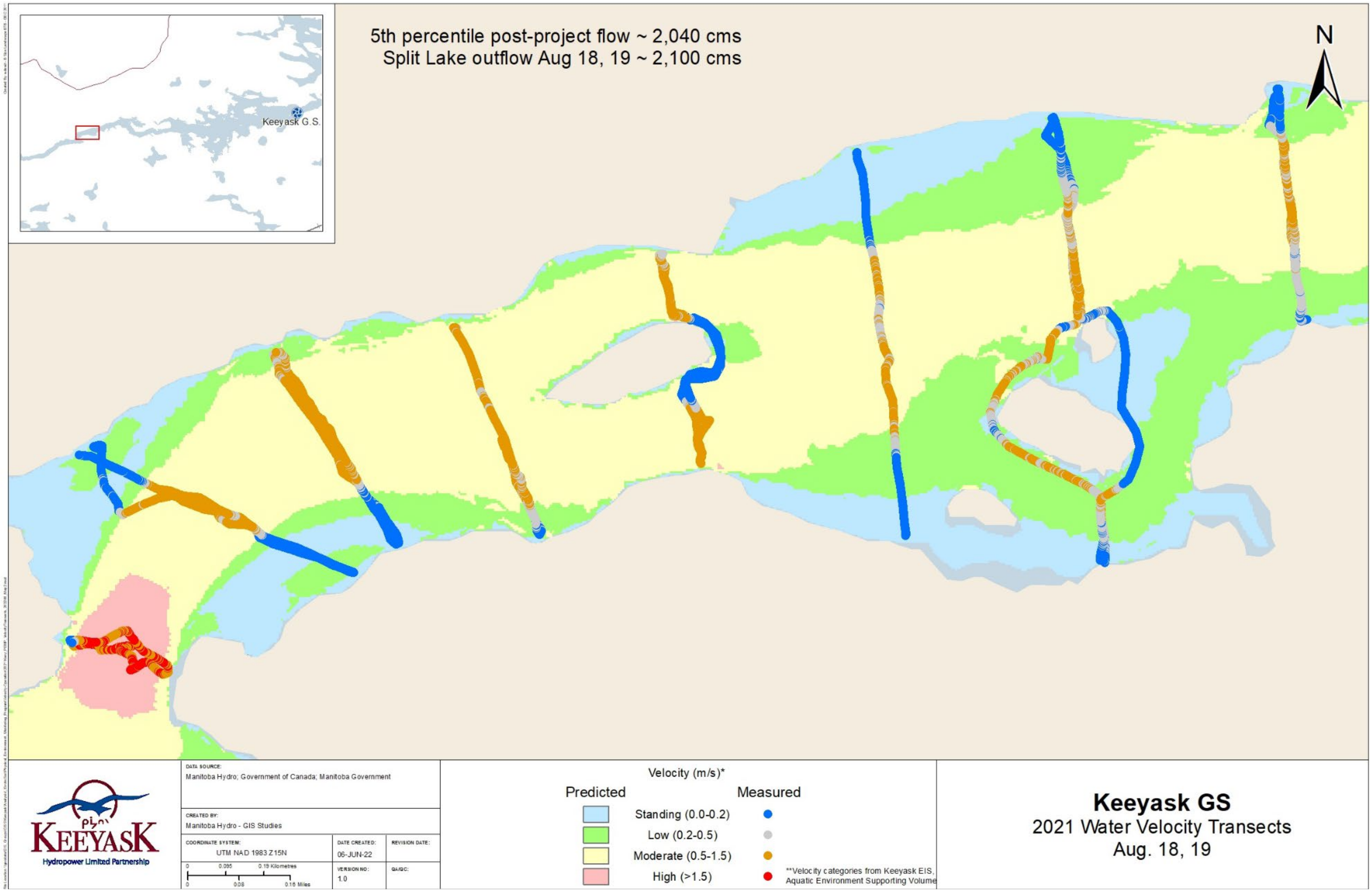

Figure 12: Velocity transects below Birthday Rapids

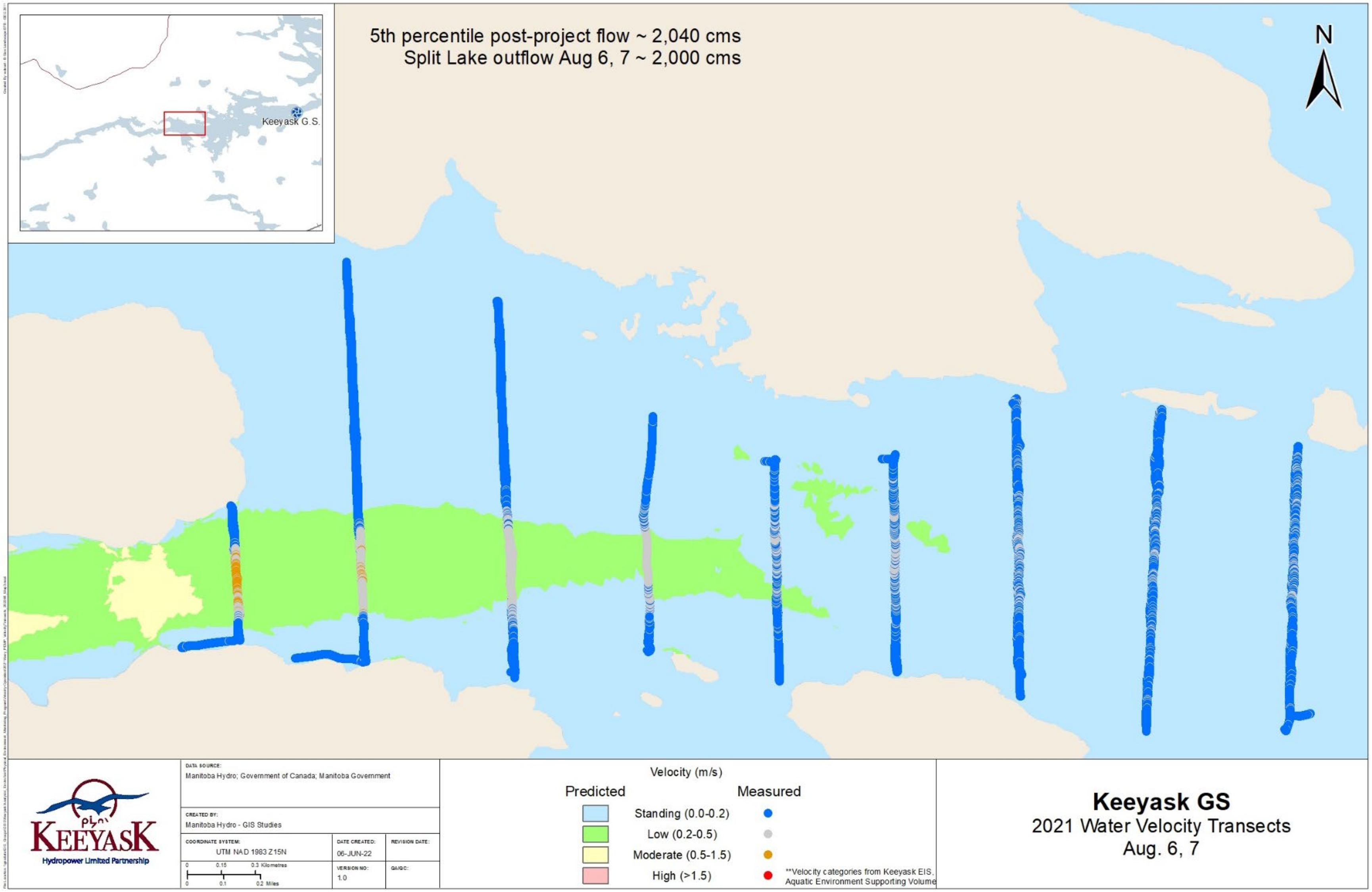

Figure 13: Velocity transects at entrance to Gull Lake

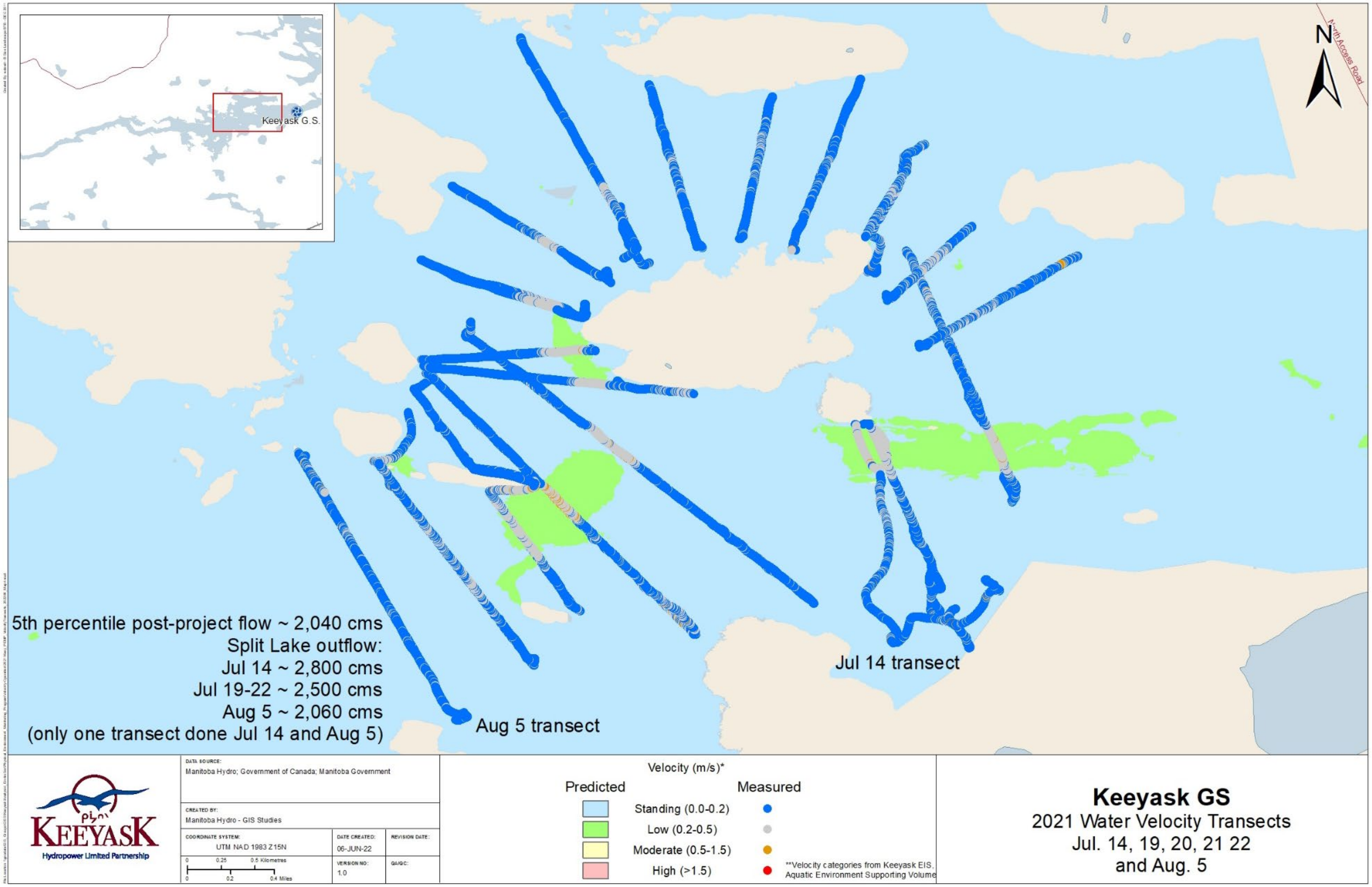

Figure 14: Velocity transects around Caribou Island

3.0 SHORELINE EROSION

Shoreline erosion monitoring during construction consists of mapping the shoreline position (edge of peat for peat shorelines, top-of-bluff for mineral banks) prior to full impoundment of the reservoir. In 2014 a high-resolution satellite imagery was collected at the start of the construction period. In 2019 another similar satellite image was collected to represent the conditions prior to impoundment that occurred in 2020, and another set of images was obtained in late summer 2021. The shorelines at the start and end of construction will be compared to see if any substantive shoreline erosion occurred during construction. Images collected after impoundment will be used to determine the actual extent of flooding and reservoir expansion over time.

4.0 SEDIMENTATION

Sedimentation monitoring includes monitoring the transport and deposition of sediment; the objectives of the sedimentation monitoring include:

- confirming sediment transport and deposition predictions; and
- supporting water quality and aquatic habitat monitoring components of the AEMP (KHLP 2015b).

The largest overall effects of the Project on sedimentation are predicted to occur after impoundment of the reservoir with the highest total sediment loading predicted to occur in the first year after impoundment. During the construction period prior to reservoir impoundment the PEMP sedimentation monitoring was generally done to collect data that will support conclusions of the effects of the Project on sediment transport and deposition after impoundment. Sediment monitoring under the *Sediment Management Plan for In-stream Construction* (KHLP 2014) was discontinued in 2021 as there were no longer any in-stream construction activities.

Sediment transport monitoring is done through the collection of discrete water samples, continuous turbidity monitoring and sediment traps at locations shown in Map 3 (detailed site maps are provided in Appendix 1). Discrete sampling involves the collection of water samples and in-situ measurements by field personnel at certain times (e.g., monthly) while continuous turbidity monitoring involves the installation of automated equipment that remains in place to take readings much more frequently. The continuous turbidity sites are periodically visited for maintenance checks; typically completed while discrete monitoring is performed. Sediment loading is estimated from the continuous turbidity data.

4.1 WINTER 2020-2021

In each annual report the winter sedimentation data is reported from the previous winter (i.e. one year delay) to allow time after the end of the field season for all data to be reviewed and analyzed before reporting. This report presents the 2020-21 winter sedimentation data.

4.1.1 CONTINUOUS AND DISCRETE TURBIDITY AND TSS

Winter monitoring in 2020-21 was conducted monthly at four continuous turbidity sites (Table 4), upstream of the Project area in Clark Lake, upstream and downstream ends of Gull Lake, and downstream of the Project in entrance to Stephens Lake (seep maps Appx. 1). Equipment was installed in January after suitable ice conditions developed at all the sites and was removed in early April before ice break up. The data collected at each of the monitoring sites was reviewed to identify and remove poor quality data from factors such ice, dead batteries, and equipment

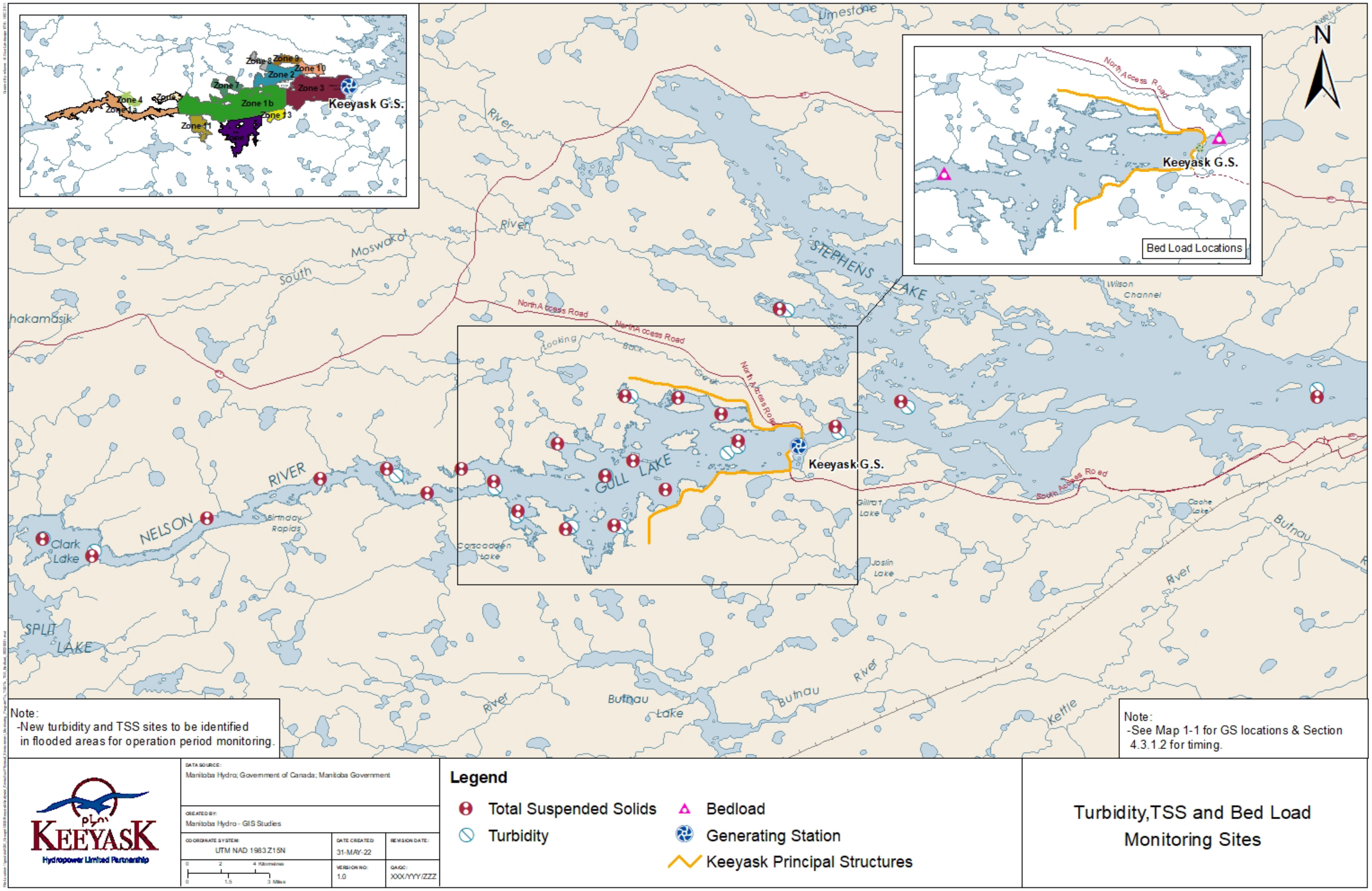

Map 3: Turbidity, total suspended solids and bed load monitoring sites

malfunction. The continuous data were also compared with the discrete readings obtained on each maintenance site visit and adjustments made for any sensor drift.

Turbidity levels were consistent between the four sites, starting out around 13 FNU in January and gradually decreasing to about 9 FNU in April, which is a typical pattern in winter seen in previous year (Figure 15). While TU at KE-4-b and KE-9 were virtually the same, TU was initially slightly lower at CL-2-b and slightly higher at STL-4, but generally within about 0.5-1 FNU of each other. After the end of February TU was essentially the same at the four sites. The range and average of the continuous turbidity in 2021 was similar to conditions in the previous five years during Keeyask construction.

Table 4: 2020-2021 winter continuous TU & discrete TSS monitoring locations

Site ID	Dates
CL-2-b (Clark Lake)	19-Jan-2021 to 8-Apr-2021
KE-4-b (Gull Lake upstream)	19-Jan-2021 to 7-Apr-2021
KE-4-b (Gull Lake downstream)	21-Jan-2021 to 7-Apr-2021
STL-4 (entrance to Stephens L)	21-Jan-2021 to 7-Apr-2021

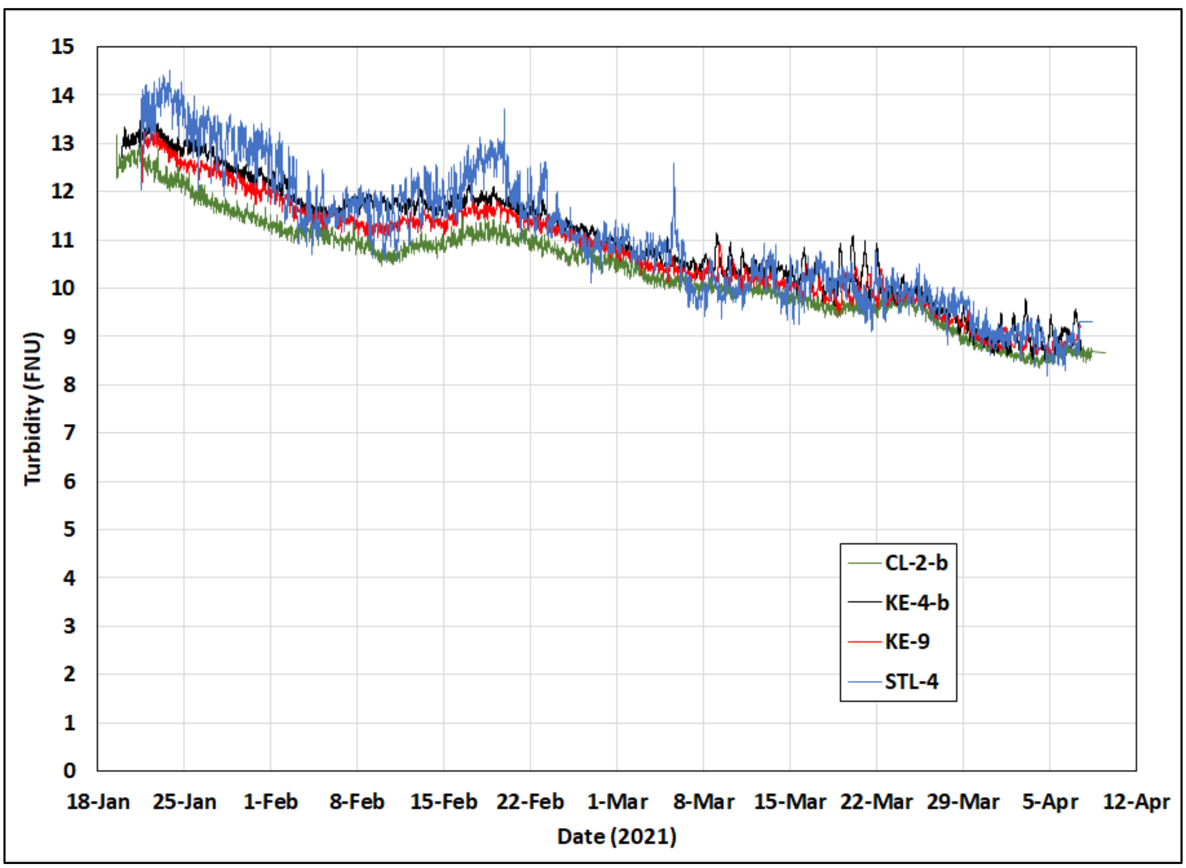

Figure 15: 2020-2021 winter continuous TU

The range and average of continuous turbidity was summarized and compared with continuous turbidity observed prior to and during construction (Figure 16). Turbidity levels in Stephens Lake downstream of the Keeyask GS were lower in 2021, the first year of operation, than observed prior to construction. This is consistent with the Keeyask EIS prediction that the Project would “significantly reduce erosion potential” downstream of the Project after construction which would result in lower turbidity downstream. Prior to the project a large hanging ice dam formed each winter at the entrance to Stephens Lake and would cause water levels to rise and flows to be redirected along erodible shorelines, which would add sediment to the river. With the Keeyask GS in operation, this hanging ice dam does not form, which mitigates the entrainment of sediment from eroding shorelines.

Discrete TSS and Turbidity data show consistent results with the continuous data (Figure 17). With the ice boom working to produce a stable ice cover upstream of the Project the downstream TSS and turbidity has dropped compared with pre-project conditions. Results from the first year of operation are similar to conditions observed in the previous 5 years during construction and average TSS was low at about 3 mg/l.

The 2020/21 monitoring period was the first winter after the Keeyask reservoir had been impounded in September 2020, resulting in the full extent of flooding in back bays upstream of the project. In addition to turbidity monitoring at the four mainstem sites (Figure 15), discrete monitoring was performed twice, once each in January and April, at 11 back bays upstream of the project and in a back bay on Stephens Lake that is unaffected by the project (Figure 18). Among all the sites, KE-Z9-1 had the lowest turbidity across its 4 sampling locations (a to d), ranging from about 2-5 FNU, while location KE-Z12-1-a also had similarly low turbidity levels. For the remaining locations, the January turbidity typically varied from about 9-13 FNU except for KE-Z8-1 and KE-Z8-2 which were low at 4-5 FNU. Turbidity averaged about 5 FNU lower in April than in January, ranging from about 6-8 FNU at all locations. This is consistent with the decline in turbidity over the course of winter that was observed from the continuous data.

At the back bay sampling sites, the four separate sampling locations (a-d, or 1-4 at site KE-Z8) are ordered with the first location (a or 1) furthest from the main channel and the last (d or 4) closest to the main channel. In the January 2021 round of monitoring many of the sites sampled had lower turbidity at the location furthest from the main channel and higher levels closer to the channel: for example, KE-Z10-1-d is about 2.5 FNU higher than KE-Z10-1-d. This likely results from sites closer to the mainstem being influenced more by the turbidity of the flow in the mainstem of the river. This effect is less prevalent in the April round of sampling when turbidity is less variable at the monitoring sites.

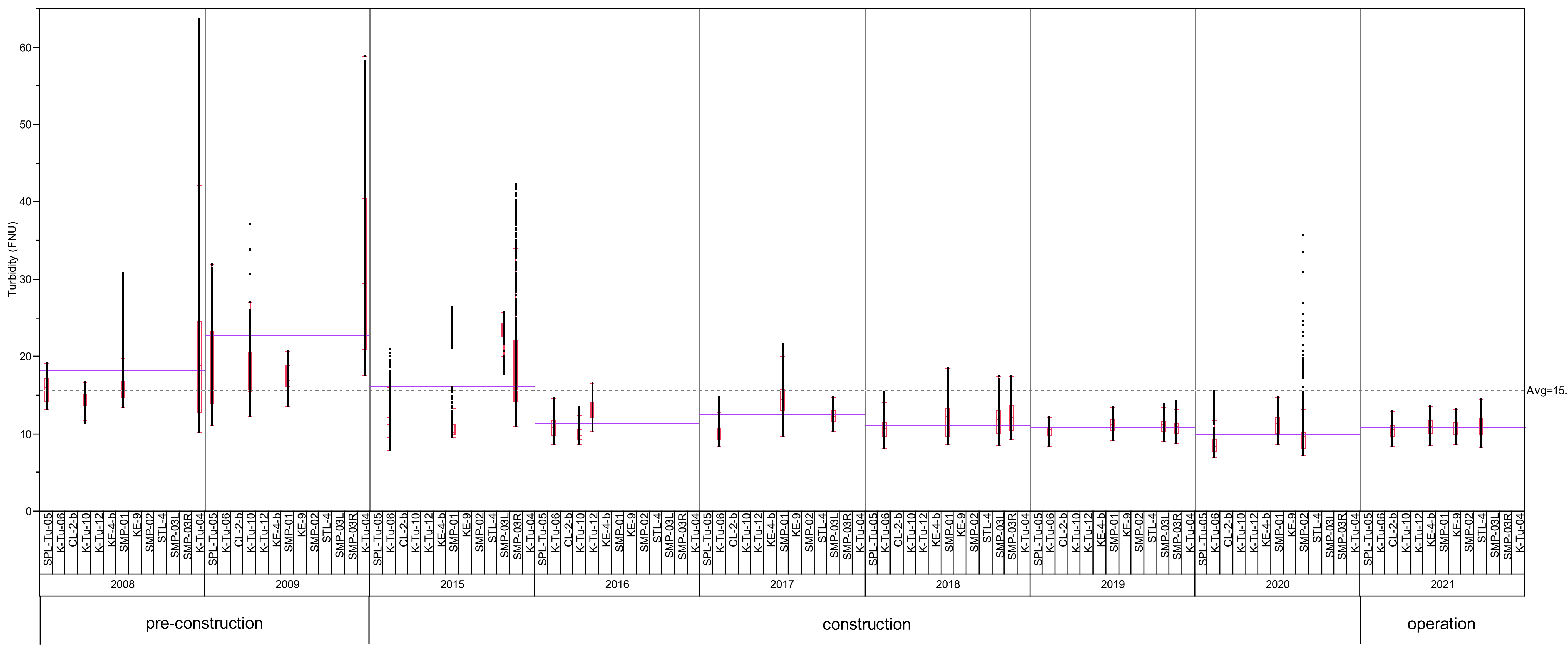

Figure 16: Summary of winter continuous TU

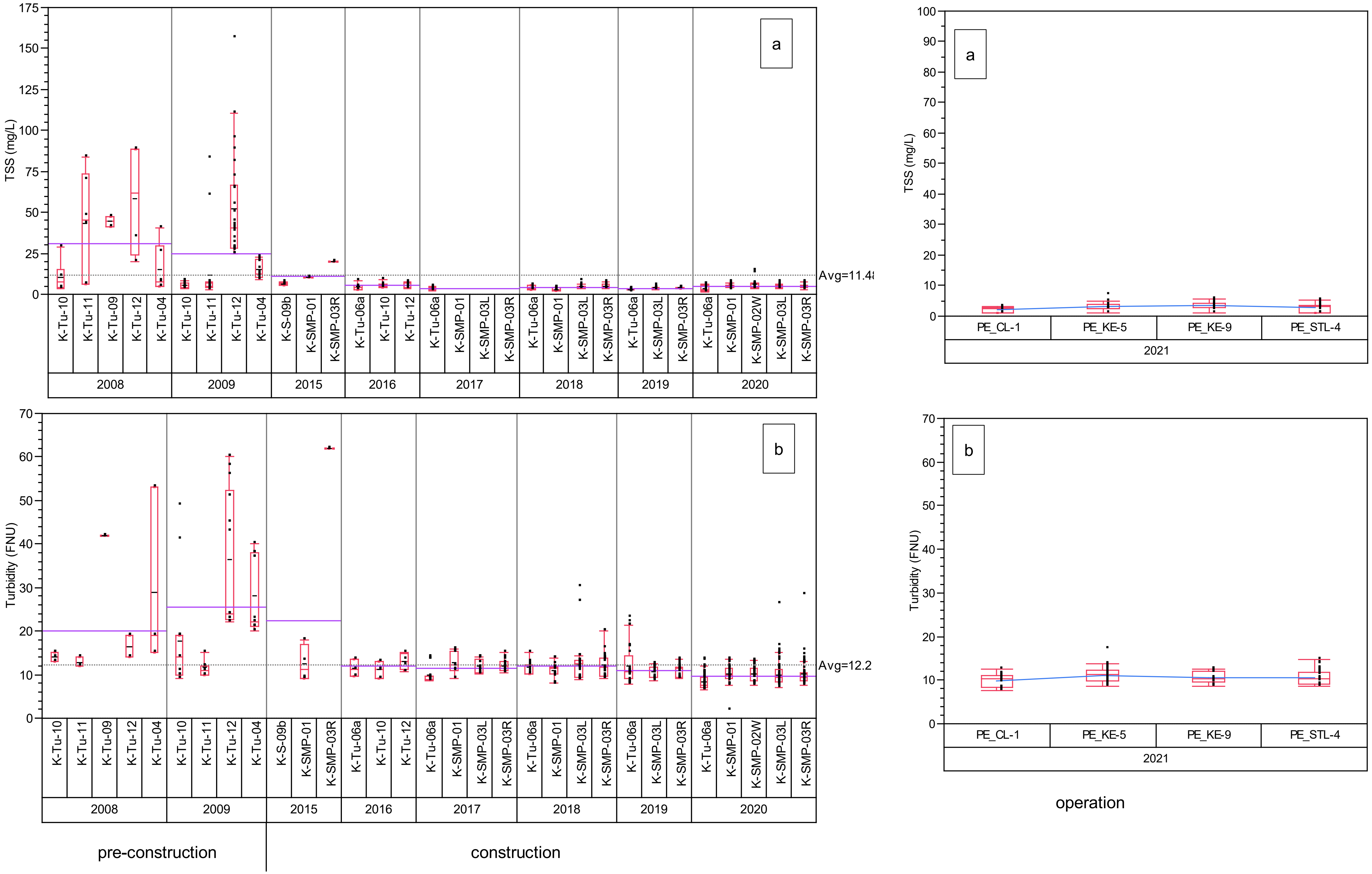

Figure 17: Summary of mainstem winter discrete TSS (a) and TU (b)

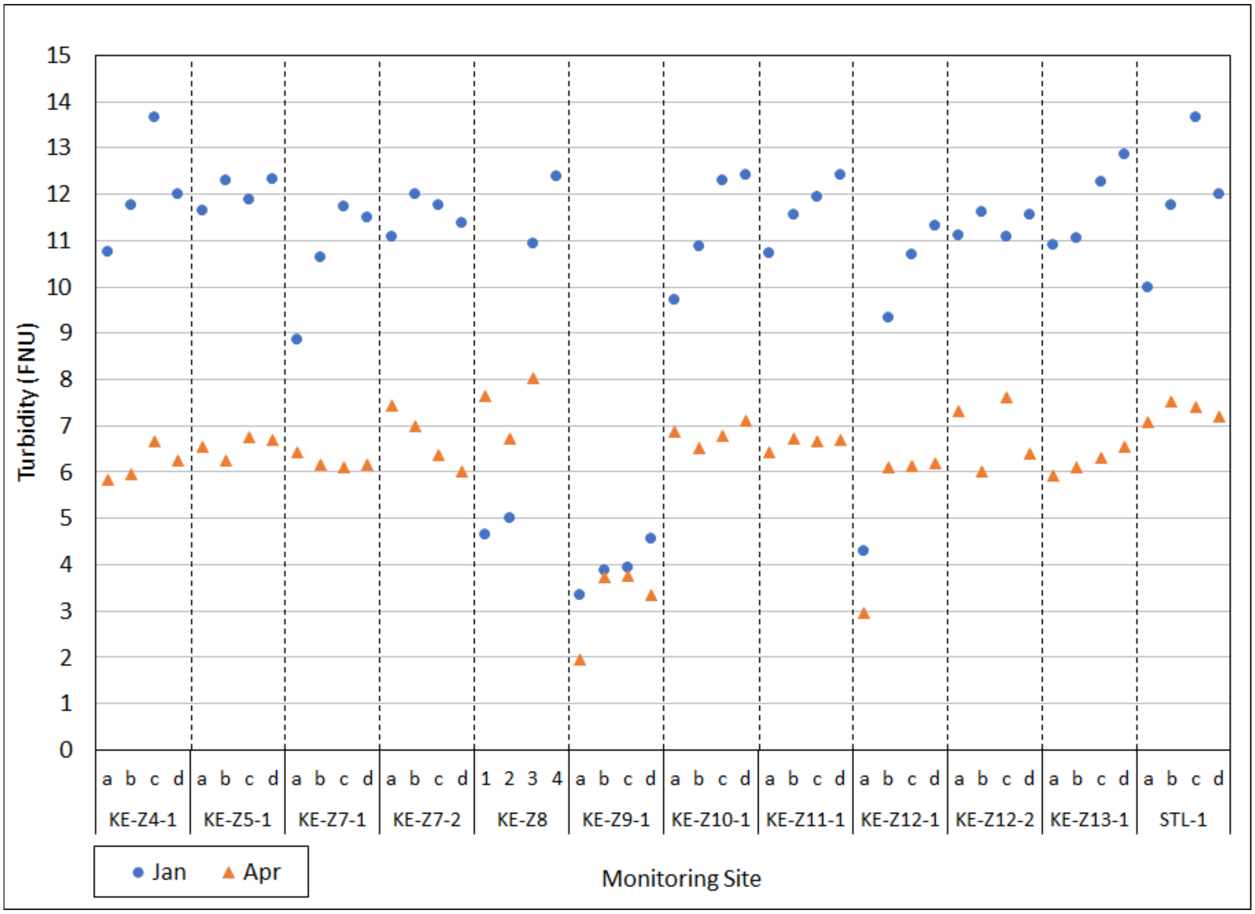

Figure 18: Discrete TU at back bay sites (winter 2020/21)

4.1.2 ESTIMATED SUSPENDED SEDIMENT LOAD

The winter suspended sediment loads (Figure 19) are estimated based on the average daily turbidity and discharge. Turbidity was converted to TSS concentrations using a Turbidity-TSS relationship developed for the Sediment Management Plan (KHLP 2014).

The estimated sediment load upstream of the area where the Project is expected to have effects (measured at SPL-Tu-05 on Split Lake and K-Tu-06 Clark Lake) indicates that the winter average was higher during the two pre-construction years than the winters monitored since construction started.

As noted above, a downstream reduction in turbidity has resulted in a reduced sediment load entering Stephens Lake from the pre-construction period and in 2014-15 when the ice boom failed. The average sediment load in winter 2020/21 is comparable to the loads observed in 3 of the last 4 years of construction.

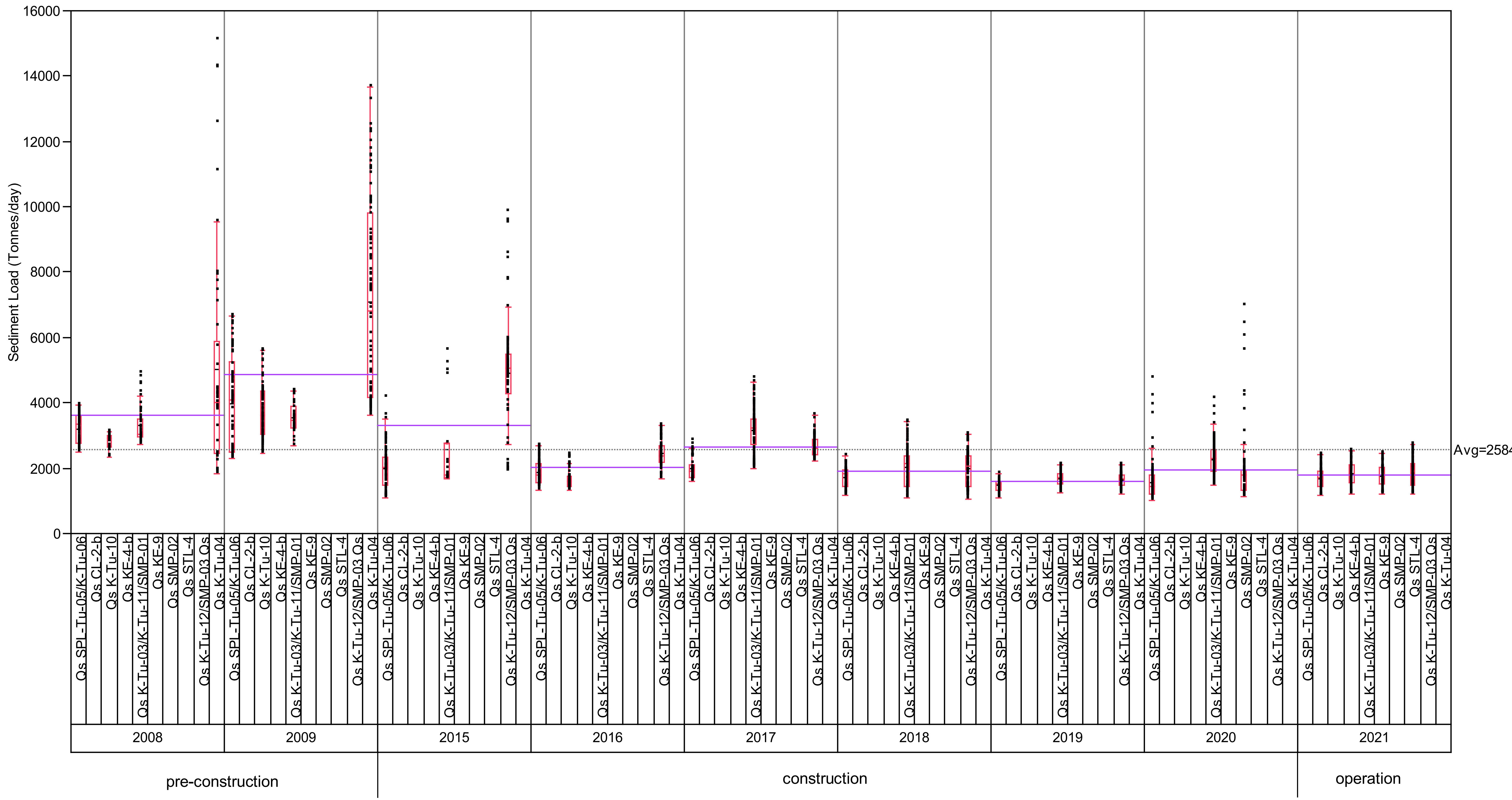

Figure 19:Summary of winter daily suspended sediment load

4.2 SUMMER 2021

The summer monitoring period extends from the time ice has melted and equipment can be safely placed in the water (typically in June) until equipment can be safely removed before winter conditions and freeze up starts (typically late September to early October).

4.2.1 CONTINUOUS TURBIDITY

Eleven continuous turbidity sites were monitored in summer 2021. This included 5 sites on the Nelson River mainstem between Clark Lake upstream of project effects to 30 km downstream of the Keeyask GS in Stephens Lake near Kettle GS, as well as 5 flooded back bays upstream of Keeyask and a bay on Stephens Lake (Table 5; location maps in Appendix 1).

The continuous turbidity monitoring stations consist of either a catamaran equipped for satellite data transmission (Photo 4) or a stand-alone buoy system requiring manual downloading of data. Both systems were equipped with a YSI multi-parameter sonde (6600 series) suspended two metres below the surface of the water.

Table 5: 2021 summer continuous turbidity monitoring locations

Site ID / Location	Dates
Mainstem Sites	
CL-2-b (Clark Lake)	Jul 21 – Sep 30
KE-4-b (entrance Gull Lake)	Jul 20 – Sep 27
KE-10-c (just upstream Keeyask GS)	Jul 20 – Sep 27
STL-2-d (entrance Stephens Lake)	Jul 22 – Sep 26
STL-5 (Stephens Lake near Kettle GS)	Jul 22 – Sep 26
Back Bay Sites	
KE-Z4-1-a	Jul 21 – Sep 30
KE-Z8-2	Jul 17 – Oct 1
KE-Z11-1-a	Jul 19 – Sep 27
KE-Z12-1-b	Jul 19 – Oct 4
KE-Z12-2-b	Jul 22 – Oct 4
STL-1-c (Stephens Lake)	Jul 23 – Sep 30

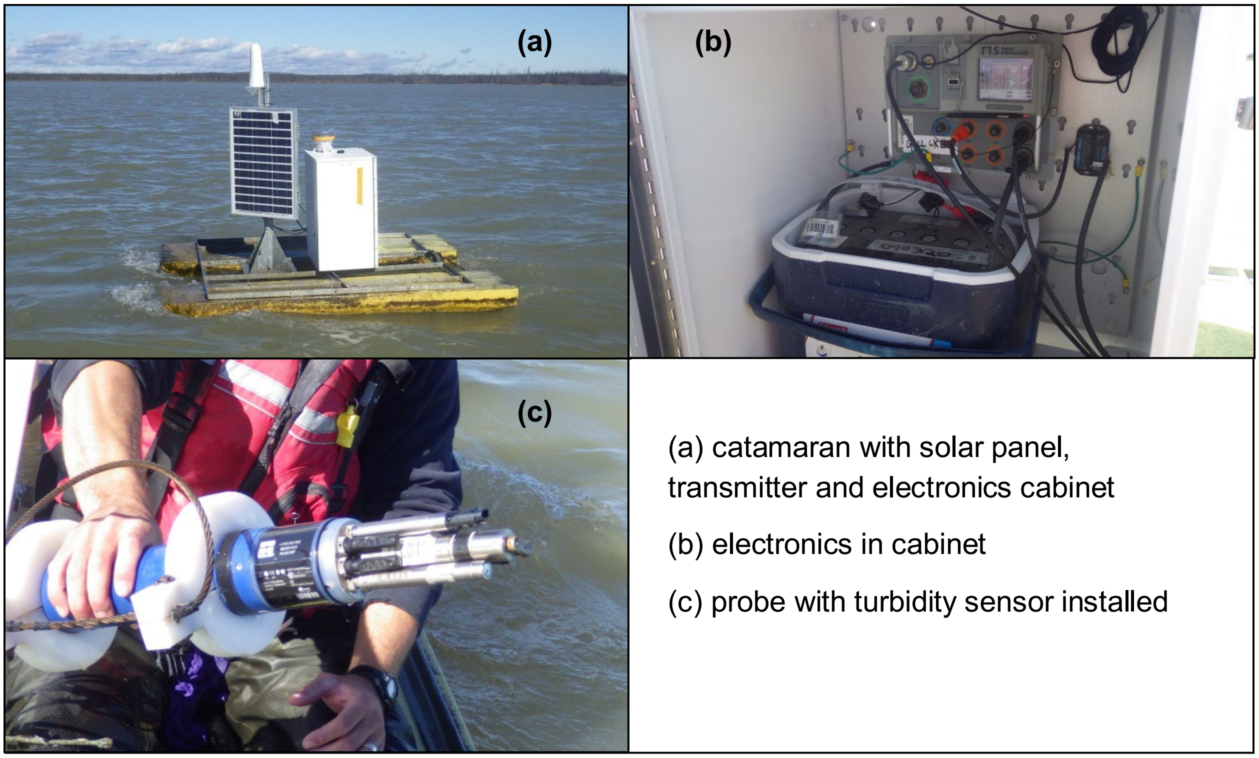

(a) catamaran with solar panel, transmitter and electronics cabinet

(b) electronics in cabinet

(c) probe with turbidity sensor installed

Photo 4: Continuous turbidity monitoring equipment

The data collected at each of the monitoring sites was reviewed to identify and remove poor quality data that may result due to factors such as algae growth and vegetation on probes, dead batteries, and equipment malfunction. The continuous data were also compared with the discrete readings obtained on each maintenance site visit and adjustments made for any sensor drift. As a result of the review, data from site KE-Z12-2-b has been excluded because the sensor produced inconsistent readings throughout the summer.

The turbidity at each of the 3 mainstem sites upstream of the Keeyask GS and STL-2-d just downstream followed each other closely, generally within about 1-2 FNU (Figure 20). Site STL-5 near Kettle GS followed the same general trend but was typically 1-2 FNU lower than the other sites, which is consistent with past observations that turbidity (and suspended sediment) and generally deceases in Stephens Lake. It is interesting to note several short duration turbidity increases of about 2 mg/l at site CL-2-b are followed closely by corresponding peaks at KE-4-b (~10-12 hr delay). These show an increase in turbidity from Split Lake (likely due to wind) moving downstream to Keeyask. There are some corresponding peaks at KE-10-c and STL-2 but not necessarily as large suggesting some attenuation of turbidity as flow passes through the reservoir.

With summer 2021 being the first year of Keeyask operation (i.e., after impoundment) under open water conditions, additional continuous turbidity monitoring was conducted in 5 back bay locations forming part of the Keeyask reservoir, plus one site downstream on Stephens Lake, which forms the Kettle GS reservoir. As noted above, continuous turbidity data for site KE-Z12-2-b was omitted from consideration, so results were only plotted for 5 of the six back bay sites (Figure 21). Each site has a good record over the entire summer except site KE-Z11-1-a, which has a gap of about

2 months due to poor quality data. For sites upstream of Keeyask, turbidity levels are typically less than 8 FNU (~90% of readings) except at KE-Z11-1-a where about 50% it is about 50%, but this is a truncated data set. Turbidity at these Keeyask back bay sites was markedly lower than at sites in the mainstem where it typically exceeded 10 mg/l (Figure 20). Turbidity in the Stephens Lake back bay (STL-1-c) was markedly higher than both the Keeyask back bay sites and the mainstem sites (Figure 21). Turbidity in this back bay exceeded 20 FNU most of the time, was between 30-40 FNU for some extended periods and peaked to almost 60 FNU. Conditions at this site are consistent with satellite imagery that shows the west side of the north basin of Stephens Lake can have much less clarity (i.e., higher turbidity) than other areas within and upstream of the lake.

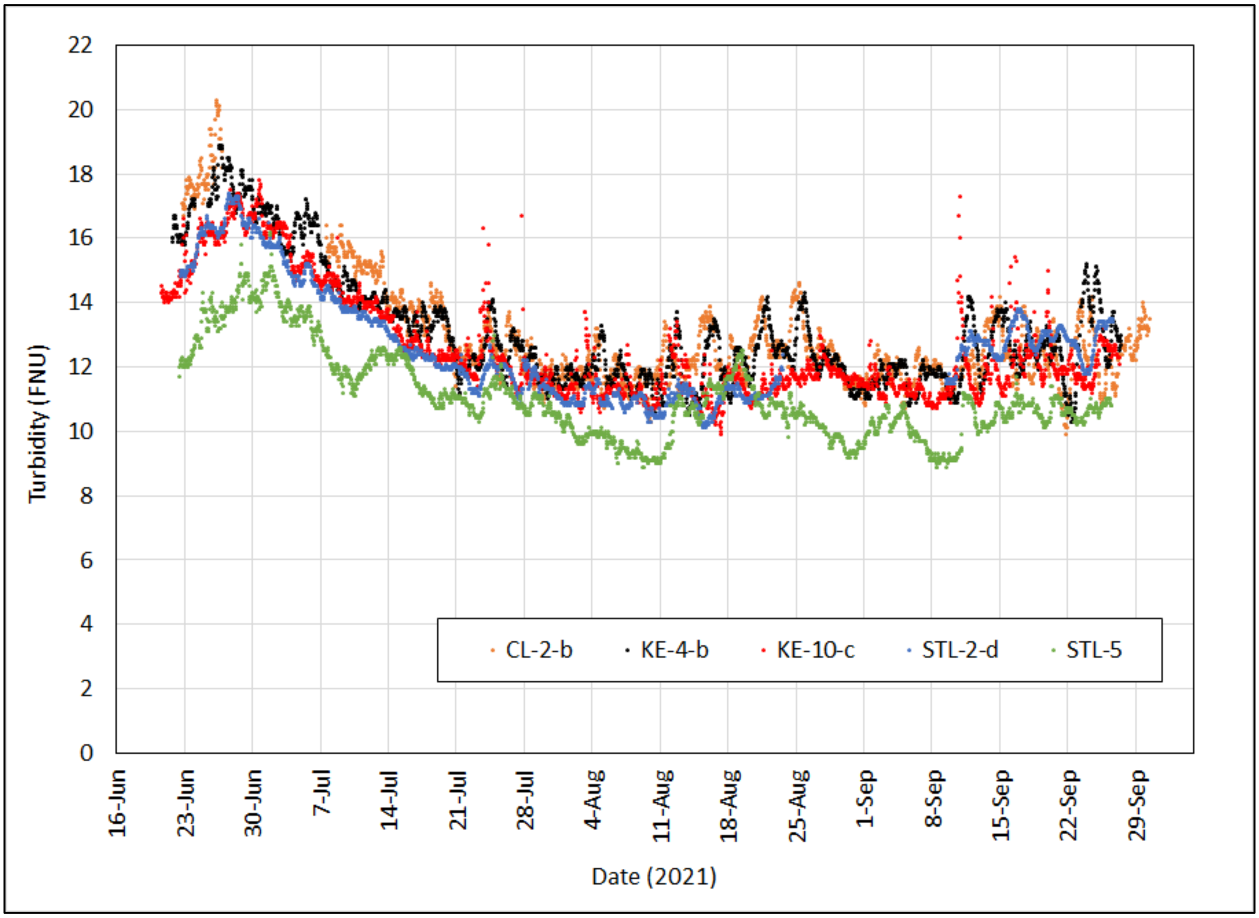

Figure 20: 2021 summer continuous TU – mainstem sites

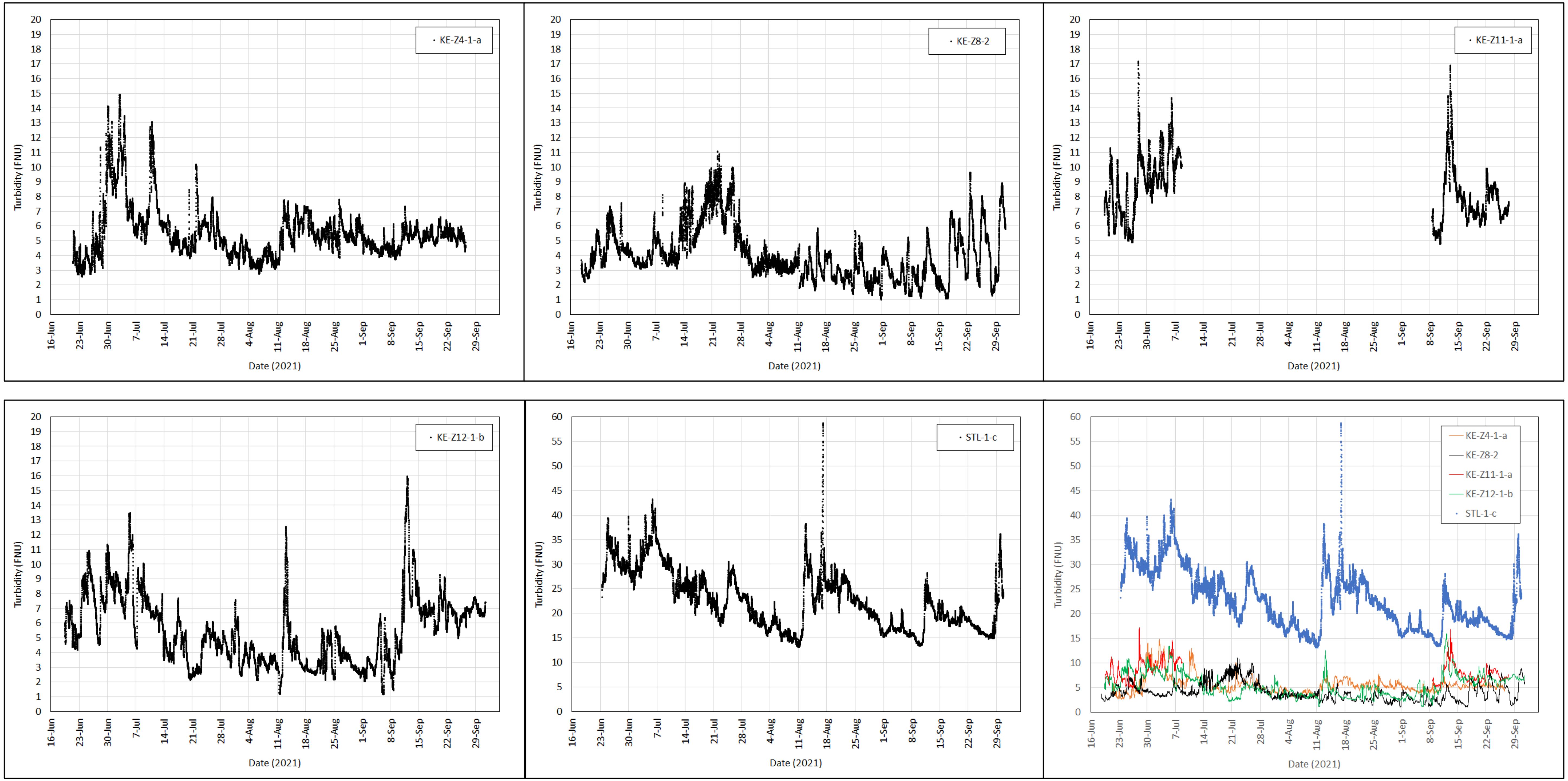

Figure 21: 2021 summer continuous TU – back bay sites

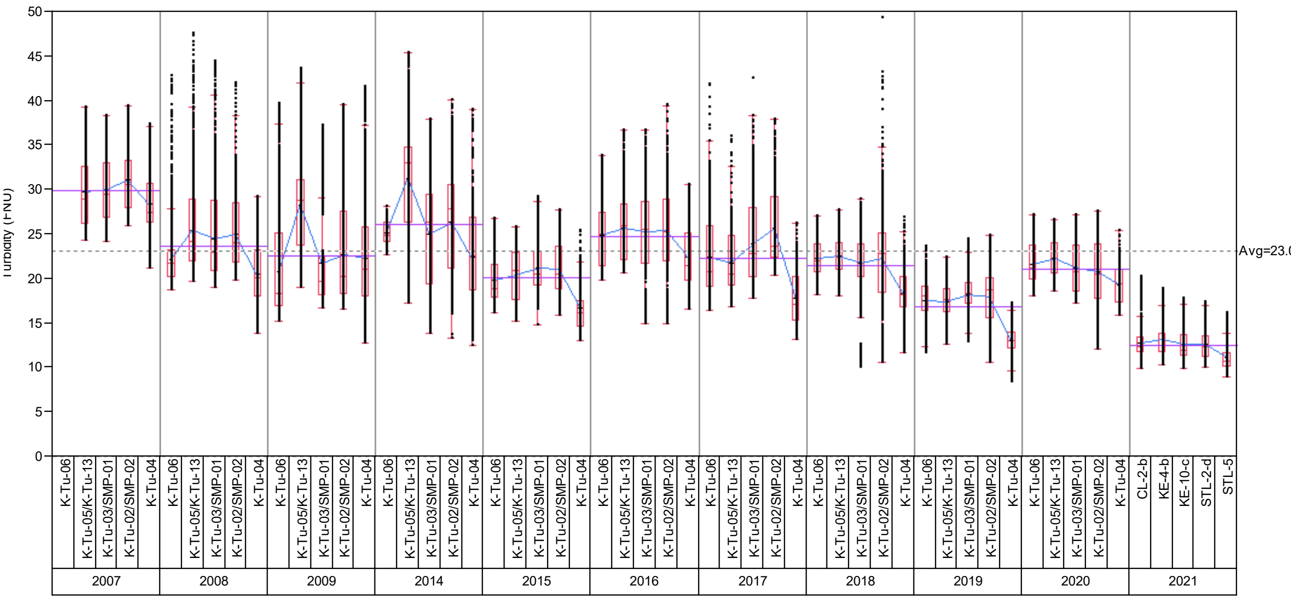

Figure 22: Summary of annual summer continuous TU

4.2.2 DISCRETE TOTAL SUSPENDED SEDIMENT AND TURBIDITY

During the summer period, site visits were performed at both the discrete monitoring sites and at the continuous turbidity sites between Clark Lake and a site in Stephens Lake just upstream of Kettle GS, about 30 km downstream of Keeyask GS (see maps in Appendix 1). Visits were performed to obtain water samples for total suspended sediment (TSS) and in-situ turbidity (TU) readings. The sites were visited 4 times, approximately monthly in June, July, August and September/October, typically coinciding with the scheduled monthly maintenance visits at the continuous turbidity sites. Discrete water samples were collected from 38 locations across 11 monitoring sites (1-6 locations sampled per site) along the mainstem and at 12 locations at 12 back bay sites. Two water samples for TSS testing were typically collected at each location at 20% & 80% of site depth. Turbidity measurements were obtained at each of the mainstem water sampling sites and at 48 locations across the 12 back bay sites (4 locations at each site). Turbidity was measured at multiple depths at the monitoring locations. The discrete readings are used to verify the continuous readings, confirm readings throughout the entire depth of the site and correlate TSS and TU. Monitoring results were reviewed for vertical variation at the sites but, since values did not have notable vertical variation, the results were summarized considering depth averaged values.

The 2021 TSS concentrations (Figure 23) generally ranged between 1 and 8 mg/L at mainstem sites and 1-6 mg/l at back bay locations excluding site STL-1. Note that the TSS laboratory detection limit is 2 mg/l and any reported results below 2 mg/l were assumed to be 1 mg/l for reporting purposes (i.e., half the detection limit): therefore, an average TSS less than 2 mg/l indicates it includes results below the detection limit. TSS was higher at mainstem sites in June and July than in August and September/October, varying from 4-6 mg/l and 1-3 mg/l respectively at mainstem sites and about 3-6 mg/l and 1-4 mg/l at back bay sites. Results from the STL-1 back bay site in Stephens were similar to the other sites in June and August at 6 mg/l and 3 mg/l respectively (Figure 23) but the July and September results were significantly higher at about 29 mg/l and 13 mg/l respectively. The results do not suggest a consistent pattern of TSS change from the upstream (CL-2) to either the site near the Keeyask GS (KE-10) or Kettle GS (STL-5): neither increasing due to sediment from erosion in the Keeyask reservoir nor decreasing due to deposition as flow passes through the reservoir.

Summer 2021 average TSS at the mainstem sites was compared with average concentrations observed previously at sites along the mainstem both prior to and during Keeyask construction (Figure 24). In both previous periods the average concentration each year varied from about 10-20 mg/l. The overall average prior to construction (2005-2010) was about 15 mg/l while the average during construction (2014-2020) was about 13 mg/l. The average in 2021 was significantly lower at approximately 4 mg/l. The Keeyask EIS (KHLP 2014b) predicted that TSS would decrease about 2-5 mg/l relative to pre-project conditions, but 2021 results indicate the concentrations in the first year of operation were more than about 10 mg/l lower than observed prior to the project.

Turbidity monitoring shows a marked difference between mainstem and back bay sampling sites, except site STL-1 which has much higher turbidity than other back bay sites, which is consistent with the TSS results (Figure 25). Generally, turbidity was higher in June and July and lower in August and September/October. Turbidity was higher at the mainstem, ranging from about 10-19 FNU, with August values being lowest from about 10-12 FNU and July being highest at about 15-19 FNU. Back bay site KE-Z9-1 (locations a to d) had lower TU than all other sites, varying from 1-4 FNU for all four sampling periods. This area is the former Little Gull Lake and is more isolated from the main flow than other back bays. At the other Keeyask back bays, TU generally ranged from about 3-15 FNU, with August being lower at about 3-10 FNU and July higher from 6-15 FNU.

As noted for the continuous TU results, STL-1, and other back bays on the west side of Stephens Lake have been observed to have high levels of turbidity due to suspended sediment so it is not unexpected that some high discrete TU an TSS values would be observed for this site. Remote sensing data from Sentinel 2 satellite imagery was used to estimate TSS in the study area from Clark Lake to Stephens Lake. The results highlight the spatial variation of TSS between areas upstream of Keeyask and the west side of Stephens Lake (Figure 26). Images from June 14, August 31 and October 7, 2021, show higher levels of turbidity along the west side of Stephens Lake north of Keeyask GS as compared with areas upstream of the GS. For example, green areas on June 14 indicate TSS near STL-1 may have been up to 50-60 mg/l while upstream of Keeyask the mainstem was around 10 mg/l or less (light blue) and back bay areas may have been 5 mg/l or less (white). Generally, the high TSS on Stephens Lake is due to wind effects, particularly strong north and east winds. The variability observed in the satellite imagery is consistent with discrete TU and TSS observations.

The back bay sampling locations are labeled in order with the ‘a’ locations (or 1 for site KE-Z8) being deeper in the bay, further from the main stem flow, while locations b, c and d (or 2, 3, 4 for

KE-Z8) are progressively nearer the mainstem. It is interesting to note that for almost each site in each month of sampling, turbidity is lowest at the ‘a’ (or 1) location furthest from the mainstem and incrementally increases to the ‘d’ location closest to the mainstem (Figure 25). This may indicate a diminishing influence of mixing from the mainstem flow into the further reaches of the back bays. Note this pattern is not observed for site KE-Z9-1 due to its relative isolation from the main body of the reservoir. This pattern is also consistent with the spatial variability observed in the satellite imagery (Figure 26).

As observed with TSS results, the average mainstem TU for the summer 2021 operating period was significantly lower than observed before and during construction. At approximately 14 FNU, summer 2021 was almost half the preconstruction summer average of 26 FNU and a third lower than the 22 FNU average during construction.

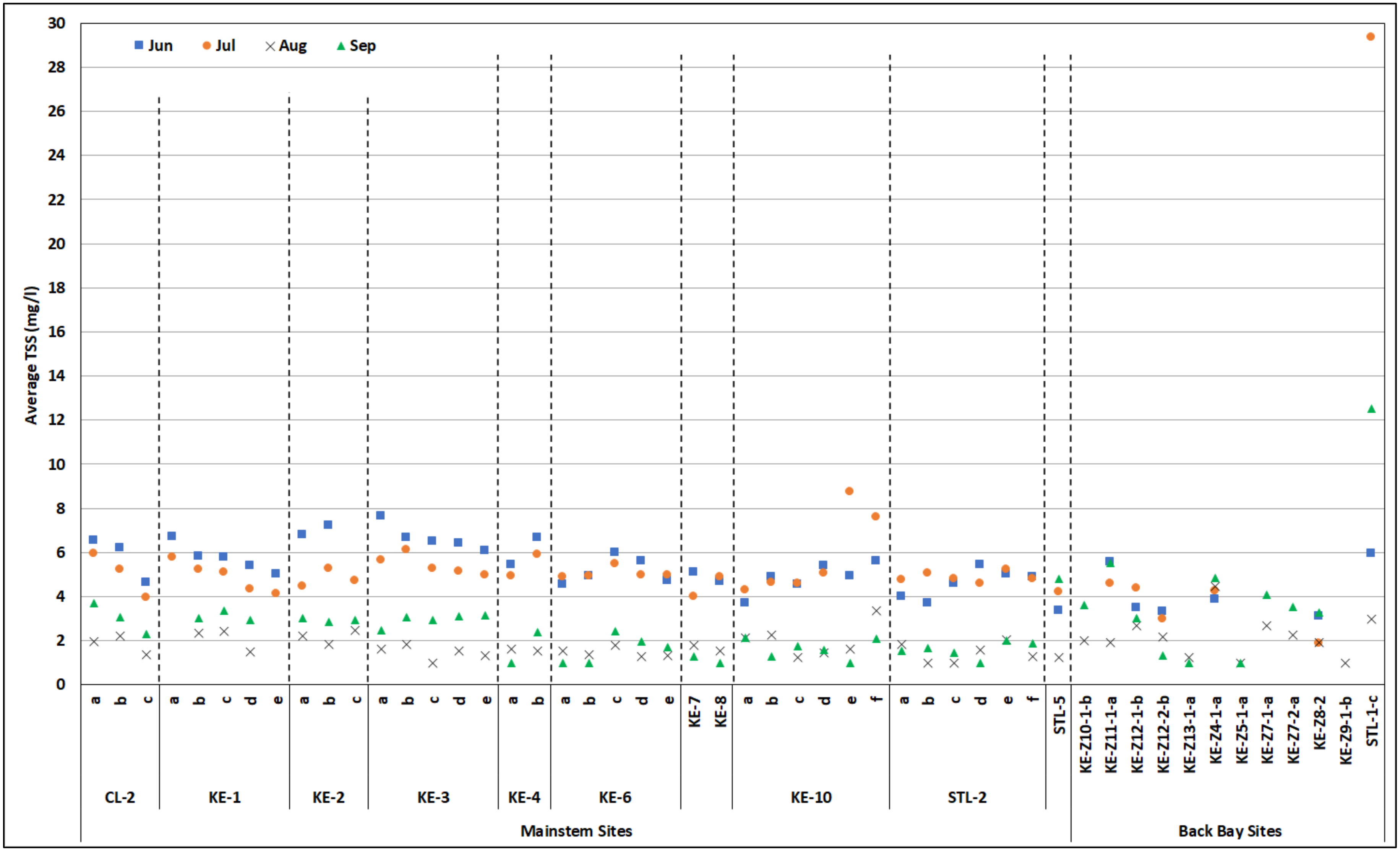

Figure 23: 2021 summer TSS

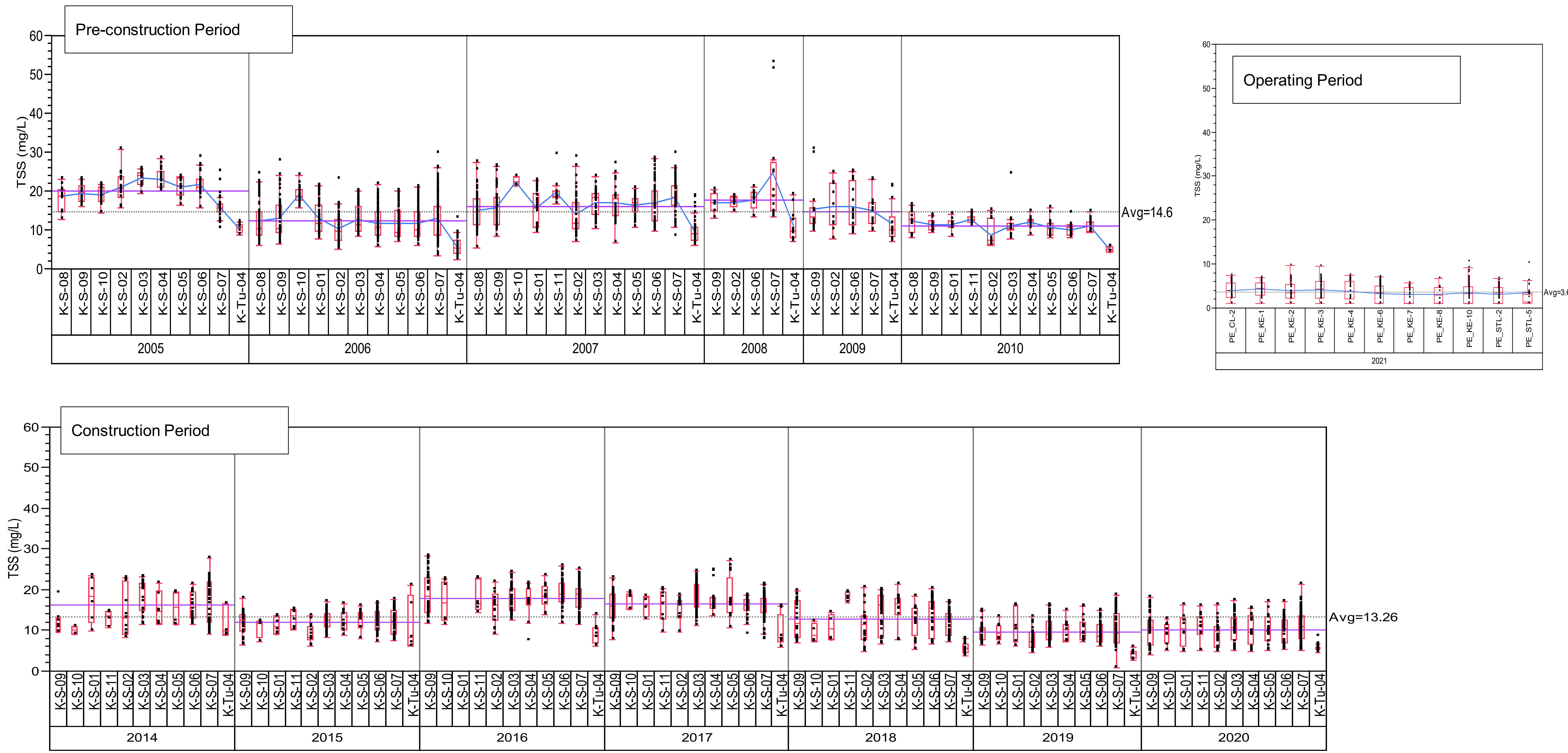

Figure 24: Summary of annual summer discrete TSS at mainstem sites (2005-2021)

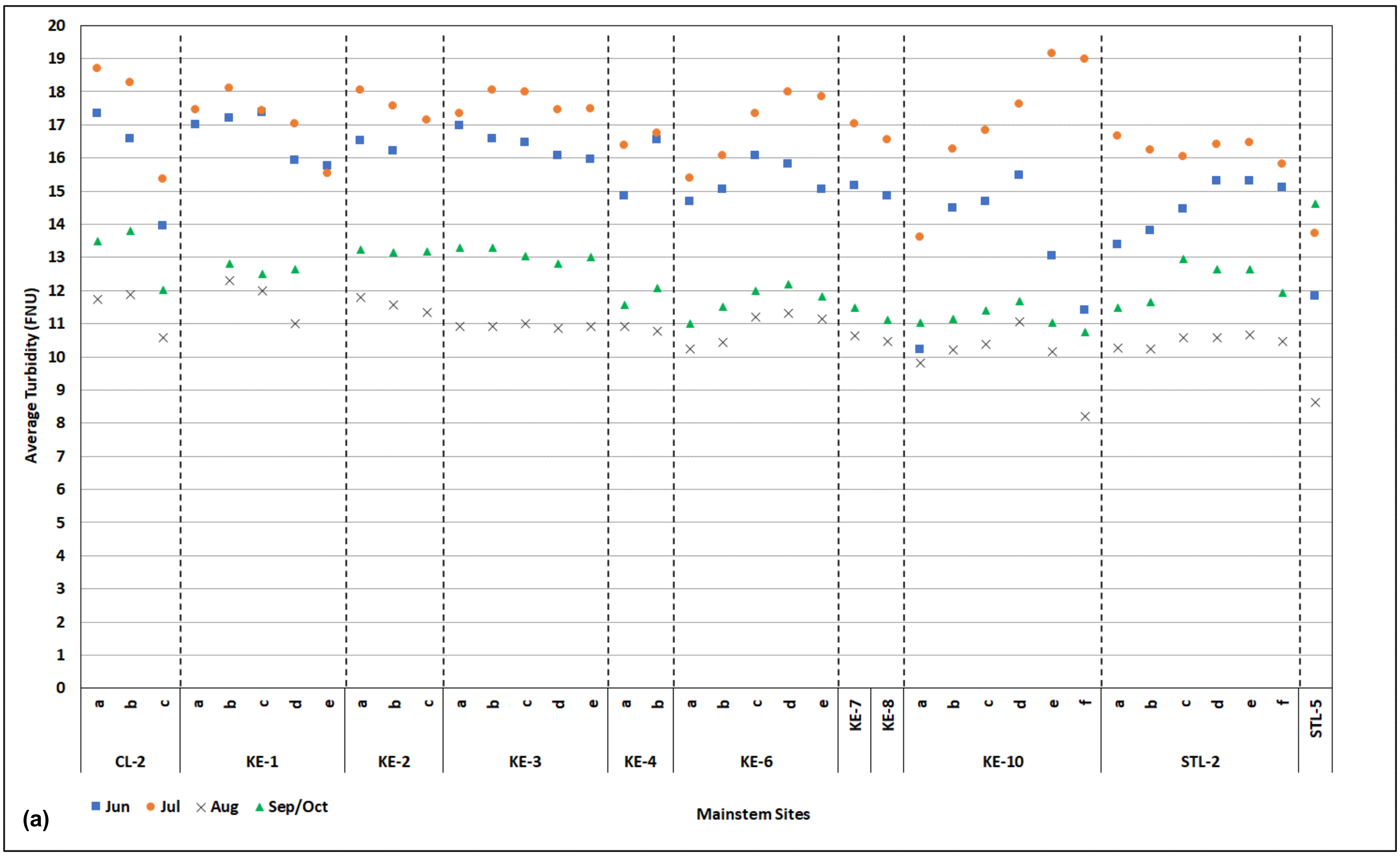

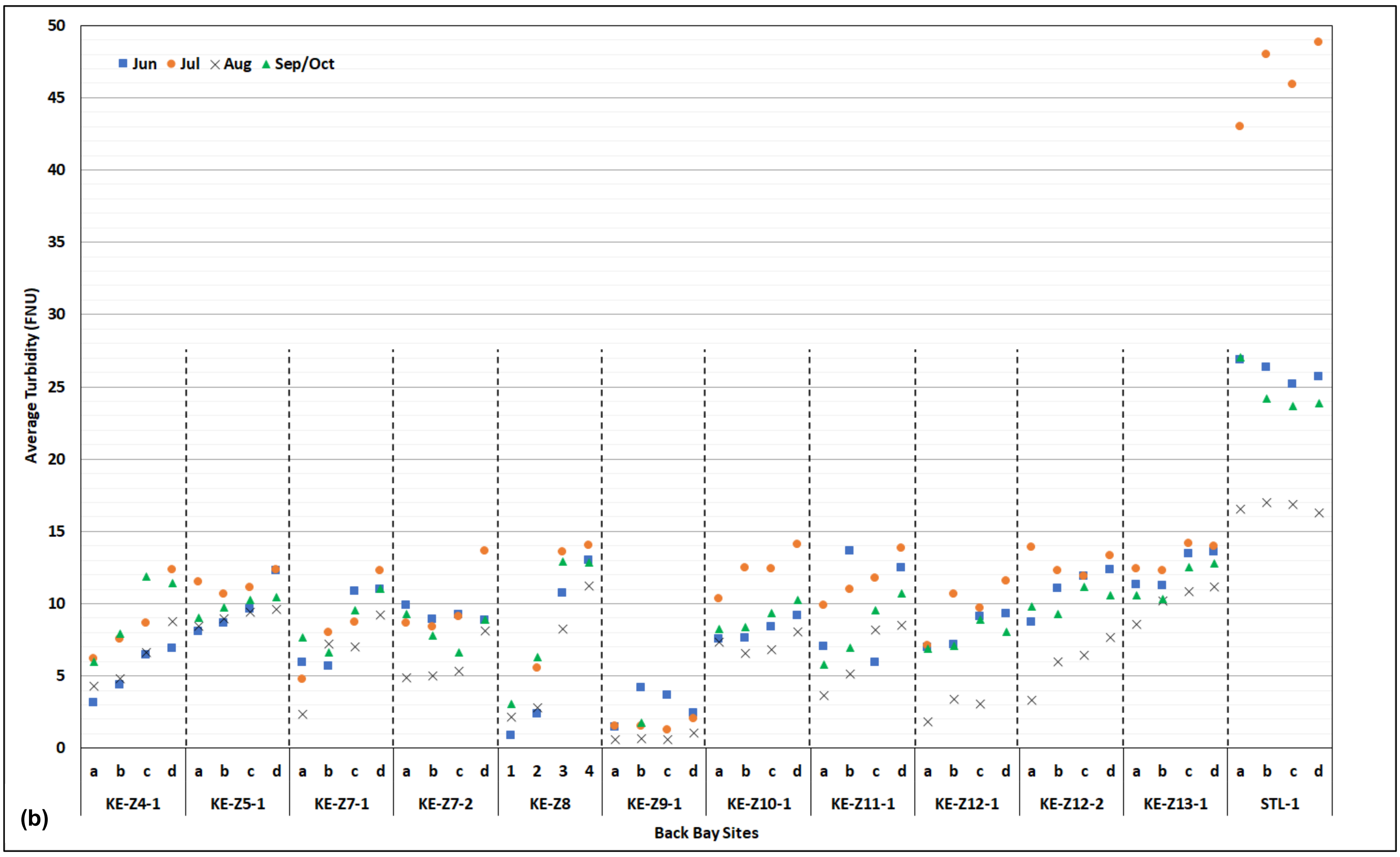

Figure 25: 2021 summer continuous TU at (a) mainstem sites, (b) back bay sites

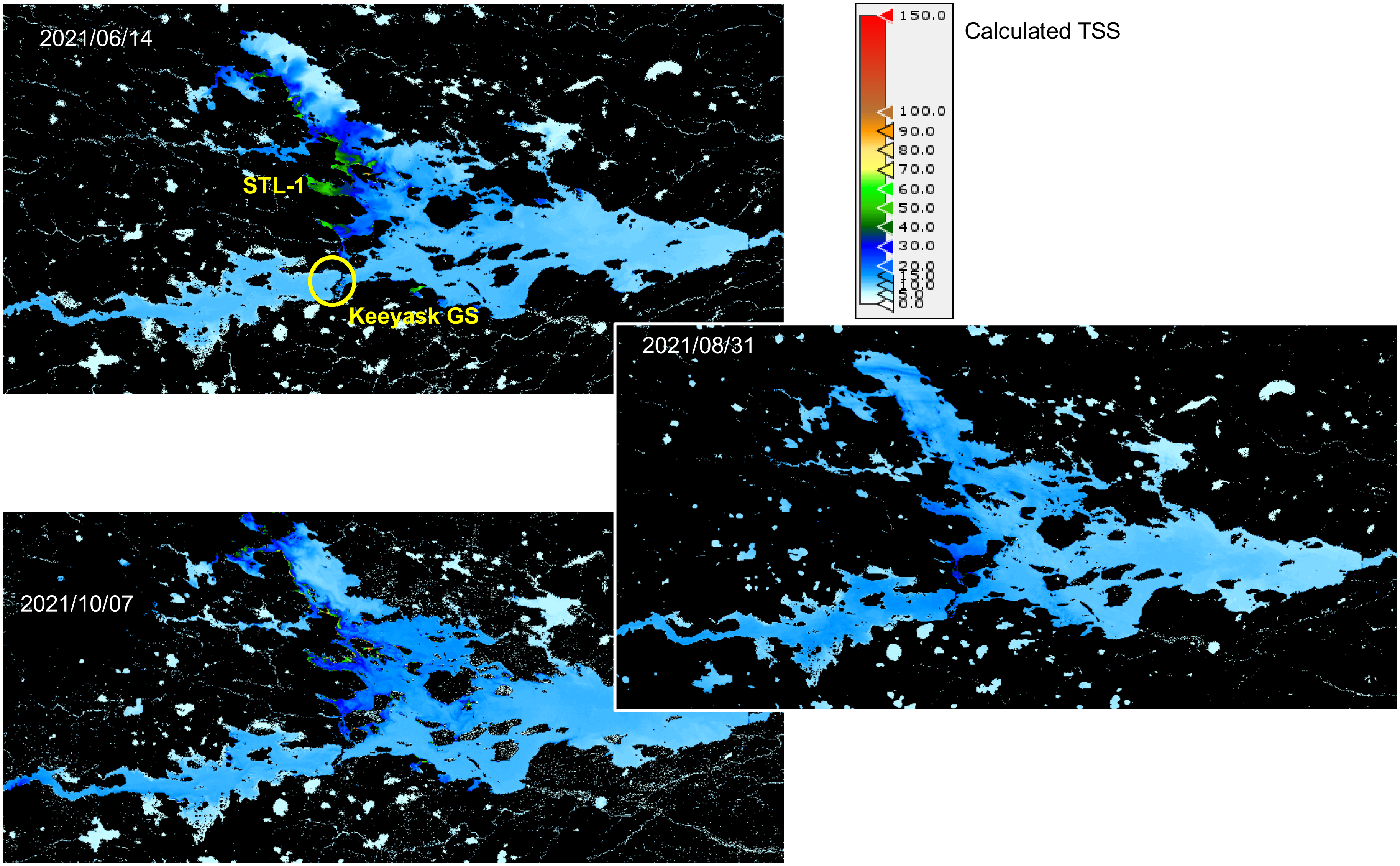

Figure 26: Spatial variation of TSS calculated from Sentinel 2 satellite data

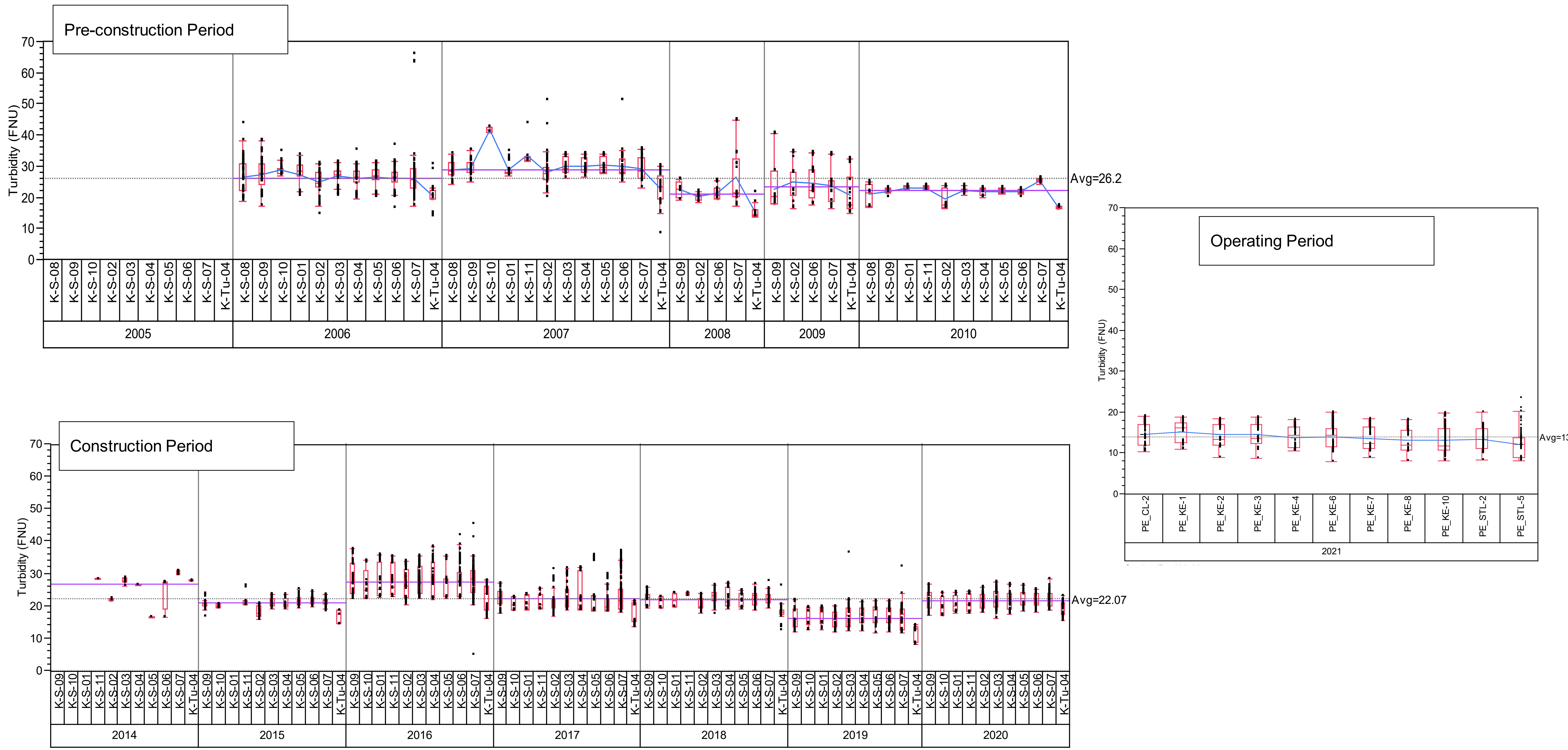

Figure 27: Summary of annual summer discrete TU at mainstem sites (2005-2021)

4.2.3 ESTIMATED SUSPENDED SEDIMENT LOAD

The summer suspended sediment loads (Figure 28) are estimated based on the average daily turbidity and Keeyask inflow discharge. Turbidity was converted to TSS concentrations using a Turbidity-TSS relationship developed for the Sediment Monitoring Program for Instream Construction (SMP; KHLP 2014).

The 2021 average summer suspended sediment load was approximately 1,500 tonnnes/day, which is roughly half the lowest sediment previously observed in 2019, and much lower than other years that have ranged up to approximately 7,000-8,500 tonnes/day. This result is not surprising given the low flow conditions that occurred in 2021 combined with the lowest TSS concentrations observed since 2005. The 2021 results indicate small decrease in sediment load through Stephens Lake, which has been observed in the past.

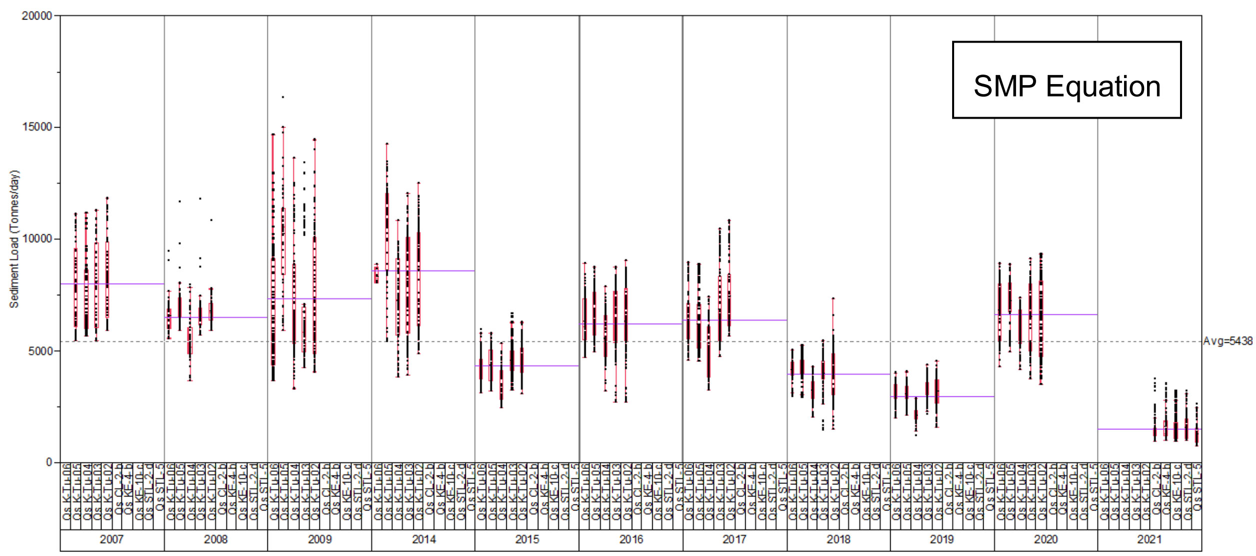

Figure 28: Summary of summer daily sediment load

4.2.4 DEPOSITION

Sediment traps with two vertical tubes (Photo 5) were installed in Gull Lake and Stephens Lake to monitor the sediment accumulation rate over the 2020/21 winter and the 2021 summer periods. One tube is a settling trap that is open at the top and the second tube is a flow through trap that has holes in the side to allow water and sediment to flow into it. Sediment trap data were still under quality review at the time of reporting.

Photo 5: Sediment traps - 2 tube design

5.0 ORGANIC CARBON

5.1 PREDICTED PROJECT EFFECTS ON ORGANIC CARBON

Organic carbon (total, dissolved and particulate) in the water was not expected to be affected by construction prior to impoundment of the reservoir but was measured during construction to provide baseline data. Although changes to organic carbon were not specifically predicted, the Keeyask EIS did estimate the potential increase in organic sediment concentration (i.e. peat, of which carbon is but one of the component elements) in the mainstem areas of Gull Lake (zones 1-3) and the flooded back bays (PESV Vol. 7, Table 7.4-5). The analysis was based on estimated volumes of broken-down peat being suspended in the different peat transport zones in Gull Lake and its flooded back bays during open water conditions. It considered the increase for year 1, the first year after impoundment when the greatest amount of breakdown was predicted, and years 2 and 5 which were predicted to have progressively less peat breakdown. Conditions in 2021 represent year 1, the first year of operating conditions after impoundment in 2020.

In the mainstem areas (zones 1-3) peak estimated increases in suspended organic sediment concentration were low, ranging from 0-2 mg/l (PESV Vol. 7, Table 7.4-5). Among back bay zones, the predicted peak increases in zones 5, 10 and 13 were low, ranging from 2-4 mg/l. More moderate peak increases of 8-10 mg/l were predicted for zones 7, 9 and 12, although this would represent a large overall increase in suspended material considering typical TSS concentrations. Large peak increases of 15 and 21 mg/l were predicted for zones 11 and 8 respectively due to the large amount of peat predicted to break down in these areas and their small overall volumes. Although changes in organic carbon concentrations were not directly predicted in Keeyask EIS, the estimates of peak suspended organic sediment effects may suggest which areas are more or less likely to experience larger or smaller effects on organic carbon concentrations.

5.2 WINTER 2021

Discrete water samples were obtained at up to 5 sites once a month from January to April 2021 between Clark Lake and the entrance to Stephens Lake along the mainstem of the river, back bays were not sampled. These water samples were tested to measure the concentrations of Dissolved Organic Carbon (DOC) and Total Organic Carbon (TOC). These results are used to calculate the amount of Particulate Organic Carbon (POC), since POC is equal to TOC minus DOC. Note that in some cases the lab reported DOC is greater than the reported TOC, although the two values tend to be relatively close (<1 mg/l difference), suggesting POC is likely limited.

Typically, water samples were obtained at two or three depths in the water column (e.g., 20% & 80% depth) on each sampling visit. For purposes of the organic carbon analysis, the respective TOC or DOC results obtained from multiple depths at a site for each sampling day were averaged to get a single concentration value for the site and the results for each month were plotted (Figure 29). The results do not suggest any apparent trend during the winter period, nor do they indicate trend from upstream to downstream.

TOC varied from about 6-10 mg/l, although most values were above 8 mg/l, while the overall average was about 8.6 mg/l (Table 6). The range and average of TOC in winter 2021 was similar to conditions observed in previous winter periods. The results do not suggest any significant change resulting from reservoir impoundment and project operation.

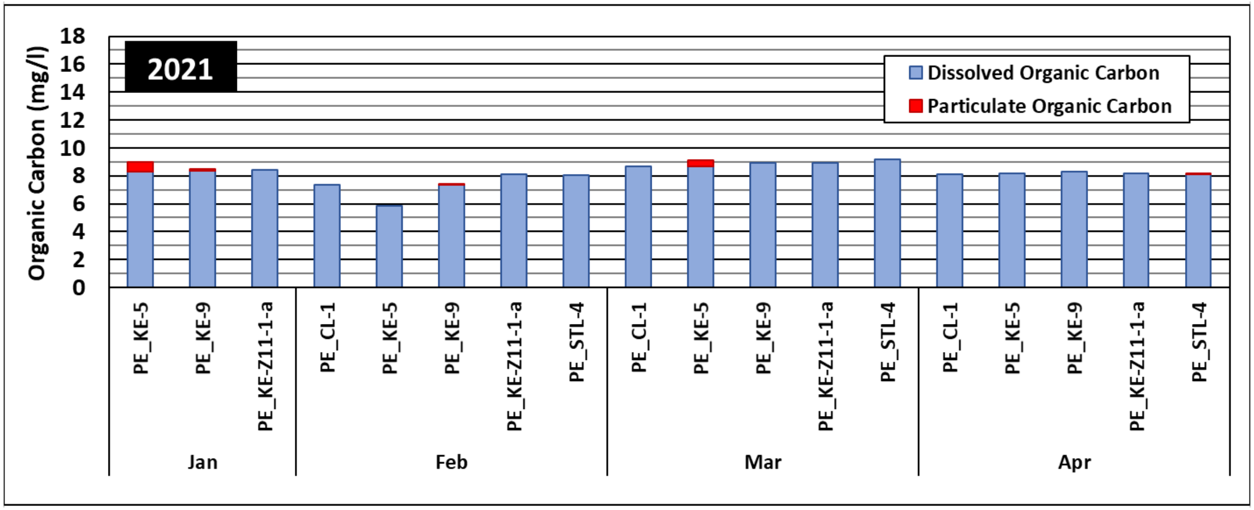

Figure 29: DOC, POC and TOC in winter 2021

Table 6: Summary of measured TOC during construction and operation

Year	Open Water (Jun-Oct)				Winter (Jan-Apr)	
	Mainstem		Back Bays		Mainstem	
	Range	Avg	Range	Avg	Range	Avg
2015	8-9	8.4				
2016	7.5-9.5	8.3				
2017	8-10	8.4			8-10	9.5
2018	9-10	9.5			9-10	9
2019	7.5-8.5	8.2			8-11	9
2020	8.5-10	9			7-9	8
2021	7.5-10.5	8.8	8-16	10.3	6-10	8.6

5.3 SUMMER 2021

Discrete water samples were obtained at up to 48 separate sampling locations at up to 23 sampling sites: e.g., sampling site STL-2 has 5 sampling locations a-f across the width of the river. Samples were obtained once a month from June to September 2021, between Clark Lake and Stephens Lake near Kettle GS. This included up to 38 locations along the mainstem of the river and up to 12 sites in flooded back bays. As was the case for winter organic carbon, the POC was calculated as the difference between lab measured TOC and DOC, but in many of the results DOC exceeds TOC (average <1 mg/l difference between the two) and for purposes of analysis and plotting the TOC is assumed to be equal to DOC where the DOC is larger.

The averaged organic carbon concentrations were plotted for each sampling location for the mainstem and back bay sites in each month (Figure 30). The results do not suggest any trend in organic carbon concentrations along the mainstem, either in an upstream to downstream direction or from month to month over the summer. Similarly, organic carbon concentrations in the back bays do not suggest a seasonal trend over the summer, while an upstream to downstream trend would not be expected for these sites. Back bay sites, however, do tend to be the locations where higher organic carbon concentrations do occur (Figure 30). Concentrations at sites in zones 4 (KE-Z4), 7 (KE-Z7), 8 (KE-Z8), and 11 (KE-Z11) are generally higher, with 8 and 11 typically among highest concentrations while zone 8 had the highest of the summer at 16 mg/l. Although organic carbon concentration is a different measure than the estimated peak increase in suspended organic material, the organic carbon results are consistent with expectations of greater organic material in the water in flooded back bays.

Concentrations in back bays varied over a higher and greater range than the mainstem, from about 8-16 mg/l in back bays (8-12.5 mg/l if the 16 mg/l value is omitted) versus about 7.5-10.5 mg/l in the mainstem (Table 6). The average concentration in the mainstem was about 1.5 mg/l lower than in the back bays, where the respective average concentrations were 8.8 mg/l and 10.3 mg/l. The 3 mg/l range of mainstem concentrations in 2021 was greater than the ranges of variation in previous years while the average in 2021 was within 0.7 mg/l of past averages (Table 6). Overall, the results from 2021 do not suggest any significant effect of the project on organic carbon concentrations along the mainstem from Clark Lake to the Keeyask GS, nor in the water discharged downstream.

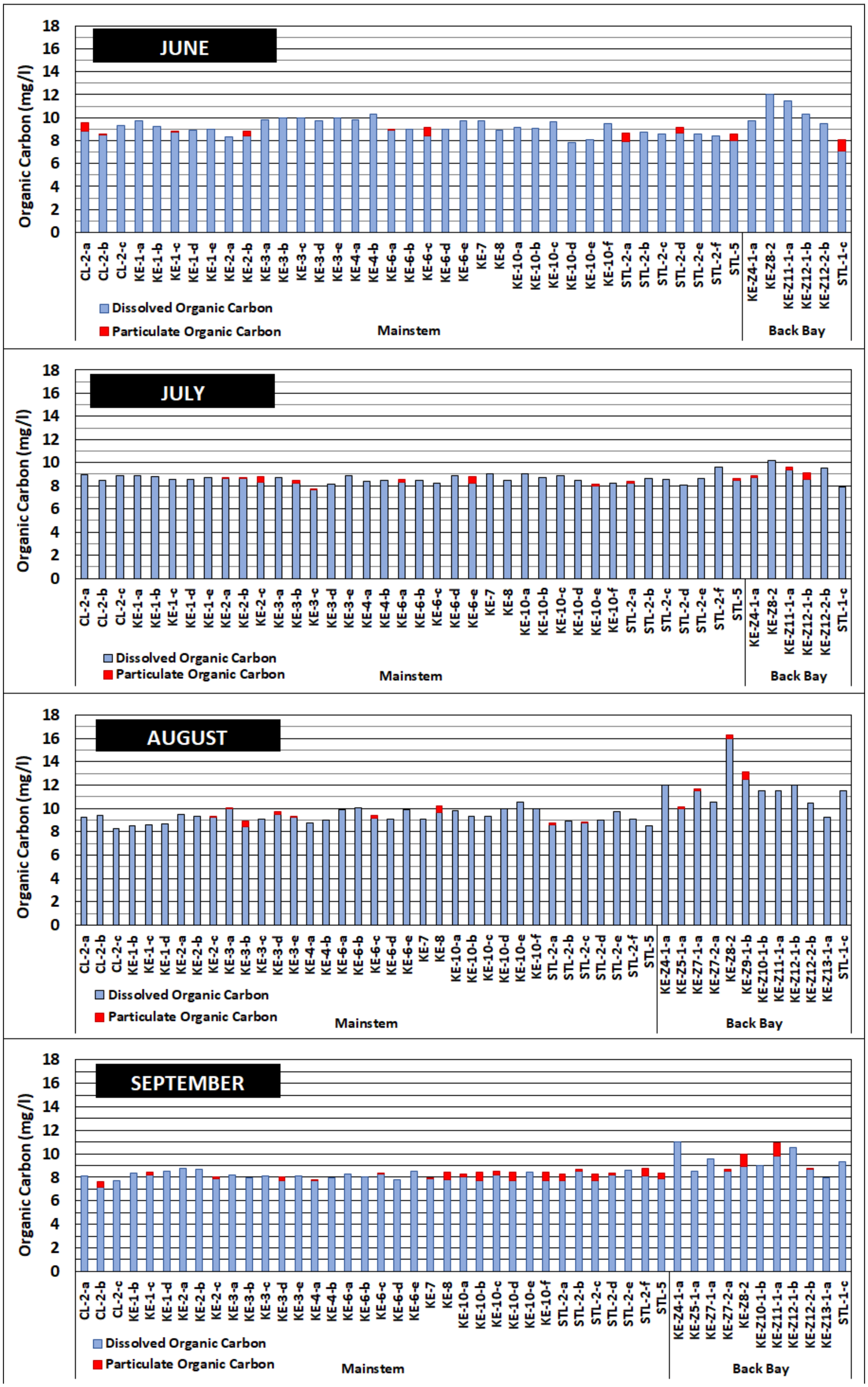

Figure 30: DOC, POC and TOC in summer 2021

6.0 DISSOLVED OXYGEN

Dissolved oxygen (DO) and water temperature (T) monitoring was performed using electronic sondes to collect in-situ measurements of these parameters along with percent saturation calculated based on ambient conditions. The monitoring included collection of discrete measurements in both winter (Jan-Apr) and summer open water period (Jun-Oct), as well as continuous monitoring at several sites in summer. Discrete monitoring involved obtaining measurements through the depth of the water column to identify vertical variability, particularly to see if DO is reduced near the bottom in water overlying flooded peat. Continuous monitoring involved placing two sondes at each monitoring site for several months during the open water period. To identify differences in the water column over time, one sonde was placed near the water surface and the other placed just above the bed. The discrete and continuous data sets were reviewed for data quality and erroneous and inconsistent data were filtered out. For the continuous data sets, the review tended to err on the side of leaving data in rather than remove potentially suspect data.

6.1 2021 WINTER DISCRETE DO

In winter 2021 (Jan-Apr), discrete dissolved oxygen (DO) and water temperature (T) monitoring was performed at 4 sites along the mainstem of the Nelson River from Clark L upstream (site CL-1) to just downstream of Keeyask GS in Stephens Lake (site STL-4), 11 sites in back bays flooded by the project and a back bay in Stephens L. At the mainstem sites only one location was sampled. In back bays, measurements were obtained at four sampling locations at each site. The sites and locations monitored were (see Appx. 1 for locations):

- Mainstem sites
  - CL-1; KE-5; KE-9; and STL-4
- Back bay sites (four locations measured at each identified as a, b, c, d, except KE-Z8 which has locations 1, 2, 3, 4)
  - KE-Z4-1; KE-Z5-1; KE-Z7-1; KE-Z7-2; KE-Z8; KE-Z9-1; KE-Z10-1; KE-Z11-1; KE-Z12-1; KE-Z12-2; KE-Z13-1; and STL-1

Charts showing the measured depth profiles of DO concentration, % saturation[1] and T are provided in Appendix 2.

Monitoring results for the mainstem sites showed that DO was high through the winter at these locations and T was just above 0°C. For the sites upstream of the GS (CL-1, KE-5, and KE-9) the DO was about 14-15 mg/l with a percent saturation between 95%-100%. Site STL-4 just downstream of the Keeyask GS had higher DO of about 15-16 mg/l and percent saturation ranging

[1] Saturation concentration is the DO concentration that water at a given temperature will tend to maintain in the absence of bio-chemical DO consumption, which reduces DO, or addition of excess DO from turbulent flow, which causes supersaturation.

from 100%-110%. Site STL-4 was supersaturated (i.e., >100% saturation) because the turbulent spillway flow entrains excess oxygen into the water and this excess does not transfer back to the atmosphere before the water reaches site STL-4.

To generally summarize discrete DO concentrations observed at the back bay monitoring sites, the DO conditions were identified as being either low, moderate, or high depending on the range of concentrations observed during the winter period. These classifications are defined based on consideration of the minimum 7-day average and instantaneous DO objectives when water temperatures are below 5°C for cool and cold aquatic species (Manitoba Water Stewardship, 2011). The 7-day average DO objectives for cool and cold-water species, 4 mg/l and 9.5 mg/l respectively while the respective instantaneous objectives are 3 mg/l and 8 mg/l. Based on these objectives, the following classifications were used to describe the DO variation between the surface and bottom for the 48 back bay sampling locations (Table 7):

- Low < 4 mg/l < Moderate < 9.5 mg/l < High.

Table 7: Summary of winter discrete DO conditions at back bay sites

Site \ Location[1]	a or 1	b or 2	c or 3	d or 4
KE-Z4-1	H / L[2, 3]	H / L	H	H / M
KE-Z5-1	H	H	H	H
KE-Z7-1	H / L	H	H	H
KE-Z7-2	H	H	H	H
KE-Z8	L	L	H	H
KE-Z9-1	L	L	L	L
KE-Z10-1	H	H / M	H / M	H
KE-Z11-1	H / L	H	H	H
KE-Z12-1	L	H / L	H	H
KE-Z12-2	H	H	H	H
KE-Z13-1	H	H	H	H
STL-1	H	H	H	H

Notes:
1) Site locations are designated by a, b, c or d (e.g., KE-Z4-1-a, KE-Z9-1-c, etc., except for KE-Z8 which is designated by 1, 2, 3, or 4 (i.e., KE-Z8-1, KE-Z8-2, etc.)
2) DO classified based on concentration where: low (L) < 4 mg/l < moderate (M) < 9.5 mg/l < high (H)
3) Single L, H or M indicates condition through depth of water column while combinations indicate variation from surface to bottom (e.g., H / L, high near surface low near bottom)

The results show that for the majority of monitoring locations, 33 of 48, the DO concentrations were classified as high through the depth of the water column. At 8 of the sites the DO varied from high near the surface to either moderate (3) or low (5) near the bottom. Only 7 of the monitoring sites had low do through the full depth, four of which occurred at the KE-Z9-1 monitoring site, two at KE-Z8, and one at KE-Z12-1. Each of the 7 sites with low DO had total water depths of less than 3 m, which is likely a significant factor in the depletion of DO at these locations. Another contributing factor would be a lack of mixing as these sites are in areas removed from the main flow, particularly for site KE-Z9, which is likely completely isolated from the reservoir in winter. Shallow depth and distance from the main flow, however, are not de-facto indicators that DO will be low: locations KE-7-2-b, c and d are all shallow but have high DO.

The majority of sites, including those identified as having high DO, show some vertical variation in DO concentration with higher levels near the surface and lower concentrations near the bottom. In most cases the variation occurs within the lower 1-2 m of the water column. The sites with high DO near the surface and low DO at the bottom show the most dramatic change from top to bottom, going from about 100% saturation down to near 0%.

Some variation in T is also observed at the back bay monitoring sites, with lower temperatures at the surface and higher temperatures near the bottom. although temperatures remain below 1°C through the water column at most of the sites. The highest water temperatures of 3-4°C were observed at monitoring locations KE-Z7-1-a and KE-Z9-1-a. Location KE-Z9-1-b was up to 2-3°C while KE-Z9-1-c, KE-Z9-1-c, and KE-Z4-1-a to d got to 1-2°C. It is notable that these sites experience low DO near the bottom in conjunction with higher water temperatures, which may be indicative of poorly mixed conditions. It is not necessarily the case that elevated T is required to reduce the DO to low levels, as sites KE-Z11-1-a and KE-Z12-1-a, and KE-Z12-1-b had low DO without significantly increased T near the bottom.

Overall, the winter DO results are generally consistent with expectations for winter DO in the Keeyask EIS (KHLP 2012b). Concentrations at monitoring sites KE-Z7-1, KE-Z7-2, KE-Z10-1 and KE-Z-11-1 may be somewhat higher than expected. It was expected that very low DO would be likely to develop in KE-Z9-1 because it is cut off from the reservoir in winter, as well as in the poorly mixed areas at KE-Z8-1, KE-Z8-2 and KE-Z12-1a.

6.2 2021 SUMMER DISCRETE & CONTINUOUS DO

6.2.1 DISCRETE DO

In summer 2021 (Jun-Oct), discrete DO and T monitoring was performed at 11 sites along the mainstem of the Nelson River from Clark L upstream (site CL-2) to about 30 km downstream of the Keeyask GS in Stephens Lake (site STL-5), plus 11 sites in back bays flooded by the project and a back bay in Stephens L. Up to six sampling locations were monitored across the width of the river at the mainstem sites. In back bays, measurements were obtained at four sampling locations at each site. The sites and locations monitored were (see Appx. 1 for locations):

- Mainstem sites
  - CL-2-a to c (i.e., PE_CL-2-a, PE_CL-2-b, PE_CL-2-c); KE-1-a to e; KE-2-a to c; KE-3-a to e; KE-4-1a and b; KE-6-1-a to e; KE-7; KE-8; KE-10-a to f; and STL-2-a to f; and STL-5
- Back bay sites (four locations measured at each identified as a, b, c, d, except KE-Z8 which has locations 1, 2, 3, 4)
  - KE-Z4-1; KE-Z5-1; KE-Z7-1; KE-Z7-2; KE-Z8; KE-Z9-1; KE-Z10-1; KE-Z11-1; KE-Z12-1; KE-Z12-2; KE-Z13-1; and STL-1

Sampling was generally done four times at each site, with site visits taking place in June, July August and either September or October. Charts showing the measured depth profiles of DO concentration, % saturation and T for each monitoring site are provided in Appendix 3. Depth profiles of back bay DO concentrations are also displayed together for comparison between the different monitoring sites (Figure 31).

Monitoring results for the mainstem sites showed that DO was high at all sites. Except for a few locations that were slightly different, the DO concentrations at mainstem sites were typically in the range of about 8.5-10.5 mg/l, with a degree of saturation between about 90%-100%. DO concentration was typically uniform through the water column depth at each sampling location. This was for conditions where water temperature ranged from a low of about 12°C in September to 19°C in August. Since DO was relatively uniform through the water depth at each site, the observed results are also apparent in the depth averaged DO concentrations at each location (Figure 32). Since the study area is aligned in a general west-east direction, the average concentrations were plotted based on the planned easting of sample locations to identify any upstream to downstream trends that may be due to the project. The results show relatively uniform DO conditions from upstream to downstream and do not suggest any significant effect of the project on mainstem DO.

As noted, there were a few locations that were slightly different from the typical trend. DO was 0.5-1 mg/l lower at locations KE-10-1-a and KE-10-1-b, just upstream of the Keeyask GS, where it varied from about 7.5-10 mg/l at 80%-95% saturation. These were the only two mainstem sites that showed a notable drop in DO between the surface and the bottom readings, although the difference of about 1 mg/l was small. The decrease is likely attributable to flooded organic material on the bed at these two locations. DO concentrations at site STL-2-e on the south side of the channel downstream of the GS were slightly higher than at other mainstem locations, including locations STL-2-a to d, ranging from about 9-11 mg/l with a saturation of 100%-110%. Concentrations at this site were elevated due to the turbulent flow coming from the spillway, which causes additional oxygen to be entrained in the water.

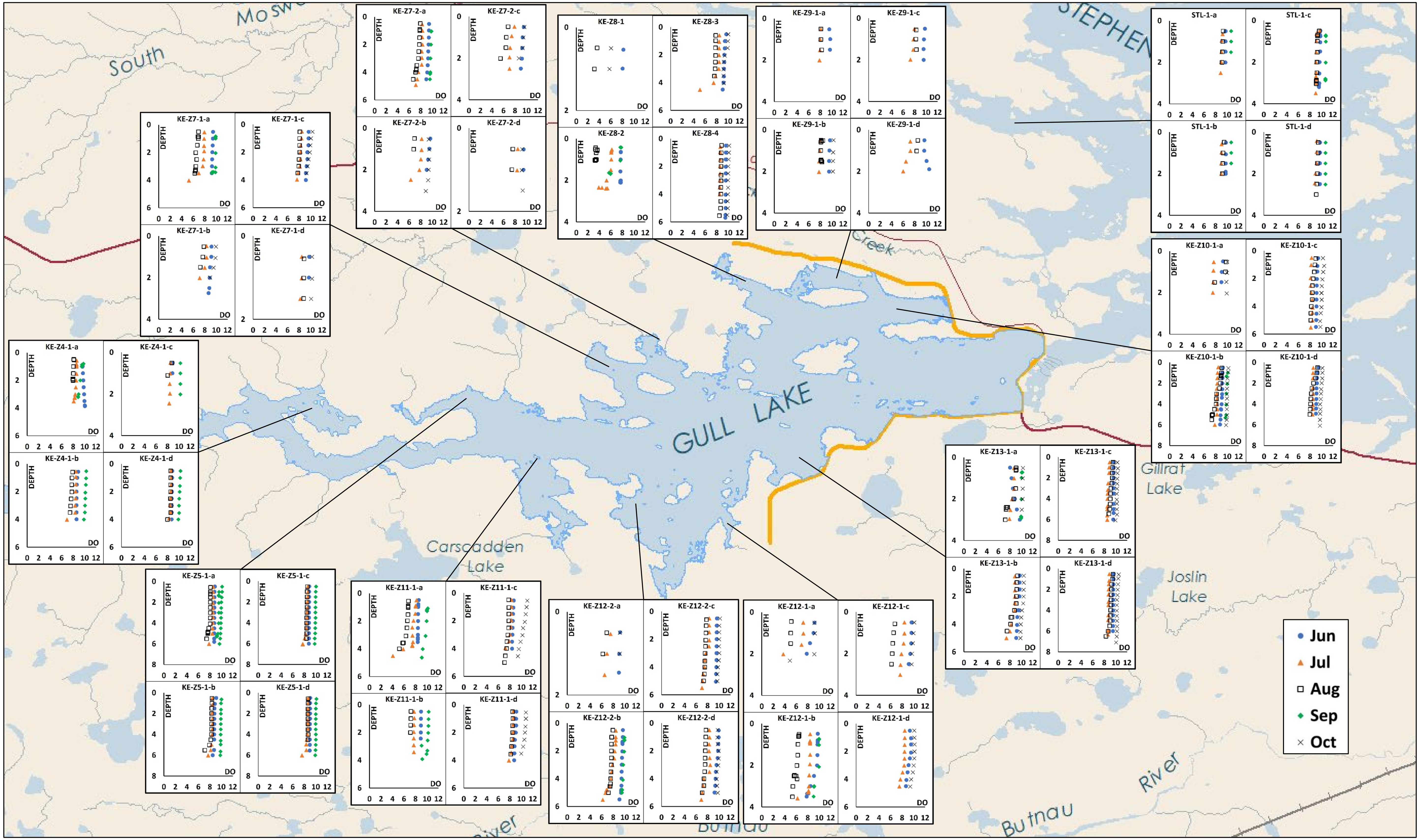

Figure 31: **DO depth profiles in back bays**

DO concentrations observed in back bays varied over a much wider range than along the mainstem (Figure 31, Appx 3). To generally summarize discrete DO concentrations observed at these sites, the DO conditions were identified as being either low, moderate, or high depending on the range of concentrations observed during the summer period. These classifications are defined based on consideration of the minimum 7-day average and instantaneous DO objectives when water temperatures are above 5°C for cool and cold aquatic species (Manitoba Water Stewardship, 2011). The 7-day average DO objectives for cool and cold-water species are 6 mg/l and 5 mg/l respectively, while the respective instantaneous minimum objectives are 5 mg/l and 4 mg/l. Based on these values, the following classifications were selected to describe the DO variation between the surface and bottom for the 48 back bay sampling locations (Table 8):

- Low < 4 mg/l < Moderate < 6 mg/l < High.

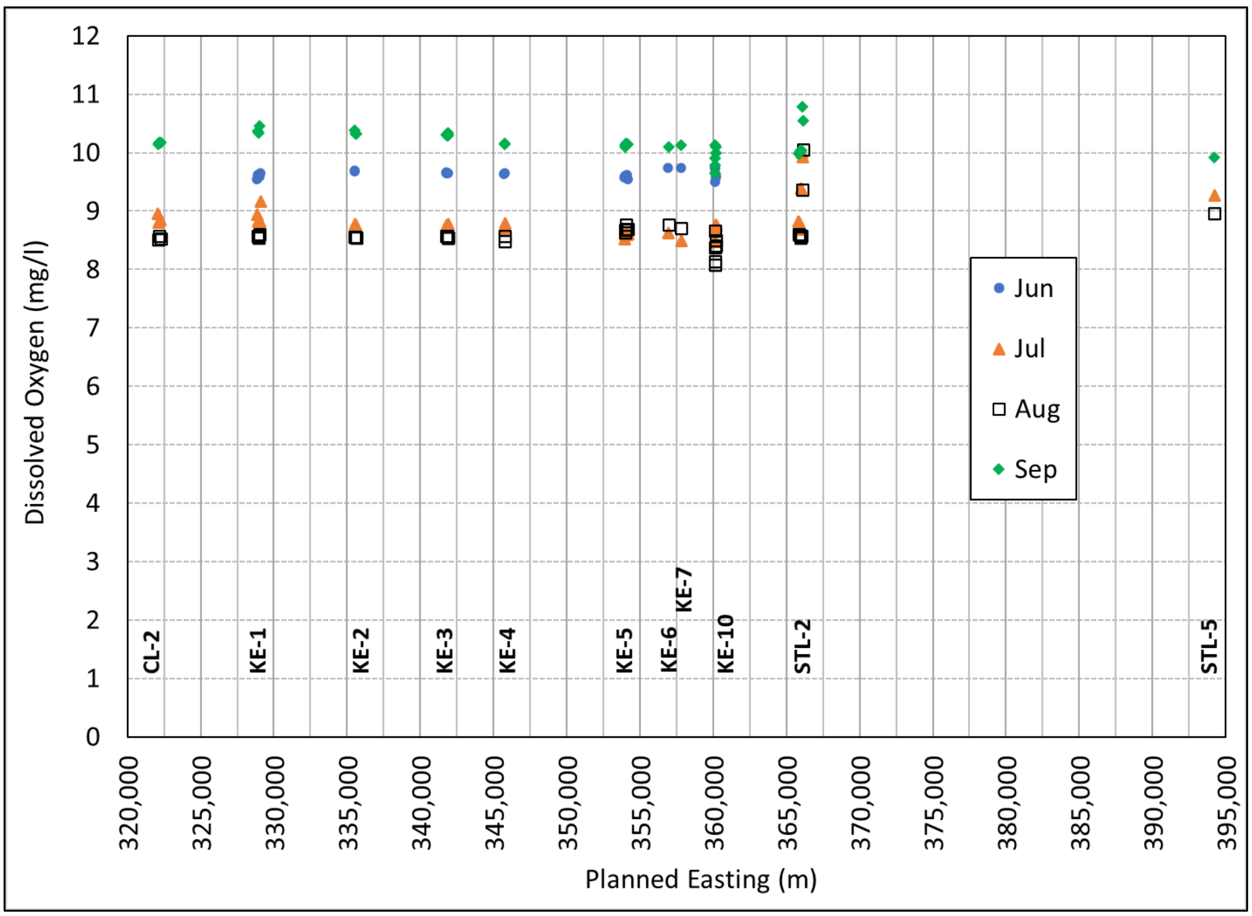

Figure 32: Average DO at mainstem sites, summer 2021

Based on the selected criteria, 40 of the 48 discrete sampling sites were classified as having high DO, with concentrations that exceeded 6 mg/l (Table 8). While DO concentration may have varied between about 6-10 mg/l at these sampling locations, many locations exceeded about 8 mg/l and had DO saturation of about 80-100%. Most of these sites also showed some vertical differentiation with a lower DO concentration near the bottom, even if it was only a small difference of less than 1 mg/l. A few sites had deviations of about 2 mg/l from top to bottom (KE-Z7-2-b, KE-Z10-1-b, KE-Z11-1-c).

Five of the back bay sampling locations had high DO near the surface that decrease to moderate DO near the bottom, while another three had high surface DO that dropped to low DO at the bottom (Table 8). In these cases, the change from top to bottom could be as much as 3-4 mg/l. While these locations may have had high DO near the surface (i.e., >6 mg/l), they generally had somewhat lower DO through much of the water column as compared with other less affected sites in the same month. Also note that since the classification considers the range over the summer, some locations my be moderate or low DO through the entire water column in a particular month. The full depth of KE-Z8-1 and KE-Z8-2 was low in August, while KE-Z8-1, KE-Z8-2 and KE-Z12-1-a were essentially moderate in October, July, and August respectively.

Table 8: Summary of summer discrete DO conditions at back bay sites

Site \ Location[1]	a or 1	b or 2	c or 3	d or 4
KE-Z4-1	H[2, 3]	H	H	H
KE-Z5-1	H	H	H	H
KE-Z7-1	H / M	H	H	H
KE-Z7-2	H	H	H / M	H
KE-Z8	H / L	H / L	H / M	H
KE-Z9-1	H	H	H	H
KE-Z10-1	H	H	H	H
KE-Z11-1	H / M	H	H	H
KE-Z12-1	H / L	H / M	H	H
KE-Z12-2	H	H	H	H
KE-Z13-1	H	H	H	H
STL-1	H	H	H	H

Notes:
1) Site locations are designated by a, b, c or d (e.g., KE-Z4-1-a, KE-Z9-1-c, etc., except for KE-Z8 which is designated by 1, 2, 3, or 4 (i.e., KE-Z8-1, KE-Z8-2, etc.)
2) DO classified based on concentration where: low (L) < 4 mg/l < moderate (M) < 6 mg/l < high (H)
3) Single L, H or M indicates condition through depth of water column while combinations indicate variation from surface to bottom (e.g., H / L, high near surface low near bottom)

For each back bay monitoring location and sampling date, the average DO concentration was calculated from the measurements obtained through the depth of the water column. For plotting purposes, depth averaged DO was plotted based on the planned easting the sample locations so that results are shown according to their relative position along the monitoring area, which has a west-east alignment (Figure 33). Unlike the mainstem sites, there would be no expectation that

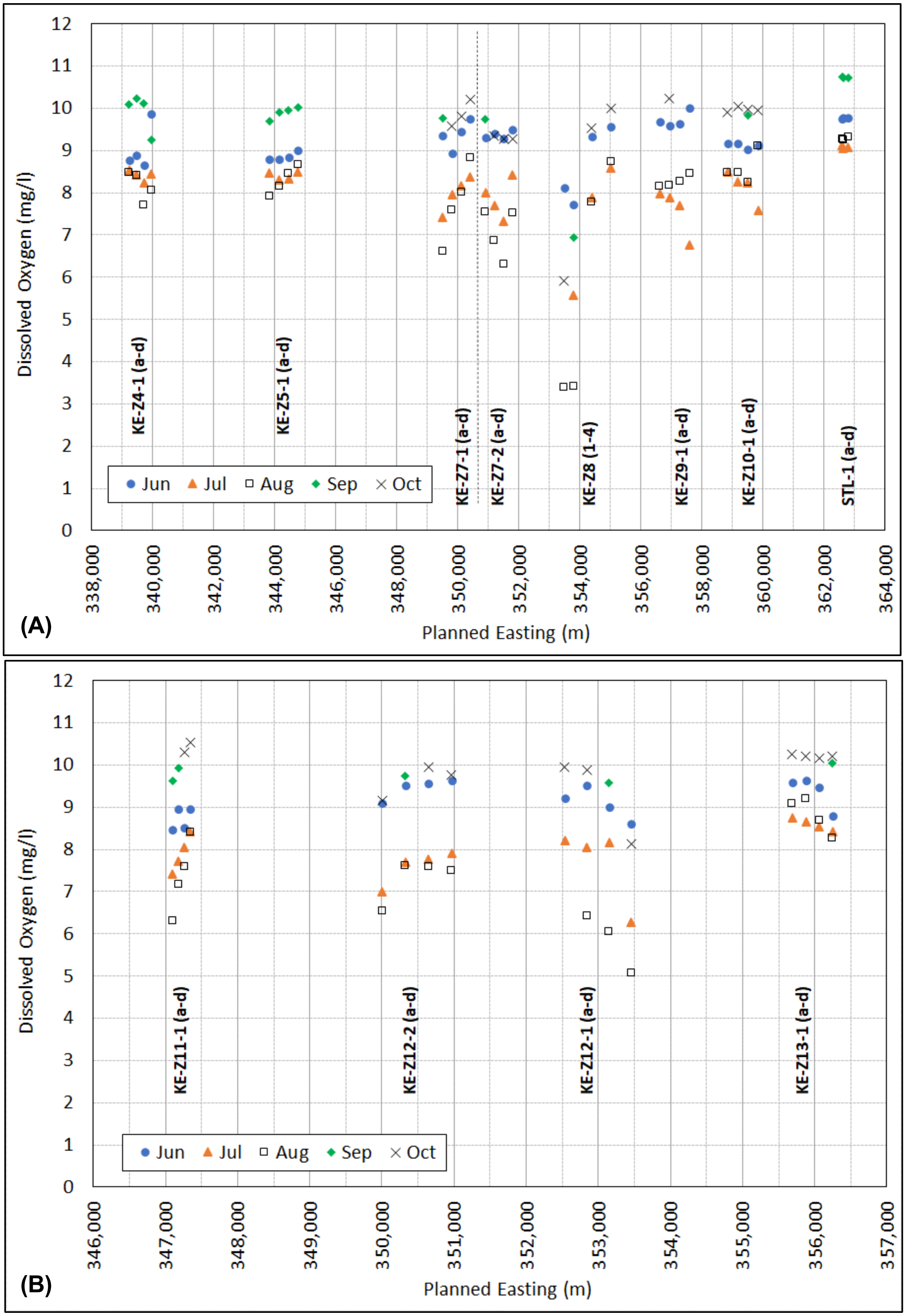

Figure 33: Average DO at north (A) and south (B) back bay sites, summer 2021

there could be an upstream to downstream trend in the results (e.g., between KE-Z11-1 and KE-Z12-2) since flow does not travel directly between them – they are independent. For clarity, the north and south back bays are plotted separately. Results show depth averaged DO is generally high, exceeding 6 mg/l at most sites during the monitoring period, although several sites have reduced DO, particularly in the warm months of July and August: notably KE-Z7-1, KE-Z7-2, KE-Z8, KE-Z11, KE-Z12-1, and KE-Z12-2. Conversely, depth averaged DO concentrations in the Stephens Lake back-bay site, which is unaffected by the project, were generally greater than the back bays upstream of Keeyask, even those where DO remained relatively high (e.g., KE-Z4-1, KE-Z5-1). This may be due to less biological activity at the STL-1 site as compared with the upstream sites in newly flooded areas with organic substrates.

The discrete monitoring results are generally consistent with expectations from the Keeyask EIS that DO would typically remain relatively high (>6 mg/l), even in flooded back bays. Reduced DO was expected to occur in some back bays, notably in association with periods of reduced winds when reaeration is decreased. Low DO observed in some locations near the bottom or through the depth of the water column was not necessarily associated with low wind conditions. These low DO levels may indicate less mixing due to wind and flow and/or higher oxygen demand from organic decay than assumed in the Keeyask EIS assessment of effects on DO.

6.2.2 CONTINUOUS DO

Continuous DO sensors were placed either near the surface (~2 m below) and bottom (~ 1m above) at the following 5 mainstem and 6 back bay locations between mid-June to the end of September:

- Mainstem:
  - CL-2-b surface
  - KE-4-b surface
  - KE-10-c surface and bottom
  - STL-2-d surface
  - STL-5 surface
- Back bay:
  - KE-Z4-1-a surface and bottom
  - KE-Z8-2 surface and bottom
  - KE-Z11-1-a surface and bottom
  - KE-Z12-1-b surface and bottom
  - KE-Z12-2-b surface and bottom
  - STL-1-c surface and bottom

Continuous DO results showed high levels of DO (>7 mg/l) from site CL-2-b upstream of project effects through to site STL-5 in Stephens Lake about 30 km downstream of the Keeyask GS (Figure 34). DO concentrations were typically within about 1-1.5 mg/l of each other. The DO concentrations were typically lowest at the KE-10-c site, with the bottom sensor at usually the lowest among the mainstem sites. Concentrations at this site may be slightly reduced due to upstream oxygen demands from the decay of flooded organic material. The KE-10-c plots also show more variability or noise than the other sites, which may be due to variations in discharge. At this location, the DO saturation varied from about 80%-100%.

DO concentrations at site STL-2 were generally quite similar to the KE-10-c (surface) concentrations, which might be expected since the two sites are close together, being immediately downstream and upstream of the Keeyask GS respectively (Figure 34). However, the STL-2 site displays several periods with DO concentrations that are about 1-1.5 mg/l higher, such as at the beginning of the data in June. Initially this was suspected to be an equipment error, but comparison with the pattern of spillway discharges shows that the periods of elevated DO

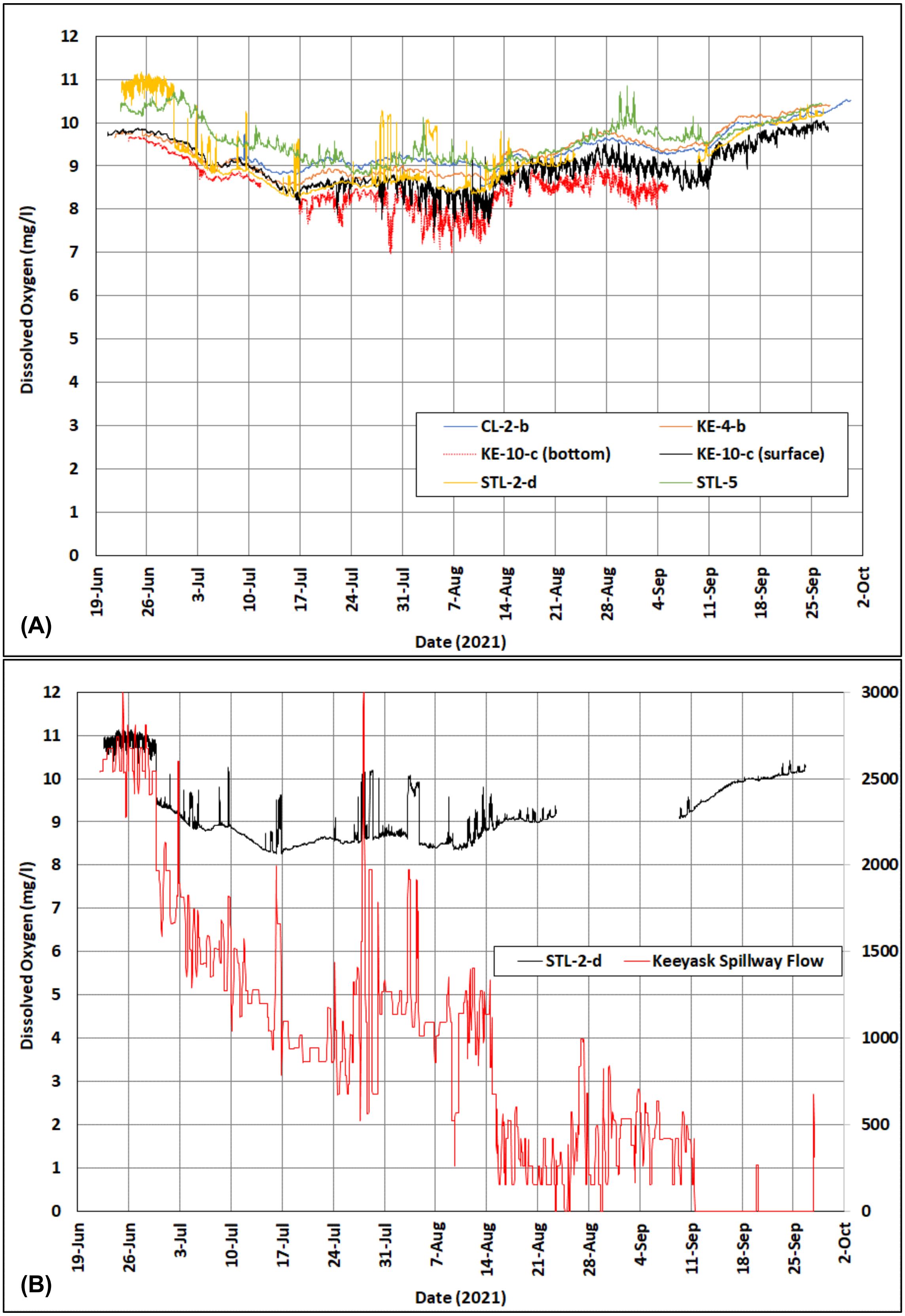

Figure 34: Continuous DO at mainstem sites (A) and site STL-2 (B)

concentrations at STL-2 correspond with periods of higher discharge from the Keeyask spillway (Figure 34). During these periods the turbulent spillway flow entrains more oxygen in the water, raising DO to the point that the water is supersaturated, with a saturation level up to about 110%.

Concentrations at CL-2-b and KE-4-b were similar through the summer with minor variations between them, varying from about 8.5-10.5 mg/l with saturation levels of about 95%-100%. The concentrations at STL-5 were close to the values at these two sites over much of the summer. However, levels were higher at STL-5 in the first month of monitoring, for a couple weeks from end of August into September, as well as some intermittent peaks at other times. During these periods the degree of saturation was elevated into the range of 105%-110%. Such elevated levels would not generally be expected at the STL-5 location. The cause is uncertain but may be partly due to variations in sensor calibration and, for short intermittent peaks, the potential influence of wind/wave events.

Among the six continuous DO sites in back bays, DO concentrations were generally highest at site STL-1-c in Stephens Lake, with DO levels exceeding 8 mg/l most almost the entire time (Figure 35). There was no apparent vertical difference in DO concentration as both the surface and bottom readings were essentially the same. Similar results were observed for the upstream site KE-Z4-1-a where DO concentrations exceeded 7 mg/l most of the time and both surface and bottom DO concentrations were essentially the same (Figure 36). Concentrations at the site dropped between 4-6 mg/l for about a day in early September. The data at this site are noisier than at STL-1. There are intermittent variations, typically reductions, of 2-3 mg/l from the prevailing level for only one to several consecutive readings. Although they may be measurement anomalies, these intermittent variations have been left in the final data set.

At back bay sites KE-Z11-1-a, KE-Z12-1-b and KE-Z12-2-b, the surface DO was typically above 6 mg/l during the summer, and only declined to 5-6 mg/l a few times for periods of less than a day (Figure 37, Figure 38, Figure 39). Bottom DO concentrations, however, dropped below 6 mg/l more frequently, decreasing to 0-1 mg/l for varying durations. This occurred less frequently at KE-Z12-2-b where there were a few intermittent decreases to 4-6 mg/l and a decrease to between 0-1 mg/l at the end of September for less than a day (Figure 39). However, due to recording errors, this site has a data gap for about a month from early July into August. Site KE-11-1-a (bottom) DO was below 6 mg/l on several occasions and for an extended period in July, with levels between 0-1 mg/l for several days during this time (Figure 37). This site has a data gap during August to early September due to equipment errors affecting results. While it is possible some of the extended low DO in July at KE-11-1-a is caused by equipment errors, the data was retained because it was not as clear that the data was anomalous. Finally, bottom DO concentrations at site KE-Z-12-b was frequently in the 4-6 mg/l range, particularly in the first two months, and at the end of August to early September (Figure 38). Intermittent decreases less than 4 mg/l occurred on several occasions, generally lasting less than a day, while a decrease to 0-1 mg/l occurred for several days in late July. DO at all three sites was generally higher (>6 mg/l) during the final month of monitoring as water temperatures cooled.

Finally, DO concentrations were generally quite low at back bay site KE-Z8-2 for both the surface and bottom measurement locations (Figure 40). In the first and last two weeks of monitoring the surface DO concentrations were generally greater than 6 mg/l. Conversely, during the intervening 3 months, the DO was largely in the range of 4-6 mg/l, with frequent intermittent reductions to 1-3 mg/l for periods up to several days. Much of the bottom DO data during this period was erroneous resulting in a data gap of about 1.5 months from July into August (Figure 40). However, based on results from other back bays, it is likely the bottom DO was lower than surface DO during this time and decreased to 0-1 mg/l for potentially several days at a time. Bottom DO did decline to 0-1 mg/l just prior to the data gap. After the data gap, the bottom DO appears to track closely with surface DO and is largely in the range of 4-6 mg/l until the last couple of weeks when the DO is generally greater than 6 mg/l.

Overall, the surface DO results are generally consistent with expectations with concentrations typically exceeding 6 mg/l at all the sites (KHLP 2012b), with site KE-Z8-2 being an exception as it experienced low DO throughout much of the summer. Except for site KS-Z4-1-a, bottom DO concentrations decreased to levels between 4-6 mg/l more frequently than may have been anticipated at sites K-Z11-1a, K-Z12-1-b and K-Z12-2-b than may have been anticipated from analyses conducted for the Keeyask EIS. Similarly, low DO below 4 mg/l occurred more frequently than may have been anticipated at sites K-Z11-1a and K-Z12-1-b.

Observed back bay conditions were more like modeled DO effects for scenarios assuming greater oxygen demands in the water or sediment, or reduced mixing from wind as compared with values used for expected conditions (TetrES 2011). The observed continuous DO results may indicate less mixing and/or greater oxygen demand from decaying organic material than assumed in DO models use for the Keeyask EIS. Notably, the low turbidity levels observed in back bays (see sec. 4.2) may be a contributing factor as greater light penetration could result in greater biological activity than assumed in the models. It may also be that resurfaced peat in the back bays that cannot be accounted for in the models impedes flow mixing between with flow in the mainstem.

Wind mixing is also an important factor, and the occurrence of low DO generally corresponds with periods of reduced wind speeds, as demonstrated for bottom DO at site KE-Z12-1-b (Figure 41). Generally, when the 24-hour average wind speed dropped below about 10-12 km/h, the bottom DO started to decline and continued to drop as low wind speeds persisted: for example, during the Jul. 16-23 period when DO drops to 0 mg/l. However, DO does not always decrease to a low level with low wind speeds. Winds were low in the days before and after Aug 27, but KE-Z12-1-b DO concentration remained above 6 mg/l. It is likely that wind direction is also a factor as a larger fetch length could facilitate larger waves that create greater mixing. This may be a factor in the consistently low DO observed at site KE-Z8-2 because the site is relatively protected and has short fetch lengths in almost all directions except to the southeast. That, however, is the least common direction that winds come from and, when they do, the wind speeds are generally low (KHLP 2012b).

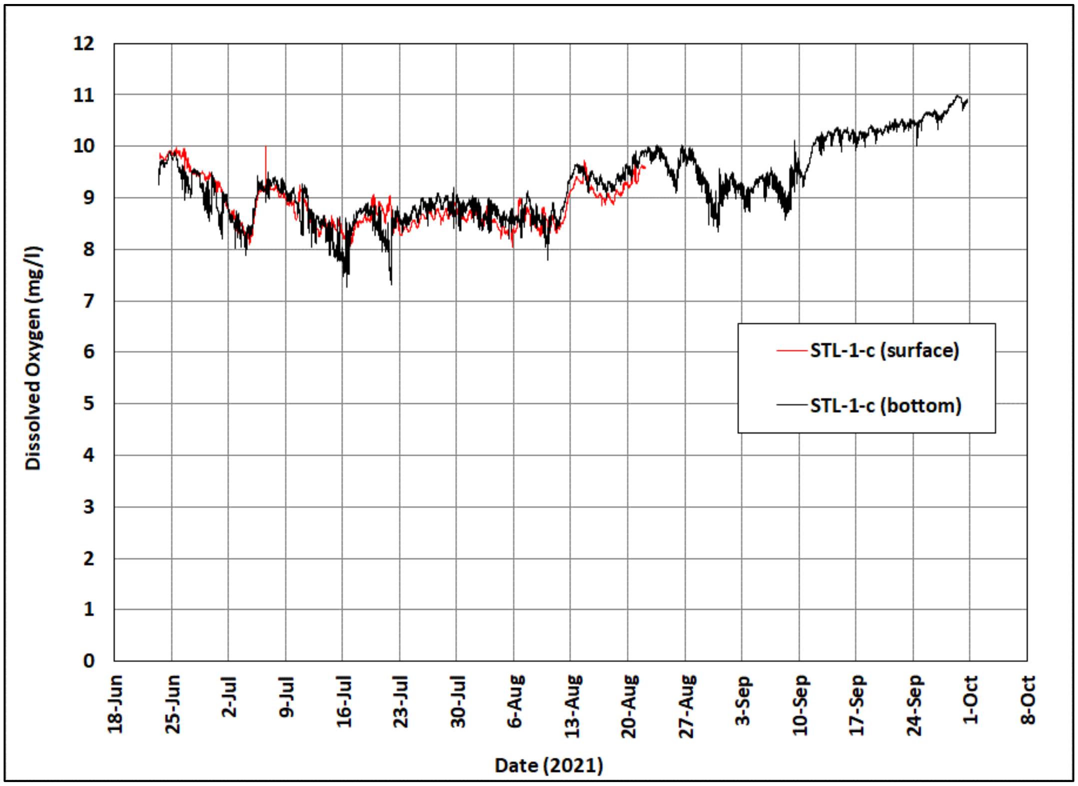

Figure 35: Continuous DO at site STL-1

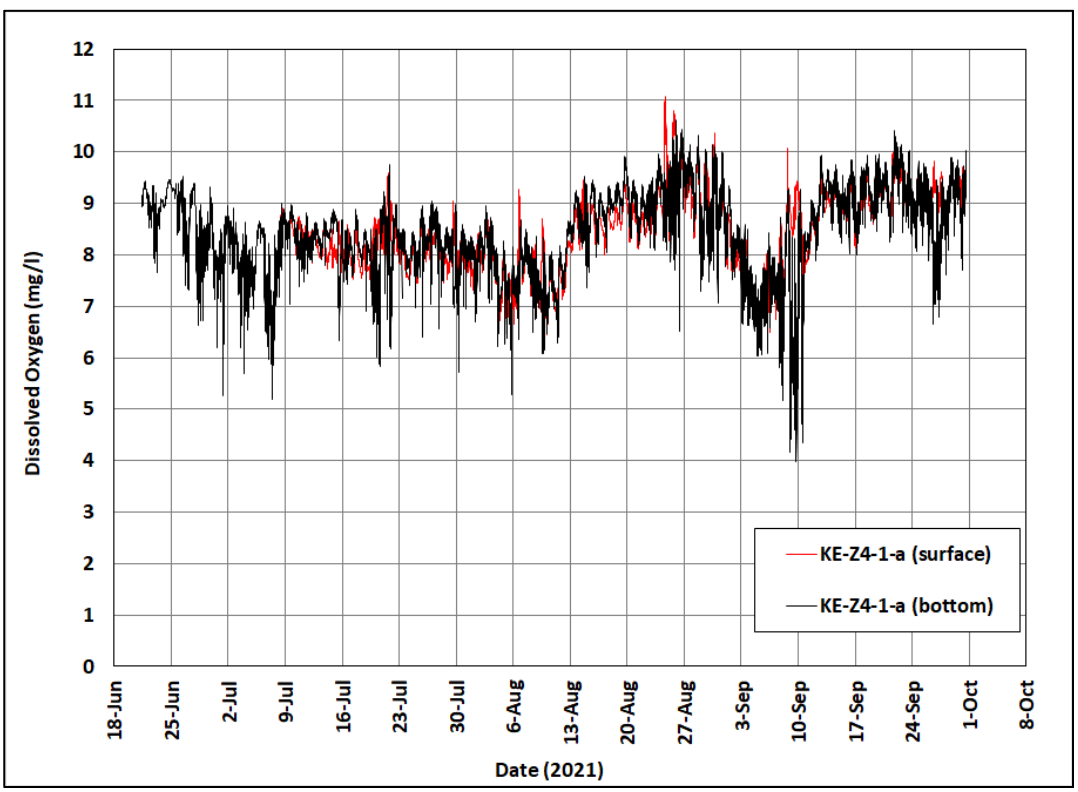

Figure 36: Continuous DO at site KE-Z4-1-a

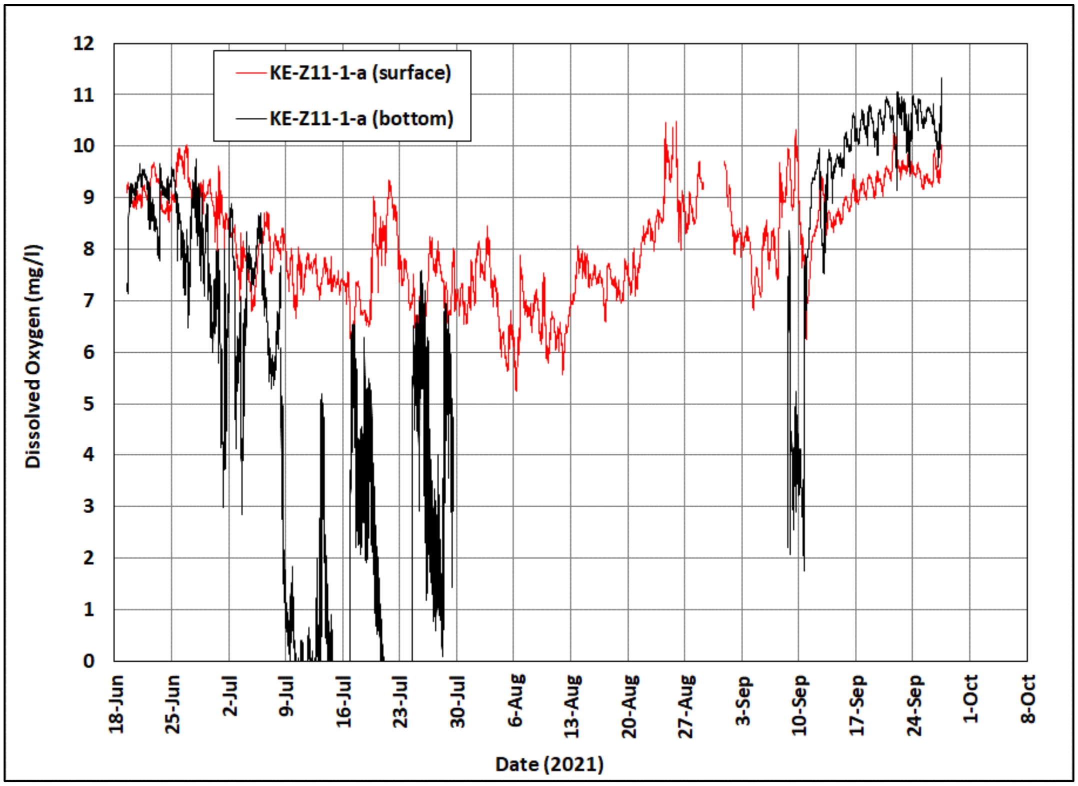

Figure 37: **Continuous DO at site KE-Z11-1-a**

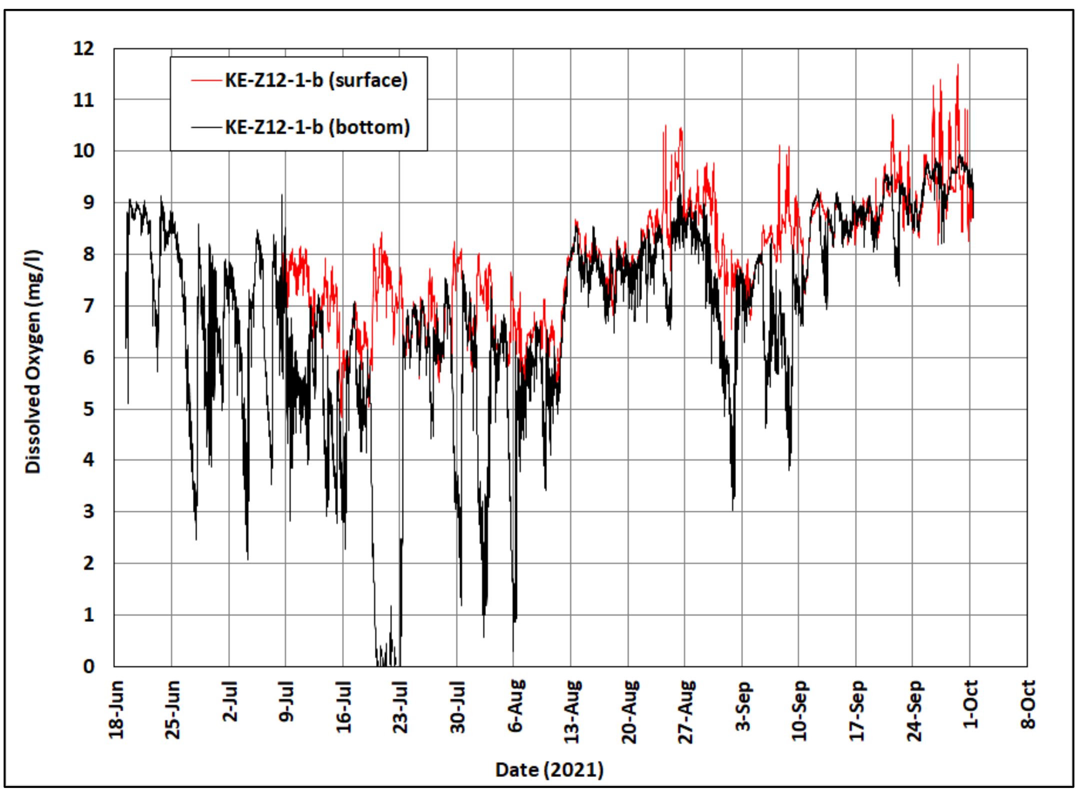

Figure 38: **Continuous DO at site KE-Z12-1-b**

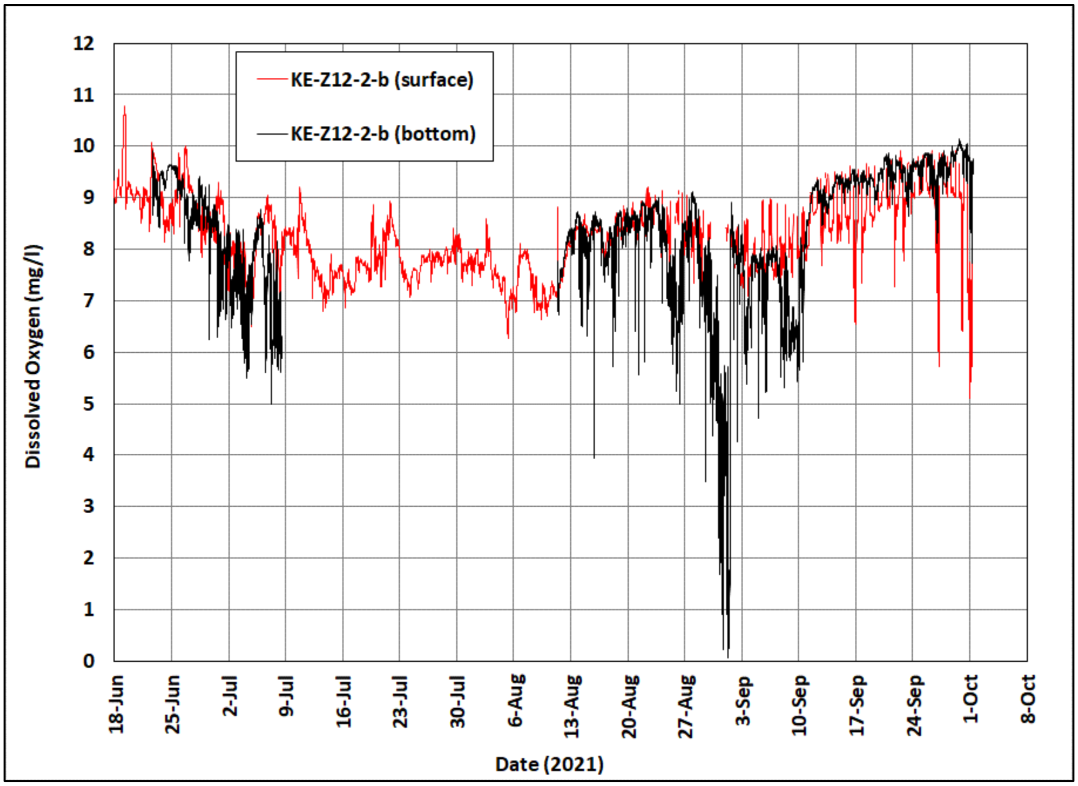

Figure 39: Continuous DO at site KE-Z12-2-b

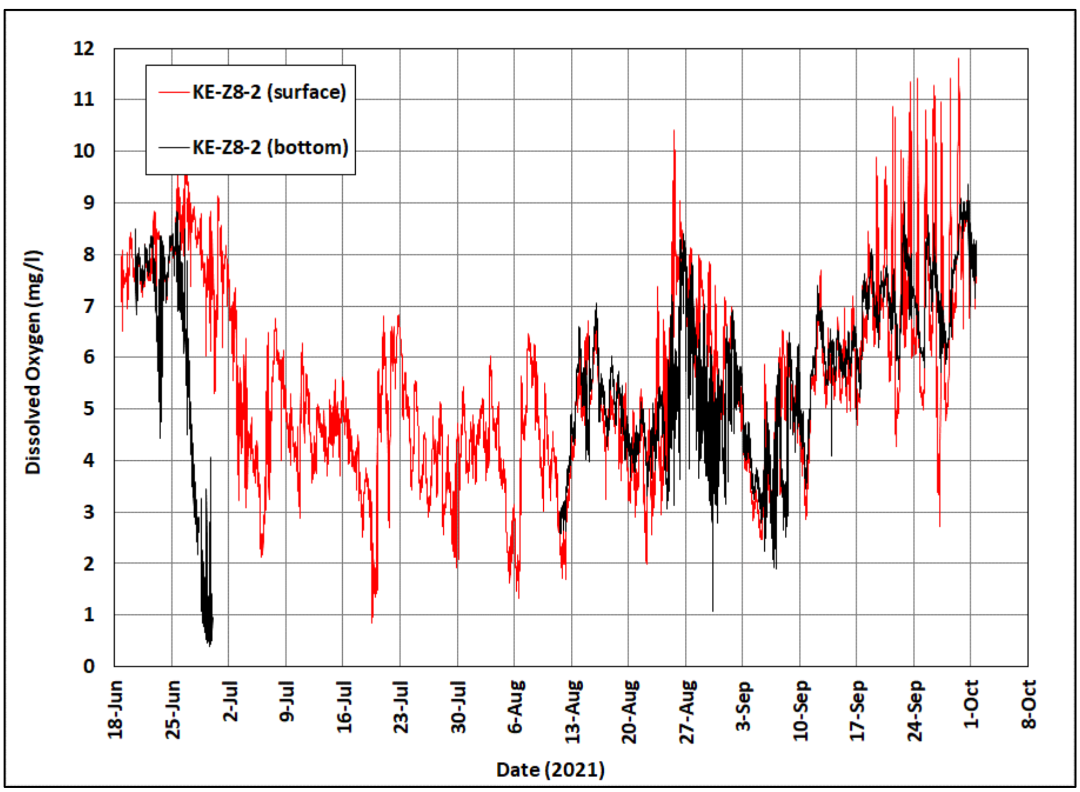

Figure 40: Continuous DO at site KE-Z8-2

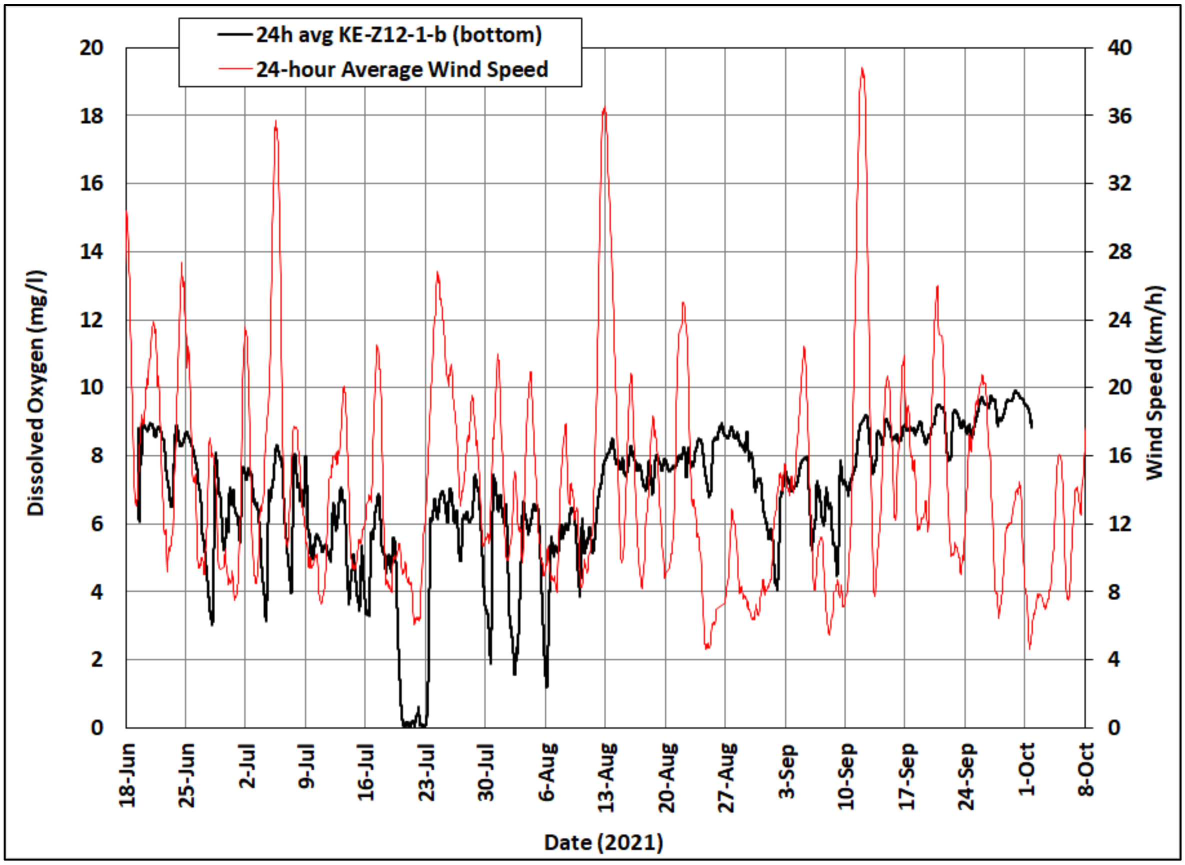

Figure 41: 24-hour average continuous DO at site KE-Z12-1-b and wind speed

6.3 LITTLE GULL LAKE AERATION SYSTEM – 2020/2021 MONITORING SUMMARY

6.3.1 BACKGROUND

Little Gull Lake was a small lake developed within peat bogs approximately 900 m to the north of Gull Lake (Figure 42). After impoundment of the Keeyask reservoir in fall 2020, Little Gull Lake was incorporated into the overall reservoir. Dissolved oxygen (DO) modeling conducted during the Keeyask environmental assessment indicated that this area would become anoxic during winter, due to restricted flows and the high oxygen demand from organic substrate. It was also identified that the water depth between the former Little Gull Lake and Gull Lake within the reservoir would be very shallow and could freeze to the bottom in the winter. This could restrict the movement of fish to areas of higher DO creating the risk of winterkill.

To mitigate the risk of winterkill an aeration system was installed on the North Shore of the former Little Gull Lake. The aeration system is comprised of four Keeton Industries SolAer aeration units. Each unit operates independently and is comprised of a solar power system (solar panel, batteries, and controller) and air supply system (compressor, manifold, air filter, self-sinking supply line, and two in-water diffusers). The on-land components are housed within a weatherproof insulated cabinet. Pumped air is introduced to the lake via Keeton Duraplate self-cleaning, non-clogging, membrane diffusers. There are eight diffusers in total, two per system.

6.3.2 AERATION SYSTEM MONITORING

Monitoring of DO included the collection of discrete measurements and continuous monitoring. Discrete DO readings were collected monthly along transects outside aeration field at the limit of safe ice (~5-10 m outside of the aeration field). Due to dangerous ice conditions, it is not possible to collect discrete samples within the aeration field. Data shows that system was elevating DO above background levels, however there is a limited increase of DO outside of the immediate area of aeration field.

The continuous DO sensors were to be deployed within the aeration field. However, pandemic related logistical challenges resulted in the loggers being installed after ice-on. Two HOBO dissolved oxygen loggers were deployed, outside of the field at the safe ice distance of ~10 m. The deployment methods used were not suitable to the conditions of Little Gull Lake, field notes indicate that the loggers had a high probability of entering the fluid sediment layer of the lake and the moorings used were damaged by ice during breakup. The data from the loggers is not useful and an improved deployment method has been developed for the winter 2021/22 monitoring program.

The system was also monitored via visual inspection of the aeration area (UAV photography). Aerial photography confirmed that the system was capable of maintaining open water through the winter (Photo 6, Photo 7, Photo 8).

Figure 42: Location of Little Gull Lake

Photo 6: Little Gull L., November 2021, looking east

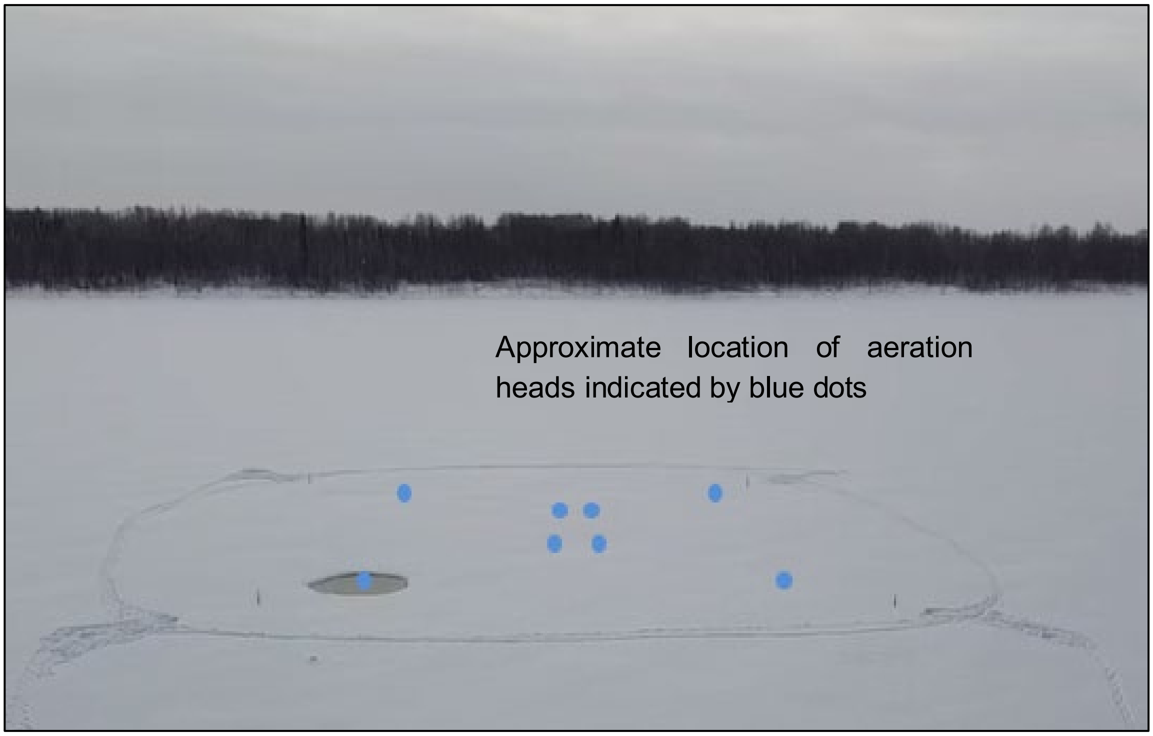

Photo 7: Little Gull L., February 2021, looking south

Photo 8: Little Gull L., March 2021, looking north

7.0 DEBRIS

As part of the Project, in accordance with the Joint Keeyask Development Agreement (JKDA; TCN et.al. 2009), a waterways management program was started in 2015 for the Project area from Clark Lake to Gull Rapids. The JKDA indicated that up to 25 workers configured as two two-person boat patrols plus supplementary work crews would operate in the Keeyask area. One boat patrol would operate downstream to implement safety measures and inform resource users of altered water conditions due to the Project while the other would operate upstream to implement safety measures, manage hazardous debris and assist the work crews.

Boat patrols identify and remove floating woody debris (Photo 9) that may pose a safety hazard to navigation. The boat patrol typically records the amount of debris removed each season, classifying it as either small (<1m length) or large (>1m length), and the large material is further classified as either new or old debris (generally with or without bark) or if it came from beaver activity.

Prior to 2015, this area was only visited about once each week (20% of the time) by the crew that also patrolled Split Lake and the amount of debris collected in the Clark Lake to Gull Rapids area was estimated to be 20% of the total amount of debris collected by this crew. Starting in 2018 a new data collection program was initiated allowing for tracking of the location of floating debris and accounting for debris in the Keeyask area. In 2018 and 2019, 10 or fewer pieces of debris were removed each year (Table 9). While the patrol operated in the area in both 2020 and 2021, they did not record the removal of any debris. Except for 2003 the quantities removed after 2014 were much less than the estimated amounts of debris removed up to 2014. This suggests that the amounts removed from the Project prior to 2015 were likely much lower than estimated by the simple assumption it was 20% of the amount collected by the Split Lake boat patrol.

In 2021, the boat patrol upstream of Keeyask GS was primarily focused on supporting a 20-person work crew that was tasked with cleaning up woody debris in the vicinity of the Keeyask south dyke (pers. comm., R. Flett, MB Hydro, May 2022). The boat patrol transported the work crew the 60 km distance between the community of Split Lake and the south dyke twice each day. One member of the boat patrol typically remained with the work crew as a supervisor and the patrol boat was used to provide support. While the boat patrol did mark navigation hazards like newly formed reefs created by reservoir impoundment, it did not conduct formal daily patrols of the waterway to find and remove floating debris, which is why the boat patrol did not record the debris removed. Floating debris was opportunistically removed but not recorded.

The 20-person work crew collected and stockpiled woody debris from about 4 km of shoreline and waterway adjacent to the south dyke (Figure 43. Photo 10). The debris was gathered into several stockpiles that were left over the winter to allow the debris to dry out. In May 2022 the stockpiles were burned to get rid of the debris.

Table 9: Debris removed from the Keeyask area

Year	Small (<1 m)	Large (> 1m)			
		New	Old	Beaver	Total
2003	3	4	7	0	11
2004	36	1	140	0	141
2005	2	6	103	0	109
2006	11	1	65	0	66
2007	0	3	81	0	84
2008	1	0	49	1	49
2012	0	1	30	1	32
2014	2	1	59	0	60
2015	4	0	6	0	10
2016	3	1	2	0	6
2017	Not available				
2018	5	0	4	1	10
2019	1	4	3		8
2020	Not available				
2020	Not available				

Photo 9: Large floating debris is removed from the water by the boat patrol team

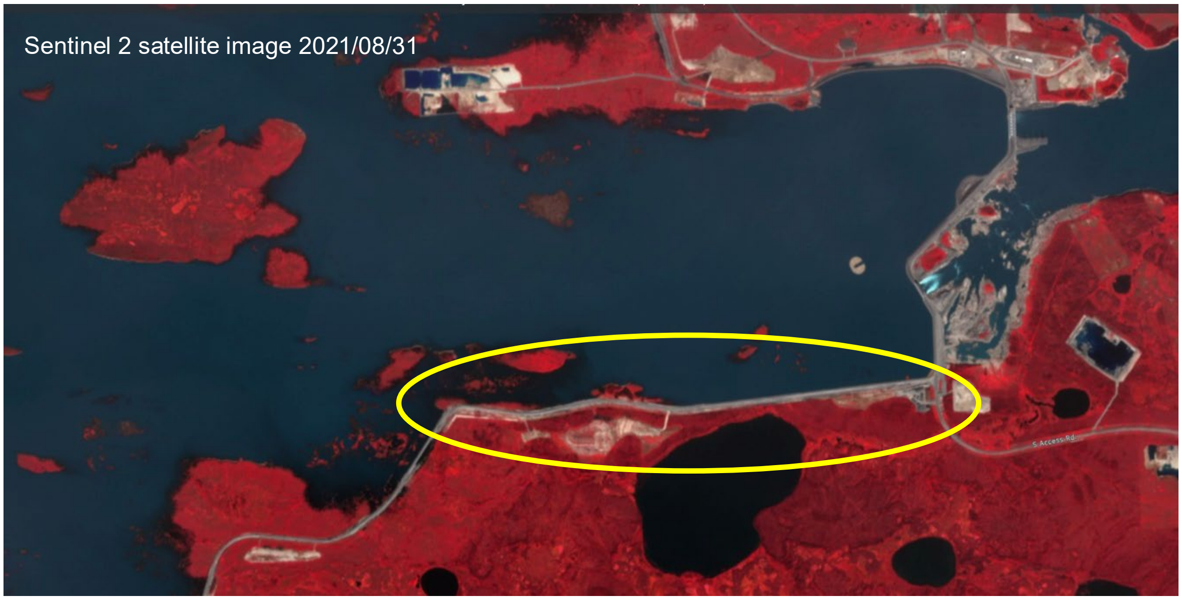

Figure 43: General work area for south dyke debris removal activities

Photo 10: Debris adjacent to south dyke after impoundment (Sep. 5, 2020)

8.0 RESERVOIR GREENHOUSE GAS

The purpose of Keeyask reservoir greenhouse gas monitoring program is to enable the comparison of aquatic greenhouse gas (GHG) concentrations and emissions before and after flooding and reservoir creation. The GHG monitoring program is implemented by Manitoba Hydro in conjunction with the Centre for Earth Observation Science at the University of Manitoba and the report in this section was prepared by the GHG monitoring team (Papakyriakou et. al. 2022).

Studies have shown that GHG emissions from hydroelectric reservoirs in boreal ecosystems increase shortly after flooding (Teodoru et al. 2012). The size and duration of the change in GHG emissions ("reservoir effect") is influenced by many factors including reservoir size, type and amount of biomass flooded, location, water residence time, temperature, etc. (Demarty and Tremblay 2017; Goldenfum 2012). The Keeyask Physical Environment Supporting Volume (KHLP 2012b) predicted that carbon dioxide (CO_2) emissions would approach background levels by approximately 10 years after impoundment and that methane (CH_4) emissions would remain elevated throughout the 100-year life of the Keeyask Generation Project. These predictions were based on IPCC (2006) guidance at that time. Since then, reservoir GHG science has continued to evolve (Delsontro et al. 2018, Prairie et al 2018). Studies have focussed on GHG processes and emission pathways, and how GHG emissions may relate to reservoir characteristics and location. Similarly, the methods used to study GHGs at the Keeyask reservoir have evolved and are described in this report.

8.1 BACKGROUND

The Greenhouse gas monitoring program was expanded in 2017 and has continued until present with the objective to obtain pre- and post-flood data on the magnitude, rates, variability and environmental influences of the GHG exchange.

The impoundment of various natural ecosystems gives rise to additional and more active routes of GHG emissions (largely CO2 and CH4) as the impounded areas adjust to the new environmental changes. The areas of interest in the current study area of the Keeyask reservoir includes flooding of former peatland areas, floating peat islands resulting from displaced peat, expansion of shoreline areas into back bays and wetlands in the areas surrounding and connected with the reservoir. The main GHG emission pathways include (1) diffusion from the water to the atmosphere, (2) ebullition or GHG bubbles originated from sediments, and (3) emission of gases from newly released floating peat areas. The GHGs released from these environments are variable in space and time so can be difficult to measure accurately with point-in-time water sampling, or short-term deployments of chambers in select locations. The micrometeorological technique, eddy covariance (EC), allows near continuous ecosystem wide measurement of GHG exchange from all pathways within an upwind area denoted as the flux footprint. The analysis of water from point-in-time sampling, and deployment of submersible sensors, provide site specific information on GHG source or sink characteristics both within and beyond the EC flux footprint.

In pre-flood seasons (2017-2019), EC monitoring was used to characterize GHG fluxes from the main channel of the Nelson River and a stream/wetland complex, that transitioned to back bay on impoundment. EC information are not available from 2020 due to COVID19 restrictions on access to the field sites. The full program (EC monitoring, point-in-time sampling and deployment of submersible sensors) continued as part of the GHG monitoring program in 2021 after full impoundment of the reservoir in 2020.

8.2 2021 MONITORING ACTIVITIES & ANALYSES

The locations of all water sample and EC monitoring sites are depicted in Figure 44.

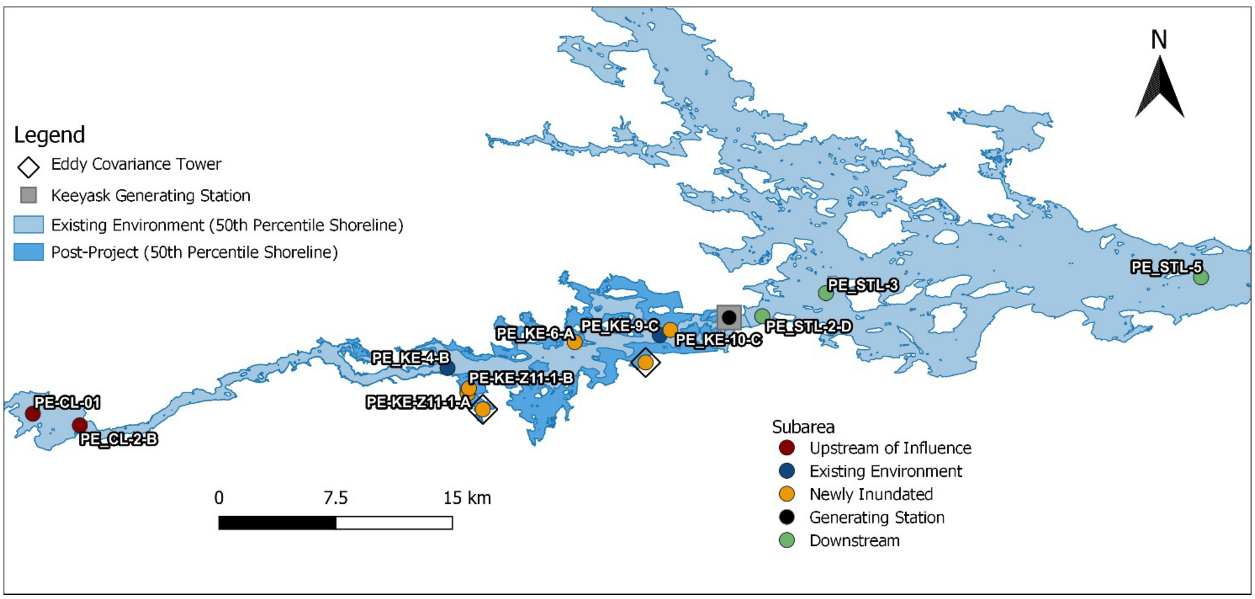

Figure 44: GHG discrete sampling locations in the Keeyask Area for 2021

8.2.1 EDDY COVARIANCE MEASUREMENTS

Two EC towers were deployed in the 2021 season; one along the south dike road (South Dike Road Tower) near the Keeyask spillway, approximately 4.5-5km upstream, and another in the Back Bay area resulting from flooding of the Rabbit Creek wetland complex connected to the Nelson River that is approximately 15-15.5km upstream of the Keeyask axis (Back Bay Tower). Towers are designated as diamonds in Figure 44. Eddy covariance resolves a flux from a contributing area (flux footprint) upwind of the instrumented tower.

8.2.2 SOUTH DIKE ROAD TOWER

The Dike Road EC tower was deployed May 6th, 2021, and ran continuously until November 9th, 2021, with the full complement of eddy covariance instrumentation (56°19'20.54"N, 95°17'15.24"W, Figure 44, Photo 11). In November, a reduced selection of instruments remained in use to monitor over winter fluxes (CO_2 and associated meteorological data).

1) LI-7500 CO¬2/H_2O Analyzer
2) Gill Windmaster Pro 3D Sonic Anemometer
3) LI-7700 CH_4 Analyzer
4) LI-7200 CO_2/H_2O Analyzer
5) Wind Turbine for additional power generation

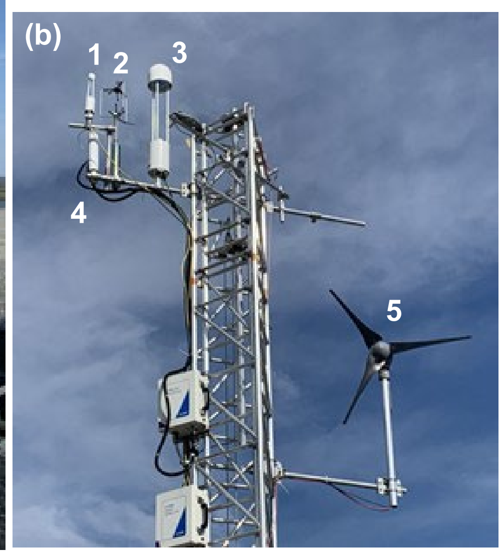

Photo: A. Soloway. Image Date: September 1, 2021

Photo 11: Dike road eddy covariance tower. (a) whole tower (b) instruments

The EC instruments measured 3D wind (Gill WindMaster Pro, Gill Instruments, Hampshire, UK), CO_2/H_2O concentrations (LI-7200, LI-COR Biosciences, Lincoln, NB, USA), CH_4 concentrations (LI-7700, LI-COR Biosciences, Lincoln, NB, USA) as well as relevant meteorological variables: temperature and relative humidity (HMP155, Vaisala, Finland), photosynthetically active radiation (PAR, LI-190R, LI-COR Biosciences, Lincoln, NB, USA). The measurement area was representative of the reservoir (mainly the new shoreline – discussed further in footprint analyses, Photo 12) near the Keeyask Generating Station and spillway.

Note emerging peat and vegetation
Photo: A. Soloway. Image Date: August 31, 2021

Photo 12: Aerial view of the south dike road tower site

8.2.3 BACK BAY TOWER

The Back Bay tower was deployed May 3rd, 2021, until removal for the winter season on November 9th, 2021 (56°17'31.56"N, 95°27'17.29"W, Figure 44, Photo 13). EC instrumentation was the same complement as at the south dike road site, but at a measurement height of 5.22m above water level. The back bay is adjacent to the Nelson River main channel, approximately 15km upstream of the generating station and spillway. The measurement footprint is representative of shallow water/flooded peatland components of the reservoir (Photo 14).

Site visits occurred approximately monthly, during which time sensors were checked for proper functioning, cleaning, maintenance and to download data.

8.2.4 DATA PROCESSING AND POST-PROCESSING

Processing of raw EC data in intensive and systematic. For example, data is removed when: sensor signal strength is low; wind speeds are outside of designated thresholds; and flux measurements vary by more than an established deviation. Modelling techniques are applied to filter out confounding variables in environments where GHG fluxes are small.

Photo: A. Soloway. Image Date: August 31, 2021

Photo 13: Back bay tower looking towards north

Photo: A. Soloway. Image Date: August 31, 2021

Photo 14: Aerial view of the Back Bay site showing heterogeneity after impoundment

8.2.5 POINT-IN-TIME WATER SAMPLE PROGRAM

Discrete water samples were taken in collaboration with the Keeyask PEMP sampling at locations spanning from Clark Lake to the Kettle Generating Station forebay throughout the year (Figure 44). Thus, including environments upstream, within and downstream of the Keeyask complex. Sampling sites differed during the ice-covered period versus the open-water period (Table 10). As in 2020, our protocol was adapted to facilitate sampling alongside those taken for the Physical Environment Monitoring Plan (PEMP) monthly survey. Samples were taken at 20% of the total water column depth, and additionally at 80% depth when possible. Point-in-time samples were also taken during UM EC tower site visits (Photo 15), and bi-weekly within the Generating Station year-round. Parameters analyzed, as well as analysis and sampling details are included in Table 11.

Table 10: Summary of monthly discrete sampling locations in 2021

SITE NAME	JAN	FEB	MAR	APR	MAY	JUN	JUL	AUG	SEP	OCT	NOV	DEC
Generating Station			X*	X	X	X	X	X	X	X	X	X
Dike Road Tower						X	X		X	X	X	
Back Bay Tower						X		X		X	X	
PE_CL-1	X	X	X	X								
PE_CL-2-B						X	X	X	X			
PE_KE-10-C						X	X	X	X			
PE_KE-4-B						X	X	X	X			
PE_KE-6-A	X	X	X	X								
PE_KE-9(-C)	X	X	X	X								
PE_KE_Z11-1-A	X	X	X	X								
PE_KE-Z11-1-B							X	X	X			
PE_STL-2-D						X	X	X	X			
PE_STL-3 (PE_STL_4)	X	X	X	X								
PE_STL-5							X	X	X			

* X indicates that a site was sampled in that month

8.2.6 AQUATIC SUBMERSIBLE GHG SENSORS

Two rafts were deployed in the 2021 field season to directly measure aquatic GHG concentration periodically throughout the day from June 26th to September 26th, 2021. A raft located mid-channel (PE_KE-4-B, Figure 44, Photo 16), and a raft located within the back bay (PE_KE_Z11-1-A, Figure 44, Photo 17) were equipped with a submersible pCO2 sensor (CO2-Pro CV, Pro-Oceanus, Halifax, NS) and a submersible pCH4 sensor (CONTROS HydroC-CH4, 4H Jena Engineering, Jena, Germany).

Photo: A. Soloway. Image Date: May 12, 2022

Photo 15: Water sampling on the dike road eddy covariance tower site

Table 11: Water analyses for 2021 Keeyask water sampling program

VARIABLE	UNITS	LOCATION OF ANALYSIS	SUBSAMPLING GLASSWARE	DETECTION LIMIT
Suspended nitrogen (SuspN)	mg L^{-1}	FWI*	N/A	0.7 mg N
Total dissolved nitrogen (TDN)	mg L^{-1}	FWI	N/A	8 mg L^{-1}
Suspended phosphorus (SuspP)	mg L^{-1}	FWI	N/A	0.4 mg L^{-1}
Total dissolved phosphorus (TDP)	mg L^{-1}	FWI	N/A	0.4 mg L^{-1}
Suspended organic carbon (SuspC)	mg L^{-1}	FWI	N/A	7.06 mg C
Dissolved organic carbon (DOC)	mmol L^{-1}	FWI	N/A	13.1 mmol L^{-1}
Chlorophyll a (Chla)	mg L^{-1}	FWI	N/A	0.52 mg L^{-1}
Total suspended sediment (TSS)	mg L^{-1}	UM	N/A	2.5 mg L^{-1}
pH	pH units	UM	N/A	± 0.01**
Conductivity	mS cm^{-1}	UM	N/A	0.1 mS cm^{-1}
Dissolved inorganic carbon (DIC)	mmol kg^{-1}	UM	12mL Exetainer	7 mmol kg^{-1}
Total alkalinity (TA)	mmol kg^{-1}	UM	12mL Exetainer	20 mmol kg^{-1}
Dissolved methane concentration	nmol L^{-1}	UBC	60mL serum vial	0.4 nmol L^{-1}
* Locations: Freshwater Institute, Department of Fisheries and Oceans (FWI): University of Manitoba (UM) and University of British Columbia (UBC)				
**Relative accuracy; detection limit not applicable				

Location of point in time sampling & where submersible GHG sensors deployed
Photo: A. Soloway. Image Date: August 31, 2021

Photo 16: Aerial view of the mid-channel raft (site: PE_KE-4-B)

Location of point in time sampling & where submersible GHG sensors deployed
Photo: A. Soloway. Image Date: August 31, 2021

Photo 17: Aerial view of the back bay raft (site: PE-KE-Z11-1-A)

The CO2 instruments were set to measure three times per day, early morning, mid-afternoon, and in the evening (5:30 am CDT, 1:30pm CDT and 9:30pm CDT).

The CH4 sensors were set to measure only once per day (due to higher power requirements) during mid-afternoon.

Incidents of low power disrupted the internal sensor programming effecting both the frequency of dissolved CH4 and CO2 measurements. CO2 measurements were affected at the main reservoir raft (PE_KE-4-B) yielding only a small number of measurements in August.

8.2.7 Bulk Flux Calculation

Bulk diffusive fluxes for CO_2 and CH_4 were calculated using the diffusion-limited stagnant film model (Liss and Slater, 1974, Wanninkhof et al. 2009) requiring measurements of windspeed, water temperature, the partial pressures of CO2 and CH4 in the waterside of the air-water inface, and in the lower atmosphere. The transfer velocity required for the flux determination was modeled after Vachon and Prairie (2013). The calculated diffusive fluxes provide an indication of gas exchange in environments beyond the EC flux footprint.

8.3 GHG MONIORING RESULTS

8.3.1 EDDY COVARIANCE GHG FLUXES – DIKE ROAD SITE

Footprint & Data Coverage

The EC flux tower measurement footprint and tower location are presented in Figure 45.

- These constitute the first direct GHG flux measurements over a seasonal transition from late spring, through fall, and into the winter over a peatland in the Canadian boreal - subarctic transition newly flooded for hydroelectric production.
- The measurement footprint is critical for interpreting flux results based on the area being measured.
- Modelled footprint indicates the tower represents fluxes measured within a radius of 600 m of the tower (only data on the reservoir side of the Dike Road were considered).
- These areas were shallower (under 2m in depth) and had patches of emerging vegetation (note aerial photograph – Photo 12).
- The flux footprint for the dike road tower best represents fluxes from the former riverbank area of the newly formed reservoir – an area experiencing high rates of change and new water inundation.
- Particularly for CH4 flux, new inundated peaty zones are responsible for the majority of released methane during hydroelectric reservoir impoundment. As will be discussed

further in this report, the EC measurements are strongly impacted by newly submerged shoreline area of the reservoir while deeper reservoir areas may best be represented by bulk flux measurements calculated using water samples and submersible sensor in deeper areas.

- Data coverage was excellent throughout the 2021 field season at the Dike Road. A gap in CH4 flux occurred in part of August (~2 weeks) because the opacity of the sensor lens degraded due to the deposition of air-borne particulates.

The blue circle (approximate 600m radius from the tower) represents the area which is representative of 90% of the fluxes. and Spillway. Note only data on the reservoir side of dike road were included in analyses.

Figure 45: Measurement footprint of the dike road tower site

Flux results from the eddy covariance measurements at the Dike Road EC tower site are presented in Figure 46 and statistically summarized in Table 12.

CO2 Flux

- CO2 Flux increased in magnitude (both emissions and uptake) rapidly between ice break in May and warmer summer months July and August following seasonal trends
- Peak average CO2 fluxes were measured in July (6.03 ± 3.81 g/m2/d, mean ± SD) while lowest average CO2 fluxes were measured during ice cover conditions in May (0.55 ± 0.82 g/m2/d), a difference of a factor of 12.
- As seasonal weather cooled, fluxes decreased in magnitude until December when the ice cover period begins again and flux processes slow, becoming more similar to fluxes in May (0.71 ± 0.47 g/m2/d).

CH4 Flux

- CH4 flux mirrored rapid initial increases in magnitude observed in CO2 flux and decreased until November when the instrument was removed for the winter.
- Overall, seasonal CH4 flux was 62.53 ± 57.10 mg/m2/d. The large standard deviation accounting for the vastly different averages in the shoulder seasons compared to open water/mid-summer season
- Mean CH4 flux increased in magnitude by nearly 20x between the ice-covered period in May (4.9 ± 7.24 mg/m2/d) and August (120.25 ± 53.85 mg/m2/d) – note sample size in August is smaller than other months.

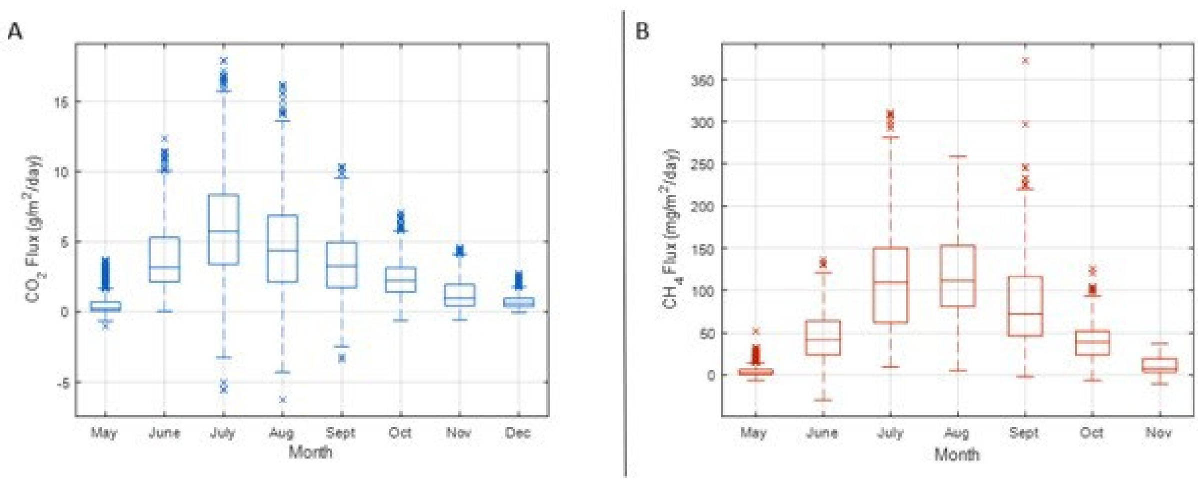

Each boxplot contains all flux measurements made during the month indicated. Note that due to the need for instrument cleaning, data available for CH4 flux during August is based on limited data (N=112 measurements).

Figure 46: Greenhouse gas fluxes by month throughout the 2021 study period at the dike road site (May – December) for (A) CO_2 and (B) CH_4

Table 12: Statistical summary of GHG fluxes measured at the dike road EC tower

	May	June	July	August	Sept	Oct	Nov	Dec	All Data
CO_2 FLUX (g/m^2/day)									
10th	-0.1	1.31	1.45	0.43	0.55	0.81	0.2	0.2	0.05
Q1	0.06	2.11	3.41	2.09	1.72	1.41	0.44	0.38	0.17
median	0.23	3.19	5.72	4.35	3.28	2.19	0.96	0.61	0.51
mean	0.55	3.85	6.03	4.66	3.4	2.35	1.29	0.71	0.75
Q3	0.7	5.29	8.35	6.82	4.94	3.16	1.91	0.94	1.09
90th	1.91	7.21	11.02	9.19	6.31	4.09	3	1.36	1.83
SD	0.82	2.33	3.81	3.46	2.19	1.31	1.07	0.47	0.77
SE	0.03	0.07	0.1	0.1	0.07	0.04	0.03	0.01	0.01
n	953	998	1400	1089	1093	1318	1314	1481	9646
CH_4 FLUX (mg/m^2/day)									
10th	-0.42	10.82	36.03	62.88	31.29	15.19	2.05		2.95
Q1	0.58	23.35	62.09	81.07	46.25	23.59	3.58		18.85
median	1.93	41.58	109.21	111.21	72.2	38.67	7.8		47.26
mean	4.9	46	111.78	120.25	86.11	39.95	11.42	N/A	62.53
Q3	6.06	64.03	150.13	153.19	116.45	52.18	19.12		92.85
90th	16.24	88.81	188.65	190.82	156.52	65.47	24.72		146.93
SD	7.24	29.93	59.76	53.85	52.37	20.41	9.48		57.10
SE	0.36	1.43	2.32	5.09	2.41	0.9	0.73		1.09
n	397	437	663	112	471	511	168		2759

CO_2 fluxes represent 15-minute averages, dictated by the ogive optimization script, while the CH_4 fluxes represent 30-minute averages. (10th and 90th signify 10th and 90th percentiles respectively).

8.3.2 EDDY COVARIANCE GHG FLUXES – BACK BAY SITE

Footprint & Data Coverage

The EC flux tower measurement footprint and tower location are presented in Figure 47.

- Measurement footprint accurately represents the makeup of the back bay area and newly inundated, heterogeneous patches of water, and emergent vegetation (note aerial imagery – Photo 14).
- Data coverage was more limited at the back bay than at the reservoir tower site – one data gap occurred from mid-August to mid-September due to power issues (tripped breaker).

- Another significant gap occurred in the CH4 data just prior to this, mid-July to early August because the opacity of the sensor lens degraded due to the deposition of air-borne particulates.

The blue circle represents the area which is representative of 90% of the fluxes (an approximate 335m radius from the tower). Inset image: Note only data north of the tower were considered in analyses. (Sentinel, Imagery Data: July 29, 2021).

Figure 47: Measurement footprint of the back bay tower site

Results from the eddy covariance measurements at the Back Bay EC tower site are presented in Figure 48 and statistically summarized in Table 13. Highlights are itemized below.

CO2 Flux

- Overall, during the 2021 study period, CO2 fluxes measured at the back bay averaged 3.92 ± 4.02 g/m2/d

- CO2 flux increased in magnitude (both emissions and uptake) from the beginning of the study period in May during the ice-covered period until July/August/September. Average CO2 flux dropped slightly in August (4.87 ± 5.9 g/m2/d), likely attributable to the presence of a greater uptake in CO2 by emerging vegetation in the back bay area during peak growing season.
- CO2 flux was largest during September (7.48 ± 3.61 g/m2/d) and smallest on average, in November (0.92 ± 0.93 mg/m2/d), the coldest month of the study period.

CH4 Flux

- Overall, throughout the 2021 study period, Back Bay CH4 fluxes were 116.66 mg/m2/d.
- Significant data loss occurred with the CH4 sensor in particular, as previously mentioned.
- Unlike the Dike Road fluxes, the Back Bay experienced a surge in CH4 flux in May (135.72 ± 186.01 mg/m2/d, corresponding with the timing of ice melt. The range of value recorded in May was also the largest (SD = 186.01 mg/m2/d). This observation is consistent with a release of GHGs, which had accumulated under the capping ice cover over the winter months, on ice thaw and break-up.
- CH4 fluxes appear to increase in magnitude through the course of the study period until September when largest average fluxes were measured (222.11 ± 18.52 mg/m2/d).

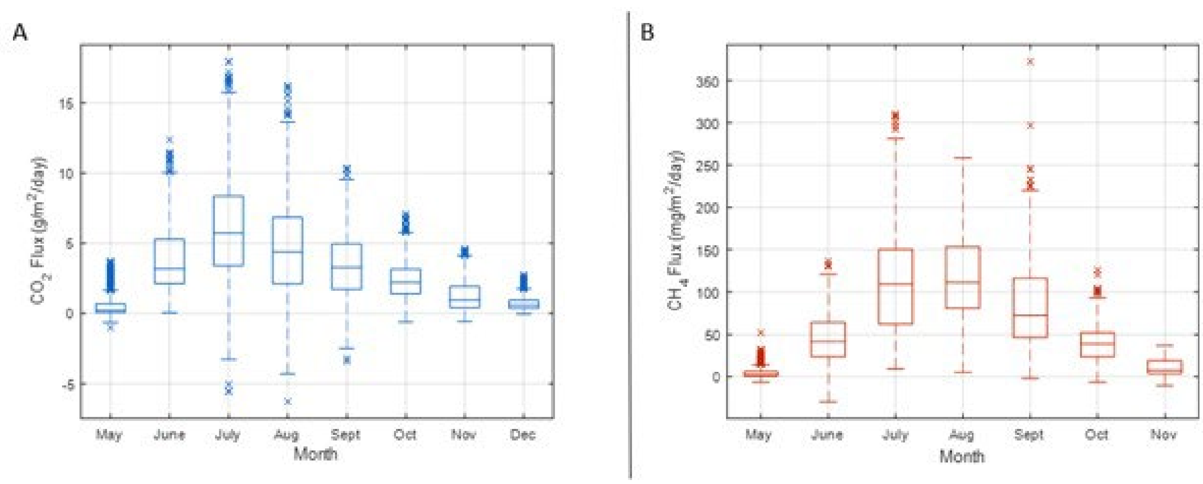

Each boxplot contains all flux measurements made during the month indicated. There was abnormally high data lost between mid-August and mid-September due to a power failure, and heightened deposition of airborne particulates on the sensor lens degrading sensor function.

Figure 48: Greenhouse gas fluxes by month throughout the 2021 study period at the back bay site (May – November) for (A) CO_2 and (B) CH_4

Table 13: Statistical summary of GHG fluxes measured at the dike road EC tower

	May	June	July	August	Sept	Oct	Nov	All Data
CO_2 FLUX ($g/m^2/d$)								
10th	0.04	1.24	1.07	-1.05	2.11	1.04	0	0.09
Q1	0.14	2.25	3.2	1.2	5.89	1.67	0.21	0.99
median	0.77	3.28	5.5	4	7.76	2.6	0.72	3.12
mean	1.93	3.7	5.67	4.87	7.48	3.08	0.92	3.92
Q3	2.75	4.67	7.76	7.33	9.43	4.06	1.24	5.9
90th	5.61	6.83	10.72	12.41	11.99	5.97	2.29	9.06
SD	2.65	2.19	3.82	5.9	3.61	1.97	0.93	4.02
SE	0.07	0.07	0.12	0.19	0.27	0.13	0.1	0.06
n	1381	1081	1065	974	178	222	88	4989
CH_4 FLUX ($mg/m^2/day$)								
10th	2	28.27	50.45	64.93	106.52	28.47	0.36	5.64
Q1	7.41	40.26	59.18	73.17	179.07	38.8	3.34	31.74
median	53.08	79.55	90.63	101.44	236.7	49.61	8.51	67.84
mean	135.72	90.53	160.34	109.16	222.11	53.01	12.91	116.66
Q3	181.81	129.23	179.14	152	279.49	65.34	24.29	150.67
90th	428.09	173.73	414.46	155.33	294.22	80.56	38.25	281.1
SD	186.01	56.51	157.55	39.58	70.37	18.52	17.28	140.28
SE	8.07	2.61	17.09	12.52	11.27	2.67	3.46	4.04
n	531	468	85	10	39	48	25	1206

CO2 fluxes represent 15-minute averages, dictated by the ogive optimization script, while the CH4 fluxes represent 30-minute averages. (10th and 90th signify 10th and 90th percentiles respectively).

8.3.3 ANALYSES ON DISCRETE WATER SAMPLES

As in 2020, delays due to COVID-19 prevented data from FWI being presented in this report (see Table 11 for relevant variables). A summary of variables important to the aquatic inorganic carbon system and methane is presented in Table 14. To illustrate the differing distributions of these variables in certain locations throughout the study area, boxplots grouped by subarea are presented in Figure 49 (refer to Figure 44 for attribution of sites to subareas).

Highlights from the analyses are:

- A spatial depiction of dissolved greenhouse gas concentrations throughout the study area is provided in Figure 50.
- Dissolved gas concentrations appeared homogenous during the ice-cover period, however, there was noticeable variation during the open-water period when compared with shallow, newly inundated areas to the existing environment.
- Median CH4 concentration during the ice-cover period was consistently low across all sites (8-100 µatm) but varied greatly in the open-water period.
- Calculated pCO2 and pCH4 (Figure 51) has been more consistent and less variable for the main channel areas than back bay areas.

Table 14: Univariate statistics for water quality parameters from all discrete water samples taken in 2021

	T (°C)	pH	TA (mmol kg^{-1})	DIC (mmol kg^{-1})	pCO_2calc (µatm)	pCH_4 (µatm)
Min	0.0	7.02	1194.61	1186.53	430.4	1.7
10th	0.6	7.55	1507.11	1466.05	769.5	8.3
Median	10.7	7.80	1582.81	1555.51	1190.0	18.0
Mean	8.7	7.75	1670.43	1645.77	1146.0	84.3
90th	19.0	7.93	1902.95	1901.65	1990.2	156.3
Max	19.9	8.01	1951.13	2048.15	7105.9	1510.8

(10th and 90th signify 10th and 90th percentiles respectively). The pCO2 was calculated using measured DIC and pH and carbonate equilibria expressions within the software, CO2SYS (Pierrot et al. 2006, Lewis and Wallace 1998)

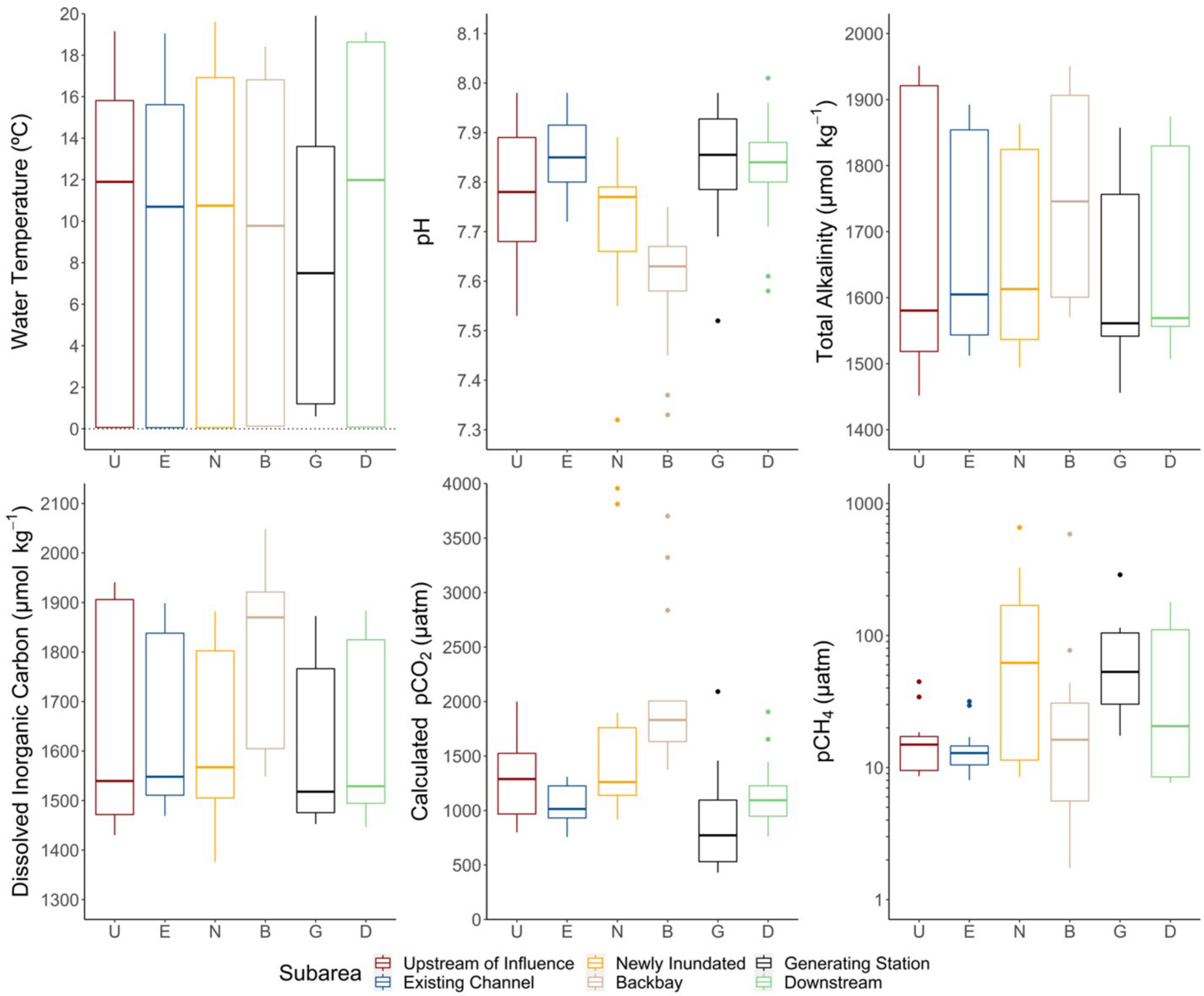

See Figure 43 for spatial presentation of subareas. “Newly Inundated” refers to locations that were flooded after impoundment, excluding sites in the back bay. Data from all discrete samples taken in 2021 is included in this figure.

Figure 49: Boxplots depicting the distribution of water quality variables for various subareas within the study area

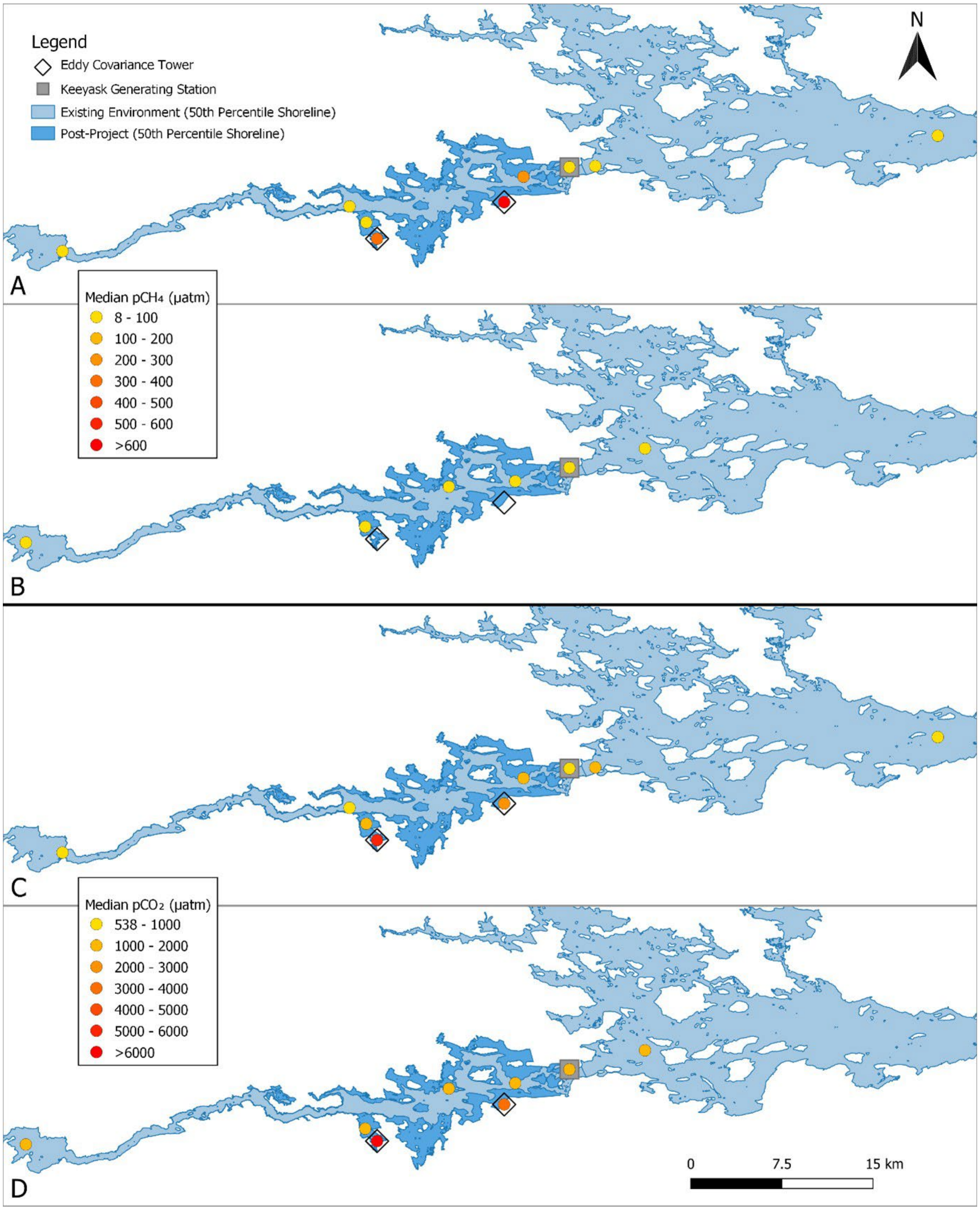

Figure 50: Spatial variation in pCH_4 during (A) open-water period and (B) ice-cover period; and pCO_{2calc} during (C) open-water period and (D) ice-cover period

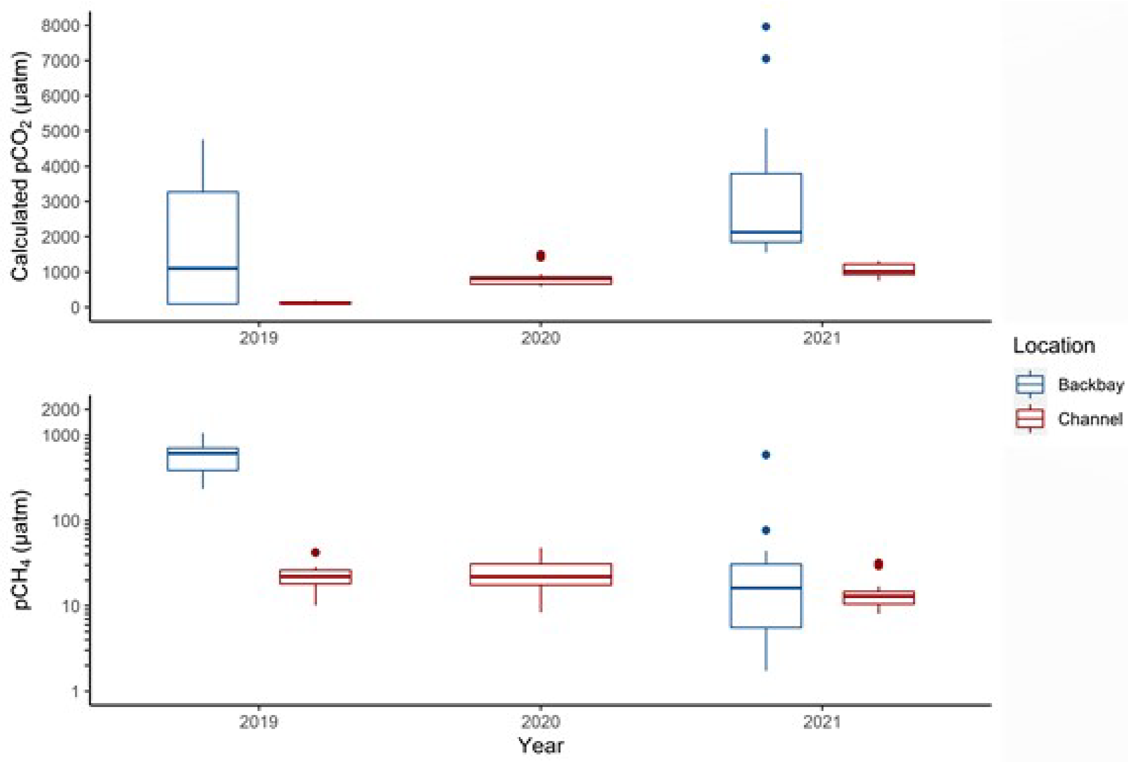

In 2019, pCO2 was calculated with DIC and TA rather than DIC and pH..

Figure 51: Comparison of calculated pCO_2 and pCH_4 for existing channel and back bay locations

8.3.4 CONTINUOUS MEASUREMENT OF pCO_2 AND pCH_4

The distribution of measurements of dissolved gases CO_2 and CH_4 (expressed as partial pressure) from the rafts at PE-KE-4-S (Channel) and PE-Z-11-1-a (Back Bay) are shown in Figure 52, and summarized in Table 15 and **Error! Reference source not found.**. An automated measure of pCO_2 was unavailable from the channel raft due to an instrument malfunction. Highlights are itemized below.

- The submersible sensors provide important information on temporal trends in dissolved gas concentration at a location.
- Median values for pCO2 from PE-Z-11-1-a (Back Bay) increased from July through to September. The degree of oversaturation relative to atmospheric levels (assuming atmospheric pCO2 of 400 µatm) ranged from ~4 in July to ~7 in September.
- Measured median pCO2 for the full data set from PE-Z-11-1-a (2227.78 µatm) is larger than the median value of pCO2Calc (1901.95 µatm) shown in Figure 13. Differences can arise from discrepancy between measured and modeled pCO2 using carbonate equilibria expressions, while also water was sampled from station PE-Z-11-1-b, that was situated

downstream of the PE-Z-11-a (location of the submerged sensor). PE-Z-11-1-b is downstream of PE-Z-11-1-a and closer to the thalweg of the pre-existing Rabbit Creek.

- Both back bay and channel sites were supersaturated in CH4. The degree of supersaturation relative to atmospheric levels was higher in the Back Bay relative to the Channel. The highest concentration of CH4 was distinctly observed in July in the Back Bay (median of 222.3 µatm), while median CH4 concentrations were similar across summer months in the Channel.
- Measured median CH4 for the entire data set from PE-Z-11-1-a (106.45 µatm) was substantially higher than CH4 measured on discrete water (16.24 µatm). The differences may be attributed to differing location of the automated sensor (upstream of the discrete water sampling station PE-Z-11-1-b, and farther from the thalweg of the pre-existing Rabbit Creek).

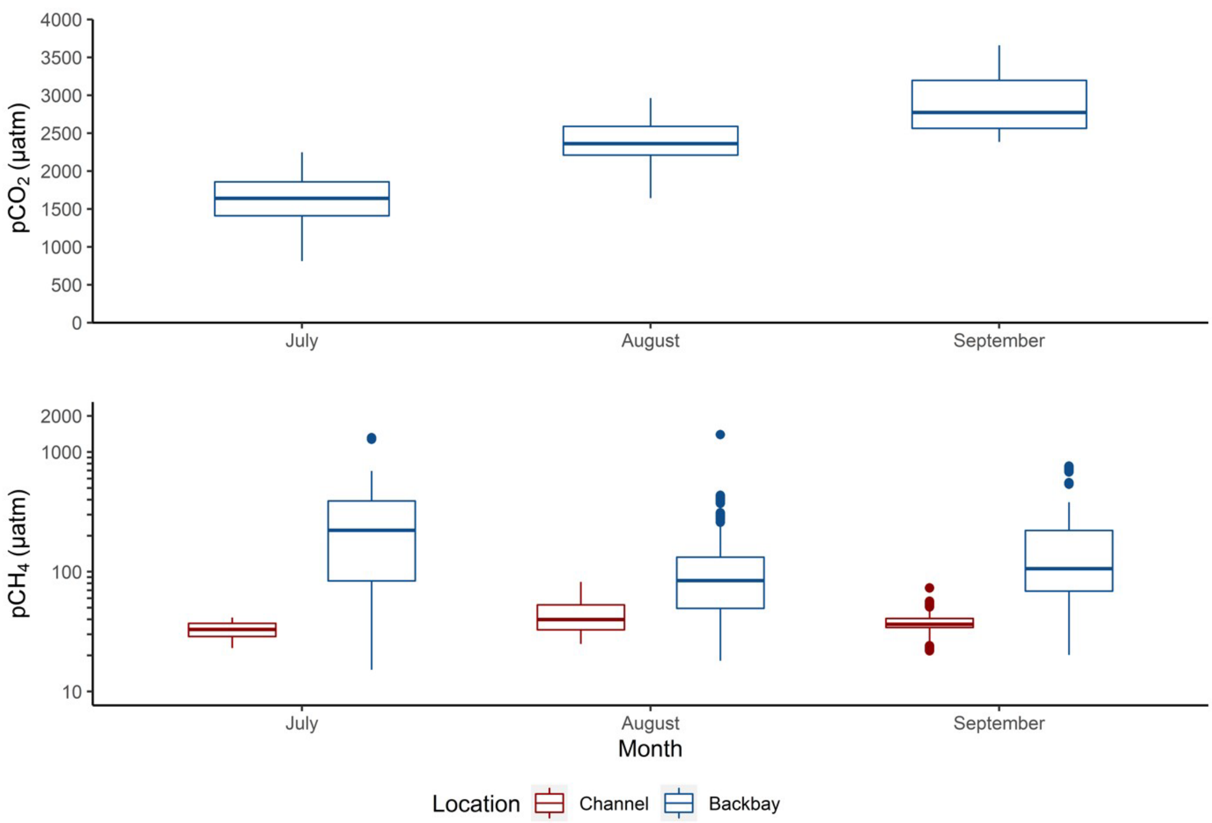

Figure 52: Monthly distributions of continuous pCO_2 and pCH_4 measured by the CO2-Pro CV and the CONTROS HydroC-CH4 in 2021 for the channel (PE-KE-4-S) and back bay (PE-Z-11-1-a) continuous monitoring locations

Table 15: Statistical summary of Back Bay submersible sensor dissolved gas concentrations

	June	July	August	September	Full Dataset
			pCO_2 (µatm)		
10th	749.59	1227.42	1975.03	2491.53	1272.83
Q1	801.06	1407.52	2209.55	2561.45	1661.52
median	928.38	1640.75	2362.96	2772.66	2227.78
mean	883.37	1620.47	2361.44	2866.89	2146.62
Q3	954.14	1858.71	2593.82	3201.27	2590.62
90th	993.58	2068.53	2686.06	3311	3011.39
SD	98.72	316.19	289.02	338.5	641.98
SE	27.38	32.79	29.97	42.65	39.66
n	13	93	93	63	262
			pCH_4 (µatm)		
10th	196.03	29.51	30.63	51.32	48.77
Q1	197.67	83.87	49.44	69.01	67.88
median	206.99	222.32	84.47	106.06	106.45
mean	233.57	257.59	116.5	159.67	163.81
Q3	296.09	390.41	132.62	221.24	230.38
90th	297.58	580.97	241.74	355.81	361.04
SD	45.67	220.49	111.15	115.24	128.01
SE	7.61	11.98	5.85	1.79	1.83
n	36	339	361	4162	4898

8.3.5 BULK FLUX CALCULATIONS FOR CO_2 AND CH_4

The distributions of the diffusive fluxes for CO_2 and CH_4 using the bulk-flux model are shown in Figure 53 and Figure 54 using dissolved gases resulting from the discrete water sampling program and submersible sensors respectively. Statistics on the distributions are provided in Table 17 and Table 18. A summary of highlights follows.

- The diffusive fluxes of CO_2 appear similar in both mean and median values among upstream, existing channel, and downstream (Figure 53 and Table 17).
- The largest diffusive fluxes of CO_2 were observed at Back Bay stations, followed by stations in the shallow water over newly inundated peatland. The lowest fluxes corresponded to concentration data from the generating station.

Table 16: Statistical summary of main Channel (PE-KE-4-S) submersible sensor dissolved CH4 concentration

	pCH$_4$ (µatm)*				
	June	July	August	September	Full Dataset
10th	15.79	27.53	32.48	26.8	26.64
Q1	17.77	28.81	32.8	34.29	32.79
median	19.34	33.02	39.91	36.41	36.36
mean	19.59	33.06	46.96	39.39	40.66
Q3	19.91	37.15	53	40.74	47.28
90th	26.46	40.2	80.71	56	56.43
SD	3.22	4.86	17.48	9.8	14.25
SE	0.35	0.39	0.69	0.33	0.34
n	84	155	650	895	1784

**CO_2 data is omitted due to insufficient data due to instrument malfunction*

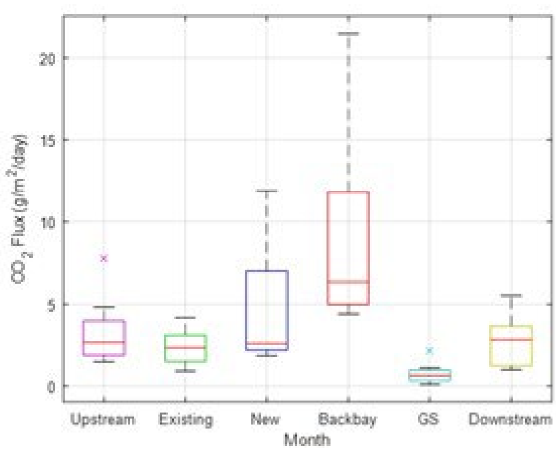

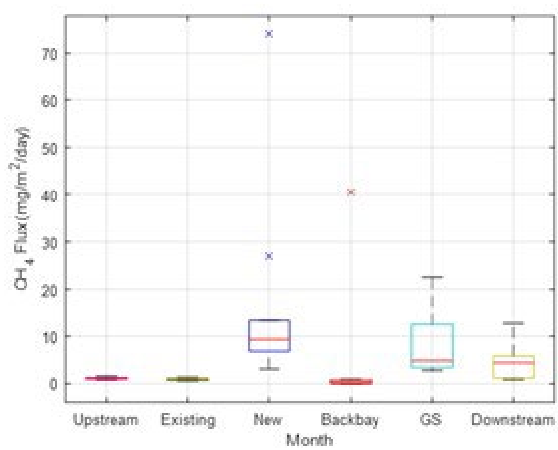

Fluxes are shown by subarea (Figure 43).

Figure 53: Bulk flux of CO_2 (a) and CH_4 (b) calculated using dissolved gases resulting from the discrete water sampling program between June and September

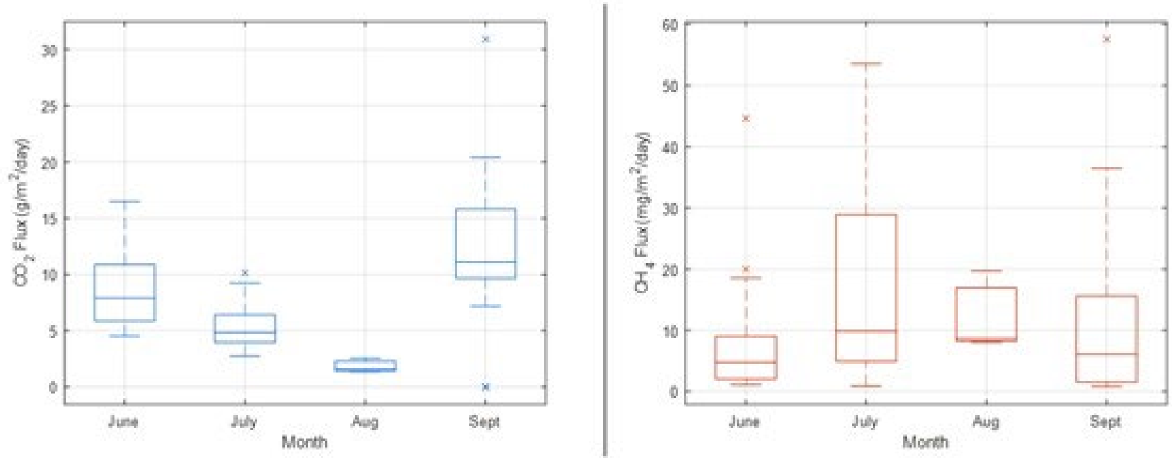

Figure 54: Bulk flux calculated from submersible sensor data at the back bay raft (PE-Z-11-1-a), by month for (a) CO2 flux, (b) CH4 flux

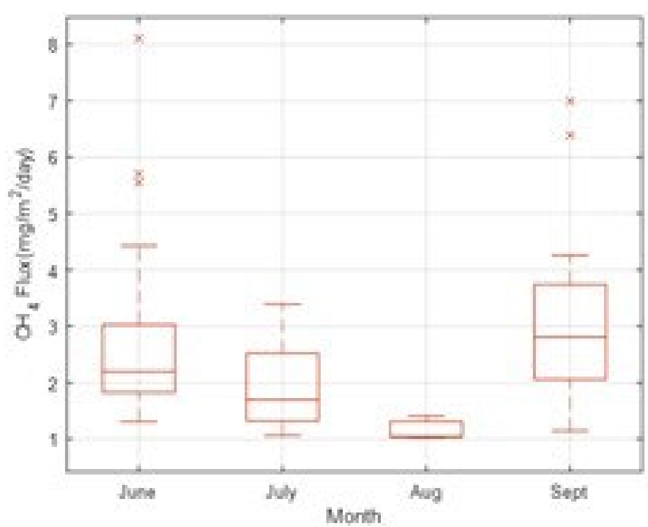

Figure 55: Bulk flux calculated from submersible sensor data at the main channel raft (PE-KE-4-S), by month for CH_4 flux

- The largest diffusive CH_4 fluxes (by mean and median) were observed at the stations in shallow water over the newly inundated peatland, followed by the generating station samples and downstream stations, in that order.
- High CO_2 and CH_4 fluxes over shallow newly inundated peatland of zone E is the direct consequence of organic carbon degradation in the water column and substrate within this zone, in conjunction with larger water residence time relative to other zones within the

reservoir complex. It is speculated the relative high outgassing of CH_4 at the generating station is associated with the high dissolved CH_4 concentrations observed in the shallow, newly inundated peatland that underlies a high areal proportion of the reservoir surface directly upstream of the station forebay. A large flux of CO_2 on the other hand is not observed from generating station water samples. The partial pressure of CO_2 is relatively low in the water samples from the existing channel, and in generator water samples. This could be the combination of lower respiration of CO_2 in these waters relative to photosynthesis, the higher water solubility for CO_2 in the marginally cooler water at the generating station intake relative to other stations (Figure 49), and higher water solubility for CO_2 relative to CH_4. Additional analysis is needed to confirm these processes.

- The diffusive flux of CO_2 at PE-Z-11-1-a is largest in September (Figure 53a), followed by June, July, and August. June values are based on only 3-days of data. While pCO_2 at the station increased from July to September (Figure 52), median, 75th and 90th percentile windspeed was larger in both July and September relative to August, supporting larger rates of outgassing. A similar trend was observed from eddy covariance fluxes shown in Figure 48.
- The highest median diffusive fluxes of CH_4 at PE-Z-11-1-a were observed in July and August, with July showing larger variability surrounding the flux (Figure 53b). The direct measures of CH_4 fluxes using eddy covariance fluxes were generally higher than the calculated diffusive fluxes. The eddy covariance flux footprint is in a shallower upstream portion (presumably longer residence time and warmer water and substrate) of the Back Bay relative to the location of PE-Z-11-1-a, and the contributing area includes diffusive emissions, in addition to emissions associated with ebullition flux.

Table 17: Statistical summary of diffusive GHG fluxes calculated using the bulk-approach and associated with the discrete water sampling program between June and September

	U	E	N	B	G	D
			CO_2 ($g/m^2/d$)			
10th	1.51	1.26	2.12	4.58	0.21	1.17
Q1	2.06	1.57	2.25	5.15	0.35	1.29
median	2.66	2.32	2.58	6.35	0.66	2.81
mean	3.28	2.36	4.57	9.02	0.77	2.79
Q3	3.52	2.84	6.52	9.97	0.93	3.58
90th	5.71	3.73	8.37	17.30	1.42	4.94
SD	2.10	1.08	3.38	6.17	0.65	1.54
SE	0.74	0.38	1.07	2.18	0.23	0.41
n	8	8	10	8	8	14
			CH_4 ($mg/m^2/d$)			
10th	0.86	0.62	5.37	0.03	2.82	1.02
Q1	0.99	0.73	6.99	0.05	3.72	1.76
median	1.14	0.86	9.32	0.28	4.83	4.39
mean	1.15	0.91	16.65	5.36	8.35	4.86
Q3	1.27	1.06	12.60	0.81	9.57	5.61
90th	1.41	1.27	31.71	12.80	19.61	10.58
SD	0.26	0.28	21.21	14.22	7.66	3.74
SE	0.09	0.10	6.71	5.03	2.71	1.00
n	8	8	10	8	8	14

U, E, N, B, G, D represent respectively upstream, existing channel, newly inundated, back bay, generating station and downstream. See Figure 44 for spatial presentation of subareas. "Newly Inundated" refers to locations that were flooded after impoundment, excluding sites in the back bay.

Table 18: Statistical summary of diffusive GHG fluxes

	Back Bay Fluxes (PE-Z-11-1-a)* CO_2 Flux ($g/m^2/day$)	CH_4 Flux ($mg/m^2/day$)
10th	3.47	1.25
Q1	4.93	2.45
Median	7.59	7.13
Mean	8.43	12.08
Q3	10.97	16.46
90th	15.02	36.40
SD	5.03	13.40
SE	0.52	1.43
n	92	88

	Channel Fluxes (PE-KE-4-S)* CH_4 Flux ($g/m^2/day$)
10th	1.22
Q1	1.55
Median	2.15
Mean	2.47
Q3	3.05
90th	3.92
SD	1.33
SE	0.14
n	87

Calculated using the bulk-approach using data from submersible sensors between June and September at the Back Bay (PE-Z-11-1-a), and channel station (PE-KE-4-S)

8.4 GHG SUMMARY

The 2021 field season marks the first opportunity given COVID-19 restrictions for post-inundation eddy covariance measurements within environments of the newly formed reservoir complex, and the second year of water sampling and submersible sensor programs.

- The EC flux observations for GHGs at the south dike road are the first for a northern peatland reservoir that span the spring through to winter season. The system was a source of CO2 to the atmosphere over the entire deployment, and source of CH4 between May and November, after which time CH4 EC measurements for the gas were discontinued. As expected, ice effectively mitigates against gas exchange during the winter and early spring. Peak outgassing occurred in the summer months. As seasonal weather cooled, fluxes decreased in magnitude until December.
- Substantial heterogeneity in both dissolved GHGs and bulk fluxes were observed across the sub environments of the reservoir complex. Larger concentrations of both CO2 and

CH4 were observed in the shallow recently inundated areas of the former river bank relative to the deeper water of the existing channel, and regions up- and downstream of the reservoir. Even in the back bay we observe large differences in dissolved CH4 at sites in close physical proximity.

- The back bay environment experienced a surge in CH4 flux in May corresponding with the timing of ice melt. This observation is consistent with a release of GHGs, which had accumulated under the capping ice cover over the winter months, on ice thaw and break-up.
- Over the months June, July, August and September, the average EC CO2 flux measured at the Keeyask reservoir ranged between 3.85 ± 2.33 g/m2/d in May and 6.03 ± 3.81 g/m2/d in July. These fluxes are larger than the May-September averages from the main channel reported in 2019 (0.65 ± 1.1 g/m2/d) and 2018 (1.9 ± 1.3 g/m2/d). The EC tower footprint in 2021, which is dominated by shallow newly submerged land is different than the flux footprints from 2018 and 2019, which largely included a southern portion of the Nelson River's channel upstream of the yet uncompleted generating station and spillway. It should be noted that our bulk CO2 fluxes calculated for the existing channel sub environment (2.84 ± 1.08 g/m2/d), while larger, are closer in line to fluxes observed in the previous years.
- The June to September EC CO2 fluxes in 2021 (4.6 ± 3.27 g/m2/d) were larger, on average than those measured from floating chambers at Gull Lake during 2009-2013 and 2014 pre-construction (1 g/m2/d and 2.2 g/m2/day). Again, the 2021 bulk CO2 fluxes, calculated for the existing channel sub environment (2.84 ± 1.08 g/m2/d), while larger, are closer in line to these fluxes.
- The June to September 2021 EC CH4 fluxes were larger post-impoundment (46 ± 29.93 mg/m2/d in June and 120.25 ± 53.85 mg/m2/d in September) relative to 2018 and 2019, during which time fluxes are not discernible from instrument noise (6.93 mg/m2/d). Again, much of the difference may be attributed to the difference in flux footprints between the 2021 EC installation on the south dike road and 2018/19 channel deployments. Note that the average diffusive flux from the existing channel averaged 0.91 mg/m2/d, which are lower than values observed in 2018 and 2019 (3.0 and 5.0 mg CH4/m2/d).

9.0 LITERATURE CITED

Demarty, M. and A. Tremblay, 2017. Long term follow-up of pCO2, pCH4 and emissions from

DelSontro, T., J. J. Beaulieu, J. A. Downing, 2018. Greenhouse gas emissions from lakes and impoundments: Upscaling in the face of global change, Limnology and Oceanography Letters 3, pp. 64–75, doi: 10.1002/lol2.10073.

Environnement Illimité inc. 2014. Keeyask Technical Summary: Monitoring Aquatic Greenhouse Gas (GHG) Emissions (2009-2014), Report prepared for Manitoba Hydro, 11 pages.

Goldenfum, J.A., 2012. Challenges and solutions for assessing the impact of freshwater reservoirs on natural GHG emissions, Ecohydrology Hydrobiology, Volume 12, No. 12, pp. 115-122.

IPPC 2006. IPCC Guidelines for National Greenhouse Gas Inventories, Volume 4 Agriculture, Forestry and Other Land Use, Chapter 7 Wetlands, 24 pages.

Keeyask Hydropower Limited Partnership (KHLP). 2012a. Keeyask Generation Project: Response to EIS Guidelines. June 2012. Winnipeg, Manitoba.

Keeyask Hydropower Limited Partnership (KHLP). 2012b. Keeyask Generation Project: Physical Environment Supporting Volume. June 2012. Winnipeg, Manitoba

Keeyask Hydropower Limited Partnership (KHLP). 2012c. Keeyask Generation Project: Aquatic Environment Supporting Volume. June 2012. Winnipeg, Manitoba

Keeyask Hydropower Limited Partnership (KHLP). 2015a. Keeyask Generation Project: Physical Environment Monitoring Plan. October 2015. Winnipeg, Manitoba.

Keeyask Hydropower Limited Partnership (KHLP). 2015b. Keeyask Generation Project: Aquatic Effects Monitoring Plan. June 2015. Winnipeg, Manitoba.

Keeyask Hydropower Limited Partnership (KHLP). 2015c. Keeyask Generation Project: Reservoir Clearing Plan. April 2015. Winnipeg, Manitoba.

Keeyask Hydropower Limited Partnership (KHLP). 2014. Keeyask Generation Project: Sediment Management Plan for In-stream Construction. July 2014. Winnipeg, Manitoba.

KGS Acres Ltd. 2011. Keeyask Generating Station, Stage IV Studies: Existing Environment Sedimentation (Memorandum GN9.2.3, Mb Hydro File No. 00195-11100-0154_03). June 2011. Winnipeg, Manitoba.

Manitoba Hydro. 2015. 2014–2015 Physical Environment Monitoring Report: Year 1 Construction. June 2016. Winnipeg, Manitoba.

Manitoba Hydro. 2016. 2015–2016 Physical Environment Monitoring Report: Year 2 Construction. June 2016. Winnipeg, Manitoba.

Manitoba Hydro. 2017. 2016–2017 Physical Environment Monitoring Report: Year 3 Construction. June 2017. Winnipeg, Manitoba.

Manitoba Hydro. 2018. 2017–2018 Physical Environment Monitoring Report: Year 4 Construction. June 2018. Winnipeg, Manitoba.

Manitoba Hydro. 2019. 2018–2019 Physical Environment Monitoring Report: Year 5 Construction. June 2019. Winnipeg, Manitoba.

Manitoba Hydro. 2020. 2019–2020 Physical Environment Monitoring Report: Year 6 Construction. June 2020. Winnipeg, Manitoba.

Manitoba Hydro. 2021. 2020–2021 Physical Environment Monitoring Report: Year 7 Construction. June 2020. Winnipeg, Manitoba.

Manitoba Hydro. 2020. Sediment Management Plan for In-Stream Construction Annual Report April 2019 – March 2020. June 2020. Winnipeg, Manitoba.

TetrES Consultants Inc., 2011. Water Temperature & Dissolved Oxygen Study – Project Effects. Keeyask Project Environmental Studies Program Report prepared for Manitoba Hydro. 100 pp.

TCN, WLFN, YFFN, FLCN and the Manitoba Hydro-Electric Board. 2009. Joint Keeyask Development Agreement. May 2009. Winnipeg, Manitoba.

Papakyriakou, T., A. Soloway, D. Gedig and R. Gill, 2022. Reservoir Greenhouse Gas Program – 2021 Report. Report prepared for Manitoba Hydro. May 2022. 28 pp. plus 1 appendix.

Prairie, Y.T., Alm, J., Beaulieu, J. and others. 2018. Greenhouse Gas Emissions from Freshwater Reservoirs: What Does the Atmosphere See? Ecosystems, 21, pp. 1058 -1071. DOI: 10.1007/s10021-017-0198-9

Teodoru, C.R., J. Bastien, M. Bonneville, P. A. del Giorgio, M. Demarty, M. Garneau, J. Hélie, L. Pelletier, Y. T. Prairie, N.T. Roulet, I.B. Strachan, A. Tremblay, 2012. The net carbon footprint of a newly created boreal hydroelectric reservoir, Global Biogeochemical Cycles, 26, Issue 2, 14 pages doi: 10.1029/2011GB004187.

UNESCO/IHA 2010. GHG Measurement Guidelines for Freshwater Reservoirs, The International Hydropower Association, London, 139 pages, ISBN 978-0-9566228-0-8.

United States Environmental Protection Agency (USEPA), 1985. Rates, Constants, and Kinetics Formulations in Surface Water Quality Modeling. Second Edition (EPA/600/3-85/040). Environmental Research Laboratory, Office of Research and Development. June 1985. Athens, GA.

APPENDIX 1:
DETAILED MAPS OF PEMP MONITORING SITES

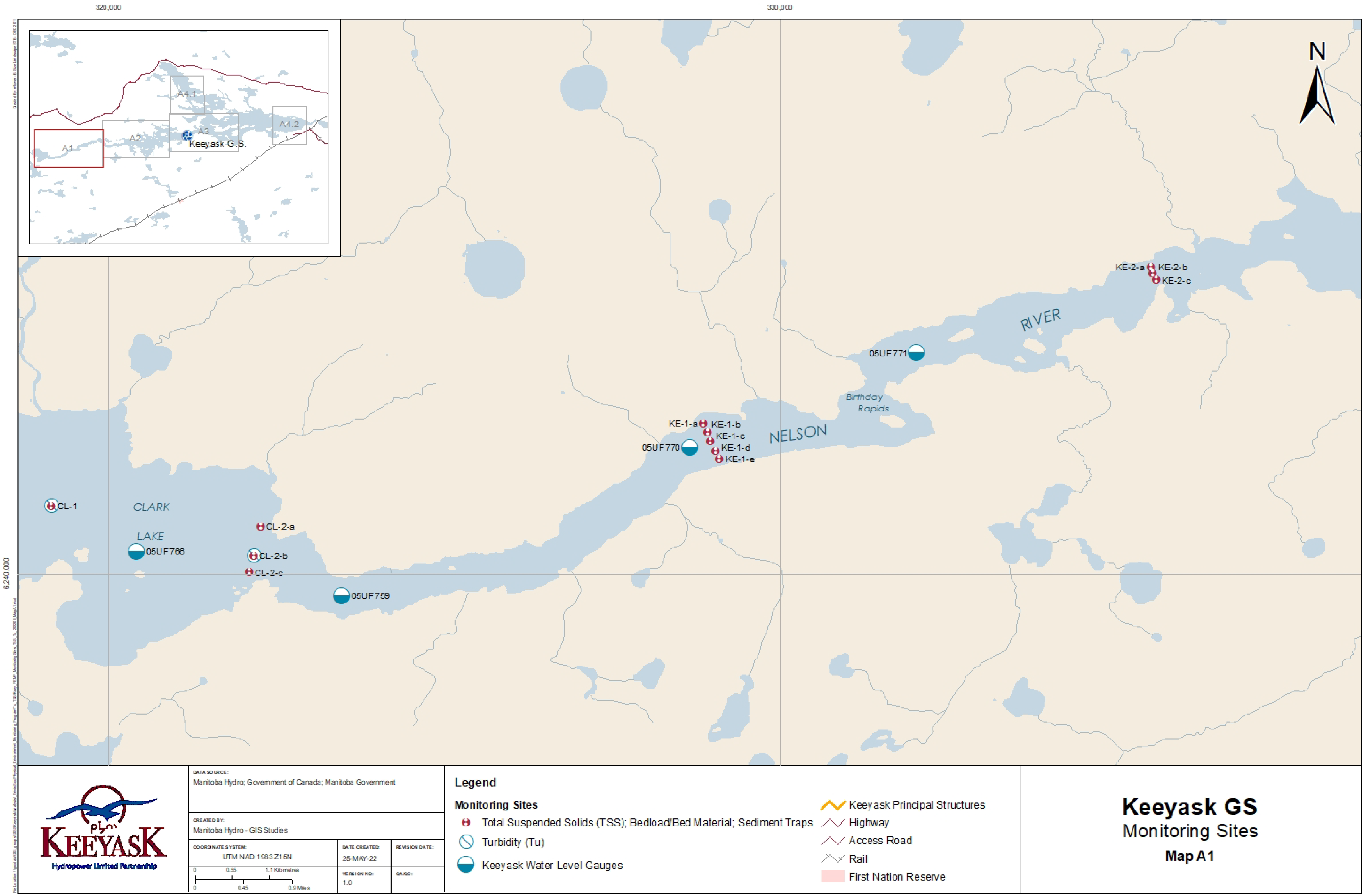
320,000
330,000
6,240,000
N
A4.1
A2
A3
A4.2
A1
Keeyask G.S.
KE-2-a
KE-2-b
KE-2-c
RIVER
05UF771
Birthday Rapids
KE-1-a
KE-1-b
KE-1-c
KE-1-d
KE-1-e
05UF770
NELSON
CL-1
CLARK
LAKE
05UF766
CL-2-a
CL-2-b
CL-2-c
05UF769
KEEYASK
Hydropower Limited Partnership
DATA SOURCE:
Manitoba Hydro; Government of Canada; Manitoba Government
CREATED BY:
Manitoba Hydro - GIS Studies
COORDINATE SYSTEM:
UTM NAD 1983 Z15N
DATE CREATED:
25-MAY-22
REVISION DATE:
VERSION NO:
1.0
QA/QC:
Legend
Monitoring Sites
Total Suspended Solids (TSS); Bedload/Bed Material; Sediment Traps
Turbidity (Tu)
Keeyask Water Level Gauges
Keeyask Principal Structures
Highway
Access Road
Rail
First Nation Reserve
Keeyask GS
Monitoring Sites
Map A1

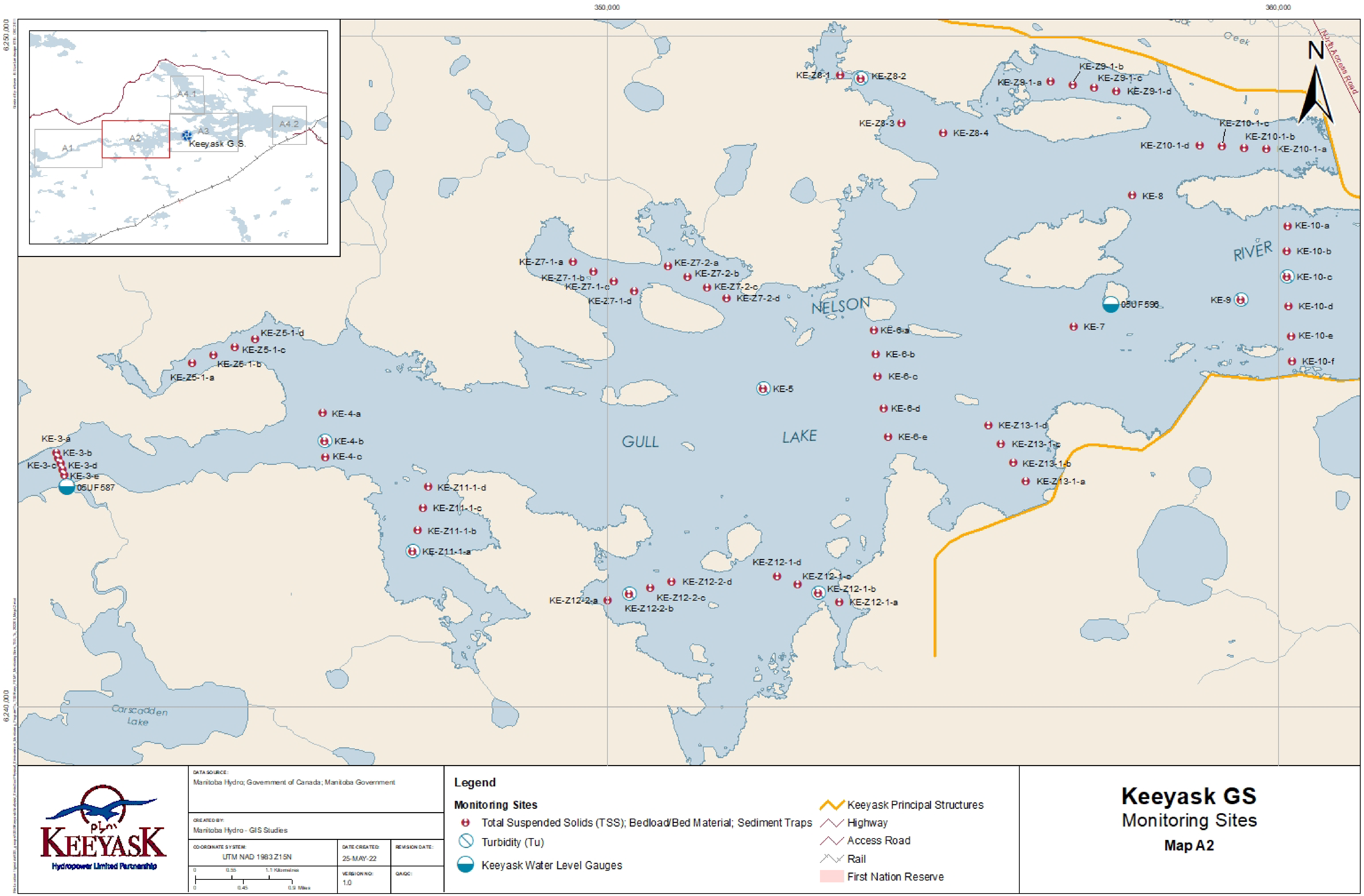
Keeyask GS
Monitoring Sites
Map A2
Legend
Monitoring Sites
Total Suspended Solids (TSS); Bedload/Bed Material; Sediment Traps
Turbidity (Tu)
Keeyask Water Level Gauges
Keeyask Principal Structures
Highway
Access Road
Rail
First Nation Reserve
DATA SOURCE:
Manitoba Hydro; Government of Canada; Manitoba Government
CREATED BY:
Manitoba Hydro - GIS Studies
COORDINATE SYSTEM:
UTM NAD 1983 Z15N
DATE CREATED:
25-MAY-22
VERSION NO:
1.0
GULL
LAKE
NELSON
RIVER
Carscadden Lake
Keeyask G.S.
A1
A2
A3
A4.1
A4.2
KE-3-a
KE-3-b
KE-3-c
KE-3-d
KE-3-e
05UF587
KE-4-a
KE-4-b
KE-4-c
KE-5
KE-6-a
KE-6-b
KE-6-c
KE-6-d
KE-6-e
KE-7
KE-8
KE-9
05UF596
KE-10-a
KE-10-b
KE-10-c
KE-10-d
KE-10-e
KE-10-f
KE-Z5-1-a
KE-Z5-1-b
KE-Z5-1-c
KE-Z5-1-d
KE-Z7-1-a
KE-Z7-1-b
KE-Z7-1-c
KE-Z7-1-d
KE-Z7-2-a
KE-Z7-2-b
KE-Z7-2-c
KE-Z7-2-d
KE-Z8-1
KE-Z8-2
KE-Z8-3
KE-Z8-4
KE-Z9-1-a
KE-Z9-1-b
KE-Z9-1-c
KE-Z9-1-d
KE-Z10-1-a
KE-Z10-1-b
KE-Z10-1-c
KE-Z10-1-d
KE-Z11-1-a
KE-Z11-1-b
KE-Z11-1-c
KE-Z11-1-d
KE-Z12-1-a
KE-Z12-1-b
KE-Z12-1-c
KE-Z12-1-d
KE-Z12-2-a
KE-Z12-2-b
KE-Z12-2-c
KE-Z12-2-d
KE-Z13-1-a
KE-Z13-1-b
KE-Z13-1-c
KE-Z13-1-d
350,000
360,000
6,250,000
6,240,000
N
KEEYASK
Hydropower Limited Partnership

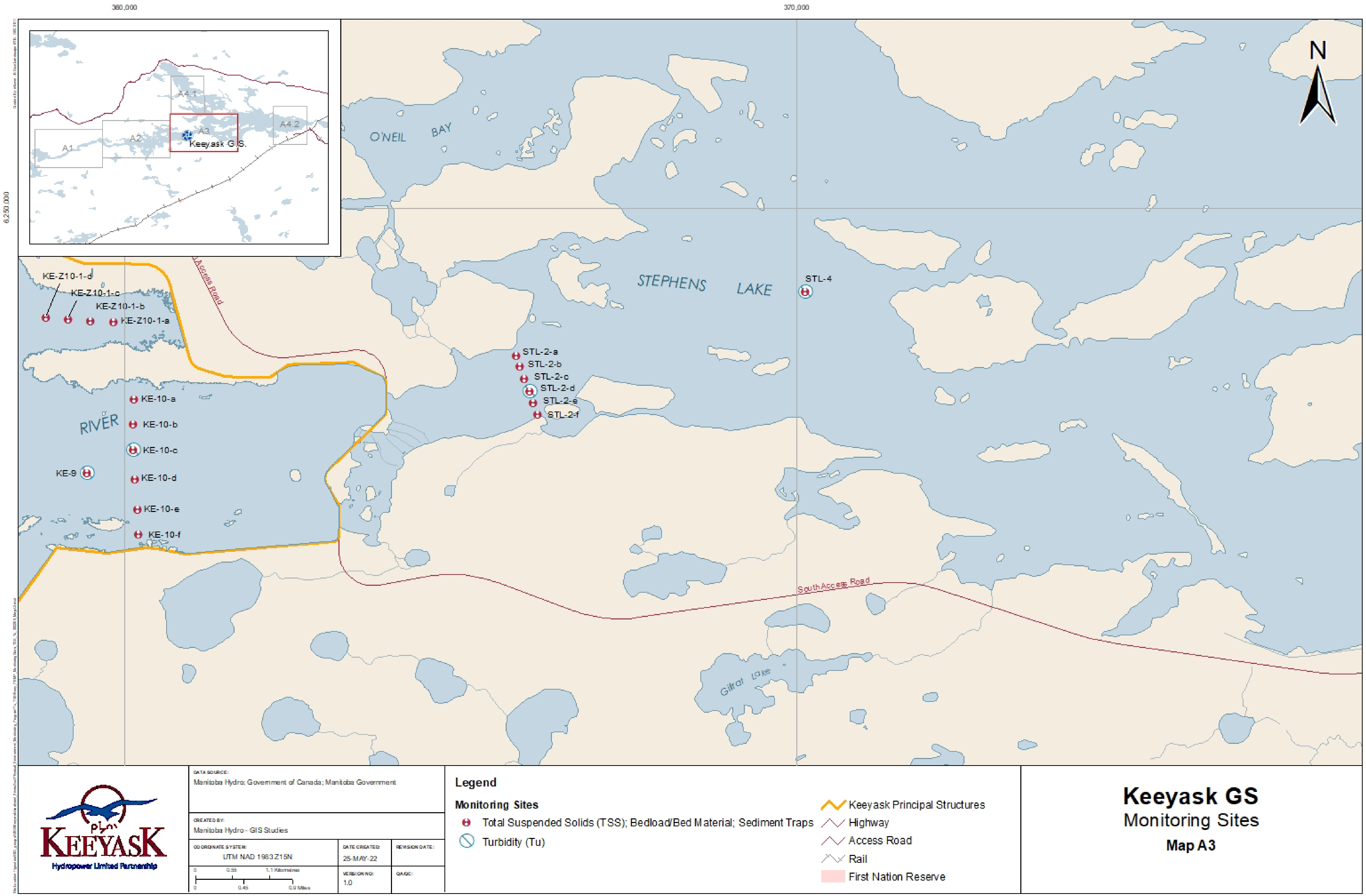
360,000
370,000
6,250,000
A4.1
A1
A2
A3
A4.2
Keeyask G.S.
N
O'NEIL BAY
STEPHENS LAKE
RIVER
Gilrat Lake
South Access Road
KE-Z10-1-d
KE-Z10-1-c
KE-Z10-1-b
KE-Z10-1-a
KE-10-a
KE-10-b
KE-10-c
KE-9
KE-10-d
KE-10-e
KE-10-f
STL-2-a
STL-2-b
STL-2-c
STL-2-d
STL-2-e
STL-2-f
STL-4
DATA SOURCE:
Manitoba Hydro; Government of Canada; Manitoba Government
CREATED BY:
Manitoba Hydro - GIS Studies
COORDINATE SYSTEM:
UTM NAD 1983 Z15N
DATE CREATED:
25-MAY-22
REVISION DATE:
VERSION NO:
1.0
QA/QC:
0 0.55 1.1 Kilometres
0 0.45 0.9 Miles
Legend
Monitoring Sites
Total Suspended Solids (TSS); Bedload/Bed Material; Sediment Traps
Turbidity (Tu)
Keeyask Principal Structures
Highway
Access Road
Rail
First Nation Reserve
Keeyask GS
Monitoring Sites
Map A3

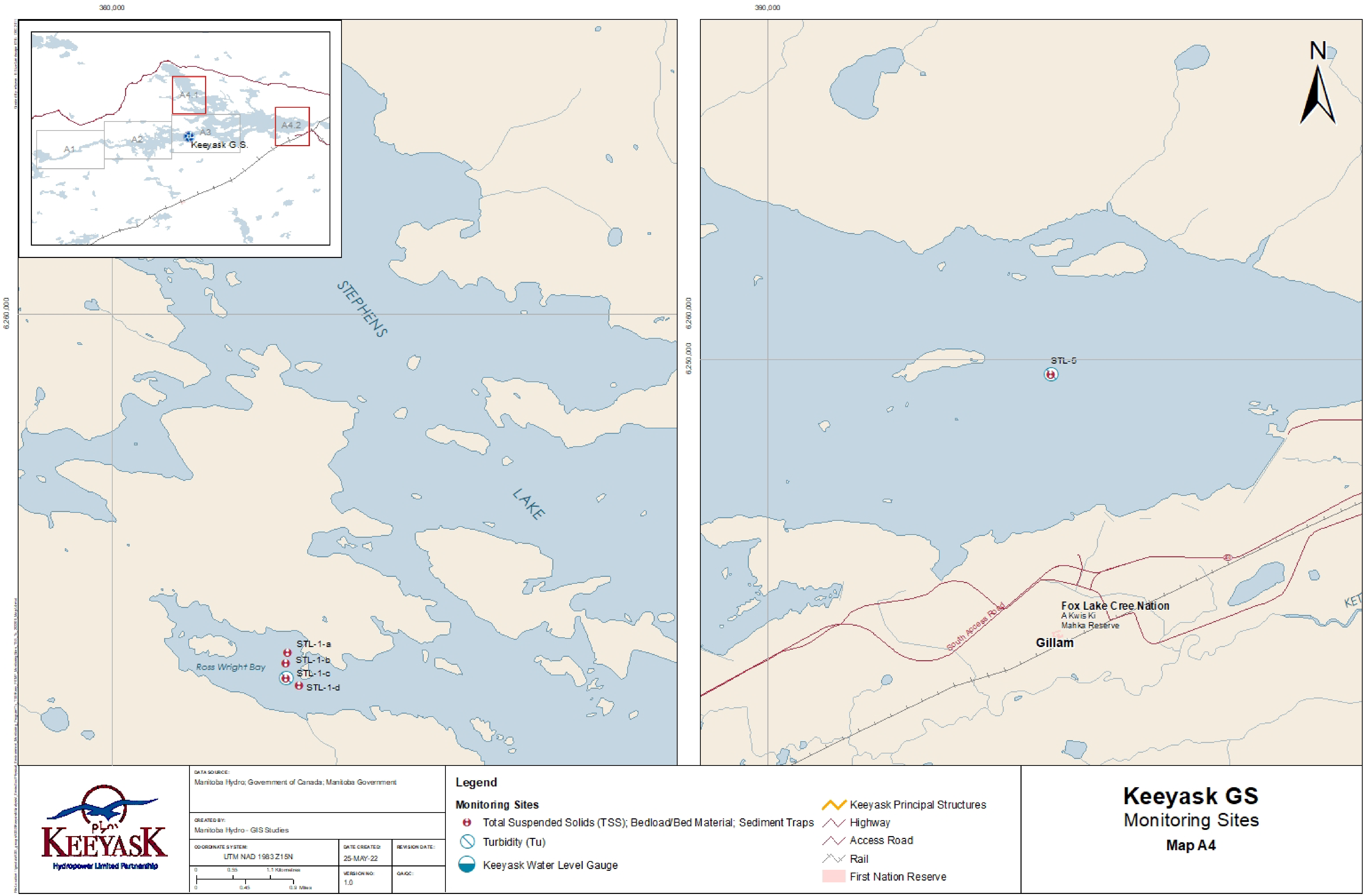

360,000
390,000
6,260,000
6,250,000
Keeyask G.S.
A1
A2
A3
A4.1
A4.2
STEPHENS
LAKE
Ross Wright Bay
STL-1-a
STL-1-b
STL-1-c
STL-1-d
STL-5
N
Fox Lake Cree Nation
A Kwis Ki
Mahka Reserve
Gillam
South Access Road
DATA SOURCE:
Manitoba Hydro; Government of Canada; Manitoba Government
CREATED BY:
Manitoba Hydro - GIS Studies
COORDINATE SYSTEM:
UTM NAD 1983 Z15N
DATE CREATED:
25-MAY-22
REVISION DATE:
VERSION NO:
1.0
QA/QC:
Legend
Monitoring Sites
Total Suspended Solids (TSS); Bedload/Bed Material; Sediment Traps
Turbidity (Tu)
Keeyask Water Level Gauge
Keeyask Principal Structures
Highway
Access Road
Rail
First Nation Reserve
Keeyask GS
Monitoring Sites
Map A4

APPENDIX 2: WINTER DEPTH PROFILE CHARTS OF DISSOLVED OXYGEN CONCENTRATION, PERCENT SATURATION, AND WATER TEMPERATURE

Site Listing in order of presentation in Appendix 2:

Note that site names on charts all include the "PE_" prefix that is an internal designation used to identify the monitoring site as part of the physical environment program.

Mainstem sites (upstream to downstream):

- PE_CL-1
- PE_KE-5
- PE_KE-9
- PE_STL-4

North back bay sites:

- PE_KE-Z4-1-a, b, c, d (i.e, PE_KE-Z4-1-a, PE_KE-Z4-1-b, PE_KE-Z4-1-c, PE_KE-Z4-1-d)
- PE_KE-Z5-1-a, b, c, d
- PE_KE-Z7-1-a, b, c, d
- PE_KE-Z7-2-a, b, c, d
- PE_KE-Z8-1, 2, 3, 4
- PE_KE-Z9-1-a, b, c, d
- PE_KE-Z10-1-a, b, c, d

South back bay sites:

- PE_KE-Z11-1-a, b, c, d
- PE_KE-Z12-1-a, b, c, d
- PE_KE-Z12-2-a, b, c, d
- PE_KE-Z13-1-a, b, c, d

Stephens Lake back bay site:

- PE_STL-1-a, b, c, d

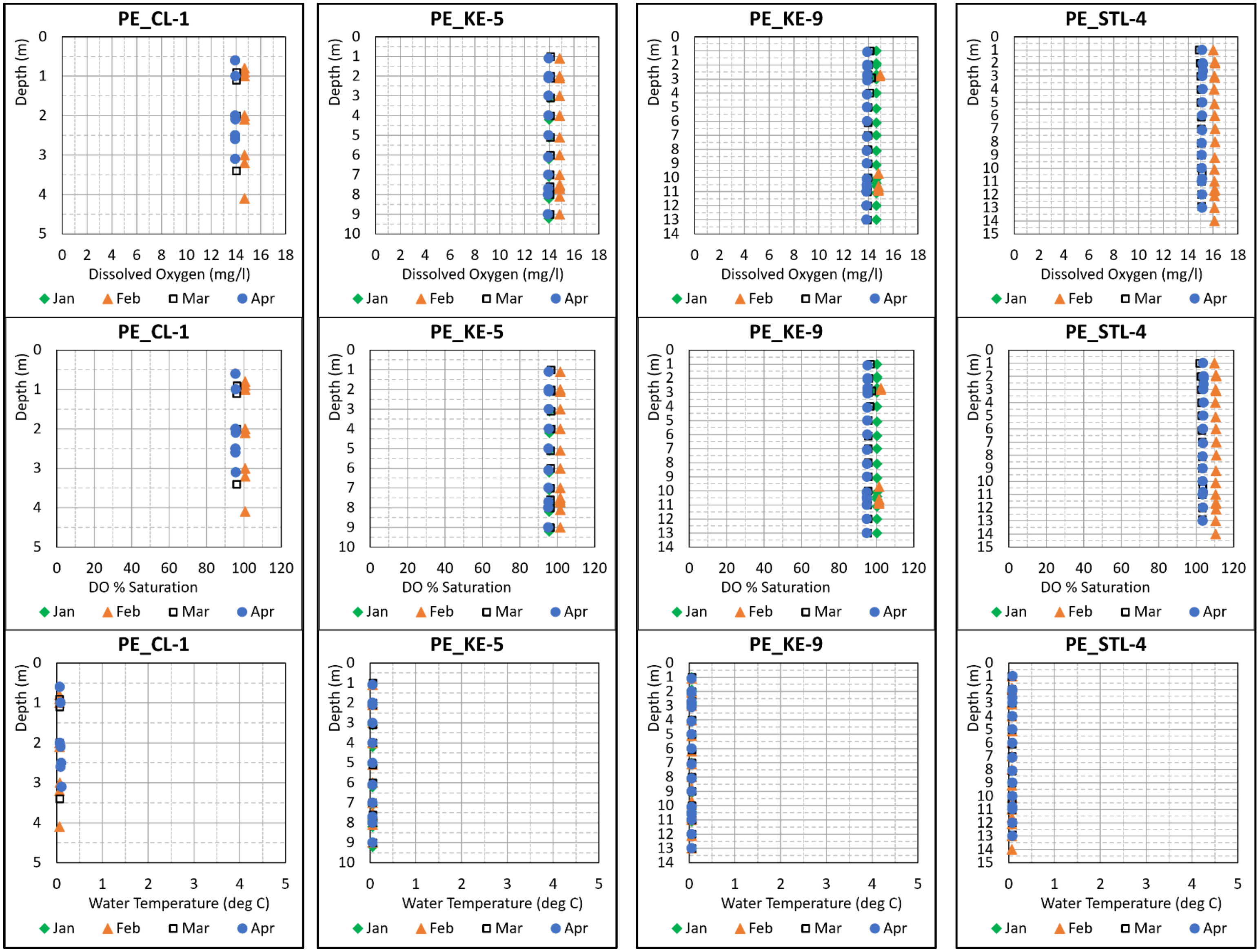
PE_CL-1
PE_KE-5
PE_KE-9
PE_STL-4
Depth (m)
Dissolved Oxygen (mg/l)
DO % Saturation
Water Temperature (deg C)
Jan
Feb
Mar
Apr

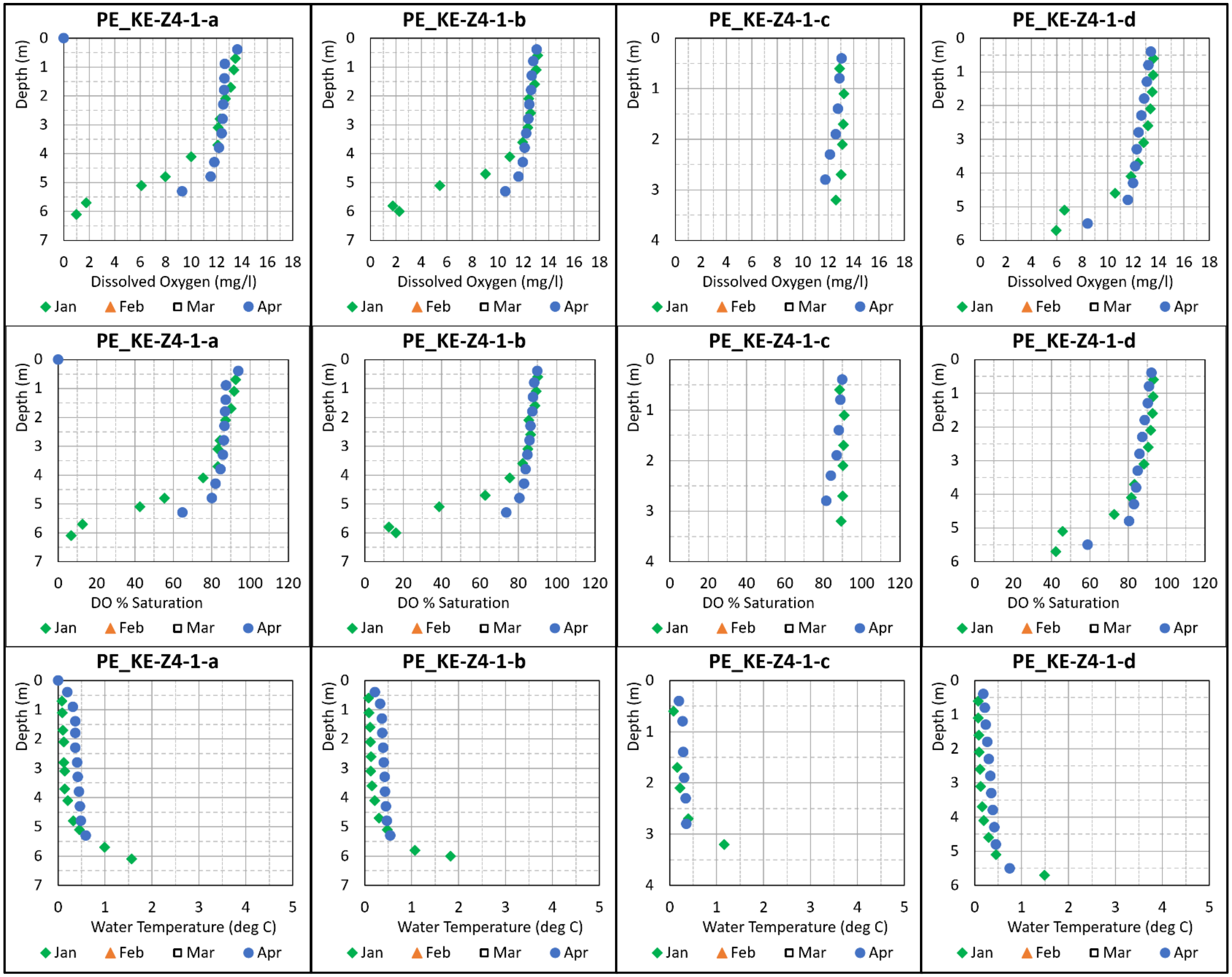
PE_KE-Z4-1-a
PE_KE-Z4-1-b
PE_KE-Z4-1-c
PE_KE-Z4-1-d
Depth (m)
Dissolved Oxygen (mg/l)
DO % Saturation
Water Temperature (deg C)
Jan
Feb
Mar
Apr

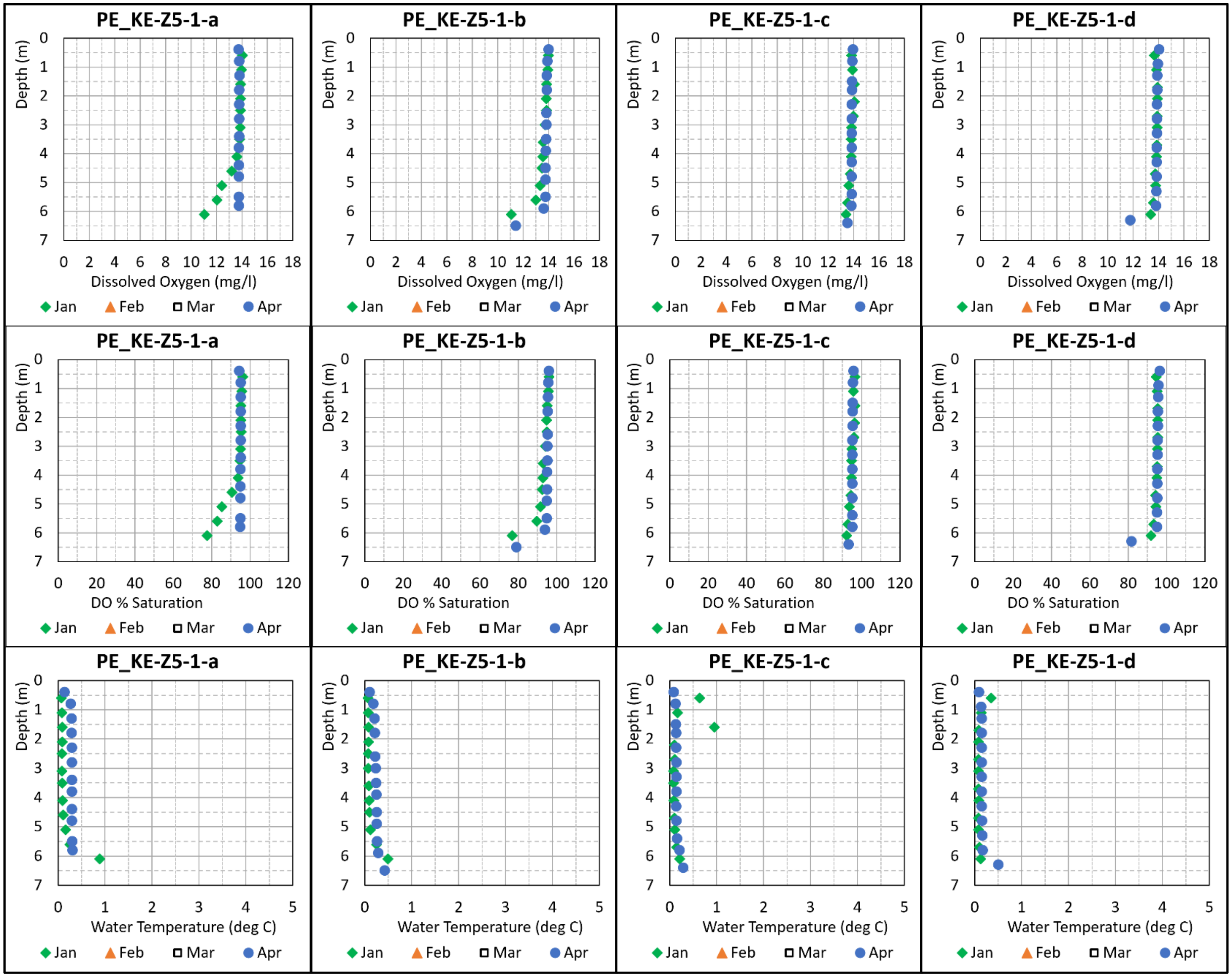
PE_KE-Z5-1-a
Depth (m)
Dissolved Oxygen (mg/l)
Jan Feb Mar Apr
PE_KE-Z5-1-b
Depth (m)
Dissolved Oxygen (mg/l)
Jan Feb Mar Apr
PE_KE-Z5-1-c
Depth (m)
Dissolved Oxygen (mg/l)
Jan Feb Mar Apr
PE_KE-Z5-1-d
Depth (m)
Dissolved Oxygen (mg/l)
Jan Feb Mar Apr
PE_KE-Z5-1-a
Depth (m)
DO % Saturation
Jan Feb Mar Apr
PE_KE-Z5-1-b
Depth (m)
DO % Saturation
Jan Feb Mar Apr
PE_KE-Z5-1-c
Depth (m)
DO % Saturation
Jan Feb Mar Apr
PE_KE-Z5-1-d
Depth (m)
DO % Saturation
Jan Feb Mar Apr
PE_KE-Z5-1-a
Depth (m)
Water Temperature (deg C)
Jan Feb Mar Apr
PE_KE-Z5-1-b
Depth (m)
Water Temperature (deg C)
Jan Feb Mar Apr
PE_KE-Z5-1-c
Depth (m)
Water Temperature (deg C)
Jan Feb Mar Apr
PE_KE-Z5-1-d
Depth (m)
Water Temperature (deg C)
Jan Feb Mar Apr

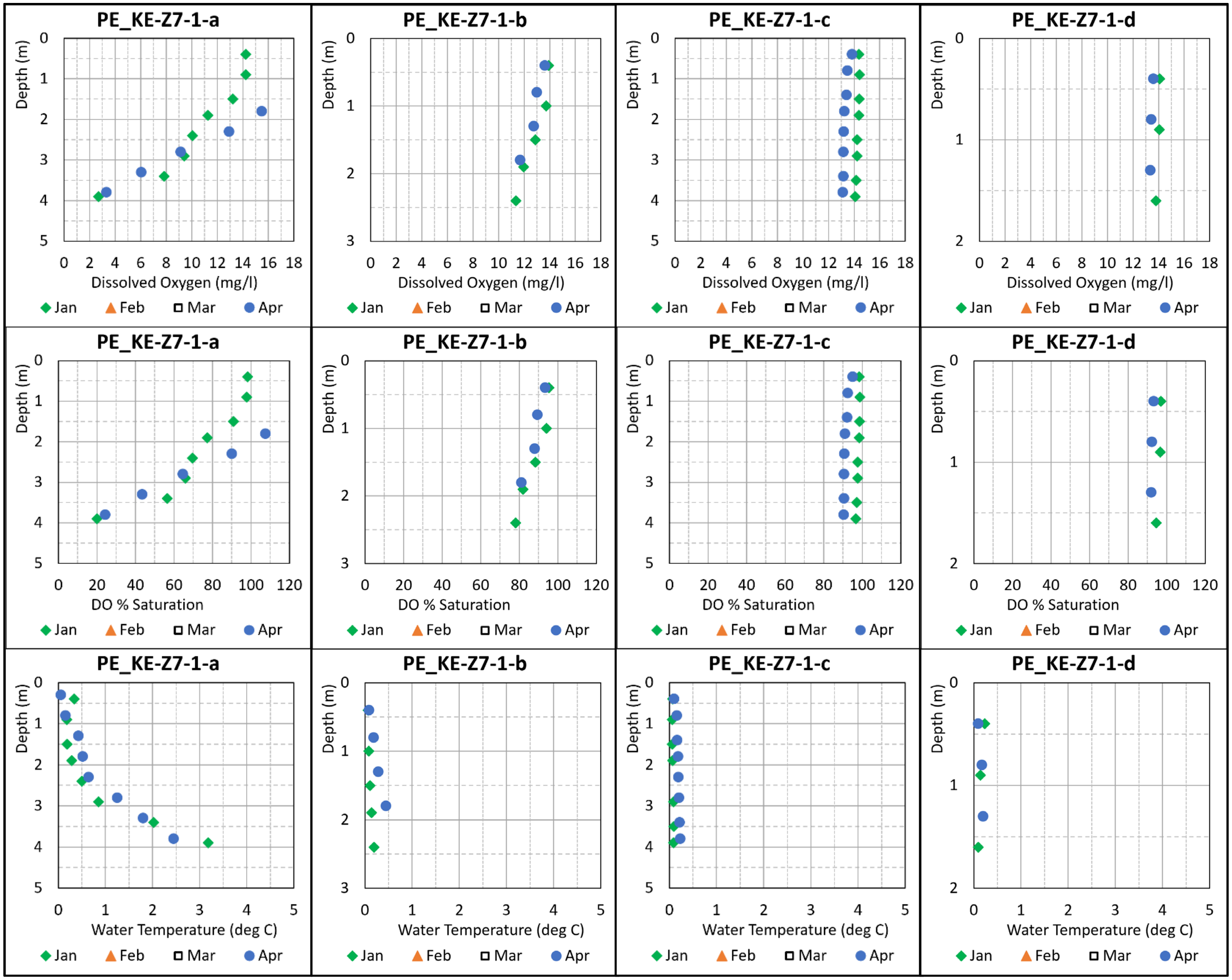
PE_KE-Z7-1-a
Depth (m)
Dissolved Oxygen (mg/l)
Jan Feb Mar Apr
PE_KE-Z7-1-b
Depth (m)
Dissolved Oxygen (mg/l)
Jan Feb Mar Apr
PE_KE-Z7-1-c
Depth (m)
Dissolved Oxygen (mg/l)
Jan Feb Mar Apr
PE_KE-Z7-1-d
Depth (m)
Dissolved Oxygen (mg/l)
Jan Feb Mar Apr
PE_KE-Z7-1-a
Depth (m)
DO % Saturation
Jan Feb Mar Apr
PE_KE-Z7-1-b
Depth (m)
DO % Saturation
Jan Feb Mar Apr
PE_KE-Z7-1-c
Depth (m)
DO % Saturation
Jan Feb Mar Apr
PE_KE-Z7-1-d
Depth (m)
DO % Saturation
Jan Feb Mar Apr
PE_KE-Z7-1-a
Depth (m)
Water Temperature (deg C)
Jan Feb Mar Apr
PE_KE-Z7-1-b
Depth (m)
Water Temperature (deg C)
Jan Feb Mar Apr
PE_KE-Z7-1-c
Depth (m)
Water Temperature (deg C)
Jan Feb Mar Apr
PE_KE-Z7-1-d
Depth (m)
Water Temperature (deg C)
Jan Feb Mar Apr

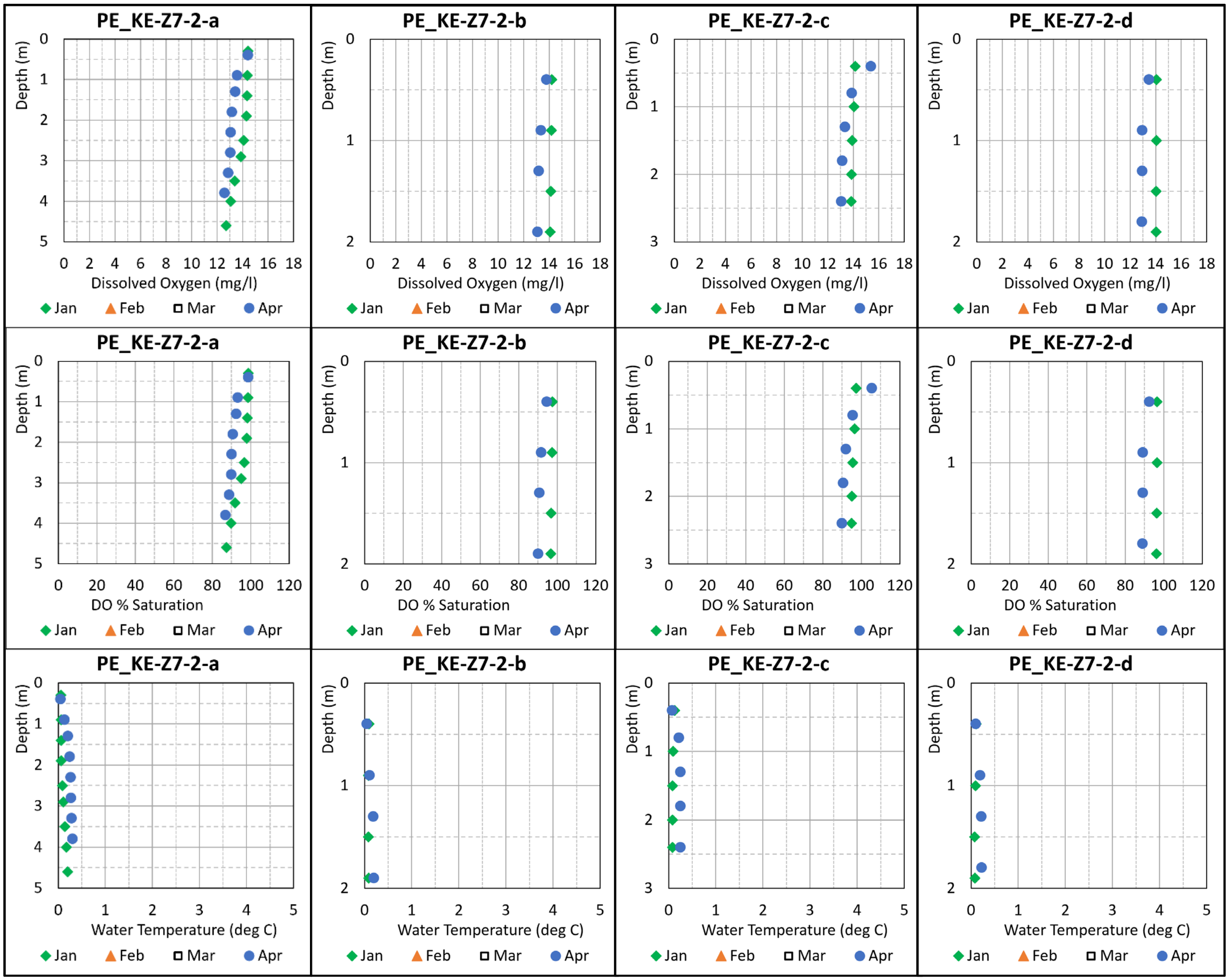
PE_KE-Z7-2-a
PE_KE-Z7-2-b
PE_KE-Z7-2-c
PE_KE-Z7-2-d
Depth (m)
Dissolved Oxygen (mg/l)
DO % Saturation
Water Temperature (deg C)
Jan
Feb
Mar
Apr
0
1
2
3
4
5
0 2 4 6 8 10 12 14 16 18
0 20 40 60 80 100 120
0 1 2 3 4 5

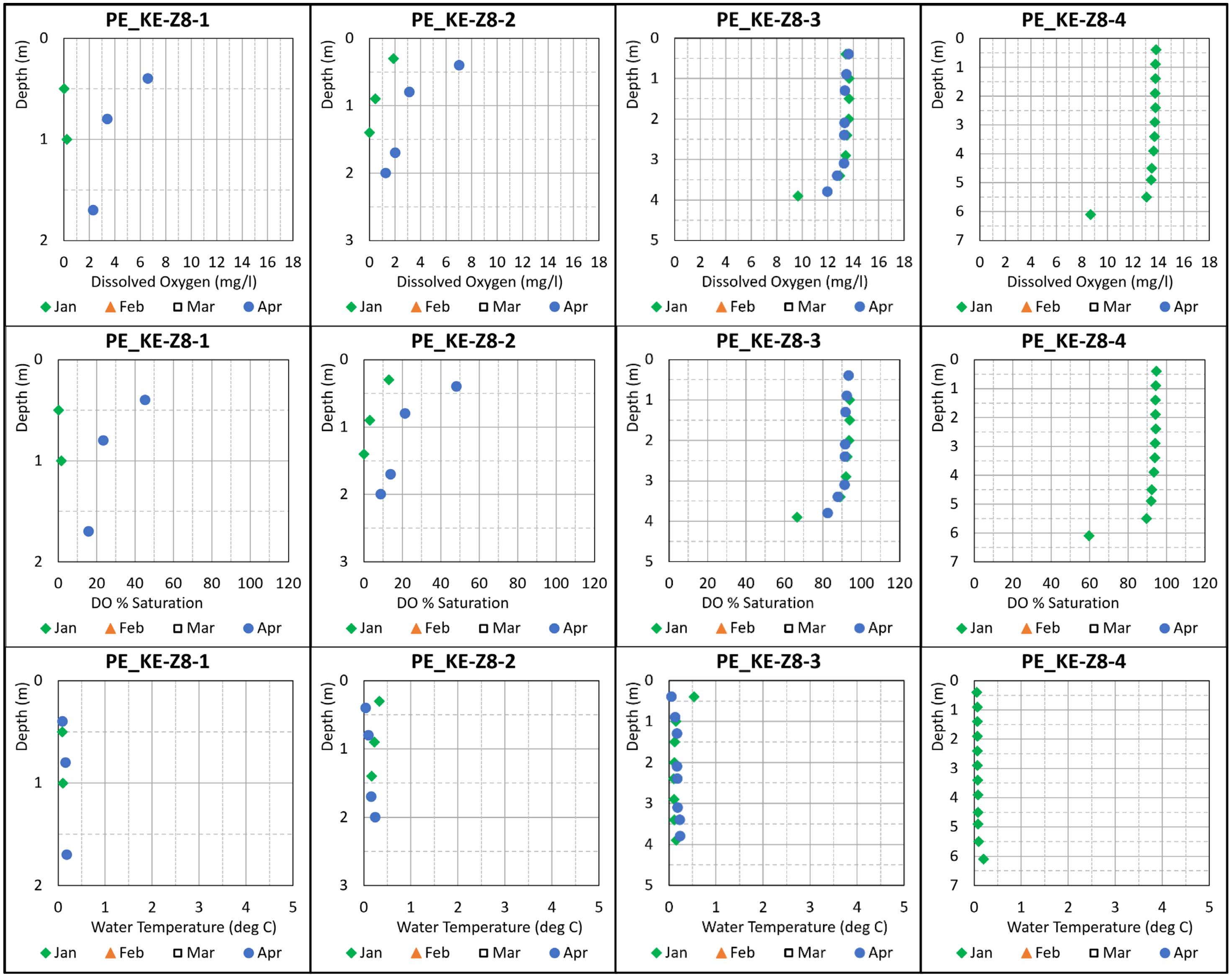
PE_KE-Z8-1
PE_KE-Z8-2
PE_KE-Z8-3
PE_KE-Z8-4
Depth (m)
Dissolved Oxygen (mg/l)
DO % Saturation
Water Temperature (deg C)
Jan
Feb
Mar
Apr

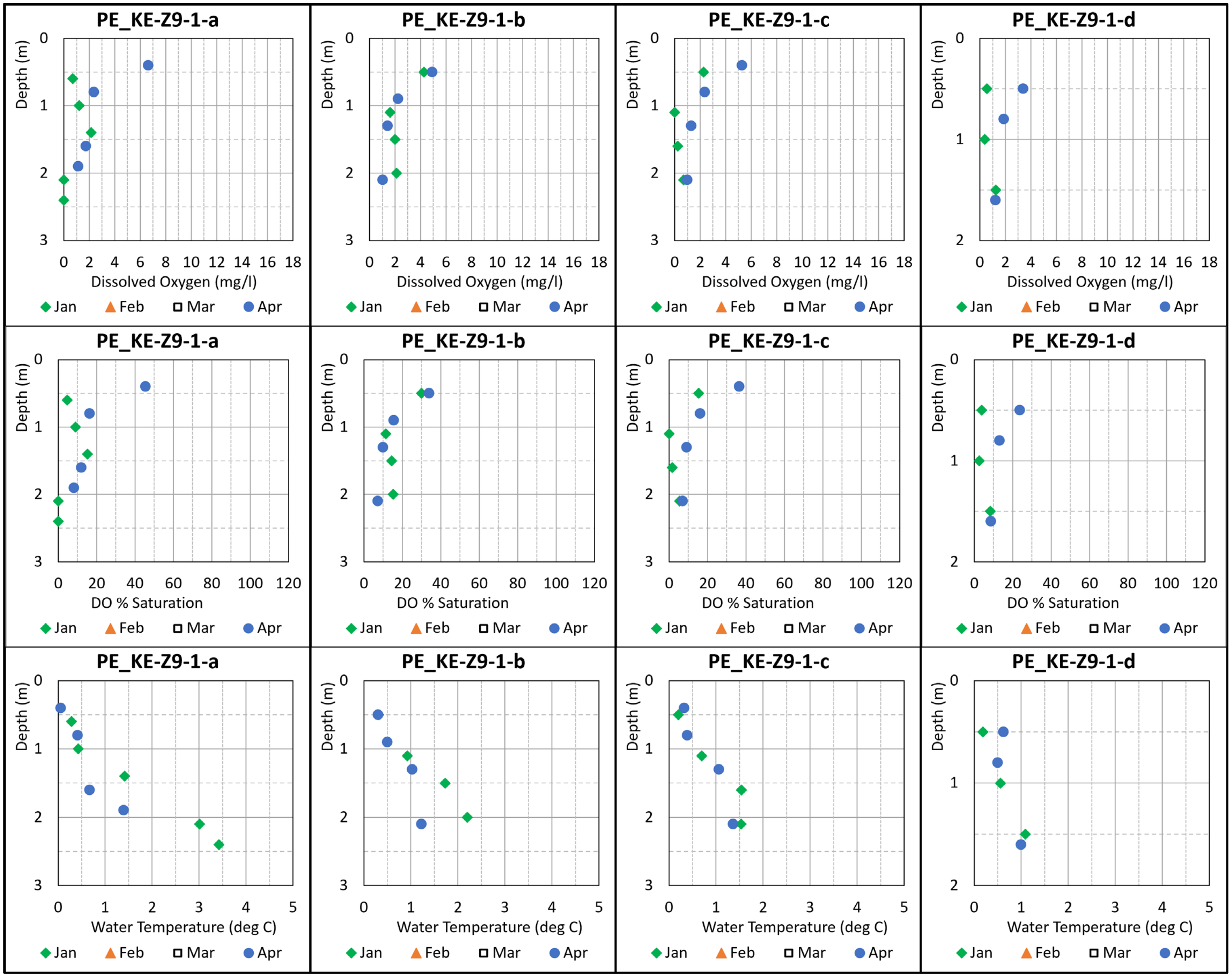
PE_KE-Z9-1-a
PE_KE-Z9-1-b
PE_KE-Z9-1-c
PE_KE-Z9-1-d
Depth (m)
Dissolved Oxygen (mg/l)
DO % Saturation
Water Temperature (deg C)
Jan
Feb
Mar
Apr

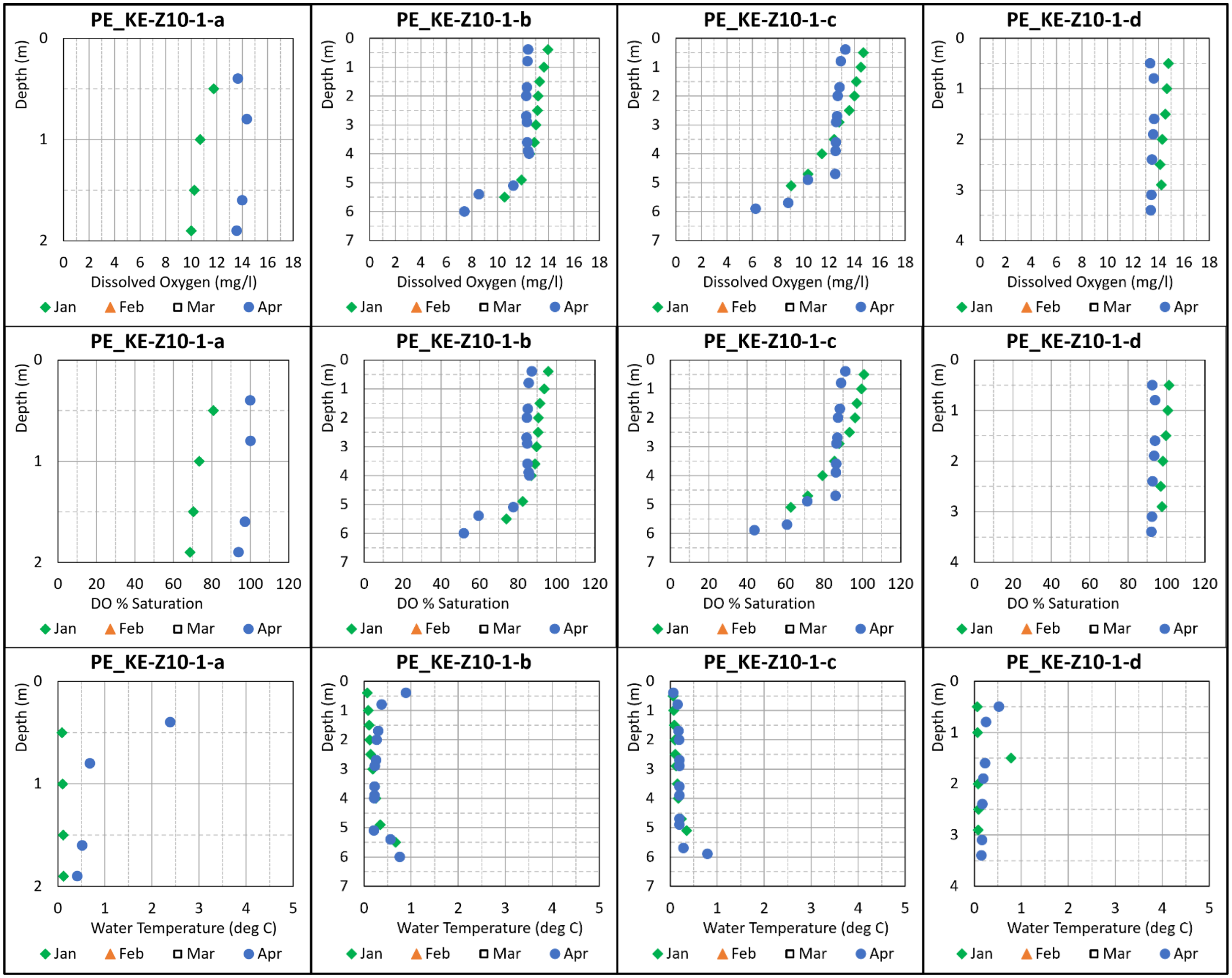
PE_KE-Z10-1-a
PE_KE-Z10-1-b
PE_KE-Z10-1-c
PE_KE-Z10-1-d
Depth (m)
Dissolved Oxygen (mg/l)
DO % Saturation
Water Temperature (deg C)
Jan
Feb
Mar
Apr

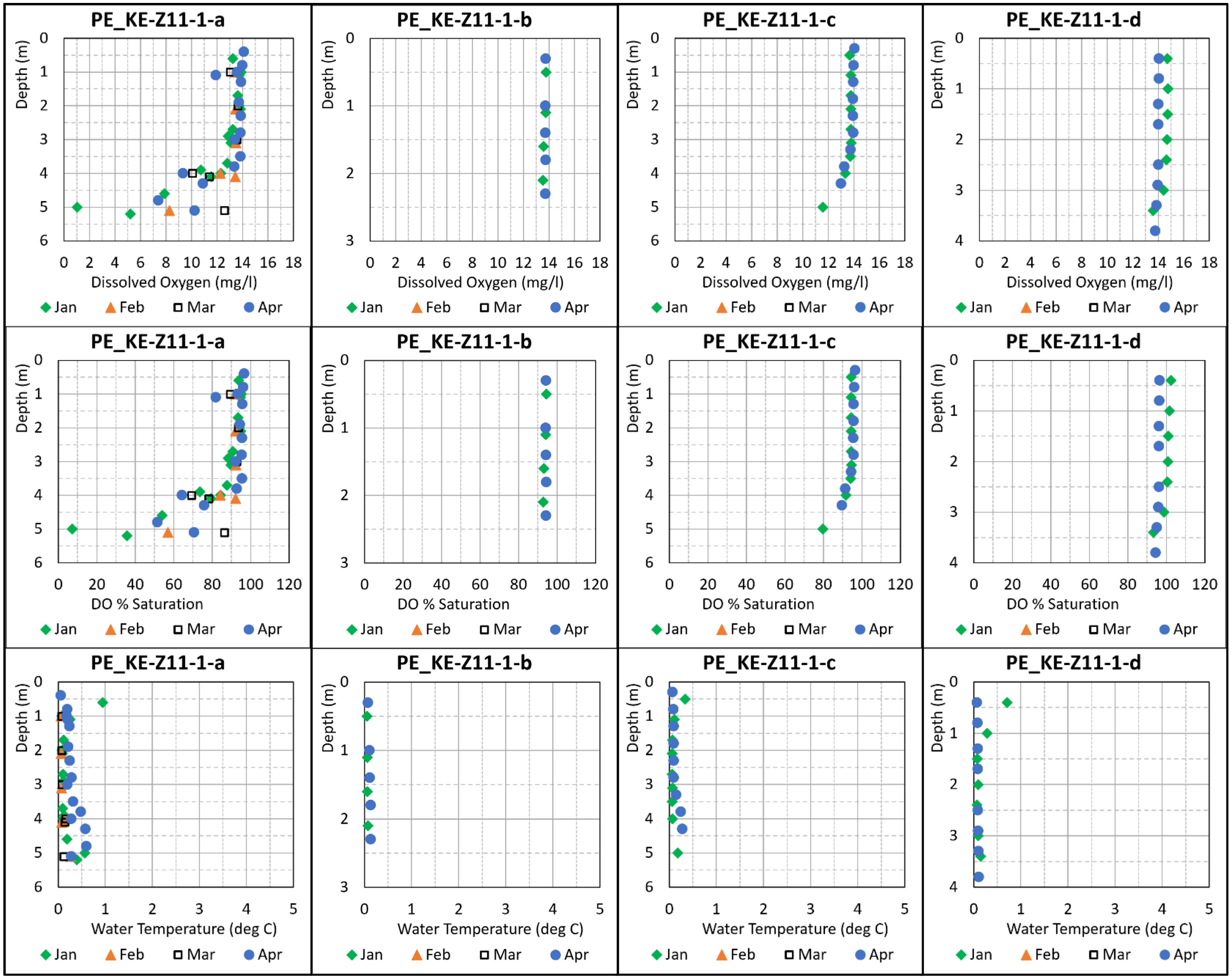
PE_KE-Z11-1-a
PE_KE-Z11-1-b
PE_KE-Z11-1-c
PE_KE-Z11-1-d
Depth (m)
Dissolved Oxygen (mg/l)
DO % Saturation
Water Temperature (deg C)
Jan
Feb
Mar
Apr

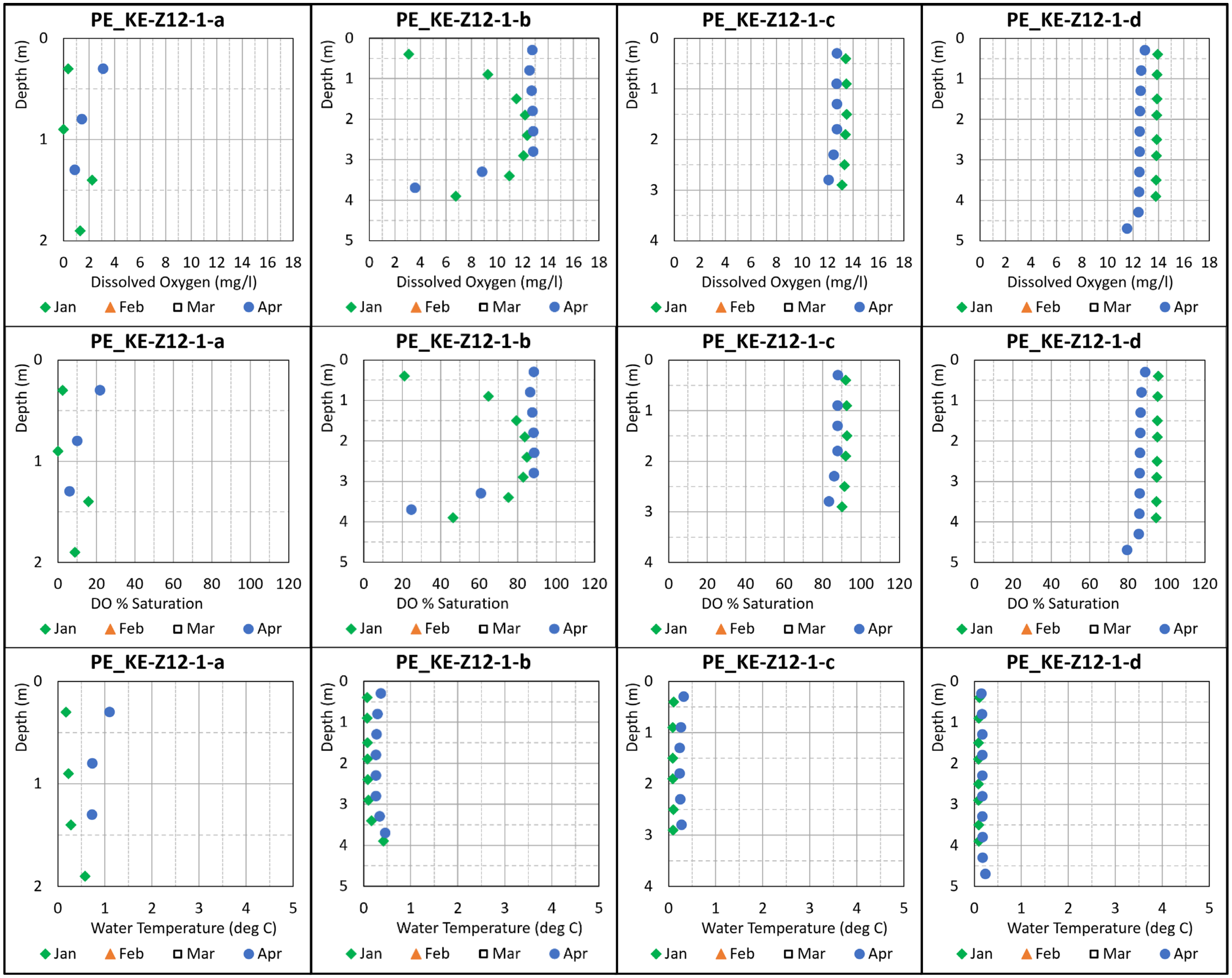
PE_KE-Z12-1-a
PE_KE-Z12-1-b
PE_KE-Z12-1-c
PE_KE-Z12-1-d
Depth (m)
Dissolved Oxygen (mg/l)
DO % Saturation
Water Temperature (deg C)
Jan
Feb
Mar
Apr

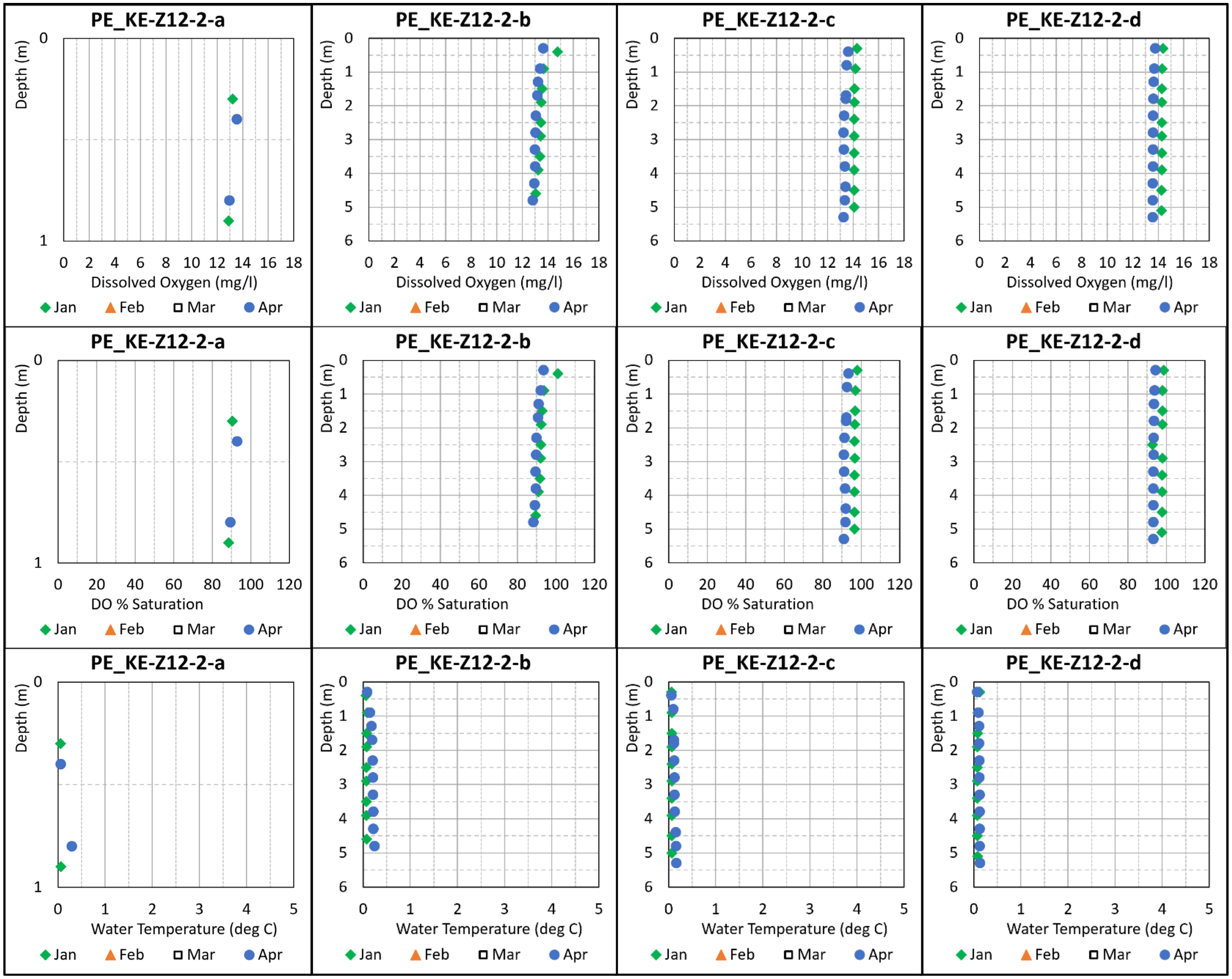
PE_KE-Z12-2-a
PE_KE-Z12-2-b
PE_KE-Z12-2-c
PE_KE-Z12-2-d
Depth (m)
Dissolved Oxygen (mg/l)
DO % Saturation
Water Temperature (deg C)
Jan
Feb
Mar
Apr

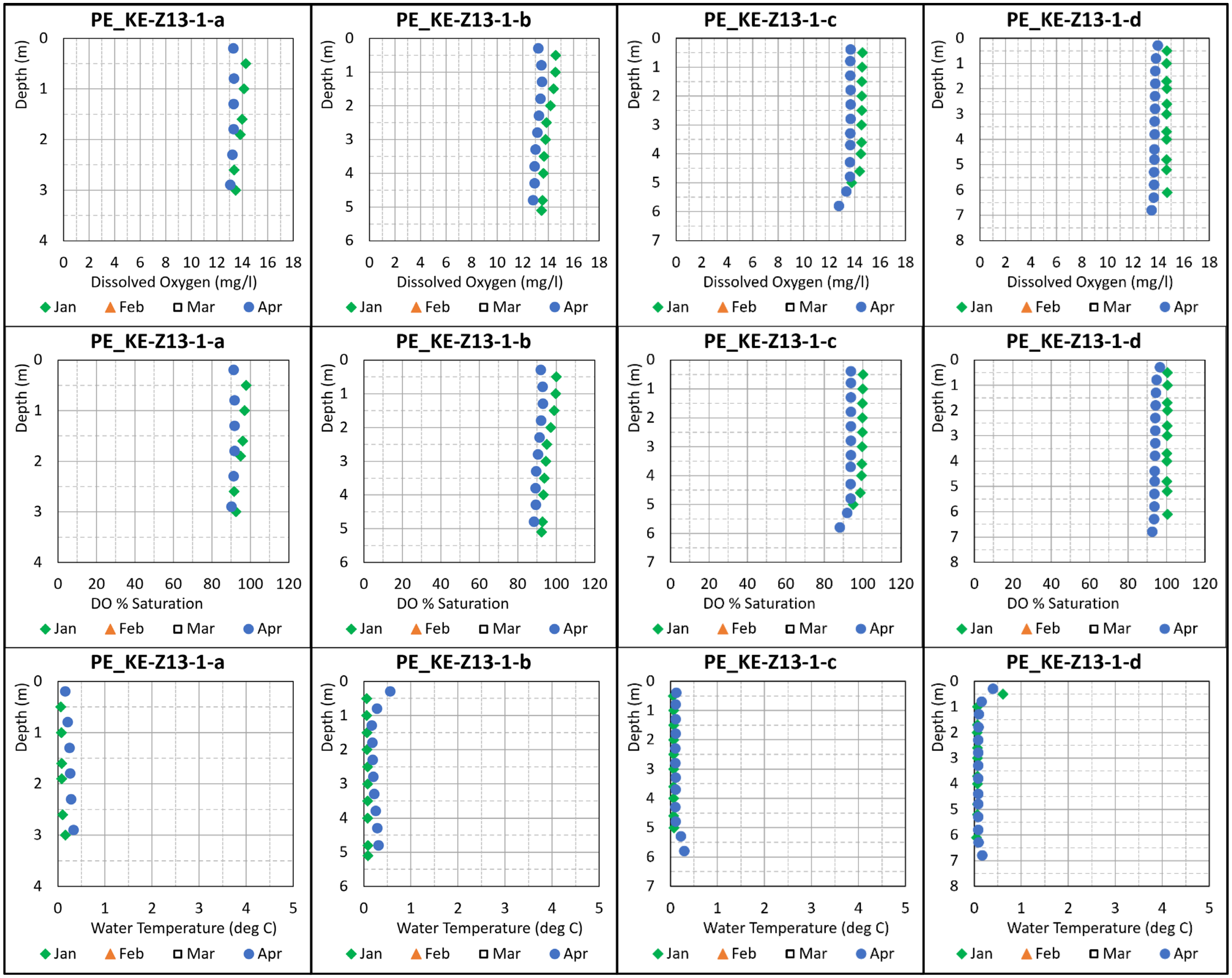
PE_KE-Z13-1-a
Depth (m)
Dissolved Oxygen (mg/l)
Jan Feb Mar Apr
PE_KE-Z13-1-b
Depth (m)
Dissolved Oxygen (mg/l)
Jan Feb Mar Apr
PE_KE-Z13-1-c
Depth (m)
Dissolved Oxygen (mg/l)
Jan Feb Mar Apr
PE_KE-Z13-1-d
Depth (m)
Dissolved Oxygen (mg/l)
Jan Feb Mar Apr
PE_KE-Z13-1-a
Depth (m)
DO % Saturation
Jan Feb Mar Apr
PE_KE-Z13-1-b
Depth (m)
DO % Saturation
Jan Feb Mar Apr
PE_KE-Z13-1-c
Depth (m)
DO % Saturation
Jan Feb Mar Apr
PE_KE-Z13-1-d
Depth (m)
DO % Saturation
Jan Feb Mar Apr
PE_KE-Z13-1-a
Depth (m)
Water Temperature (deg C)
Jan Feb Mar Apr
PE_KE-Z13-1-b
Depth (m)
Water Temperature (deg C)
Jan Feb Mar Apr
PE_KE-Z13-1-c
Depth (m)
Water Temperature (deg C)
Jan Feb Mar Apr
PE_KE-Z13-1-d
Depth (m)
Water Temperature (deg C)
Jan Feb Mar Apr

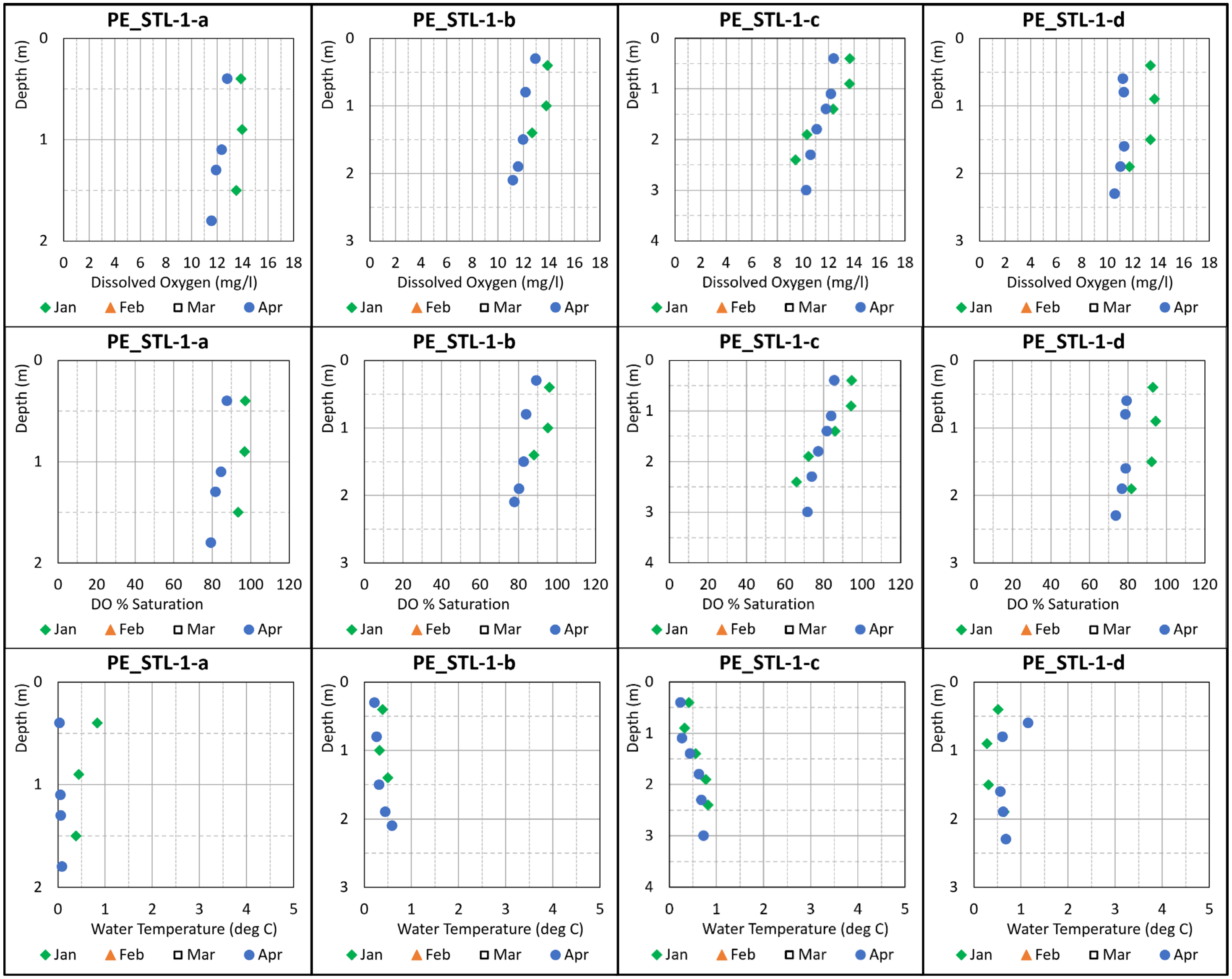
PE_STL-1-a
Depth (m)
Dissolved Oxygen (mg/l)
Jan Feb Mar Apr
PE_STL-1-b
Depth (m)
Dissolved Oxygen (mg/l)
Jan Feb Mar Apr
PE_STL-1-c
Depth (m)
Dissolved Oxygen (mg/l)
Jan Feb Mar Apr
PE_STL-1-d
Depth (m)
Dissolved Oxygen (mg/l)
Jan Feb Mar Apr
PE_STL-1-a
Depth (m)
DO % Saturation
Jan Feb Mar Apr
PE_STL-1-b
Depth (m)
DO % Saturation
Jan Feb Mar Apr
PE_STL-1-c
Depth (m)
DO % Saturation
Jan Feb Mar Apr
PE_STL-1-d
Depth (m)
DO % Saturation
Jan Feb Mar Apr
PE_STL-1-a
Depth (m)
Water Temperature (deg C)
Jan Feb Mar Apr
PE_STL-1-b
Depth (m)
Water Temperature (deg C)
Jan Feb Mar Apr
PE_STL-1-c
Depth (m)
Water Temperature (deg C)
Jan Feb Mar Apr
PE_STL-1-d
Depth (m)
Water Temperature (deg C)
Jan Feb Mar Apr

APPENDIX 3: SUMMER DEPTH PROFILE CHARTS OF DISSOLVED OXYGEN CONCENTRATION & PERCENT SATURATION, AND WATER TEMPERATURE

Site Listing in order of presentation in Appendix 3:

Note that site names on charts all include the "PE_" prefix that is an internal designation used to identify the monitoring site as part of the physical environment program.

Mainstem sites (upstream to downstream):

- PE_CL-2-a, b, c (i.e, PE_CL-2-a, PE_CL-2-b, PE_CL-2-c)
- PE_KE-1-a, b, c, d, e
- PE_KE-2-1-a, b, c
- PE_KE-3-1-a, b, c, d, e
- PE_KE-4-1-a, b
- PE_KE-6-1-a, b, c, d, e
- PE_KE-7
- PE_KE-8
- PE_KE-10-1-a, b, c, d, e, f
- PE_STL-2-a, b, c, d, e, f
- PE_STL-5

North back bay sites:

- PE_KE-Z4-1-a, b, c, d
- PE_KE-Z5-1-a, b, c, d
- PE_KE-Z7-1-a, b, c, d
- PE_KE-Z7-2-a, b, c, d
- PE_KE-Z8-1, 2, 3, 4
- PE_KE-Z9-1-a, b, c, d
- PE_KE-Z10-1-a, b, c, d

South back bay sites:

- PE_KE-Z11-1-a, b, c, d
- PE_KE-Z12-1-a, b, c, d
- PE_KE-Z12-2-a, b, c, d
- PE_KE-Z13-1-a, b, c, d

Stephens Lake back bay site:

- PE_STL-1-a, b, c, d

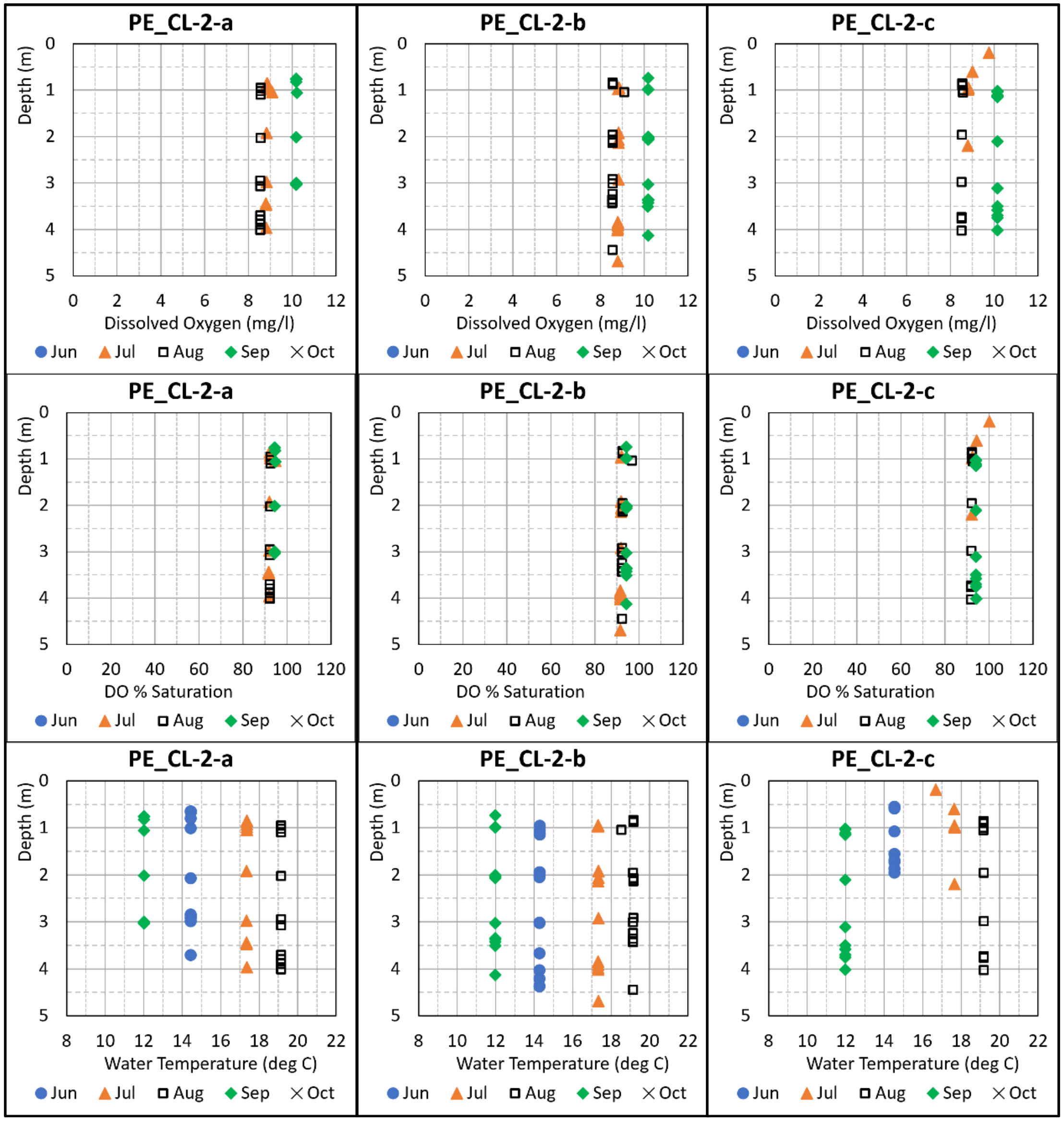
PE_CL-2-a
PE_CL-2-b
PE_CL-2-c
Depth (m)
Dissolved Oxygen (mg/l)
DO % Saturation
Water Temperature (deg C)
Jun
Jul
Aug
Sep
Oct

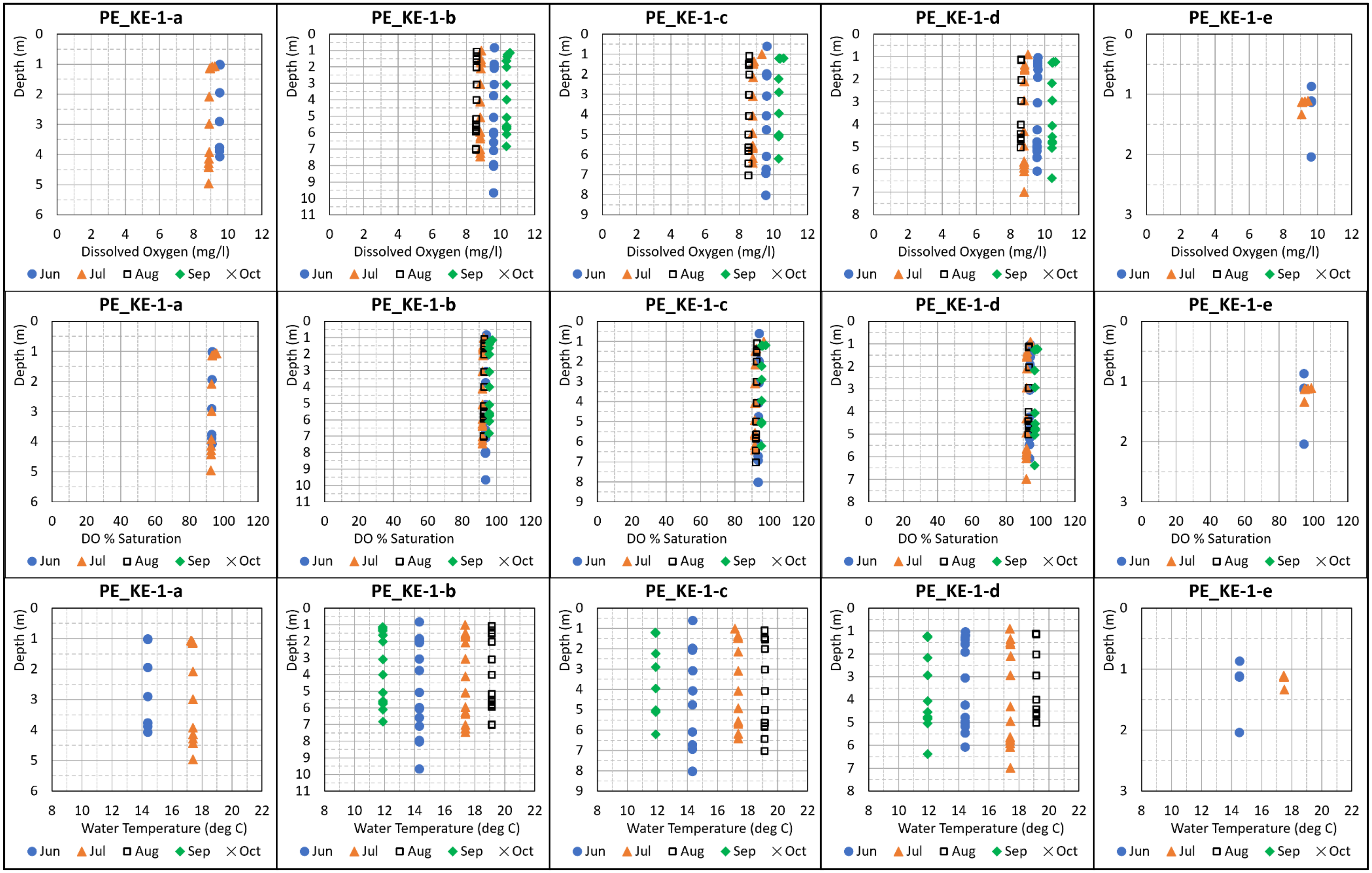
PE_KE-1-a
PE_KE-1-b
PE_KE-1-c
PE_KE-1-d
PE_KE-1-e
Depth (m)
Dissolved Oxygen (mg/l)
DO % Saturation
Water Temperature (deg C)
Jun
Jul
Aug
Sep
Oct

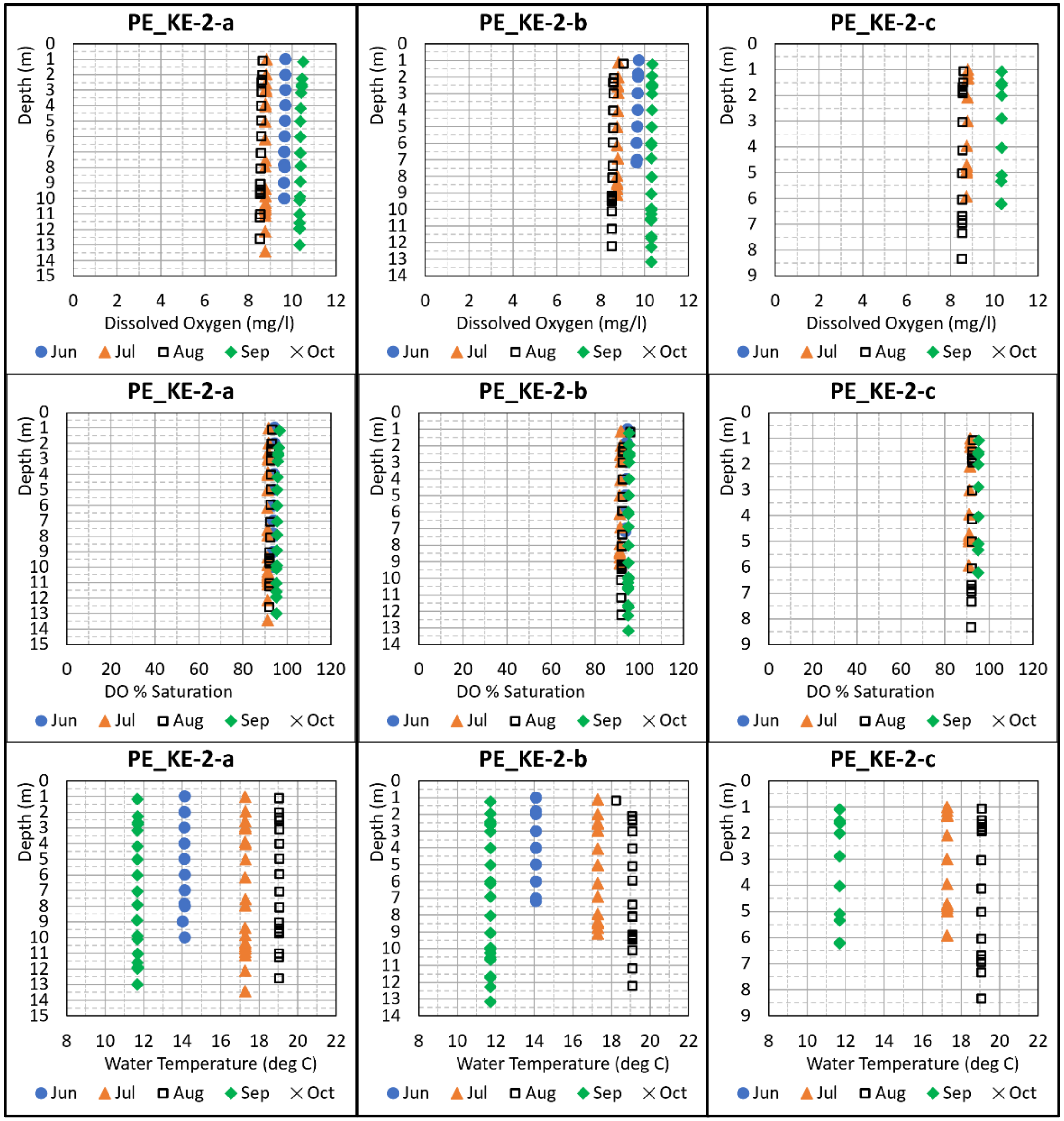
PE_KE-2-a
PE_KE-2-b
PE_KE-2-c
Depth (m)
Dissolved Oxygen (mg/l)
DO % Saturation
Water Temperature (deg C)
Jun Jul Aug Sep Oct

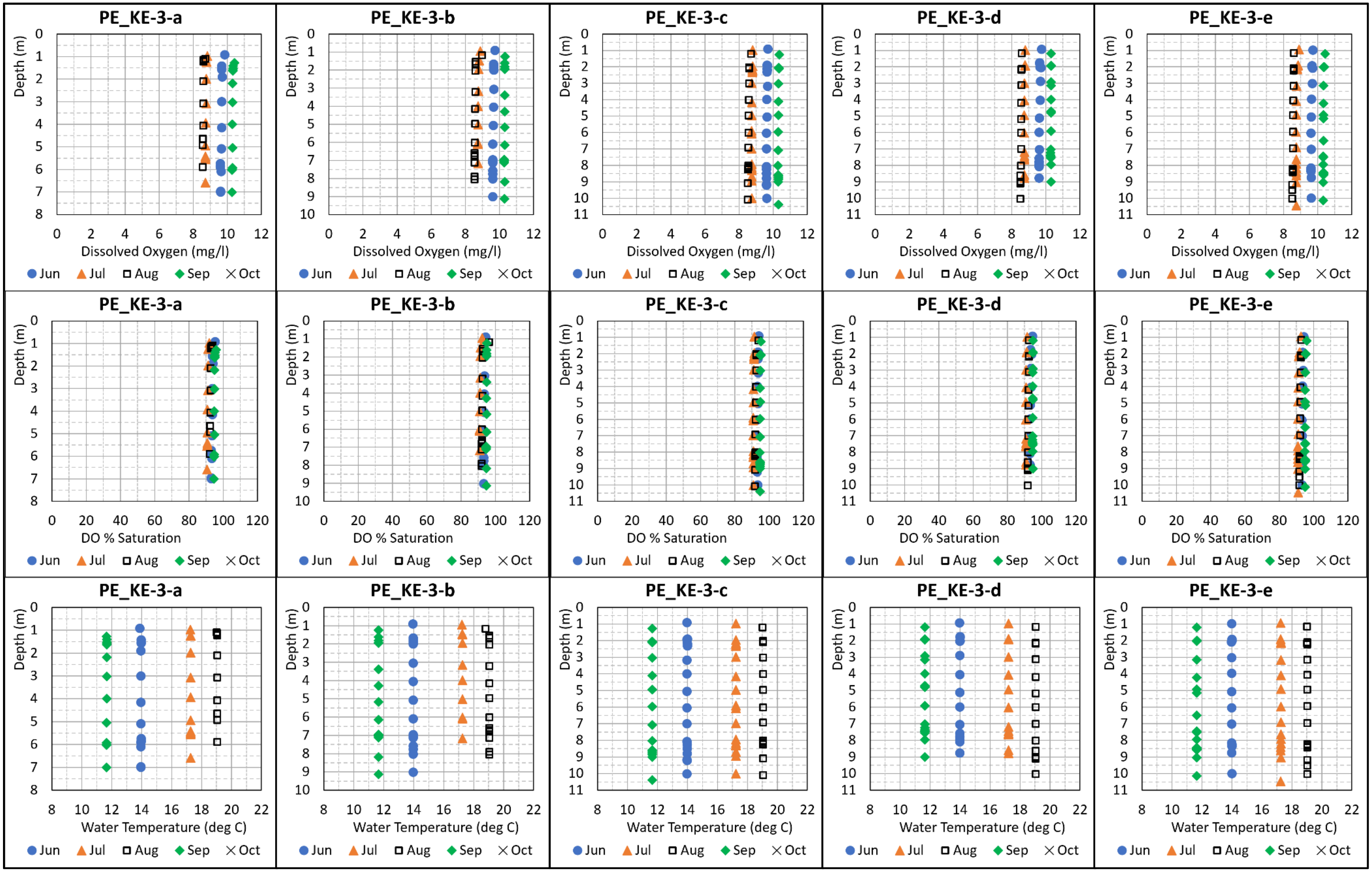
PE_KE-3-a
PE_KE-3-b
PE_KE-3-c
PE_KE-3-d
PE_KE-3-e
Depth (m)
Dissolved Oxygen (mg/l)
DO % Saturation
Water Temperature (deg C)
Jun
Jul
Aug
Sep
Oct

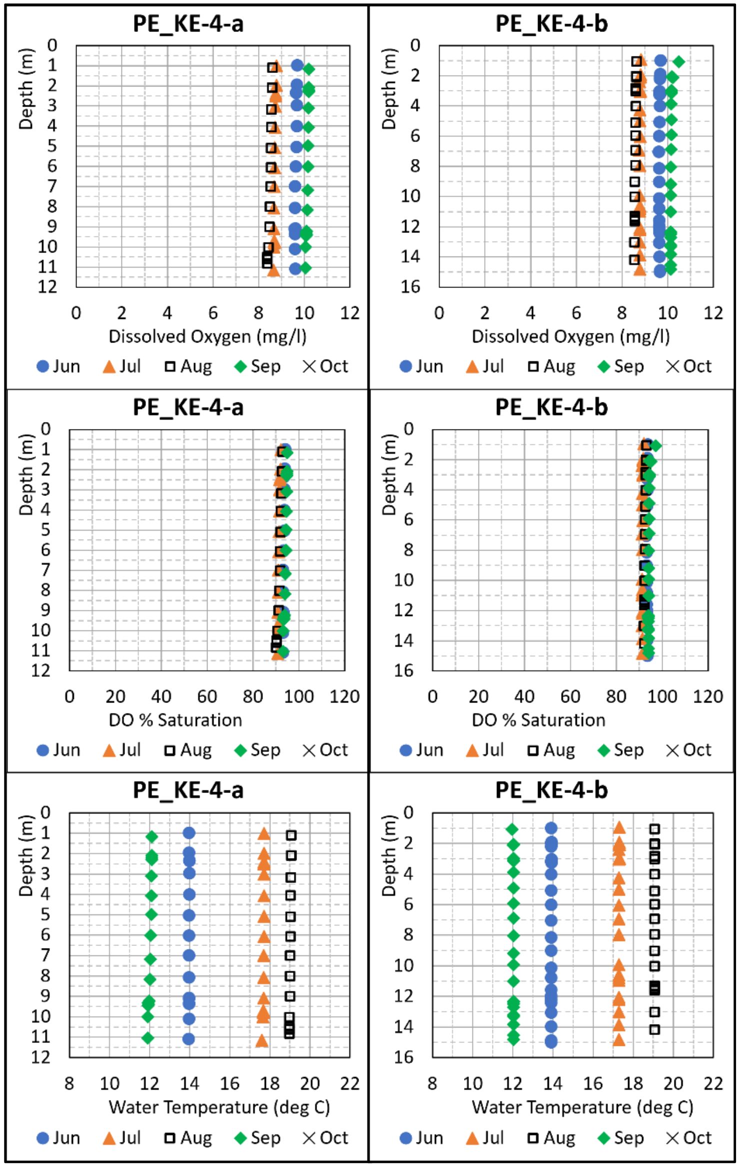
PE_KE-4-a
PE_KE-4-b
Depth (m)
Dissolved Oxygen (mg/l)
DO % Saturation
Water Temperature (deg C)
Jun
Jul
Aug
Sep
Oct

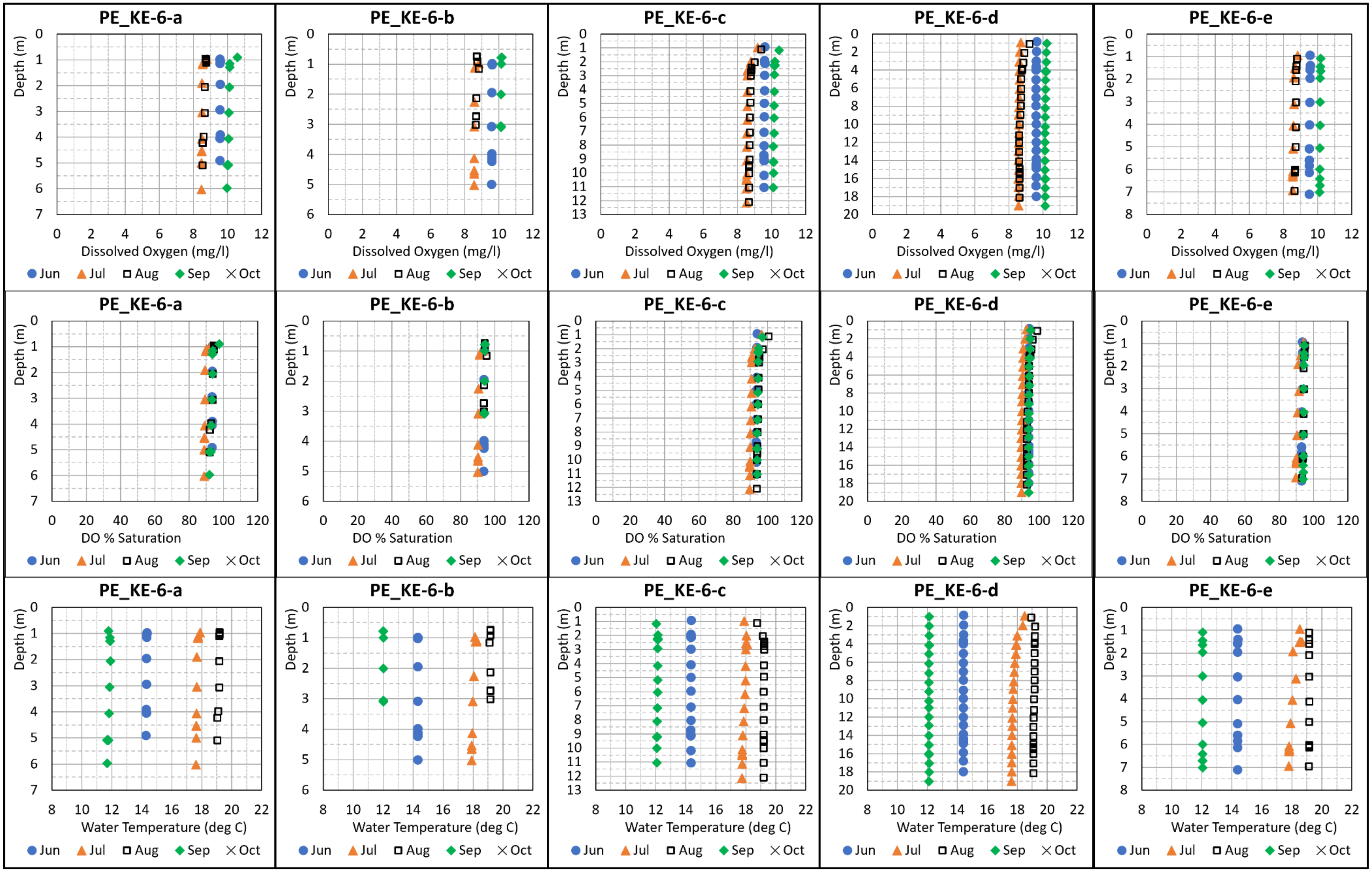
PE_KE-6-a
PE_KE-6-b
PE_KE-6-c
PE_KE-6-d
PE_KE-6-e
Depth (m)
Dissolved Oxygen (mg/l)
DO % Saturation
Water Temperature (deg C)
Jun
Jul
Aug
Sep
Oct

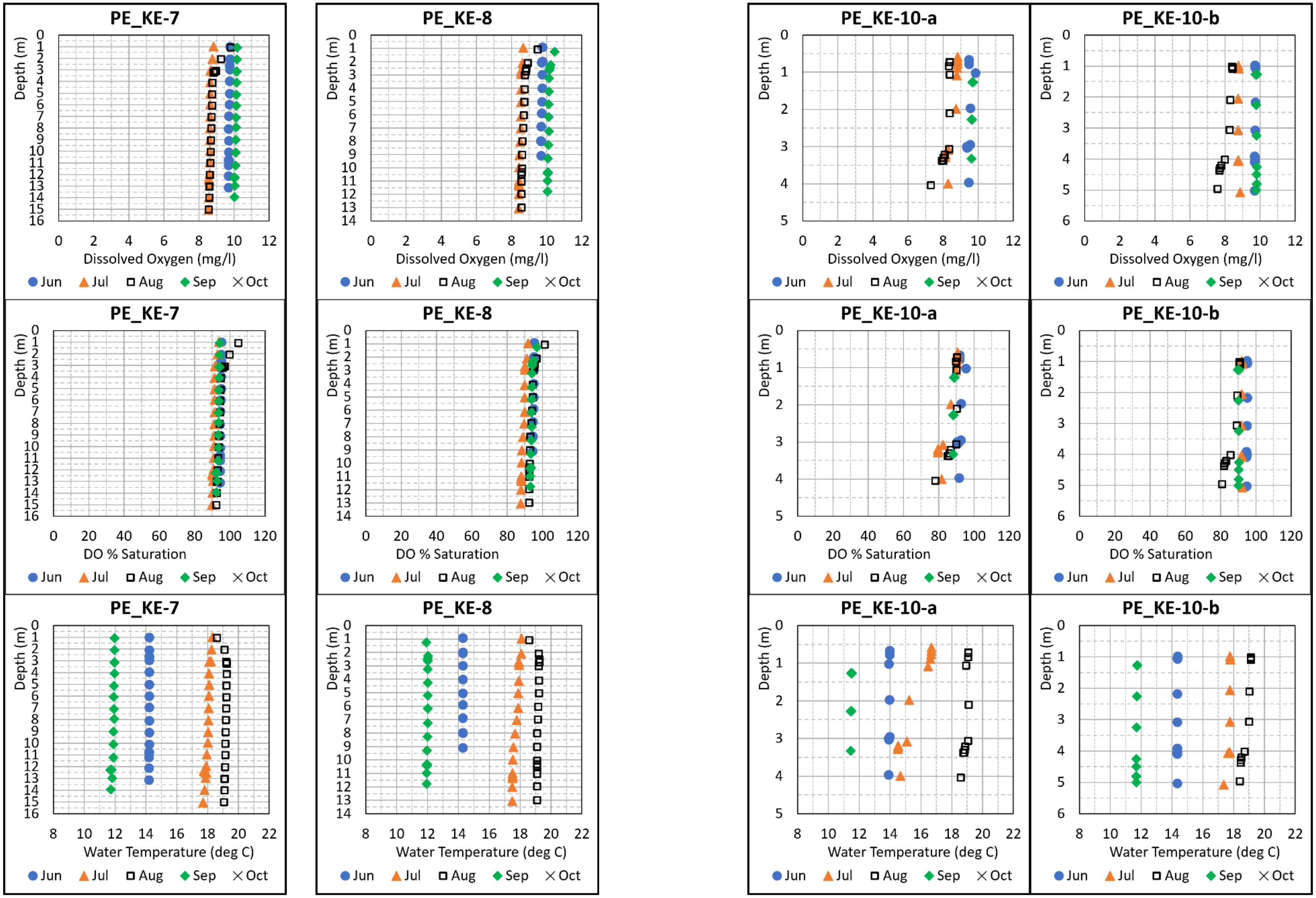
PE_KE-7
Depth (m)
Dissolved Oxygen (mg/l)
Jun Jul Aug Sep Oct
PE_KE-8
Depth (m)
Dissolved Oxygen (mg/l)
Jun Jul Aug Sep Oct
PE_KE-10-a
Depth (m)
Dissolved Oxygen (mg/l)
Jun Jul Aug Sep Oct
PE_KE-10-b
Depth (m)
Dissolved Oxygen (mg/l)
Jun Jul Aug Sep Oct
PE_KE-7
Depth (m)
DO % Saturation
Jun Jul Aug Sep Oct
PE_KE-8
Depth (m)
DO % Saturation
Jun Jul Aug Sep Oct
PE_KE-10-a
Depth (m)
DO % Saturation
Jun Jul Aug Sep Oct
PE_KE-10-b
Depth (m)
DO % Saturation
Jun Jul Aug Sep Oct
PE_KE-7
Depth (m)
Water Temperature (deg C)
Jun Jul Aug Sep Oct
PE_KE-8
Depth (m)
Water Temperature (deg C)
Jun Jul Aug Sep Oct
PE_KE-10-a
Depth (m)
Water Temperature (deg C)
Jun Jul Aug Sep Oct
PE_KE-10-b
Depth (m)
Water Temperature (deg C)
Jun Jul Aug Sep Oct

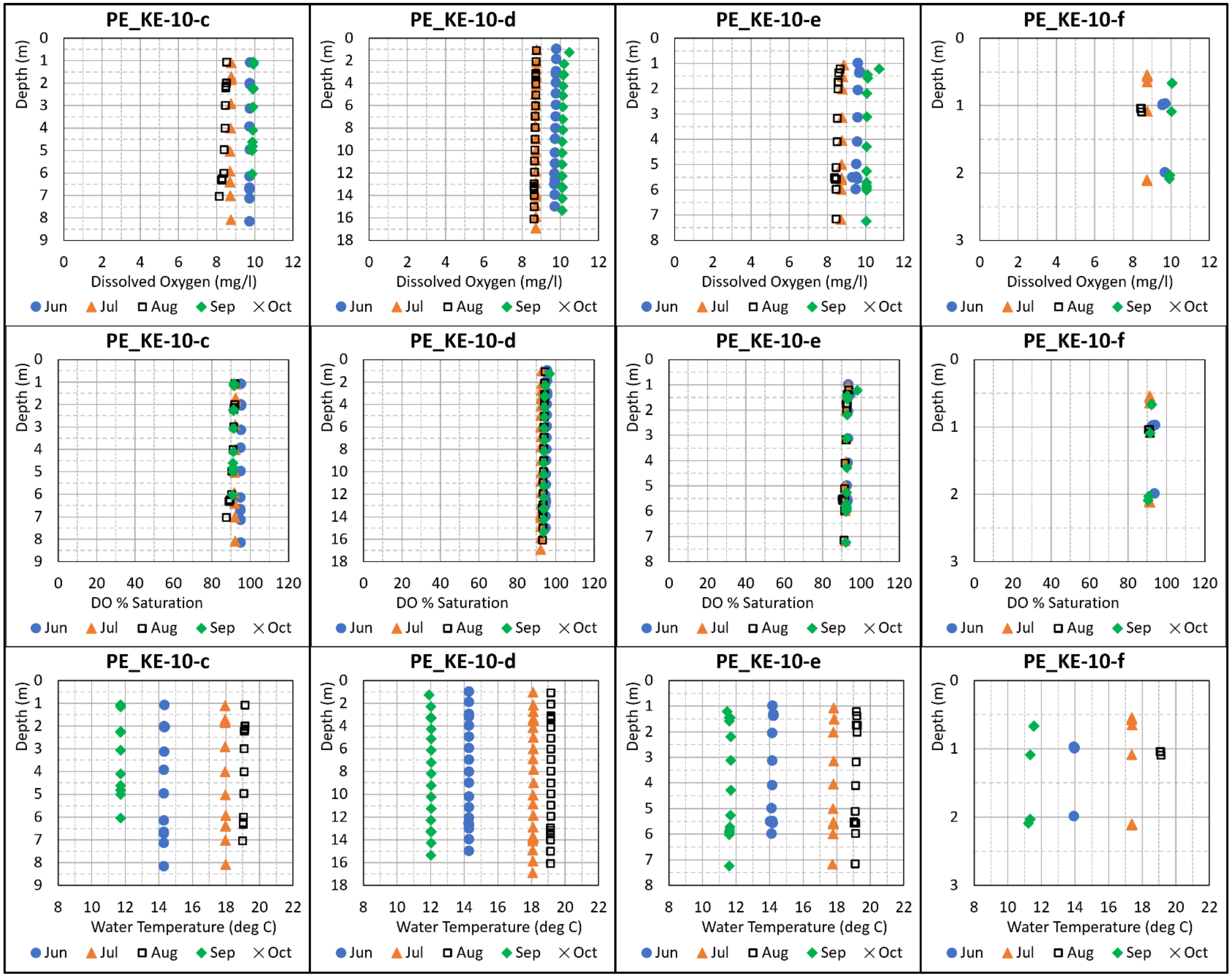
PE_KE-10-c
PE_KE-10-d
PE_KE-10-e
PE_KE-10-f
Depth (m)
Dissolved Oxygen (mg/l)
DO % Saturation
Water Temperature (deg C)
Jun
Jul
Aug
Sep
Oct

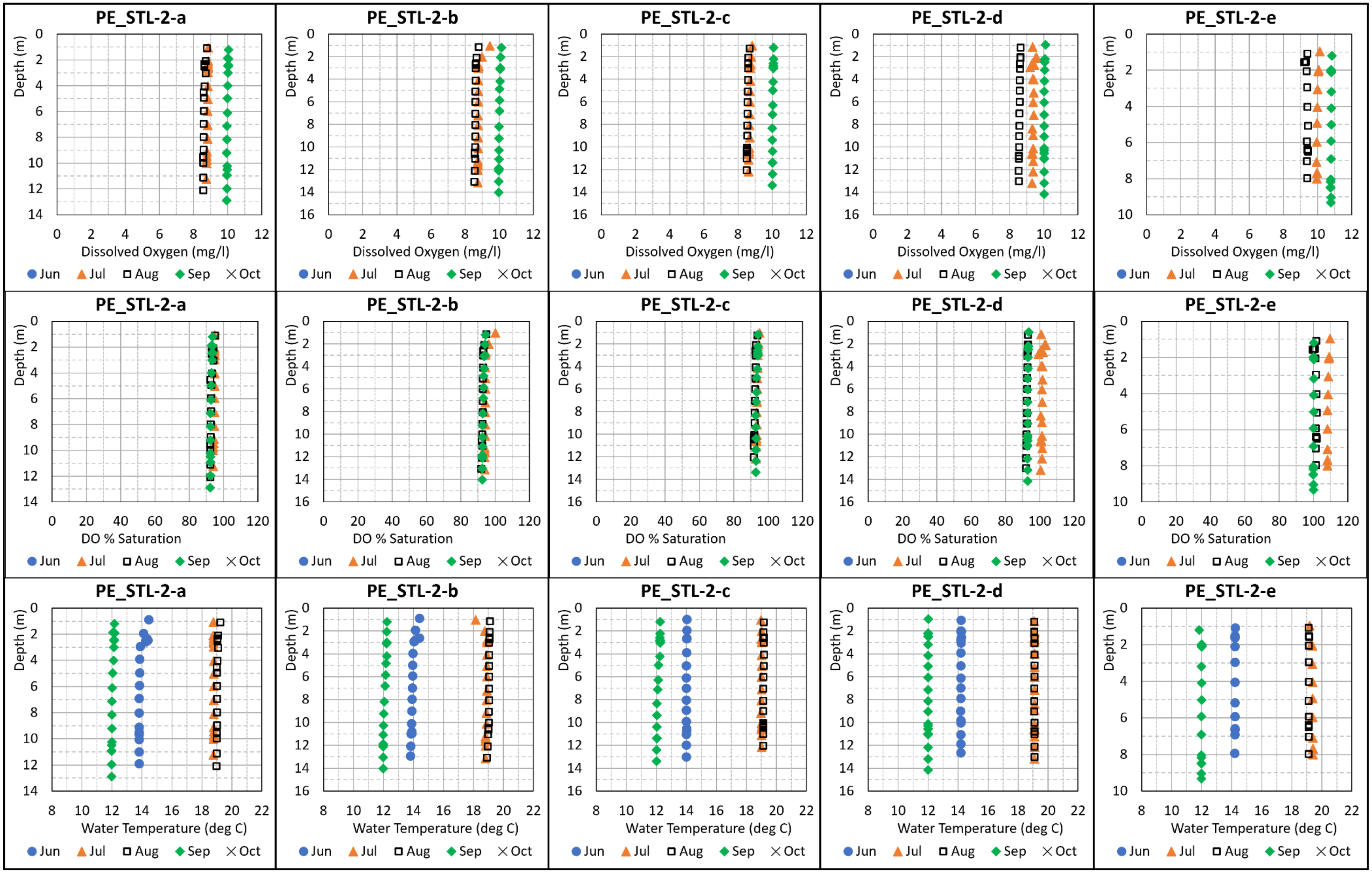
PE_STL-2-a
PE_STL-2-b
PE_STL-2-c
PE_STL-2-d
PE_STL-2-e
Depth (m)
Dissolved Oxygen (mg/l)
DO % Saturation
Water Temperature (deg C)
Jun Jul Aug Sep Oct

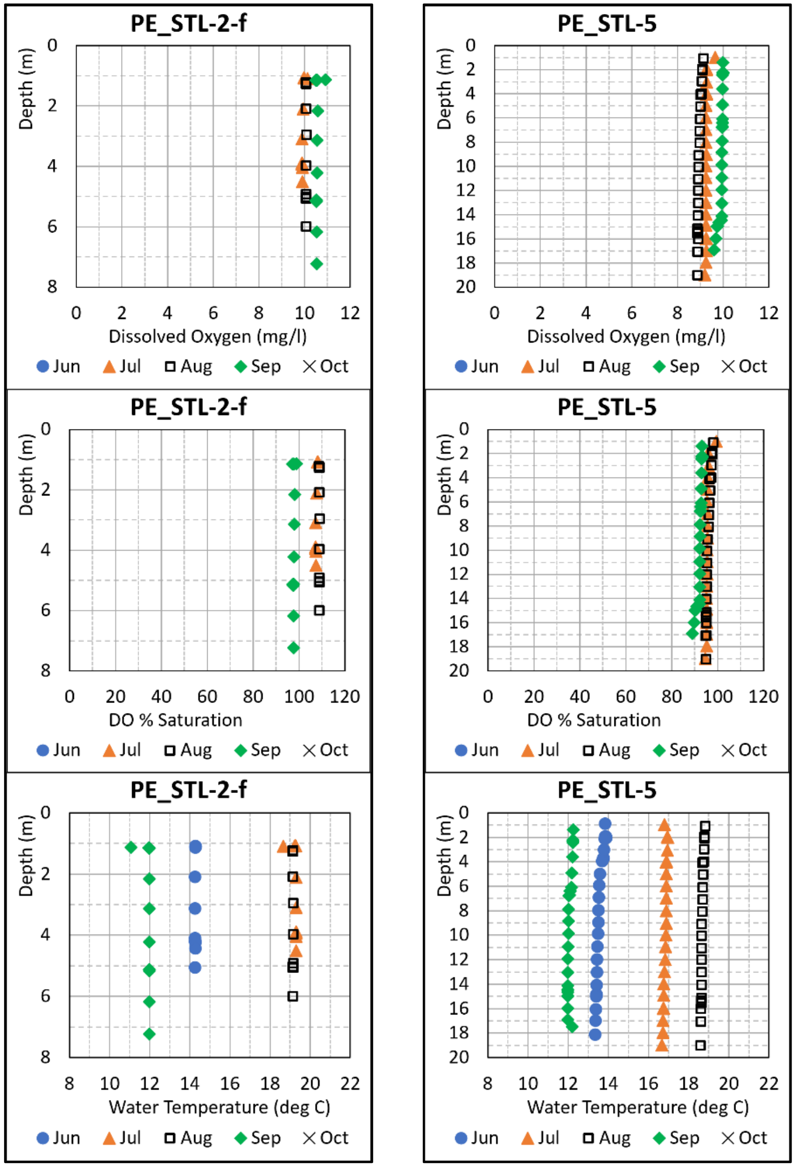
PE_STL-2-f
Depth (m)
Dissolved Oxygen (mg/l)
Jun Jul Aug Sep Oct
PE_STL-5
Depth (m)
Dissolved Oxygen (mg/l)
Jun Jul Aug Sep Oct
PE_STL-2-f
Depth (m)
DO % Saturation
Jun Jul Aug Sep Oct
PE_STL-5
Depth (m)
DO % Saturation
Jun Jul Aug Sep Oct
PE_STL-2-f
Depth (m)
Water Temperature (deg C)
Jun Jul Aug Sep Oct
PE_STL-5
Depth (m)
Water Temperature (deg C)
Jun Jul Aug Sep Oct

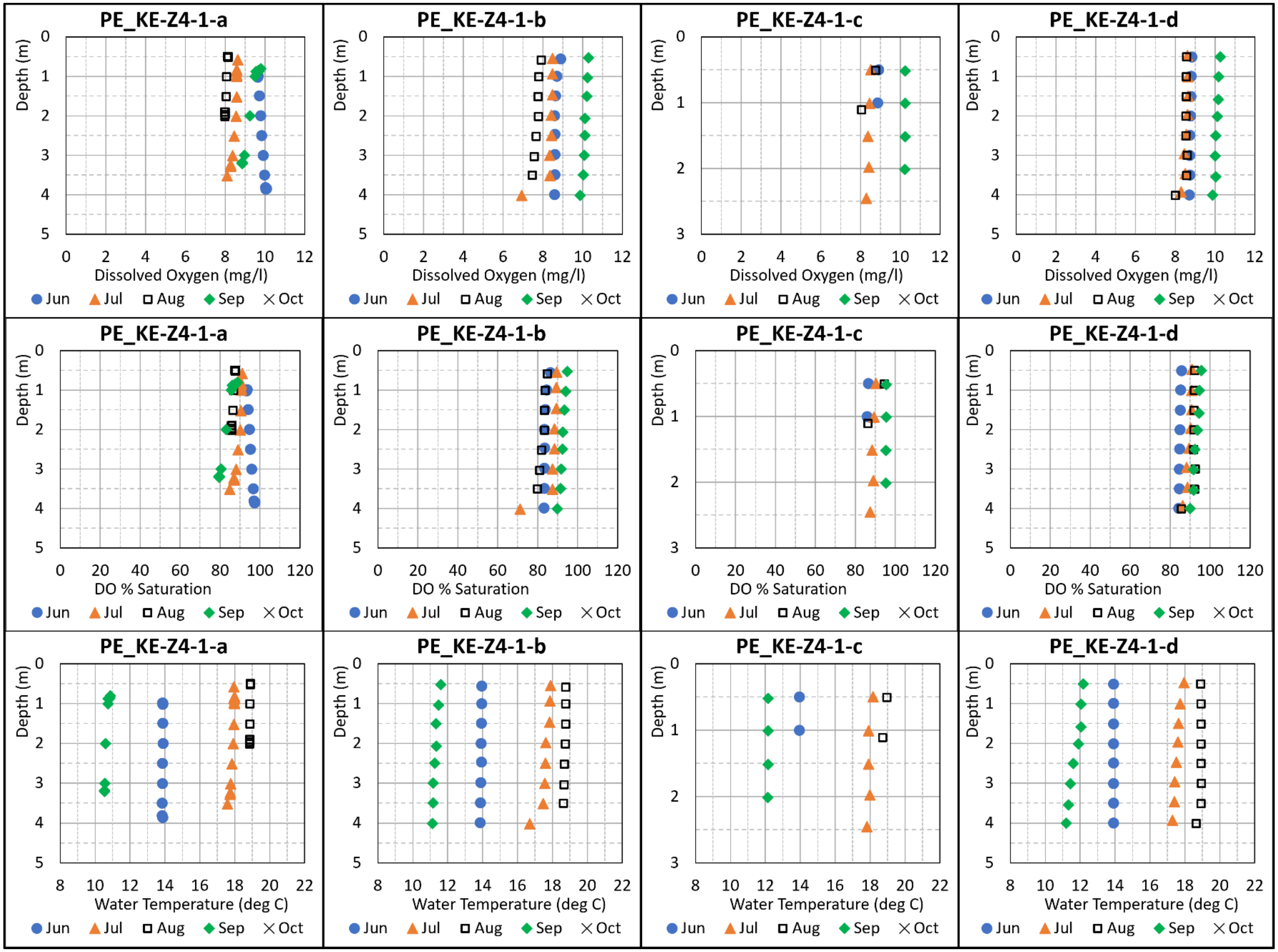
PE_KE-Z4-1-a
PE_KE-Z4-1-b
PE_KE-Z4-1-c
PE_KE-Z4-1-d
Depth (m)
Dissolved Oxygen (mg/l)
DO % Saturation
Water Temperature (deg C)
Jun
Jul
Aug
Sep
Oct

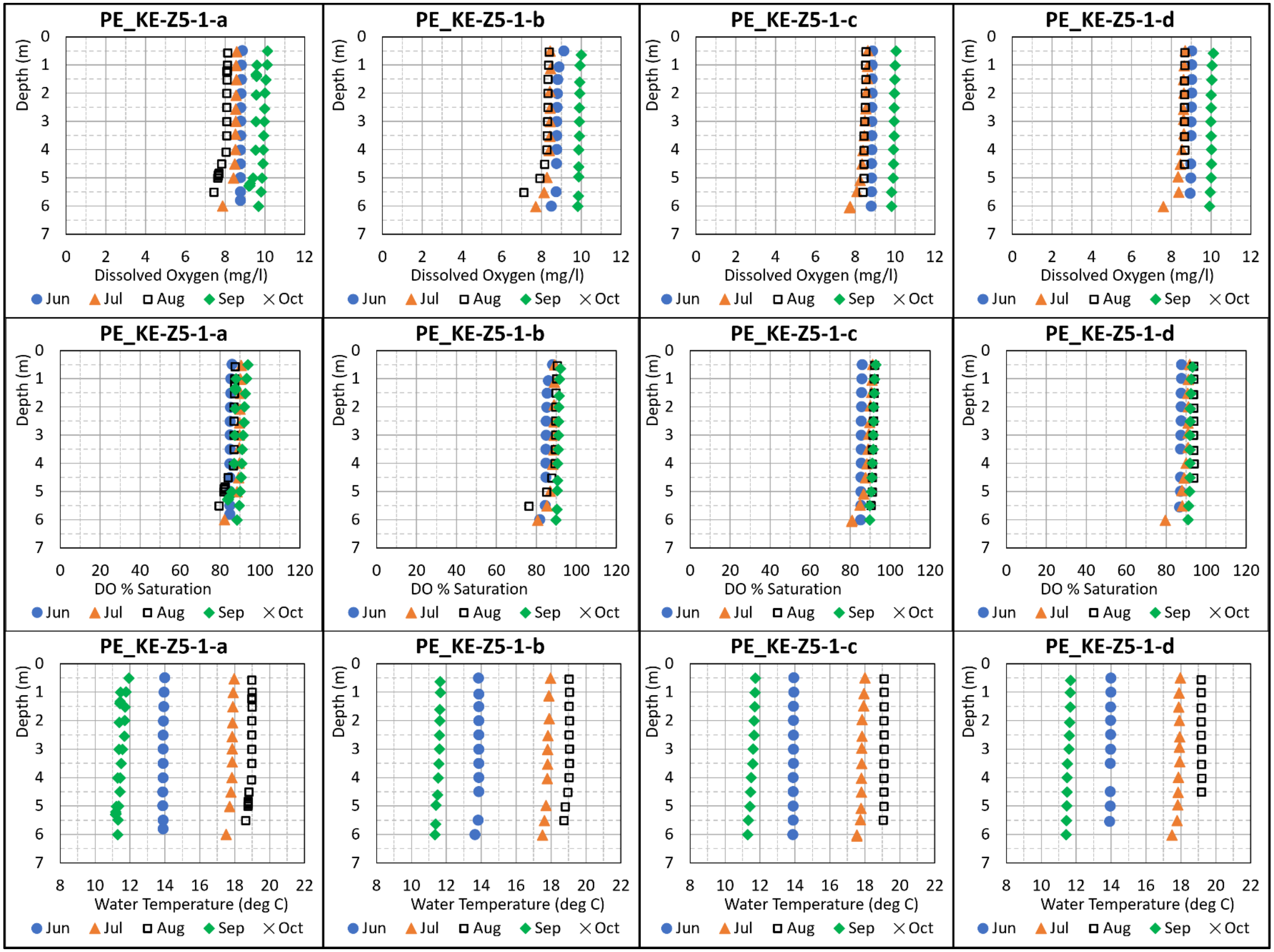
PE_KE-Z5-1-a
PE_KE-Z5-1-b
PE_KE-Z5-1-c
PE_KE-Z5-1-d
Depth (m)
Dissolved Oxygen (mg/l)
DO % Saturation
Water Temperature (deg C)
Jun Jul Aug Sep Oct

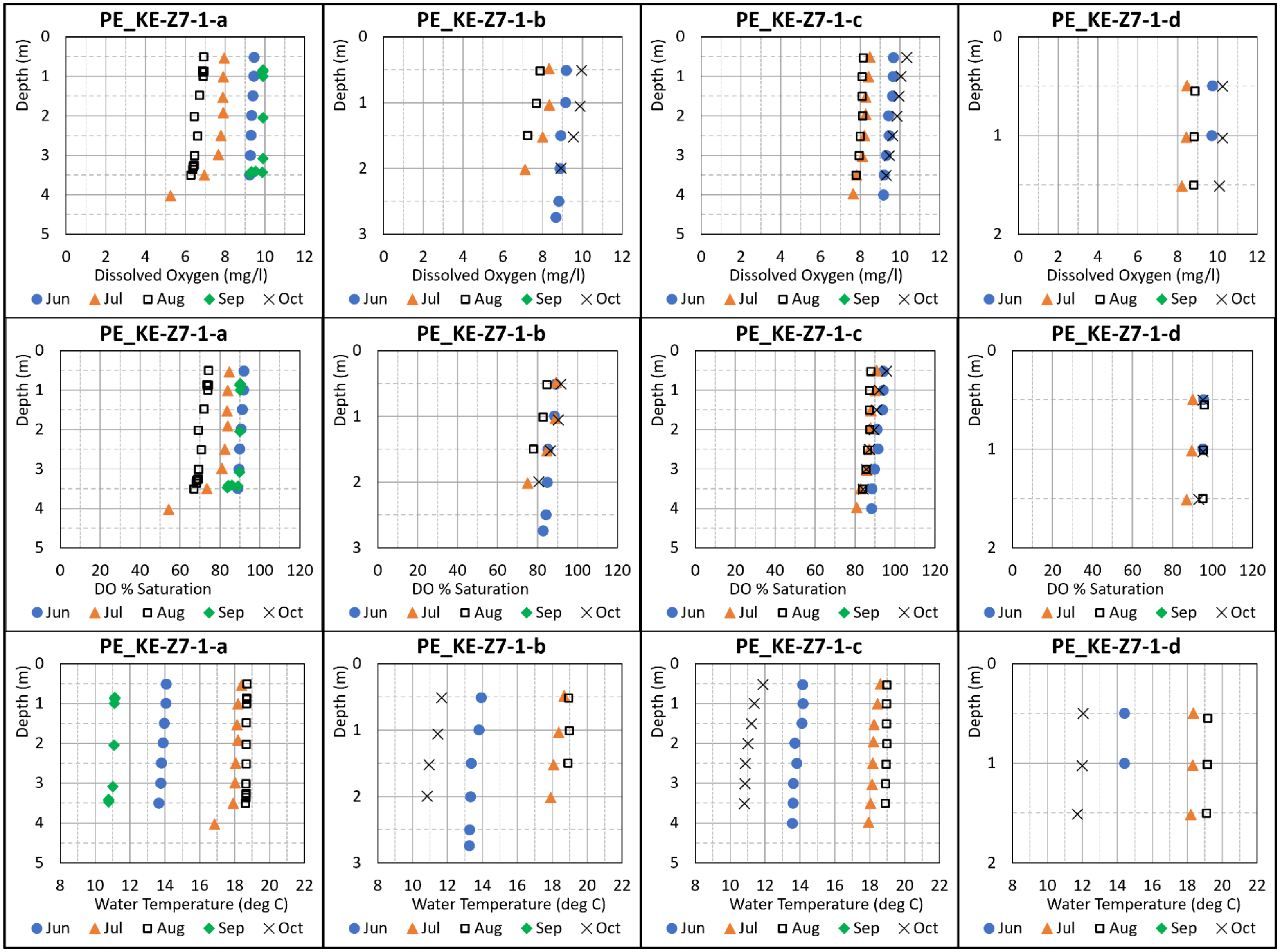
PE_KE-Z7-1-a
PE_KE-Z7-1-b
PE_KE-Z7-1-c
PE_KE-Z7-1-d
Depth (m)
Dissolved Oxygen (mg/l)
DO % Saturation
Water Temperature (deg C)
Jun
Jul
Aug
Sep
Oct

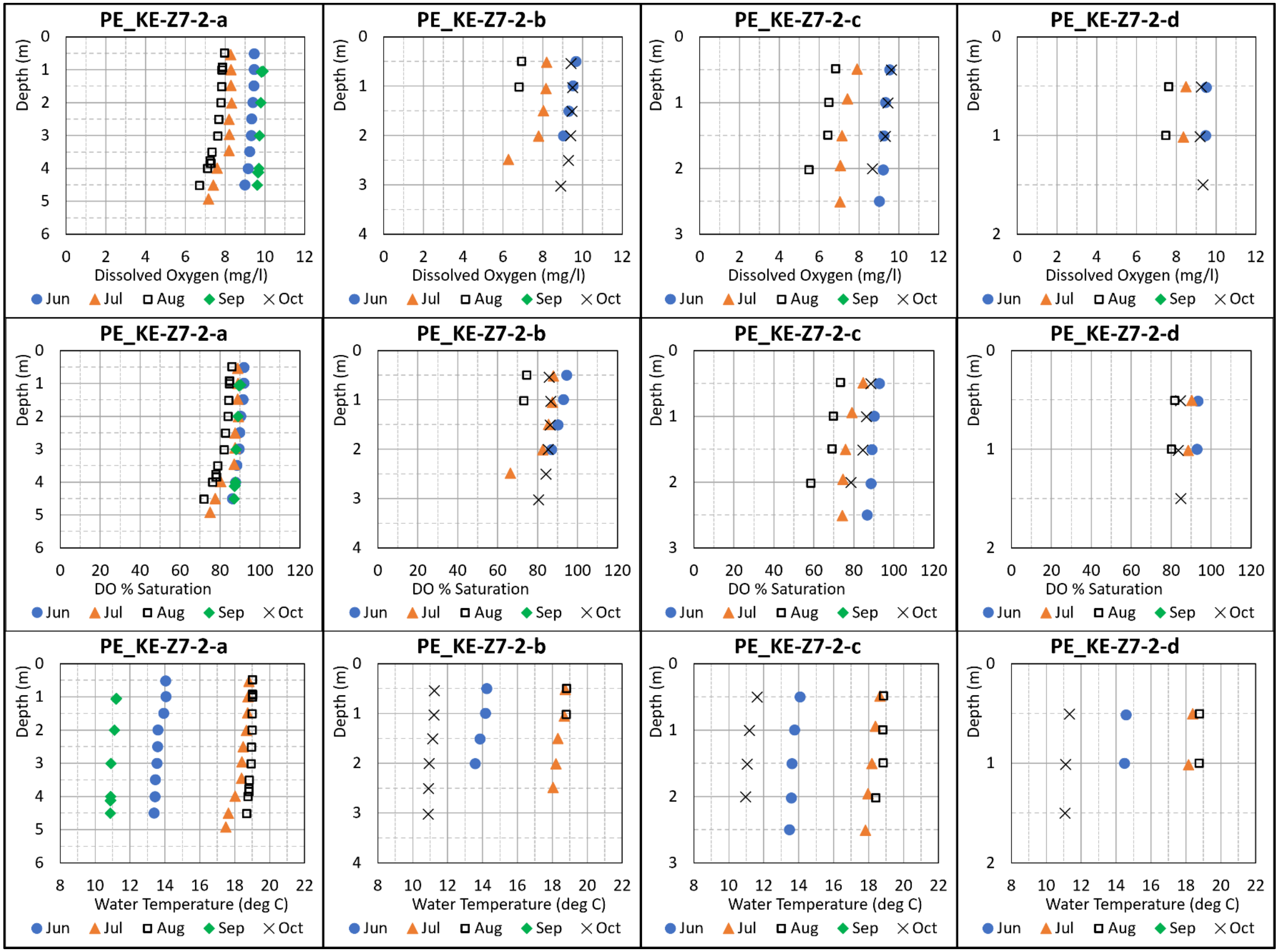
PE_KE-Z7-2-a
PE_KE-Z7-2-b
PE_KE-Z7-2-c
PE_KE-Z7-2-d
Depth (m)
Dissolved Oxygen (mg/l)
Jun Jul Aug Sep Oct
PE_KE-Z7-2-a
PE_KE-Z7-2-b
PE_KE-Z7-2-c
PE_KE-Z7-2-d
Depth (m)
DO % Saturation
Jun Jul Aug Sep Oct
PE_KE-Z7-2-a
PE_KE-Z7-2-b
PE_KE-Z7-2-c
PE_KE-Z7-2-d
Depth (m)
Water Temperature (deg C)
Jun Jul Aug Sep Oct

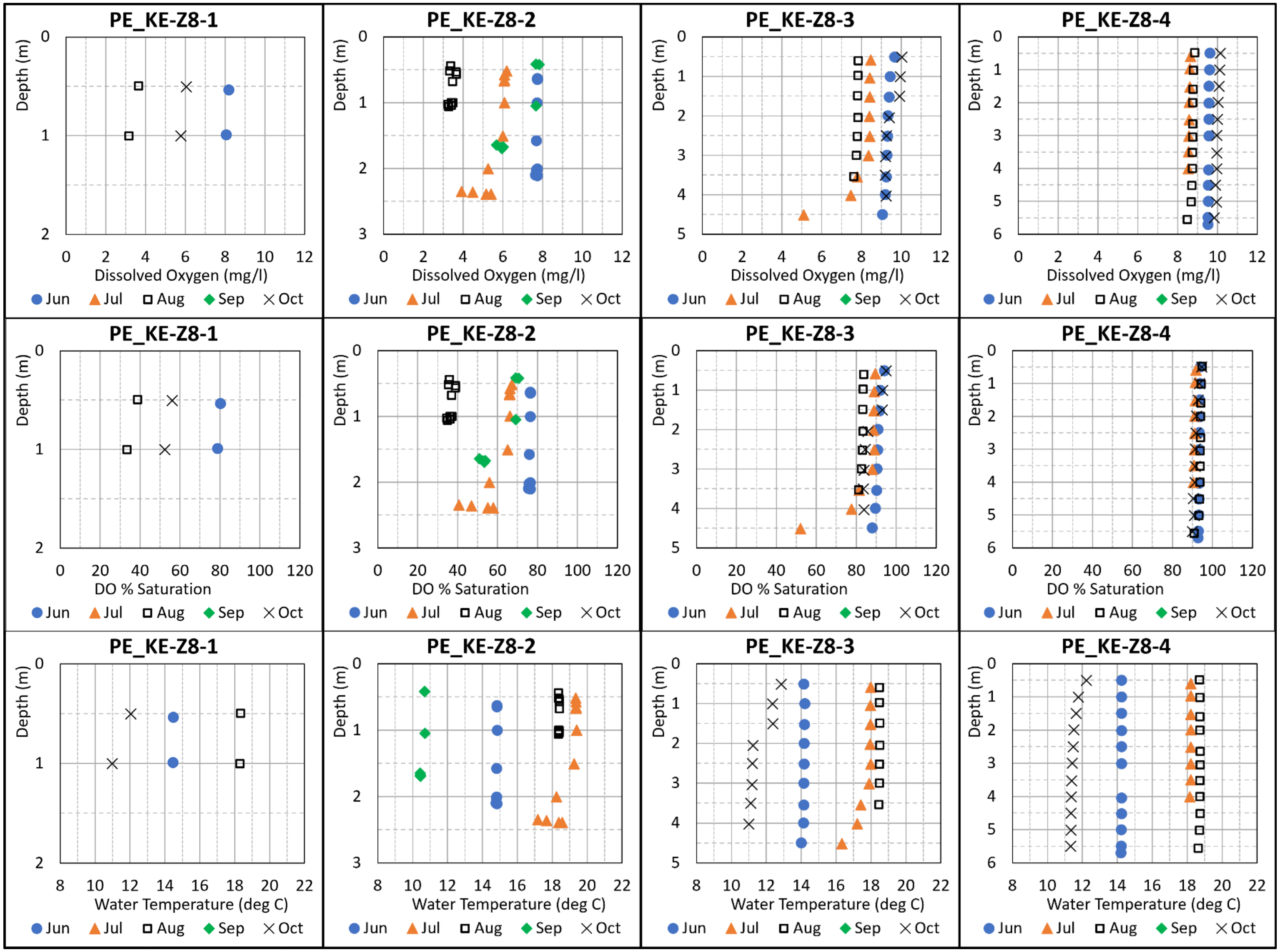
PE_KE-Z8-1
Depth (m)
0
1
2
0 2 4 6 8 10 12
Dissolved Oxygen (mg/l)
Jun Jul Aug Sep Oct
PE_KE-Z8-2
Depth (m)
0
1
2
3
0 2 4 6 8 10 12
Dissolved Oxygen (mg/l)
Jun Jul Aug Sep Oct
PE_KE-Z8-3
Depth (m)
0
1
2
3
4
5
0 2 4 6 8 10 12
Dissolved Oxygen (mg/l)
Jun Jul Aug Sep Oct
PE_KE-Z8-4
Depth (m)
0
1
2
3
4
5
6
0 2 4 6 8 10 12
Dissolved Oxygen (mg/l)
Jun Jul Aug Sep Oct
PE_KE-Z8-1
Depth (m)
0
1
2
0 20 40 60 80 100 120
DO % Saturation
Jun Jul Aug Sep Oct
PE_KE-Z8-2
Depth (m)
0
1
2
3
0 20 40 60 80 100 120
DO % Saturation
Jun Jul Aug Sep Oct
PE_KE-Z8-3
Depth (m)
0
1
2
3
4
5
0 20 40 60 80 100 120
DO % Saturation
Jun Jul Aug Sep Oct
PE_KE-Z8-4
Depth (m)
0
1
2
3
4
5
6
0 20 40 60 80 100 120
DO % Saturation
Jun Jul Aug Sep Oct
PE_KE-Z8-1
Depth (m)
0
1
2
8 10 12 14 16 18 20 22
Water Temperature (deg C)
Jun Jul Aug Sep Oct
PE_KE-Z8-2
Depth (m)
0
1
2
3
8 10 12 14 16 18 20 22
Water Temperature (deg C)
Jun Jul Aug Sep Oct
PE_KE-Z8-3
Depth (m)
0
1
2
3
4
5
8 10 12 14 16 18 20 22
Water Temperature (deg C)
Jun Jul Aug Sep Oct
PE_KE-Z8-4
Depth (m)
0
1
2
3
4
5
6
8 10 12 14 16 18 20 22
Water Temperature (deg C)
Jun Jul Aug Sep Oct

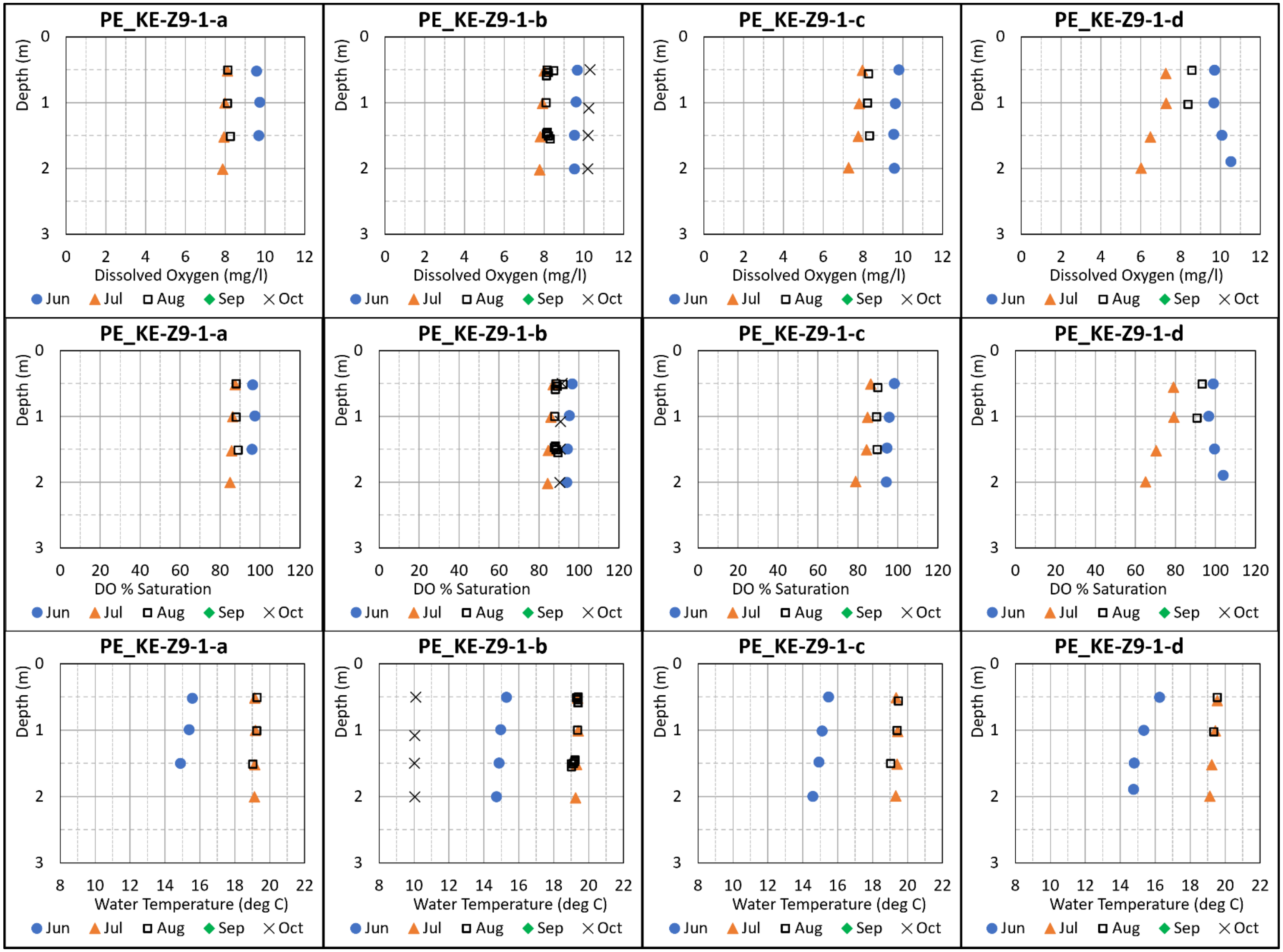
PE_KE-Z9-1-a
PE_KE-Z9-1-b
PE_KE-Z9-1-c
PE_KE-Z9-1-d
Depth (m)
Dissolved Oxygen (mg/l)
DO % Saturation
Water Temperature (deg C)
Jun
Jul
Aug
Sep
Oct

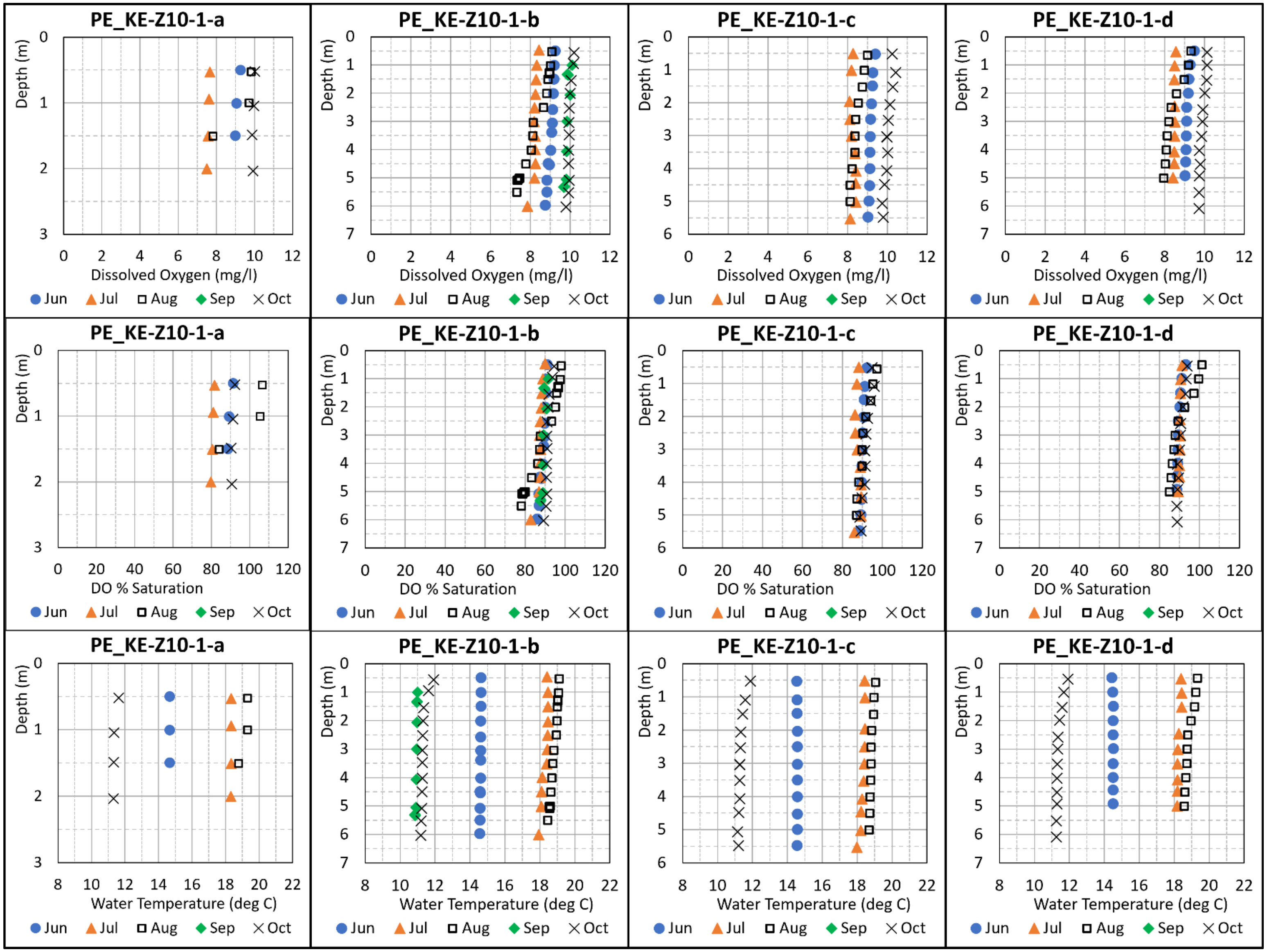
PE_KE-Z10-1-a
PE_KE-Z10-1-b
PE_KE-Z10-1-c
PE_KE-Z10-1-d
Depth (m)
Dissolved Oxygen (mg/l)
DO % Saturation
Water Temperature (deg C)
Jun Jul Aug Sep Oct

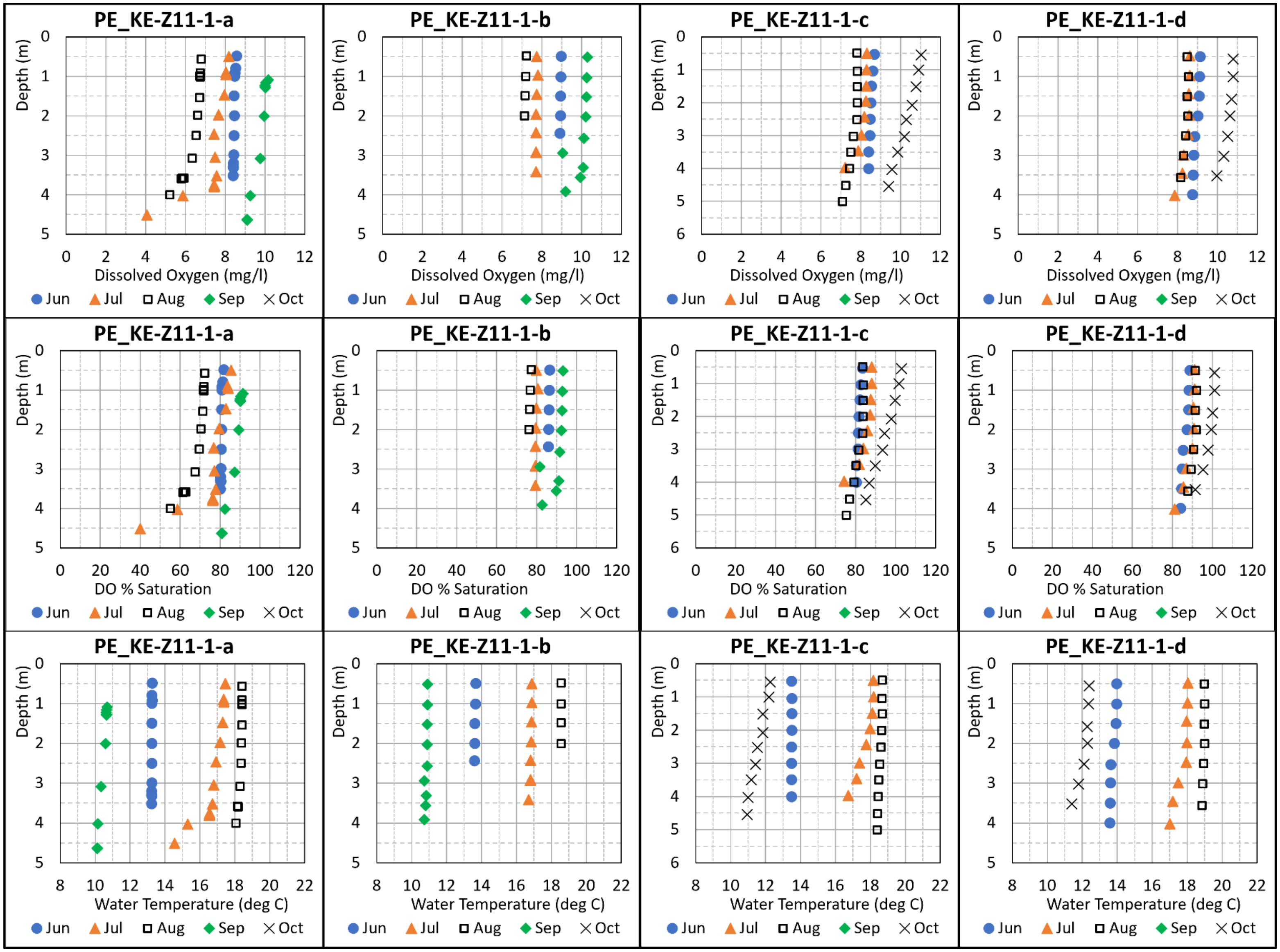
PE_KE-Z11-1-a
PE_KE-Z11-1-b
PE_KE-Z11-1-c
PE_KE-Z11-1-d
Depth (m)
Dissolved Oxygen (mg/l)
DO % Saturation
Water Temperature (deg C)
Jun
Jul
Aug
Sep
Oct

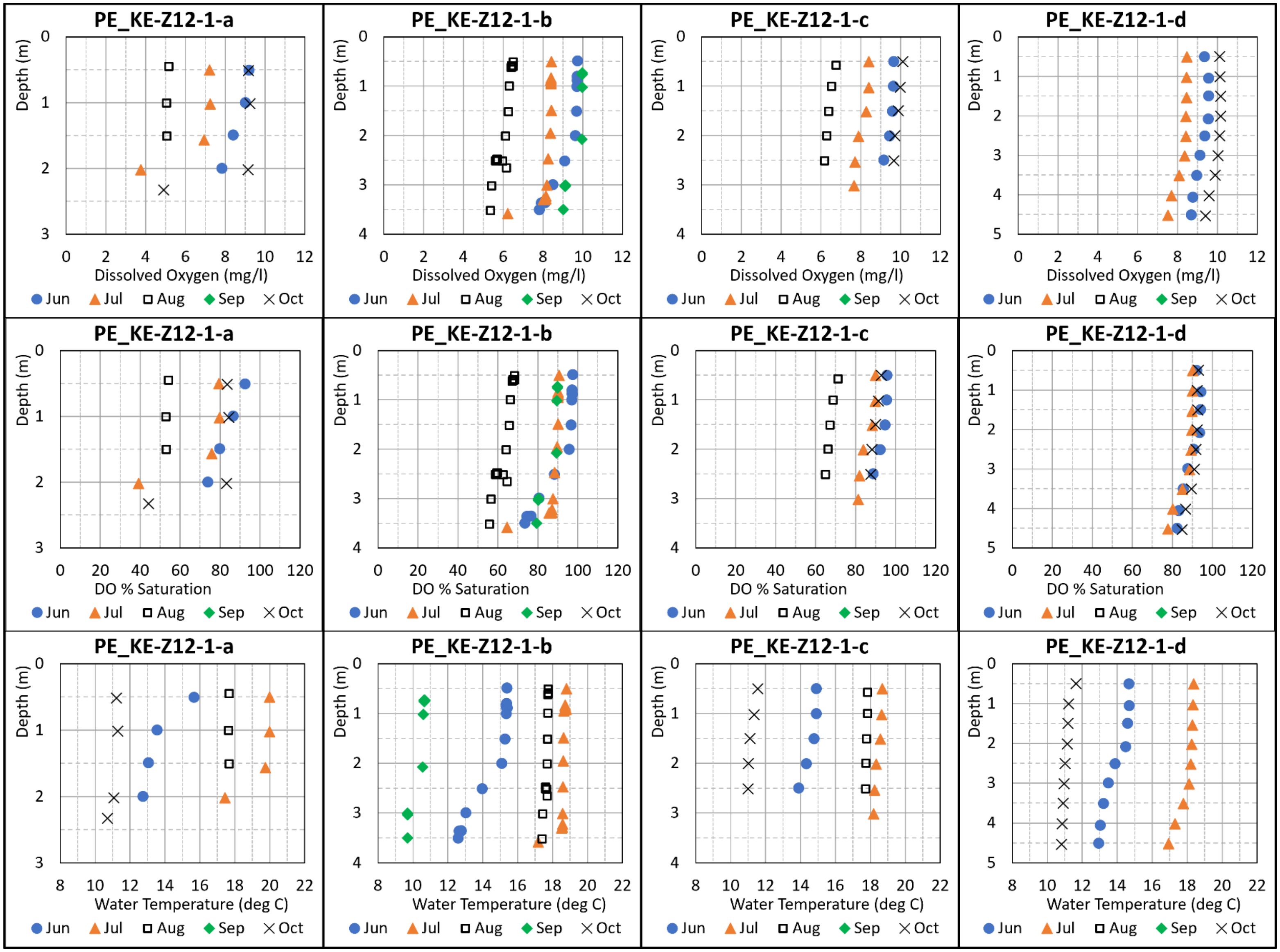
PE_KE-Z12-1-a
Depth (m)
Dissolved Oxygen (mg/l)
Jun Jul Aug Sep Oct
PE_KE-Z12-1-b
Depth (m)
Dissolved Oxygen (mg/l)
Jun Jul Aug Sep Oct
PE_KE-Z12-1-c
Depth (m)
Dissolved Oxygen (mg/l)
Jun Jul Aug Sep Oct
PE_KE-Z12-1-d
Depth (m)
Dissolved Oxygen (mg/l)
Jun Jul Aug Sep Oct
PE_KE-Z12-1-a
Depth (m)
DO % Saturation
Jun Jul Aug Sep Oct
PE_KE-Z12-1-b
Depth (m)
DO % Saturation
Jun Jul Aug Sep Oct
PE_KE-Z12-1-c
Depth (m)
DO % Saturation
Jun Jul Aug Sep Oct
PE_KE-Z12-1-d
Depth (m)
DO % Saturation
Jun Jul Aug Sep Oct
PE_KE-Z12-1-a
Depth (m)
Water Temperature (deg C)
Jun Jul Aug Sep Oct
PE_KE-Z12-1-b
Depth (m)
Water Temperature (deg C)
Jun Jul Aug Sep Oct
PE_KE-Z12-1-c
Depth (m)
Water Temperature (deg C)
Jun Jul Aug Sep Oct
PE_KE-Z12-1-d
Depth (m)
Water Temperature (deg C)
Jun Jul Aug Sep Oct

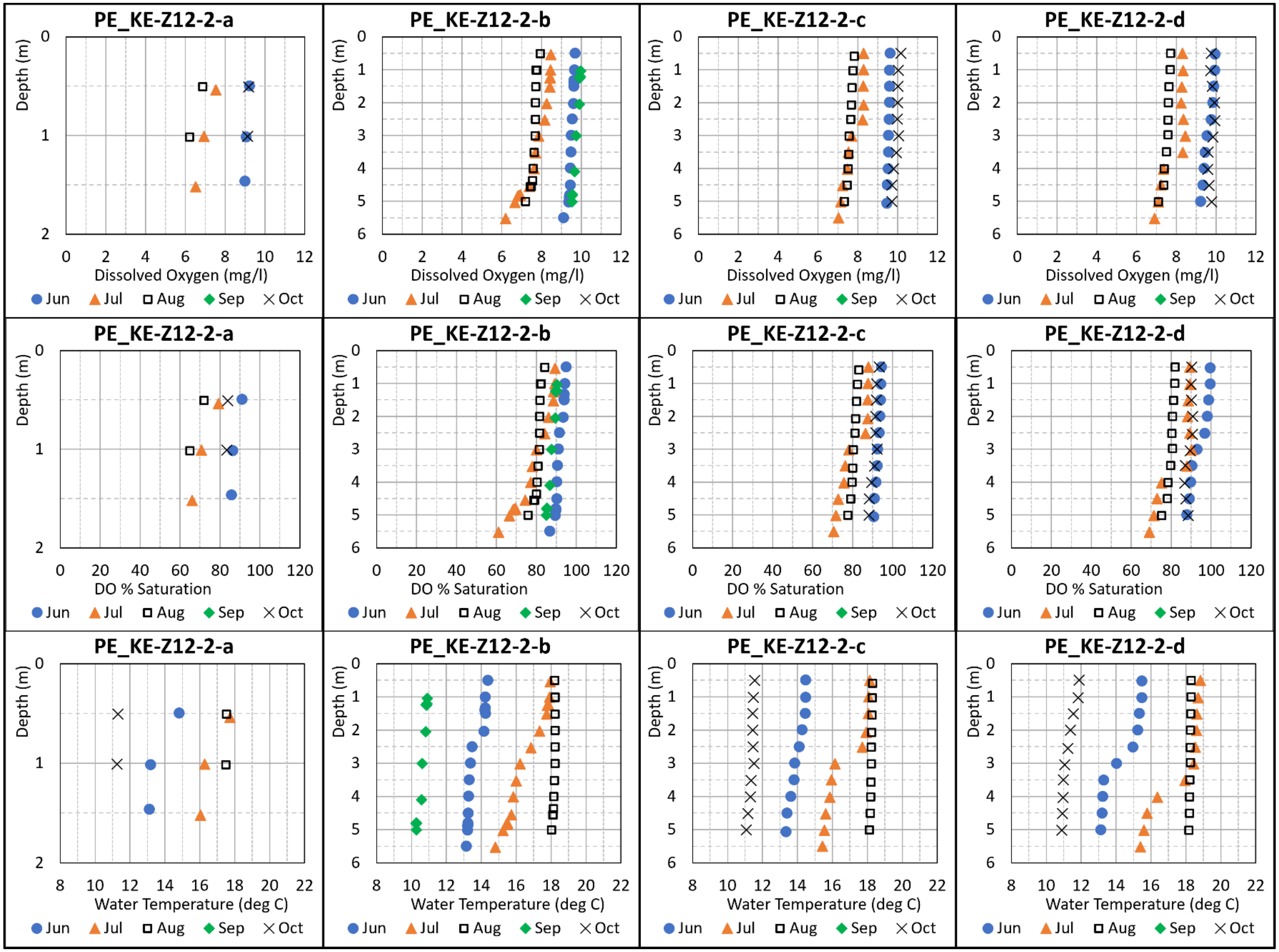
PE_KE-Z12-2-a
Depth (m)
Dissolved Oxygen (mg/l)
Jun Jul Aug Sep Oct
PE_KE-Z12-2-b
Depth (m)
Dissolved Oxygen (mg/l)
Jun Jul Aug Sep Oct
PE_KE-Z12-2-c
Depth (m)
Dissolved Oxygen (mg/l)
Jun Jul Aug Sep Oct
PE_KE-Z12-2-d
Depth (m)
Dissolved Oxygen (mg/l)
Jun Jul Aug Sep Oct
PE_KE-Z12-2-a
Depth (m)
DO % Saturation
Jun Jul Aug Sep Oct
PE_KE-Z12-2-b
Depth (m)
DO % Saturation
Jun Jul Aug Sep Oct
PE_KE-Z12-2-c
Depth (m)
DO % Saturation
Jun Jul Aug Sep Oct
PE_KE-Z12-2-d
Depth (m)
DO % Saturation
Jun Jul Aug Sep Oct
PE_KE-Z12-2-a
Depth (m)
Water Temperature (deg C)
Jun Jul Aug Sep Oct
PE_KE-Z12-2-b
Depth (m)
Water Temperature (deg C)
Jun Jul Aug Sep Oct
PE_KE-Z12-2-c
Depth (m)
Water Temperature (deg C)
Jun Jul Aug Sep Oct
PE_KE-Z12-2-d
Depth (m)
Water Temperature (deg C)
Jun Jul Aug Sep Oct

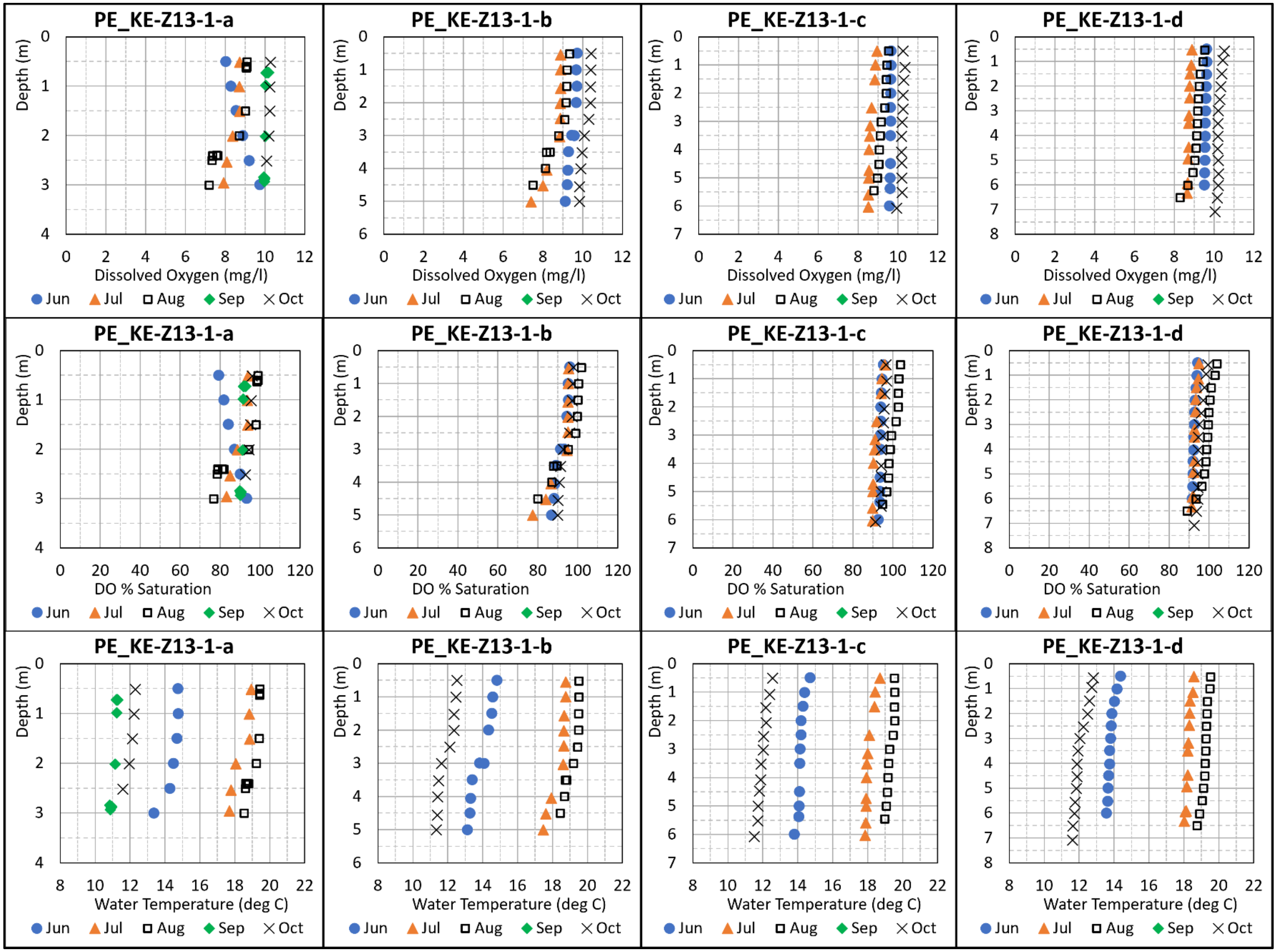
PE_KE-Z13-1-a
PE_KE-Z13-1-b
PE_KE-Z13-1-c
PE_KE-Z13-1-d
Depth (m)
Dissolved Oxygen (mg/l)
DO % Saturation
Water Temperature (deg C)
Jun
Jul
Aug
Sep
Oct

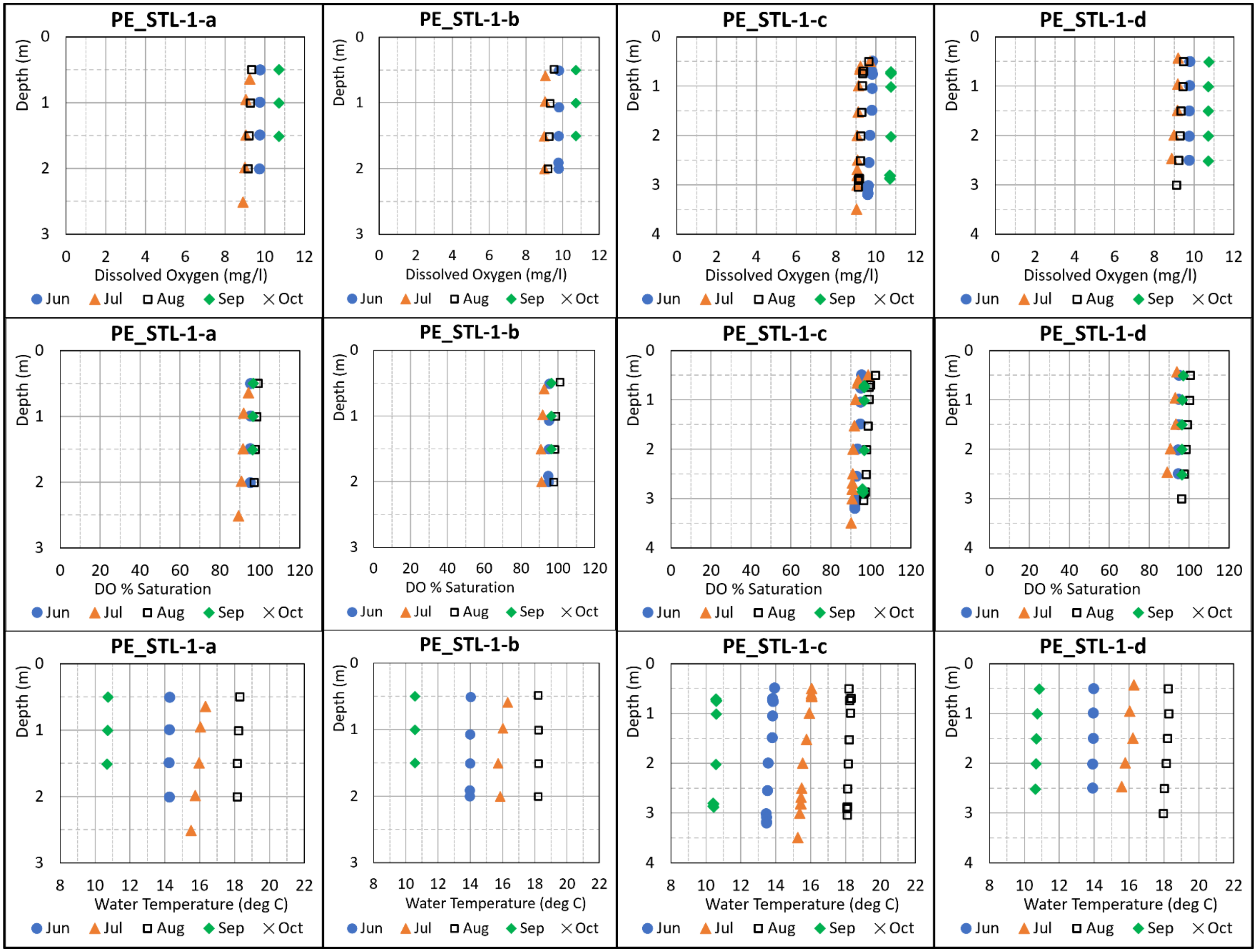
PE_STL-1-a
PE_STL-1-b
PE_STL-1-c
PE_STL-1-d
Depth (m)
Dissolved Oxygen (mg/l)
DO % Saturation
Water Temperature (deg C)
Jun
Jul
Aug
Sep
Oct